

The Role of Small RNAs in C₄ Photosynthesis



E.L.C. Gage

Magdalene College
University of Cambridge

A thesis submitted for the degree of

Doctor of Philosophy

June 2012

Contents

Declaration	i
Acknowledgements.....	iii
Abstract	v
List of Figures.....	vii
List of Tables	viii
Abbreviations	ix
1. Introduction.....	1
1.1: A Requirement for Improved Crop Productivity.....	1
1.2: The Effects of Photorespiration	1
1.3: The C ₄ Cycle	3
1.4: miRNA Regulation of the C ₄ Cycle	14
1.5: miRNA Regulation.....	15
1.6: Experimental Approach	17
1.7: Project Aims.....	21
2. Materials and Methods	23
2.1: General Plant Cultivation.....	23
2.2: Molecular Techniques	24
2.3: Quantification of Protein	30
2.4: Plasmid Design and Construction	32
2.5: Microbial Techniques	35
2.6: Transformation of <i>Cleome gynandra</i>	37
2.7: Transformation of <i>Arabidopsis thaliana</i>	39
2.8: Analysis of Transgenics	40
2.9: Anatomical Analysis	41
2.10: Photosynthetic Analysis.....	42
2.11: Hybridisations of <i>C. hassleriana</i> and <i>C. gynandra</i>	43
2.11.2: In vitro Ovule Culture	44
3. Do miRNAs regulate the C ₄ Cycle? Analysis of sRNAs and their Inhibition.....	45
3.1: Introduction.....	45
3.1.4: Experimental Design	48

3.3: Discussion	76
4. Changes in Gene Regulation during Cotyledon Development.....	87
4.1: Introduction	87
4.2: Results	90
4.3: Discussion	96
5. The Generation of Hybrids within <i>Cleome</i>	103
5.1: Introduction.....	103
5.2: Results	106
5.3: Discussion	110
6. Final Discussion	115
6.1: The potential for miRNAs to regulate the C ₄ Cycle.....	115
6.2: miRNAs actively regulate Development in <i>C. gynandra</i>	115
6.3: sRNAs may act as Regulators of the C ₄ Cycle in <i>C. gynandra</i>	116
6.4: Light Influences Development in <i>C. gynandra</i>	120
6.5: Final Conclusions	121
7. References.....	123
Appendix 1: Primer List.....	141
Appendix 2: sRNA Target List	144
Appendix 3: Plasmid Maps	147

Declaration

This dissertation is the result of my own work and includes nothing which is the outcome of work done in collaboration except where specifically indicated in the text. It does not exceed the word limit set out by the Degree Committee for Biology and is not substantially the same as any work that has been, or is being submitted to any other university for any degree, diploma or any other qualification.

E.L.C. Gage

Acknowledgements

I wish to thank my supervisor Julian Hibberd for his invaluable instruction and support throughout this project. Secondly, John Grey, John Carr and Howard Griffiths have all provided excellent advice and motivation throughout the project. Thanks are due to Kaiser Kajala, Naomi Brown and Holly Astley for advice on molecular techniques, Christine Newell for instruction on *in vitro* techniques, Padubidri Shiaprasad for advice and assistance on small RNA sequencing, Risha Narayan and Kim Rutherford for assistance with the bioinformatic analysis, Maria Herse and Jessica Royles for advice regarding photosynthetic analysis and to Susan Stanley and Britta Kuempers for advice on histological techniques.

Thanks are due to all the members of the Molecular Physiology group for making this project a uniquely enjoyable experience and for putting up with my eccentricities as a scientist. Helen Woodfield and Jane Knerova have made working in the lab a constant pleasure, while Ben Williams and Marek Szecowka never fail to brighten my day. Considerable thanks are due to my parents, Harriet Dickinson, Alice Chang, Peter Brierley, Miranda de Graaf and Cheryl Snowdon for their unfailing support, advice and all-round-greatness.

Finally, I would like to thank the Biotechnology and Biological Sciences Research Council, the Department of Plant Sciences, Magdalene College and the Cambridge Philosophical Society for the funding and support that made this work possible.

Si scientia modo per ruinam confecta est, completa scientia modo per ruinam hominis ipsius confecta est. Immolatio operi factus sum, sed scientia mentis, corporis et plantae perfecta est.

Abstract

The C₄ cycle represents a series of biochemical and anatomical modifications that are targeted to overcome the effects of photorespiration caused by the oxygenase capability of Ribulose Bisphosphate Carboxylase/Oxygenase (RuBisCO). The cycle has evolved independently in over 60 lineages, which suggests that recruitment of genes into the C₄ cycle is a relatively easy process. However, the mechanisms by which the anatomy and cell-specificity of the components of the C₄ cycle is achieved is poorly understood.

Preliminary work in maize indicated several components of the C₄ cycle may be targeted by microRNAs (miRNAs). To explore this, a library of sRNA sequences from mature leaf tissue of the model C₄ species *Cleome gynandra* L. was generated and then searched against a list of expressed sequence tag sequences for candidate genes of the C₄ cycle. To complement this, transgenic *C. gynandra* containing the viral p19 protein, which is capable of suppressing miRNA activity, were produced.

A limited subset of the candidate C₄ genes showed a high level of sRNA read alignment. In *C. gynandra* plants expressing p19 photosynthesis was compromised and transcripts of several genes (most notably *RbcS* and *RCA*) were upregulated. These data were complemented by examining the effect of illumination on developing *C. gynandra* cotyledons, and attempts to generate a hybrid between *C. gynandra* and the C₃ *C. hassleriana* Chodat. *RbcS* also showed elevated abundance in etiolated cotyledons, although this rapidly declined after illumination. The remainder of the C₄ genes profiled accumulated in etiolated tissue, but were upregulated within 6 hours of illumination. Therefore, this study has illustrated that miRNA activity may play a role in maintaining the C₄ photosynthetic cycle at optimum efficiency, although it has not been possible to identify at which point(s) this regulation is applied. Secondly, *RbcS* appears to be subject to multiple regulatory mechanisms in *C. gynandra*, and it is possible that miRNAs have a role in negatively regulating expression of *RbcS*.

List of Figures

Figure	Contents	Page
1.1	Outline of the NAD-ME subtype of the C ₄ Cycle	4
1.2	The distribution of C ₄ lineages	7
1.3	miRNA Formation and activity	15
2.1	Sequencing and Processing of the sRNA Library	28
2.2	Design of p ₁₉ expression constructs	47
3.1	Function of the pOp promoter	50
3.2	Size distribution of reads in the <i>C. gynandra</i> sRNA library	50
3.3	Distribution of sRNA hits against target sequences	54
3.4	Alignment patterns of sRNA hits against target sequences	58
3.5	Alignments of potential miRNA sequences to <i>NAD-ME</i> ₂ transcripts	58
3.6	Products of a 5' RACE of <i>PPDK</i> transcripts	59
3.7	p ₁₉ accumulation in transgenic Arabidopsis lines	60
3.8	p ₁₉ expression alters leaf morphology in Arabidopsis	61
3.9	p ₁₉ expression alters reproductive anatomy in Arabidopsis	62
3.10	A correlation between p ₁₉ abundance and Arabidopsis rosette diameter	62
3.11	p ₁₉ expression in transgenic <i>C. gynandra</i> lines	63
3.12	p ₁₉ expression effects leaf anatomy in <i>C. gynandra</i>	64
3.13	p ₁₉ expression effects leaf anatomy in <i>C. gynandra</i>	64
3.14	Creation of the pOp::p ₁₉ construct	65
3.15	GUS expression in Arabidopsis lines containing pOp::p ₁₉	67
3.16	p ₁₉ transcript and protein abundance in pOp::p ₁₉ Arabidopsis lines	67
3.17	p ₁₉ expression in pOp::p ₁₉ Arabidopsis lines alters leaf morphology	69
3.18	Grafting transgenic <i>C. gynandra</i> scions	710
3.19	GUS expression in <i>C. gynandra</i> transgenics containing pOp::p ₁₉	71
3.20	p ₁₉ expression in pOp::p ₁₉ <i>C. gynandra</i> transgenics	71
3.21	p ₁₉ expression does not alter Kranz development in <i>C. gynandra</i>	73
3.22	Photosynthetic response of <i>C. gynandra</i> transgenics expressing p ₁₉	73
3.23	Changes in transcript abundance in <i>C. gynandra</i> plants expressing p ₁₉	74
3.24	Protein abundance in <i>C. gynandra</i> transgenics expressing p ₁₉	75
4.1	Etiolated cotyledons possess Kranz anatomy	90
4.2	Etiolated cotyledons possess Kranz anatomy	90
4.3	Chlorophyll abundance in <i>C. gynandra</i> cotyledons	91
4.4	Light-induced changes in transcript abundance in <i>C. gynandra</i> cotyledons	93
4.5	Light-induced changes in transcript abundance in <i>C. gynandra</i> cotyledons	94
4.6	Light-induced changes in protein abundance in <i>C. gynandra</i> cotyledons	96
5.1	Reproductive anatomy of <i>C. gynandra</i> and <i>C. hassleriana</i>	107
5.2	Stigma receptivity in <i>C. gynandra</i> and <i>C. hassleriana</i>	108
5.3	Pollen tube growth in heterospecific pollen crosses	108
5.4	Hybrid embryo growth <i>in plant</i>	119
5.5	Response of hybrid embryos to <i>in vitro</i> culture	110
5.6	Stages of Embryo development	111

List of Tables

Table	Contents	Page
1.1	sRNA reads aligning against C ₄ genes in Maize	13
3.1	Statistics of sRNA library composition	51
3.2	Numbers of sRNA reads aligning against candidate EST sequences	53
3.3	Distribution of mismatched sRNA hits against candidate EST sequences	55/56
3.4	Conserved sequences present in predicted miRNA sequences	58
3.5	p19 expression effects photosynthesis in <i>C. gynandra</i>	63

Abbreviations

Gene and transcript names are given in *italics* while protein names are given in Roman text. In the following list only the protein name is given in the gene and protein names correspond. This is supplementary to abbreviations stated in the text.

ABA	Abscisic Acid
AlaAT	Alanine Aminotransferase
AspAT	Asparate Aminotransferase
<i>At</i>	<i>Arabidopsis thaliana</i>
bp	Base Pair
BS	Bundle Sheath
CA	Carbonic Anhydrase
CaMV	Cauliflower Mosaic Virus
cDNA	Complementary DNA
<i>Cg</i>	<i>Cleome gynandra</i>
CO ₂	Carbonic Dioxide
Chp	chloroplastic
<i>Cs</i>	<i>Cleome hassleriana</i>
cyt	cytosolic
DNA	Deoxyribonucleic Acid
dNTP	Deoxyribonucleotide triphosphate
EDTA	Ethylene Diaminetetra-acetic Acid
gDNA	Genomic DNA
GUS	β-Glucuronidase
HCO ₃ ⁻	Bicarbonate
LB	Lysogeny Broth
LHC	Light Harvesting Complex
LHCA ₁	Light Harvesting Complex of PSI
M	Mesophyll
MDH	Malate Dehydrogenase
miRNA	micro RNA
mRNA	Messenger RNA
MS	Murashige-Skoog medium
mt	mitochondrial
NAD	Nicotinamide Adenine Dinucleotide
NAD-ME	NAD-Malic Enzyme
NADP	Nicotinamide Adenine Dinucleotide Phosphate
NADP-ME	NADP-Malic Enzyme
NHD ₁	Sodium : Hydrogen Antiporter
<i>nosT</i>	Nopaline Synthase Terminator
OAA	Oxaloacetate
PCR	Polymerase Chain Reaction
PEP	Phosphoenolpyruvate
PEPC	Phosphoenolpyruvate Carboxylase
PEPCK	Phosphoenolpyruvate Carboxykinase
PFD	Photon Flux Density
Pi	Inorganic Phosphate
PIP	Plasma membrane Intrinsic Protein

Chapter1: Introduction

PM	Plasma Membrane
PPCK	PEPC kinase
PPDK	Pyruvate,orthophosphate dikinase
PPi	Pyrophosphate
PPT	Plastidial PEP/Pi Translocator
PSBQ ₂	Subunit Q of PSII
PSI	Photosystem I
PSII	Photosystem II
PyT ₁	Chloroplastic Pyruvate Transporter
qRT-PCR	Quantitative Reverse Transcription Polymerase Chain Reaction
RACE	Rapid Amplification of cDNA Ends
<i>RbcS</i>	Gene encoding RuBisCO small subunit
RCA	RuBisCO Activase
RNA	Ribonucleic Acid
RT-PCR	Reverse Transcription Polymerase Chain Reaction
RuBisCO	Ribulose 1,5-Bis-Phosphate Carboxylase Oxygenase
sRNA	Small RNA
SOC	Super Optimal Broth, Catabolite Repression
TBE	Tris-Borate-EDTA buffer
Tris	Tris(hydroxymethyl)aminomethane
<i>uidA</i>	Gene encoding β -Glucuronidase
UTR	Untranslated Region
X-Gluc	5-Bromo-4-Chloro-3-Indolyl-Beta-D Glucuronic Acid, Cyclohexylammonium Salt

1. Introduction

1.1: A Requirement for Improved Crop Productivity

Over 200 years ago it was proposed that the demands of the human population would outstrip agricultural output (Malthus, 1798) although this stark prediction has not yet been fully realised. The human population has increased by around 125% since 1950, with conservative estimates of a further 65% increase over the next 50 years (Fischer & Heilig, 1997). The increase in population has so far been sustained through the “Green Revolution” that combined high-yielding varieties of wheat and rice with increased mechanisation and agrichemical use to increase crop yields (Evenson & Gollin, 2003). However, the rate of yield increase has slowed since the 1990’s to the extent that the increase in food production is now below that of the rate of predicted population increase (McCalla, 1994; Khush, 1999).

Besides a reduction in the rate of yield increase, a number of additional factors may negatively impact food production. For example, while climate change may lead to a slight increase in yields at high latitudes, significant reductions are likely to be seen nearer the equator affecting the developing world where increases in population are likely to be greatest (Parry *et al.*, 2004). A reduction in yield may be brought about by reduced growing seasons, decreased water availability or increased losses to pests and disease (Parry *et al.*, 1999; Wallace, 2004). As a result of these factors, sustained increases in crop yields are required. This is especially the case for crops grown in southern Africa and Asia as these regions are likely to be subject to the greatest climate-change related effects (Lobell *et al.*, 2008).

The yield potential of crops under ideal conditions is determined by the efficiency of light capture, the conversion of light into biomass and the proportion of biomass partitioned into the grain (Evans & Fischer, 1999). The latter two components are considered to have been developed to an optimum by breeding, and it has been suggested that increasing photosynthetic efficiency is likely to be the key area for improving crop yields (Long *et al.*, 2006). In addition, the predicted effects of climate change on water availability may mean that increases in crop water use efficiency will be required if production levels are to be sustained (Wallace, 2000).

1.2: The Effects of Photorespiration

One potential method to increase photosynthetic efficiency may be to reduce the effects of photorespiration. A key step in photosynthesis is the carboxylation of ribulose biphosphate through the activity of Ribulose Biphosphate Carboxylase/Oxygenase (RuBisCO). Due to the

active site conformation of RuBisCO, Ribulose BisPhosphate (RuBP) can be either carboxylated or oxygenated (Andrews & Lorimer, 1987). The phosphoglycolate that is produced by the oxygenation reaction is wasteful, and its generation and subsequent metabolism is collectively termed photorespiration. At low temperatures, the comparative rate of oxygenation and carboxylation of RuBP makes the generation of phosphoglycolate negligible, but once temperatures exceed 30°C photorespiration can reduce photosynthesis by 30-40% at ambient CO₂ concentrations (Ehleringer *et al.*, 1991).

One solution to this problem is to concentrate CO₂ around RuBisCO to the point that the oxygenation reaction is inhibited (Chollet & Ogren, 1975), a mechanism which is employed in the C₄ cycle (Hatch & Slack, 1966). The cycle operates to initially fix HCO₃⁻ using phosphoenolpyruvate carboxylase (PEPC) to form a 4C acid which is subsequently decarboxylated in a separate compartment close to RuBisCO for refixing and entry into the Calvin cycle. PEPC is specific to bicarbonate, for which it shows a high affinity (Maruyama *et al.*, 1966) so that the operation of this cycle can effectively suppress photorespiration. The ability to overcome the oxygenation problem of RuBisCO generates a competitive advantage in high light, high temperature environments with the effect that C₄ species can become dominant in warmer climates (Sage *et al.*, 1999). Such increased photosynthetic efficiency means C₄ photosynthesis increases the radiation use efficiency by c.50% compared to C₃ taxa in the same environment (Kiniry *et al.*, 1989). The C₄ pathway is utilized by maize, sugarcane and sorghum, representing some of our most productive crops (Brown, 1999).

Besides allowing increased rates of carbon fixation, the C₄ cycle allows increased nitrogen use efficiency (Gallaher & Brown, 1977). For example, maize shows higher nitrogen use efficiency compared with wheat and rice (both C₃) irrespective of temperature and therefore the extent of photorespiration (Schmitt & Edwards, 1980). The increased efficiency of CO₂ fixation seen in the C₄ system allows for decreased stomatal conductance in C₄ species relative to C₃ species. Therefore, the C₄ cycle can also increase water use efficiency. This is thought to impact on the dominance of C₄ photosynthesis in hot, dry environments (Knapp *et al.*, 1994; Sage *et al.*, 1999). Growth of C₄ species tends to be less competitive at cooler temperatures, either due to evolutionary weakness of plants which evolved under hotter conditions (Long, 2004) or the increased metabolic cost of the C₄ pathway: a need to regenerate the metabolic precursors increases the net ATP cost of operating the C₄ cycle above that of the C₃ system, lowering quantum yield (Ehleringer & Björkman, 1977). This means that the C₄ system ceases to have competitive advantage under low temperatures when C₃ plants show reduced

photorespiration, but C₄ species can still become dominant in low temperature ecosystems by virtue of the other physiological benefits of the C₄ cycle. For example, C₄ species have become dominant in north European saline habitats as a result of the increased water use efficiency associated with the C₄ cycle (Collins & Jones, 1986).

Therefore, operation of the C₄ cycle can confer significant benefits in overcoming environmental limitations in the form of elevated temperature, nutrient scarcity or limited water availability. Given the concerns regarding food production (see above), the C₄ cycle is considered a trait that could improve yields (Long *et al.*, 2006). The ability of the C₄ cycle to confer increased water use efficiency in particular has led to the suggestion that the C₄ cycle may be helpful in promoting yield increases in rice (Hibberd *et al.*, 2008). Rice represents the principal foodstuff in Asia, a region which is already subject to food scarcity, the problems caused by the high irrigation requirements of the crop are likely to be exacerbated by the effects of climate change (Shehy *et al.*, 2007). Therefore, the introduction of the C₄ cycle may help to maintain a yield increase in line with population requirements. The C₄ system represents a number of significant anatomical and biochemical modifications from the C₃ state. However, the genetic origin of the C₄ system is not yet fully understood, and it will be necessary to develop this understanding if the C₄ system is to be replicated in a previously C₃ species.

1.3: The C₄ Cycle

1.3.1: Operation of the C₄ Cycle

While C₄ cycles based on a single-cell system have been described (e.g. *Bienertia cycloptera*, Voznesenskaya *et al.*, 2005), in most cases the cycle is shared between two cell types. Initial carbon fixation occurs in the mesophyll (M) to form a C₄ acid, typically aspartate or malate. The C₄ acid then diffuses into specially modified bundle sheath (BS) cells where it is decarboxylated and the CO₂ produced is refixed by RuBisCO. The C₃ by-products of the decarboxylation reaction then diffuse back into the M to be used in the regeneration of the cycle precursors (Hatch, 1971). The BS cells surrounding the vasculature are enlarged and contain increased numbers of chloroplasts that can show altered ultrastructure. Such specialised so-called “Kranz” anatomy was first described by Haberlandt (1882) and the anatomical modifications are closely linked to the underpinning biochemistry of the cycle (Dengler & Nelson, 1999). BS cell walls are frequently thickened and contain a suberized lamella to limit CO₂ leakage, although the wall is permeated by an increased number of plasmodesmatal linkages to the M to promote diffusion of metabolites through the symplast.

Starch formation is predominately limited to the BS, where the chloroplasts may show reduced granal stacking and asymmetric arrangement (discussed below). The M resemble normal C₃ cells, although these may be radialised to increase contact with the BS. Finally, leaf venation is increased to reduce the diffusive pathway distance between the M and BS. Some variation is seen in the orchestration of the cycle, and three principal biochemical subtypes have been described which vary primarily in the method of decarboxylation in the BS (reviewed by Kanai & Edwards, 1999; Furbank, 2011).

The presence of Kranz anatomy allows for each cell types to be adapted to a separate role in the C₄ cycle, as outlined in Figure 1.2. CO₂ is initially fixed in the M through the carboxylation of phosphoenolpyruvate (PEP) using phosphoenolpyruvate carboxylase (PEPC). The oxaloacetate (OAA) that is formed is converted into either aspartate or malate. In the NADP-malic enzyme (NADP-ME) subtype, malate is produced and diffuses into the BS where it is decarboxylated by NADP-ME in the chloroplast. The pyruvate that is produced as a by-product is returned back to the M where it is used to regenerate PEP using pyruvate, orthophosphate dikinase (PPDK) in the chloroplast. In the NAD-ME subtype, the OAA is converted into aspartate *via* aspartate aminotransferase which diffuses into the BS, is transaminated back into OAA before reduction to malate *via* malate dehydrogenase which is then decarboxylated by NAD-ME, reactions which all occur in the mitochondria. Again, pyruvate is produced as a by-product, but this is transferred back into the M in the form of alanine *via* alanine aminotransferase. In the PEP carboxykinase (PEPCK) subtype, two alternate reactions can occur. Aspartate can be formed from OAA, and this aspartate diffuses into the BS where it is transaminated back into OAA before decarboxylation into PEP and CO₂ *via* PEPCK. Alternately, the OAA can be converted into malate *via* NADP-malate dehydrogenase in the M chloroplasts, and the malate is then transferred into the BS mitochondria before being metabolised into pyruvate using NAD-malic enzyme. The pyruvate is then returned to the M as alanine where it is used to regenerate PEP using PPDK. While diffusive transport is considered sufficient for the bulk of metabolite exchange between the two cell types in the C₄ cycle, active transport across organellar membranes is also necessary. For example, the sodium-dependant pyruvate transporter BASS2 and a PEP/phosphate translocator are required for pyruvate/PEP transport across the chloroplast envelope (Weber *et al.*, 2010; Furumoto *et al.*, 2011).

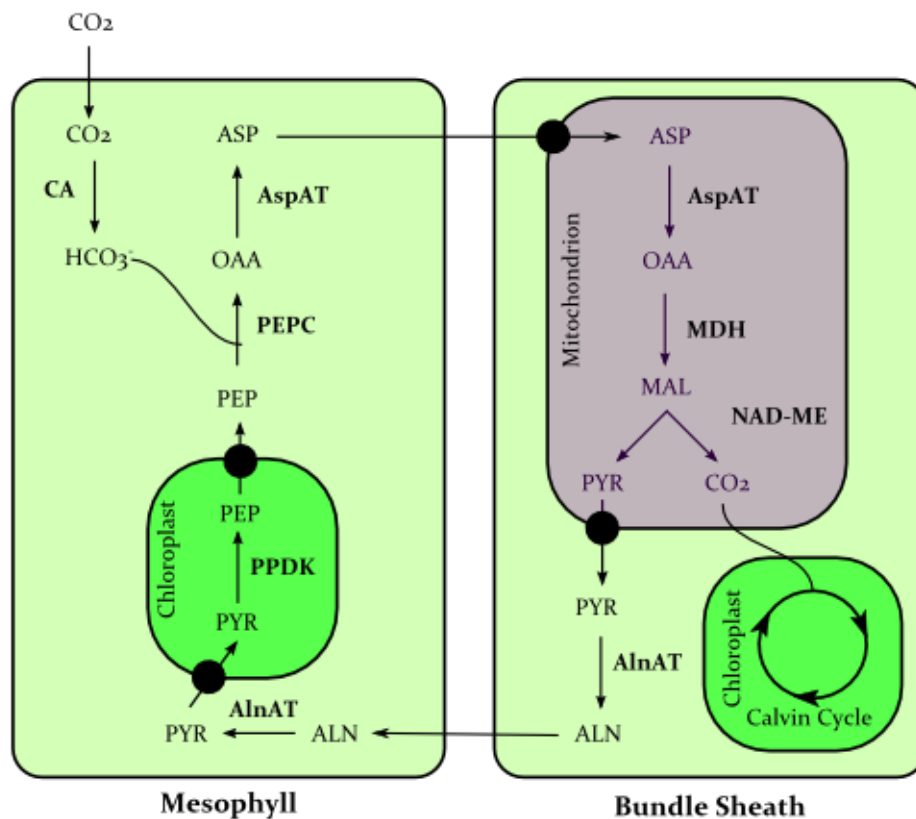


Figure 1.1: Outline of the NAD-ME subtype of the C₄ Cycle. The fixation of CO₂ in the mesophyll (M) initially forms oxaloacetate (OAA) which then diffuses into the bundle sheath (BS) in the form of aspartate (ASP) before reduction to malate (MAL) and decarboxylation with NAD-malic enzyme (NAD-ME), creating a CO₂-enriched environment which reduces photorespiratory reactions from occurring. The pyruvate (PYR) that is also produced diffuses back to the M in the form of alanine (ALN) where it is used to regenerate the phosphoenolpyruvate (PEP) consumed in the initial carboxylation step. Sites of active transport are marked with a black dot, as discussed in the text.

CA: carbonic anhydrase, PEPC: PEP carboxylase, AspAT: aspartate aminotransferase, MDH: malate dehydrogenase, AInAT: alanine aminotransferase, PPDK: pyruvate, orthophosphate dikinase

1.3.2: Evolution of the C₄ Cycle

Despite the significant changes that are likely to have occurred during the evolution of the C₄ cycle, it is found in 66 independent angiosperm lineages (Sage, 2012). While the first fossil evidence of the C₄ cycle has been dated to the Miocene at 12.5 Mya (Nambudiri *et al.*, 1978), molecular clock analysis has placed the first occurrences of the C₄ cycle to 32 Mya, a point which coincides with the rapid decline in atmospheric CO₂ that occurred during the Oligocene around 35 Mya (Kellogg, 1999; Christin *et al.*, 2008). This would indicate that evolution of C₄ photosynthesis was in response to increased oxygen concentrations rather than temperature increases, although the delayed response of c.3 million years was necessary for evolutionary preconditioning events to occur, such as gene duplication events prior to recruitment into novel photosynthetic roles or the anatomical modifications required for efficient operation of the cycle (Monson & Rawsthorne, 2004).

Once sufficient environmental conditions existed to promote evolution of the C₄ cycle (i.e. depressed atmospheric CO₂ concentrations and/or elevated temperatures), then a number of step-wise evolutionary stages are considered likely to have occurred (Sage, 2004). A measure of general preconditioning would have been necessary. It has been proposed that the enlargement of gene families *via* duplication events allowed for divergent evolution needed for the C₄ cycle (Monson, 1999). However, recent evidence suggests that evolution of *trans*-acting factors (as discussed below) may be important in the evolution of the C₄ cycle, bypassing the requirement for gene duplication events, which may explain why gene families in C₄ lineages are not significantly enlarged (Williams *et al.*, In Press). This would have been followed by anatomical alterations such as reduced intervein distance or enlargement of the BS although such modifications may have served other ecological benefits such as enhanced leaf water status (Dengler *et al.*, 1993; Sage, 2004). Increased capacity of BS organelles would then enable them to assume a greater photosynthetic role, along with increased plasmodesmatal links with the M to facilitate increased transport of metabolites. The development of a glycine shuttle is then proposed (Monson, 1999) so that photorespiratory products would accumulate in the bundle sheath for metabolic breakdown. Once metabolite transport is established, increased activity of PEPC and PPDK in the mesophyll and a decarboxylase in the bundle sheath, twined with a reduction of RuBisCO activity in the mesophyll would facilitate a transition from a C₃-like to a C₄-like system. Finally, optimisation of individual C₄ components and whole-plant optimisation would allow for the obtainment of full C₄ status.

Genes required for the C₄ cycle existed previously, but typically these were involved with alternative non-photosynthetic processes such as the proposed role of PPDK (utilised in the regeneration of PEP used in the initial fixation step) in nitrogen remobilisation from leaves during senescence (Taylor *et al.*, 2010; Aoyagi *et al.*, 1984; Liu *et al.*, 2008). Expression of these genes would have to be modified to alter abundance, acquire cell-type specific expression, and in some instances altered reaction kinetics (Monson *et al.*, 2004; Sheen, 1999), a process that would have to be concurrent with anatomical modification. However, while no novel elements are required for the utilisation of the C₄ cycle, considerable changes in gene expression are required leading to cell-type specific accumulation of enzymes, changes in enzyme kinetics and regulation and the development of the M/BS anatomy (Sage, 1999).

Despite the complexity of the evolutionary requirements of the C₄ cycle, it is predicted to have evolved at least 66 separate times (Sage *et al.*, 2011, Figure 1.2) which would indicate that the changes in gene expression and anatomy required for the effective operation of the C₄ cycle do not require any substantial evolutionary steps. The evolutionary steps towards the C₄ cycle must either infer neutral or positive competitive advantage to prevent negative selection pressures from eliminating them, a hypothesis that is supported by the abundance of C₃/C₄ intermediates throughout various C₄ lineages, as discussed below. These may represent discrete evolutionary stages or prematurely terminated evolutionary pathways, but their persistence would indicate evolutionary fitness (Monson & Moore, 1989; Sage *et al.*, 2011).

The multiple points of evolution have given rise to considerable variation in the operation of the cycle. Anatomically, the origin and number of BS layers, extent of suberin deposition, and the position and extent of granal development of BS chloroplasts varies greatly between lineages (reviewed by Dengler & Nelson, 1999). While this may be due to evolutionary divergence, such variation may be attributable to ecological factors. For example, *Cleome angustifolia* (Cleomaceae) shows modified Kranz anatomy to incorporate water storage tissues while other C₄ members of the genus show the more standard atriplicoid Kranz anatomy (Koteyeva *et al.*, 2011).

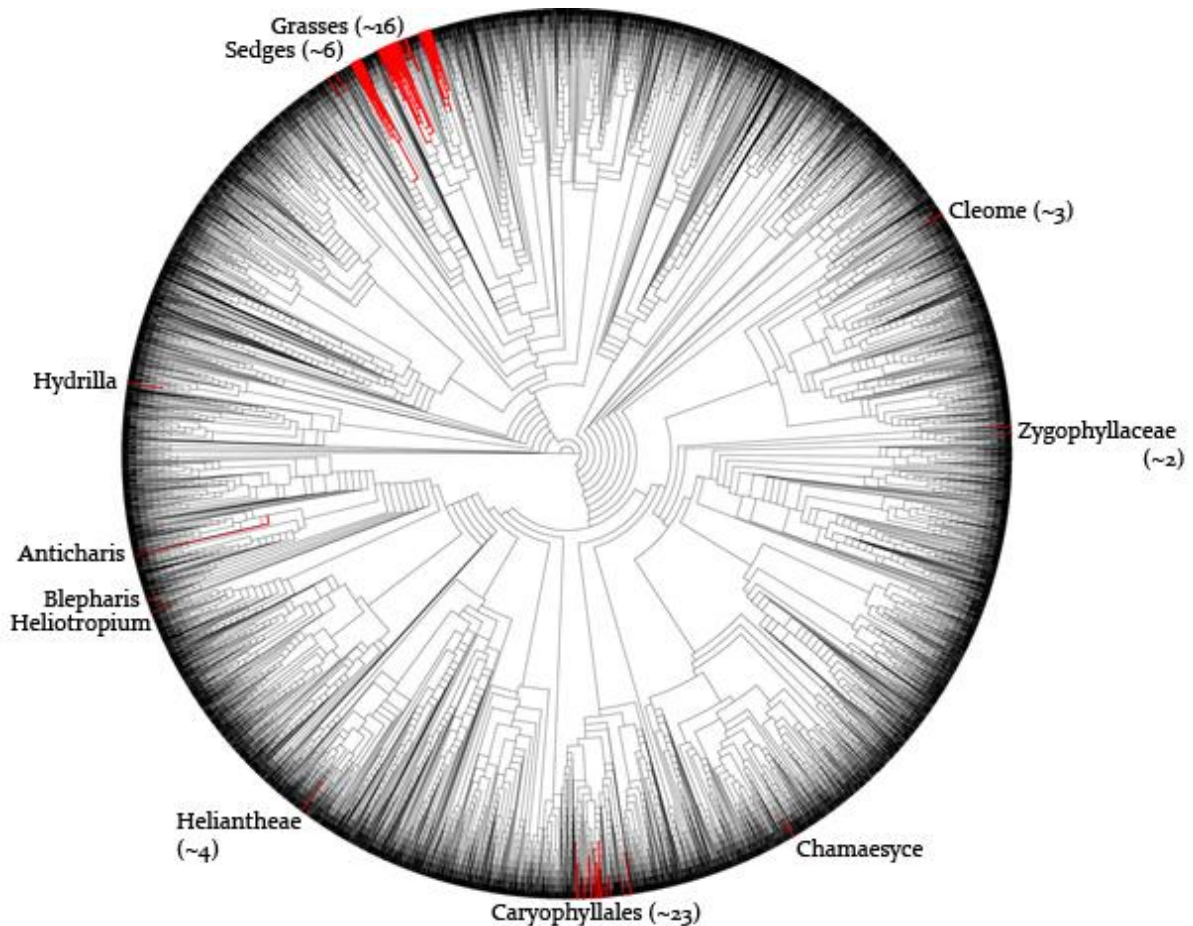


Figure 1.2: The distribution of C₄ lineages within the angiosperms. 47 of the predicted 62 independent origins of the C₄ cycle are overlaid in red upon the phylogeny of 9400 angiosperms of Smith *et al.* (1999). The values quoted with each clade indicate the number of independent origins of the C₄ system within each clade. Figure adapted from Sage *et al.*, 2011.

Biochemical variation is seen in the operation of the cycle, with separate lineages being classified on the basis of the principal enzyme utilised at the decarboxylase step which may either be NAD-Malic Enzyme (NAD-ME), NADP-Malic Enzyme (NADP-ME) or PEP carboxykinase (PEPCK), the biochemistry of which is discussed below. The presence of a particular decarboxylation subtype demonstrates some patterning with evolutionary lineage, although there is also some correlation between C₄ subtype and precipitation levels in which each subtype is predominant indicating that decarboxylase variation may serve additional ecological roles (Cabido *et al.*, 2008). Furthermore, the decarboxylation subtype may correlate with anatomical features, such as the reduction in granal stacking and PSII components seen in the BS chloroplasts of NADP-ME species to reduce oxygen evolution (Meierhoff & Westhoff, 1993) or the centripetal accumulation of chloroplasts in the BS of NAD-ME species in an attempt to limit CO₂ leakage in the absence of a suberized lamella (Sage, 2004).

The stepwise nature of the evolution of the C₄ cycle, and the ability of each stage to be competitive in its own right, is supported by a number of stable C₃/C₄ intermediates (e.g. Edwards *et al.*, 1982). The ability of the C₄ cycle to suppress photorespiration leads to a significant depression in the CO₂ compensation point (Γ) from 4-5.5 kPa CO₂ in C₃ species to 0-0.5 kPa CO₂, with C₃/C₄ species showing values intermediate to these values, although this can be in a light-dependant manner (Hunt *et al.*, 1987). Such intermediates can contain Kranz-like anatomy with the formation of distinct BS cells with increased organelle abundance, although this does not correlate with an increased activity of C₄ enzymes, indicating that the biochemical partitioning has not occurred (Edwards & Ku, 1987). A number of “C₄-like” members of *Flaveria* show a more intermediate metabolism with increased carbon fixation into C₄ acids and more extensive Kranz formation (Moore, 1989).

The presence of C₃, C₄, and intermediate species within the same genus has led to a number of hybridisation attempts between photosynthetic types within *Panicum*, *Flaveria* and *Atriplex* (as reviewed by Brown & Bouton, 1993). *Panicum* C₃/C₄ x C₃ hybrids showed intermediate characteristics in the F₁ generation, and while segregation in the F₂ hybrids was sufficient to recover the parental C₃/C₄ anatomy, Γ did not approach that of the C₃/C₄ parent, indicating that strict compartmentalisation is required for true repression of photorespiration (Bouton *et al.*, 1986). Hybrids between C₃ and C₄ members of *Atriplex* showed similar intermediary traits in anatomy, physiology and expression patterns of C₄ enzymes. For example, C₃ dominance was shown on the expression of PEPC in *Atriplex* C₃ x C₄ hybrids (Percy & Björkman, 1970), PPK levels resembled *F. floridana* (C₃/C₄) when crossed with *F. brownii* (C₄-like) (Cheng *et al.*, 1987) and NADP-ME expression was significantly depressed in hybrids between *F. trinervia* and a number of C₃/C₄ intermediates (summarised by Brown & Bouton, 1993). RuBisCO activity varied, with activity in separate hybrids resembling both the C₃ (Percy & Björkman, 1970) and C₄ (Björkman *et al.*, 1969) parent, although expression of RuBisCO is complicated by the biparental inheritance of the SSU/LSU.

A general trend in these data is that C₃ is predominant, although this could be attributable to several causes. Repression of genes may be seen in the C₃ parent which has been lost during the evolution of the C₄ lineage, or the *trans*-acting factors (see below) required for altered levels of expression are absent from the C₃ parent and are inherited independently. The variation in both biochemical and anatomical traits seen in hybrids between C₃ and C₄ species indicates that traits of the C₄ cycle are independently inherited due to their apparent lack of segregation.

1.3.3: Regulation of the C₄ Cycle

While recruitment of genes into the C₄ cycle was heavily dependent on altering regulatory methods to bring about modified expression patterns, our understanding of the regulatory mechanisms functioning in the current C₄ cycle is far from complete. The regulation that underpins the cell-type specific protein accumulation necessary for the C₄ cycle is likely to operate at multiple levels, varying between gene, developmental stage and lineage.

At the transcriptional level, exclusion of PEPC transcripts from *Flaveria bidentis* BS cells is dependent on promoter activity (Stockhaus *et al.*, 1997) which is attributable to the presence of the mesophyll enhancing module 1 (MEM₁), a 41bp sequence that is sufficient to inhibit expression in the BS. The MEM₁ of the C₃ *F. pringlei* did not direct M-specific expression in *F. bidentis* when fused to the native C₄ *Ppc* promoter, but inhibition in the BS was recovered by insertion of the *F. bidentis* MEM₁ sequence (Gowik *et al.*, 2004; Akyildiz *et al.*, 2007). Separate regions within the promoter may be responsible for elevated transcription and cell-type specificity. The -211 to +434 region of the *RbcSm3* promoter in maize is required for light-induced expression, while a region between -907 and -445 in combination with a sequence within the 3' region of the gene is required for suppression of *RbcS* transcription in the M (Viret *et al.*, 1994). Transcriptional control may not relate to the promoter sequence itself: 240bp sequences within the *Cleome gynandra* *NAD-ME1* and 2 transcripts are sufficient to grant BS-specific accumulation (Brown *et al.*, 2011). This element retains this function when placed in the antisense direction which would infer their mode of action is unlikely to be based on interaction with the mRNA molecules (Williams *et al.*, unpublished).

In maize, illumination may promote the activity of Dof1/2 transcription factors which have been implicated in coordinating the patterning of *Ppc* transcripts in maize (Yanagisawa, 2000; Kalamajka *et al.*, 2003). In addition, Langdale *et al.* (1991) proposed a demethylation event 3.3kb upstream of the *Ppc* promoter is linked to M-specific expression in response to light. However, Tolley *et al.* (2011) did not identify any methylated sites within the 0.6kb region that is required for M-specific expression (Kaush *et al.*, 2001), which would infer the absence of PEPC in maize BS cells is not attributable to modifications to DNA methylation.

While promoter components such as these have been identified as inferring C₄-like expression patterns, the *trans*-acting factors and the sequence specific targets with which they interact remain largely undefined. The *Golden2* and *Golden-like1* transcription factors have been suggested as potential *trans* factors in maize due to their ability to target high numbers of photosynthesis-related genes in Arabidopsis (Hall *et al.*, 1998; Waters *et al.*, 2009), although

whether they are capable of directing the C₄ expression patterns of the previously non-photosynthetic genes has yet to be explicitly determined.

Transcriptional control is likely to be combined with additional levels of control. For example, while higher rates of chloroplastic *rbcL* and *psbB* transcription are seen in maize BS cells, the rate difference does not correlate with observed differences in transcript abundance between the M and BS (Kubicki *et al.*, 1994). Post-transcriptional processes may involve increased transcript stability, transport, elevated decay rates or alternative processing methods. Transcript-specific *cis*-acting elements have been described in a number of instances, and the placement of the *cis*-acting element within the coding regions could infer post-transcriptional methods are in action. For example, *PPDK* and *CA₄* transcripts have also been shown to contain sequences in the UTR regions that confer M-specific accumulation (Kajala *et al.*, 2011). UTR regions in *RbcS* transcripts of *A. hypochondriacus* generate translational enhancement in BS cells while triggering transcript degradation in the M (Patel *et al.*, 2004). *Cis*-acting elements in *F. bidentis* *RbcS* UTRs may also direct BS-specific accumulation either by enhanced BS stability or decay rates of transcripts in the M (Patel *et al.*, 2006).

Beyond the transcriptional level, control may be exerted at the translational level. In the non-photosynthetic foliar regions of *Amaranthus tricolor*, a loss of transcript specificity does not correspond to a loss of BS-specificity of both subunits of RuBisCO (McCormac *et al.*, 1997), while in dark-grown *A. hypochondriacus* both subunits remain BS specific despite a collapse of transcript specificity (Berry *et al.*, 1985) so that while transcriptional-level regulation has ceased, a formerly redundant method of control is being exerted at the translational level. When grown in light, chloroplastic *rbcL* is still transcribed but fails to show protein accumulation in the M of *A. hypochondriacus* (Boinski *et al.*, 1993).

Trans-acting factors may be involved in translational processes, such as the BSD₂ zinc-binding protein which is believed to prevent aggregation and misfolding of large subunit polypeptides prior to incorporation into the RuBisCO holoenzyme (Brutnell *et al.*, 1999). Transcript regulation may be combined with translational control. Variation is seen in *rbcL* transcript length in *A. hypochondriacus* which impacts the binding of a 47kDa protein required for ribosome attachment (McCormac *et al.*, 2001) while 5'UTR regions of *RbcS* function as a translational enhancer in the same species (Patel *et al.*, 2004).

Post-translational regulation may also be possible, such as the inactivation of PPDK by phosphorylation by a regulatory protein correlating with developmental age or illumination

(Chastain *et al.*, 2006; 2008). In addition to the transcriptional control of maize PEPC discussed above, the mature protein is subject to reversible phosphorylation by PEPC kinase, the abundance of which is regulated at the transcriptional level in response to light (Jiao & Chollet, 1988; Hartwell *et al.*, 1999) and PPDK demonstrates reversible phosphorylation in light (Astley *et al.*, 2011)

1.3.4: Development of the C₄ Cycle

During leaf development, the onset of cellular patterning associated with the C₄ cycle shows considerable variation between lineages in terms of timing and response to developmental or environmental signals. RuBisCO, PPDK, PEPC, and NAD- malic enzyme accumulation in maize is tightly linked to light exposure combined with acropetal vein development as demonstrated by a lack of accumulation mutants that lack chlorophyll (Langdale *et al.*, 1987; Nelson *et al.*, 1984). Similarly, CA shows an increase in development but requires light exposure for high levels of expression (Burnell *et al.*, 1990).

While light is necessary for C₄ development in maize, the patterning of RuBisCO, PEPC and PPDK occurs as a response to developmental signals in etiolated Amaranth cotyledons (Wang *et al.*, 1993a), indicating that light is not required for this process. In *A. hypochondraicus*, PEPC and PPDK are localised to the M from an early stage in development, while both subunits of RuBisCO only become localised to the BS once a developmental barrier has been crossed and transcriptional suppression has become active (Wang *et al.*, 1992). In contrast, partitioning of the large subunit of RuBisCO occurs before the maturation of the BS in *Atriplex rosea* (Hudson *et al.*, 1992).

Therefore, if light is not required for activation of the C₄ cycle, then alternative signals must be responded to. The acquisition of BS-specific RuBisCO accumulation *Amaranthus* is tightly correlated to the transition from photosynthate sink to source (Wang *et al.*, 1993b), although whether this correlation is due to active photosynthetic metabolism or coincident developmental events remains to be explored. PEPC expression in maize has been shown to be depressed by glucose and acetate application (Kausch *et al.*, 2001), and various metabolites have been shown to negatively regulate photosynthesis genes (Sheen, 1990) so the former hypothesis is not without merit. Finally, there is some suggestion that the acquisition of C₄ traits is spatially regulated in maize by a transmissible signal from the vasculature (Langdale *et al.*, 1988; Langdale & Nelson, 1991), although this hypothesis remains to be validated.

Besides the biochemical adaptation, the formation of Kranz anatomy is considered a general prerequisite for the evolution of an effective C₄ cycle (Sage, 2004), with the exception of the unicellular systems discussed above. In maize, the close vascularisation is present from leaf initiation with M/BS initialisation closely following the same pattern of vein maturation in both an acropetal and basipetal direction, depending on vein position (Langdale & Nelson, 1991; Langdale *et al.*, 1987). Dicot C₄ species (e.g. *Amaranthus*) do not show such a developmental gradient, but instead the development of Kranz anatomy occurs after the formation of the secondary veins in a basipetal direction, an event which tends to coincide with the onset of C₄ biochemical patterning and the transition from source to sink tissues (Ramsperger *et al.*, 1996; Wang *et al.*, 1993b). The genetic origin of Kranz anatomy has yet to be determined. Hybridisation experiments in *Atriplex* shows intermediate and non-segregating forms of Kranz anatomy are expressed in F₁ and F₂ hybrids between C₃ and C₄ taxa, which may infer this is a polygenic trait as the failure of the Kranz-like anatomy to show segregation between the F₁ and F₂ generations would infer independent polygenic control (Björkman *et al.*, 1970; 1971).

As such, the regulation methods employed in establishing the expression patterns associated with the C₄ cycle are varied at multiple levels, and while there is some understanding of the *cis*-elements required the *trans* factors that interact with them are poorly understood. The abundance of post-transcriptional regulatory methods may provide some insight into the evolution of the C₄ cycle, however. Modified gene expression may be brought about by altering either the *cis*-regulating sequence or the activity of the *trans*-acting component with which it interacts (Love *et al.*, 2007). The latter path would enable recruitment of genes into the C₄ cycle without modification of the coding sequence itself, a situation which has been demonstrated in the C₄ cycle previously. For example, the UTR sequences of *NAD-ME*, *PPDK* and *CA* transcripts required to grant M-specific expression are found in C₃ orthologs (Brown *et al.*, 2011; Kajala *et al.*, 2011) which would suggest that the *cis* elements required for M specific expression are ancestral and that the *trans* factor itself has undergone recruitment into the cycle. As noted previously, understanding of the *trans*-acting factors in the C₄ cycle is poor, limiting the extent to which their evolution and regulation can be studied. Therefore, it is considered that the identification of *trans*-acting factors, especially of a suppressive or silencing role, would be of considerable benefit in extending our understanding of the C₄ cycle.

1.4: miRNA Regulation of the C₄ Cycle

A class of *trans*-acting factors which have been increasingly shown to have regulatory roles in plant systems are a number of small non-coding RNAs (sRNA, Hamilton & Baulcombe 1999). These are short sequences of RNA around 24nt in length which interact with a target gene through possession of a complementary sequence to either the genomic or transcript sequence, bringing about negative repression through a number of routes (see below). As a measure of complementarity between an sRNA and its target it required, prediction of sRNA-target genes can be carried out by comparison of sRNA sequences aligning against a gene of interest (Ambros, 2004). When sRNA libraries were aligned against photosynthesis genes in Arabidopsis, Rice and Maize, a disproportionate accumulation of sRNA sequences against these genes was demonstrated in maize (Table 1.1). A large number of sRNA sequences aligning against a gene may indicate that an underlying sRNA is present which is capable of negative regulation. The absence of high sequence aggregations in both C₃ species may suggest that sRNAs have evolved to negatively regulate components of the C₄ cycle in maize, promoting cell-type specific accumulation of protein.

Table 1.1: *In silico* predictions of sRNA sequences aligning against key photosynthesis genes in both C₃ and C₄ backgrounds. (Tolley *et al.*, unpublished data taken from a study restricted to known photosynthesis genes)

Protein Encoded	Arabidopsis (C ₃)	Rice (C ₃)	Maize (C ₄)
CA	0	0	2
PEPC	0	0	11
PPCK	0	0	10
MDH	-	0	1
OMT ₁	-	0	2
NADP-ME	0	2	4
RbcS ₁	0	1	6
RbcS ₂	1	1	3
PRK	0	0	7
PPDK	0	1	2

This hypothesis is attractive on a number of levels. MicroRNAs (miRNAs), a subset of sRNAs, have been heavily implicated in a number of developmental and regulatory roles (discussed below). Given this background, miRNAs may play a role in the development of Kranz anatomy during leaf maturation. If a regulatory miRNA were to accumulate in a cell-type specific manner after leaf maturation exclusion of a gene could be achieved *via* post-transcriptional regulation. The non-mobile nature of miRNAs (Parizotto *et al.*, 2004) would mean that

separate miRNA populations in the M and BS could be in place, facilitating cell-type specific suppression of gene expression. Despite high levels of miRNA sequence conservation between diverse lineages, a rapid rate of proto-miRNA sequence generation and evolution has been implicated *via* inverted duplication events occurring during gene family expansion (Allan *et al.*, 2004; Fahlgren *et al.*, 2007). If such rapid evolution did occur then it may provide a mechanism by which rapid C4 evolution could occur along divergent lineages.

1.5: miRNA Regulation

Various classes of small non-coding RNAs between 20–28nt have been shown to direct target-specific gene regulation (Hamilton & Baulcombe, 1999; Ambros, 2004; Bartel *et al.*, 2004). Classification within general sRNA regulation is derived from the origin of the regulatory fragment, which may involve different precursors and processing methods (reviewed by Brodersen & Voinnet, 2006). In short, a double-stranded RNA (dsRNA) molecule is cleaved to produce single-stranded RNA (ssRNA) fragments of 20–28nt which can then be incorporated into an RNA-Induced Silencing Complex (RISC), capable of directing a regulatory effect. Three principal sRNA forms are active in plants: short interfering RNA (siRNA) which target exogenous transcripts, and *trans*-acting short interfering RNA (tasi-RNA) and micro RNA (miRNA), both of which target endogenous transcripts. These differ both on methods of biosynthesis and the origin of the dsRNA utilised to produce the sRNA. The dsRNA precursor may be produced from a single-stranded target *via* an RNA-dependant RNA polymerase (RDRP), as occurs in the suppression of ssRNA viral transcripts or the post-transcriptional silencing of exogenous transgenes, or it may be formed by a transcript which contains an inverted repeat sequence which allows the transcript to fold to produce a secondary structure which contains a double stranded region (a hairpin bend). siRNAs may be generated from natural dsRNA (e.g. viral genomes) , or through the action of an RDRP prior to cleavage. The production of tasiRNA occurs from endogenous genes, the transcripts of which are targeted by a miRNA. One of the cleavage products is used to produce dsRNA using RDRP which is subsequently processed into a functional miRNA.

miRNAs represent the greatest proportion of endogenous regulatory sRNAs in plants (Schwab *et al.*, 2009), and have received the greatest extent of scientific exploration to date. The predominant method of regulation is through targeted transcript cleavage although translational repression and miRNA-directed DNA methylation also have been described (Brodersen *et al.*, 2008; Chellappan *et al.*, 2010). Such miRNAs demonstrate a regulatory effect on numerous developmental processes including leaf formation (Chuck *et al.*, 2007) and organ

polarity (Kidner & Martienssen, 2004). The roles of miRNA in leaf development are well documented. The miRNA-mediated regulation of *PHABULOSA*/*PHAVOLUTA* during leaf formation has provided significant insights into the mechanisms of miRNA regulatory pathways (Mallory *et al.*, 2004; McHale *et al.*, 2004), while tasiRNA have been shown to be capable of creating tissue patterns during development based on differential spatial distribution (Chitwood *et al.*, 2009). The role of miRNAs in regulating organ formation is continued with determined roles for miRNAs in petal and root formation (e.g. Chen, 2004; Llave *et al.*, 2002). Besides developmental roles, miRNAs have been implicated in a range of abiotic stress responses including phosphate starvation (Fujii *et al.*, 2005), salt stress (Ding *et al.*, 2009), arsenic toxicity (Srivastava *et al.*, 2005) and mechanical stress (Lu *et al.*, 2005). In these instances upregulation of miRNAs has been detected as part of a given stress response. For example, *Arabidopsis* plants that were subject to copper starvation showed an upregulation of miR398 which targets copper/zinc superoxide dismutases, subsequently downregulating these genes in response to copper depletion (Beauclair *et al.*, 2010).

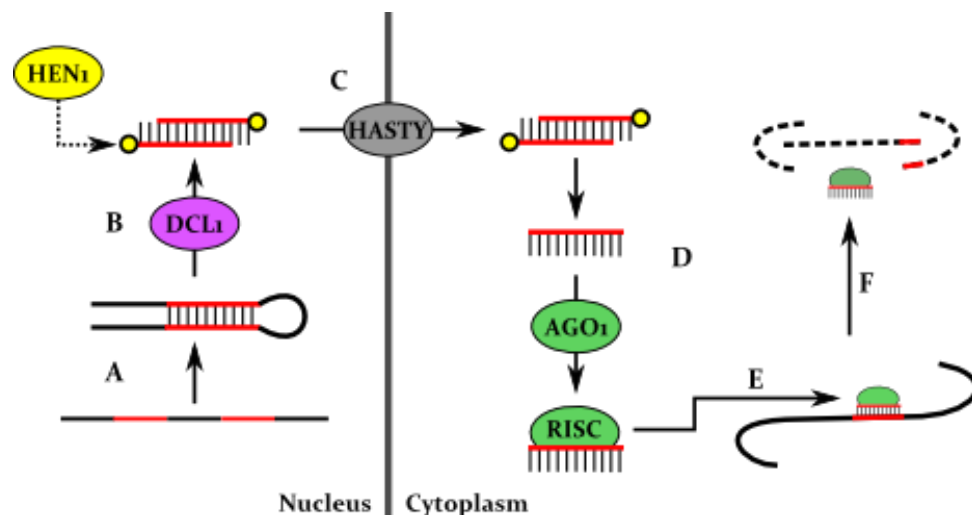


Figure 1.3: miRNA formation and activity. Pri-miRNA transcripts contain an inverted complementary sequence capable of forming a hairpin fold-back structure containing a stretch of dsRNA (A). This acts as a substrate for Dicer-like 1 (DCL1), which cleaves the hairpin into a short dsRNA fragment which is stabilised by methylation by Hua-Enhancer 1 (HEN1) (B). The dsRNA fragment is then exported out of the nucleus *via* HASTY (C) where it is processed into the single-stranded miRNA and incorporated into the RNA-induced silencing complex (RISC), the chief component of which is the Argonaute 1 (AGO1) endonuclease. The complementarity of the miRNA is utilised to guide the RISC to the target transcript (E) which is then cleaved before subsequent degradation (F). (After Brodersen & Voinnet, 2006)

miRNAs are derived from longer length transcripts (including those taken from intergene, UTR and intronic regions) (Figure 1.3) which are processed into short double-stranded RNA (dsRNA) duplexes by the DICER-LIKE1 protein (DCL1) (Kurihara & Watanabe, 2004) prior to stabilisation by methylation *via* HUA-ENHANCER1 (HEN1; Yang *et al.*, 2006). The resultant

duplex is then exported to the cytosol *via* HASTY (HST, Bollman *et al.*, 2003) whereupon the duplex is separated and the functional miRNA is incorporated into an RNA-induced silencing complex (RISC), of which the RNA slicer ARGONAUTE₁ (AGO₁) is an integral component.

Transcript targeting is achieved *via* near-perfect complementarity between miRNA and its target mRNA (Rhoades *et al.*, 2002) which will promote cleavage and subsequent degradation of the target transcript (Llave *et al.*, 2002a). Translational repression tends to be linked to less-perfect base pairing, although there are some exceptions such as the translational repression of APETALA₂ (Chen, 2004). A significant proportion of plant miRNA targets have been classified as transcription factors (Rhoades *et al.*, 2002) and regulation on a spatial or temporal scale has been demonstrated through regulation of the promoter sequences of the pre-miRNA or parent transcript (Obernosterer *et al.*, 2006; Chitwood *et al.*, 2007) or through the expression of RNA-binding proteins which specifically target certain pre-miRNAs (Viswanathan *et al.*, 2008). In addition to posttranscriptional processes, miRNA has been illustrated as having an impact on the epigenetic level, such as the chromatin methylation of *PHABULOSA* by miR165/6 (Bao *et al.*, 2004). While some sRNA forms have been shown to be mobile (moving between cells) these tend to be associated with the suppression of exogenous viral or transgene transcripts by siRNAs (Voinnet, 2009; Molnar *et al.*, 2010). miRNAs linked with developmental roles show zones of activity which appear to coincide entirely with the zones of transcription of miRNA-encoding genes, so a lack of mobility is demonstrated (Parizotto *et al.*, 2004). This would be a requirement for regulation of the C₄ cycle: if miRNAs were mobile their application to cell-type specificity would be limited.

1.6: Experimental Approach

1.6.1: miRNA Prediction

miRNA sequences may be identified by computational analysis of the target genome to predict pre-miRNA sequences based on ability to form dsRNA duplexes (e.g. Jones-Rhoades & Bartel, 2004), although this requires a well-annotated genome if it is to be effective. Alternatively, by sequencing the sRNA population of the target organism it is possible to identify miRNAs by comparing sRNA reads against the sequences of target genes. Such combined computational/cloning based strategies have been applied in the identification of miRNA sequences in a range of circumstances such as the identification of mechanical stress-responsive miRNAs in *Populus* (Lu *et al.*, 2005) and varied stresses in *Arabidopsis* (Sunkar & Zhu, 2004). While direct the computational analysis of miRNA precursors can yield predictions, the latter authors note the detection of miRNAs by cloning methods that would

not have been predicted *in silico*. Therefore, the construction of a library of miRNA sequences via the cloning methods of Havecker (2011) was considered to be the primary step in profiling regulatory miRNAs active in a C₄ leaf.

This strategy has two key limitations however. Firstly, a well-annotated genome is required for full miRNA prediction. A key part of validating a potential miRNA is the presence of a precursor transcript within the target genome, the flanking regions of which must be capable of generating a minimal free-energy folding hairpin structure capable of generating a pre-miRNA duplex (Ambros *et al.*, 2004). Secondly, the lack of a gene-specific understanding of the origin of many C₄-traits would hamper the identification of regulatory miRNA on the basis of sequence complementarity. As a result of this, a second strategy was implemented utilising viral miRNA inhibitors.

1.6.2: Viral Inhibition of sRNA Activity

The biosynthesis of short-interfering RNAs (siRNA) by a pathway closely related to that of miRNA production is considered to be an immune response in plants to virus infection (Voinnet 2001; Vance & Vaucheret, 2001). In response to this, a number of viral proteins have been demonstrated to suppress the activity of si/miRNAs as a pathogenicity factor. p21 of the *Beet Yellow Virus* (Reed *et al.*, 2003), AC₄ of the *African Cassava Mosaic Virus* (Chellappan *et al.*, 2005) and p19 of the *Tomato Bushy Stunt Virus* (Voinnet *et al.*, 2003, Lakatos *et al.*, 2004) have been shown to inhibit miRNA function by acting as competitors with DCL/HEN₁ for miRNA*/miRNA dsRNA duplexes before they can be processed into a functional RISC complex. A fourth inhibitor, P₁/HC-Pro of the *Turnip Mosaic Virus* has been well studied (Kasschau *et al.*, 2003) although its exact method of function is still unclear (Lakatos *et al.*, 2006).

Due to the similarity between biosynthesis pathways of siRNAs and miRNAs, expression of such viral inhibitors can interfere with the function of endogenous miRNAs (Chapman *et al.*, 2004), promoting a phenotype that matches that of *dcl-1* mutants in *Arabidopsis* (Kasschau *et al.*, 2003; Dunoyer *et al.*, 2004). Due to the competitive nature of the inhibitory mechanism a dose-dependent response was generally seen, although p19 was shown to be the most potent inhibitor (Lakatos *et al.*, 2006, Dunoyer *et al.*, 2004). Cytosolic p19 selectively binds to 21nt dsRNA (Vargason *et al.*, 2003) prior to RISC formation, but has no effect on existing functional RISC complexes (Lakatos *et al.*, 2006). In addition, Uhrig *et al.* (2004) reported a relocalisation effect of p19 upon nuclear ALY proteins, although the effects of this interaction are unclear.

Given the efficiency with which p19 has been shown to inhibit sRNA biosynthetic pathways, its reduced size (19 kDa) and well-documented phenotype in Arabidopsis, it was chosen as an inhibitory protein for introduction into *C. gynandra*. The benefits of establishing a stable transgenic line would be three-fold. Firstly, leaf development could be examined to identify any effects of miRNA inhibition on the formation of Kranz anatomy. Secondly, gross phenotypic quantification may highlight any effects at the physiological level attributable to interference by p19 expression. Finally, components of the C₄ cycle can be quantified at the transcript and protein level to screen for any p19-induced changes in abundance that could be associated with a relief from miRNA inhibition.

1.6.3: Inducible Expression Systems

Due to the effects of p19 expression on development as discussed above, it was considered likely that high levels of constitutive expression may impact leaf development and reduce pollen fertility. Inducible promoters have been used previously to allow for temporal control of genes (e.g. *CLAVATA1/2*, Schoof *et al.*, 2000) and so the placement of p19 under the control of a chemically inducible promoter was investigated. The dexamethasone-inducible pOp/LhGR system has been shown to generate specific induction of transgenes in tobacco (Samalova *et al.*, 2005) and Arabidopsis (Craft *et al.*, 2005) and so this system was selected for inducible expression of p19.

The ability to induce expression of p19 would allow transgenic lines to be cultivated until maturity and then p19 to be induced over a short timescale. This would limit the impact of inhibition of the small RNA pathway to an established C₄ system, allowing for effects of such inhibition to be assessed. Long-term exposure to dexamethasone during earlier plant development would also enable the effect of removing small RNA regulation on leaf anatomy to be examined.

1.6.4: A Combined Experimental Approach

Following the considerations discussed previously, a twin-tailed approach was taken to examine the potential for sRNAs to regulate the C₄ cycle. The production and analysis of a library of small RNA sequences present in mature leaf tissue would allow the identification of potential regulatory sequences on the basis of complementary target/miRNA pairing through computational methods. Any such sequence could then be verified through a number of experimental methods to identify the sites and nature of miRNA activity. This work was carried out in conjunction with the analysis of transgenic lines expressing the viral p19 inhibitor of miRNA biosynthesis. The use of this inhibitor both supports the computational

prediction of miRNAs and extends to the scope of the study beyond that which would be possible with a bioinformatic approach alone. The unknown genetic origin of many aspects of the C₄ cycle would prevent a full exploration of the effects of miRNAs upon the cycle by computational analysis alone and so it was hoped that the utilisation of the p19 inhibitor would allow an exploration of these areas. In addition the utilisation of such an inhibitor would provide an additional method of validating predictions made by the computational analysis: should a miRNA be targeting a component of the system, then a disruption of miRNA synthesis may cause detectable changes in the expression of the target gene.

1.6.5: Choice of Model Species

A considerable amount of knowledge has been accumulated relating to the control of C₄ gene expression in maize with examples of regulation occurring at multiple levels as discussed above. The C₄ cycle was initially described from maize and sugarcane (reviewed by Hatch, 1999) and the utilisation of maize as a tool to study C₄ has been promoted by its importance as a crop plant and technical benefits such as the ease of preparation of purified mesophyll or bundle sheath cellular extracts (Kanai & Edwards, 1973). Genetic resources for maize include an annotated genome sequence (Schnable *et al.*, 2009), transcriptome (Li *et al.*, 2010) and plastid proteome data (Majeran *et al.*, 2008). Small RNA sequencing attempts have enabled miRNA identification in maize (Zhang *et al.*, 2009) with roles in leaf development (Juarez *et al.*, 2004) and stress metabolism (Ding *et al.*, 2009). Maize, however, is deficient in a number of areas as a model species. These include the lack of phylogenetically proximal C₃ taxa, limiting the extent to which the value of potential regulators of the C₄ cycle can be examined. While a method for maize transformation has been described (Frame *et al.*, 2002) it is laborious and its long life cycle would limit the extent to which stable expressing lines could be established within the timeframe of a PhD program.

Various other taxa have been used as model C₄ species, including *Amaranthus*, *Flaveria* and *Atriplex*. The presence of C₃, C₄ and C₃/C₄ intermediates within *Flaveria* have enabled various evolutionary trajectories that may lead to C₄ to be explored (for example, Holaday *et al.*, 1985; Moore *et al.*, 1989) and a method for transforming the C₄ *F. bidentis* has been described (Chitty *et al.*, 1994). Similar examples of gene-specific regulatory mechanisms have been described in *Amaranthus* and *Atriplex* (as discussed above), and transformation systems exist for C₄ member of both genera (Jofre-Garfias *et al.*, 1997; Uchida *et al.*, 2003). While the transcriptomes for C₃ and C₄ members of *Flaveria* have been published (Gowick *et al.*, 2011) the genetic resources for *Amaranthus*, *Flaveria* and *Atriplex* are still sparse and the application

of the resources accumulated for *Arabidopsis* would be difficult given the phylogenetic distances between the respective taxa. These taxa also have relatively long lifecycles, and only *Flaveria* has been used as a model C₄ species in recent literature.

In order to exploit the genetic resources associated with *Arabidopsis*, Brown *et al.* (2005) proposed the utilisation members of *Cleome* (Cleomeaceae) in order to examine the control of C₄ photosynthesis. Cleomeaceae has recently been resolved as being sister to Brassicaceae (Hall *et al.*, 2002), and possesses a number of C₄ species (Marshall *et al.*, 2007; Voznesenskaya *et al.*, 2007). While a predominately C₃ genus, *Cleome* includes the C₃/C₄ intermediate *C. paradoxa* and two NAD-ME subtype C₄ species (*C. gynandra* and *C. oxalidea*). A third C₄ member, *C. angustifolia* shows novel leaf anatomy which represents an adaptation of traditional Kranz-like anatomy to incorporate additional water storage tissues (Koteyeva *et al.*, 2011). While a genomic sequence is not available for *C. gynandra*, transcriptome data is available for *C. gynandra* and the C₃ *C. hassleriana* (Braütigam *et al.*, 2011) and a phylogeny for the genus has been reconstructed (Inda *et al.*, 2008). *C. gynandra* is transformable (Newell *et al.*, 2010) and has relatively short generation times. The phylogenetic proximity of *Cleome* to *Arabidopsis* has enabled the transfer of genetic systems between the two to screen for conserved regulatory elements (Brown *et al.*, 2011; Kajala *et al.*, 2011). Due to the flexibility of *Cleome* as a potential model system, it was decided that this system would be utilised to examine the potential roles of regulatory small RNAs in the C₄ cycle.

1.7: Project Aims

1.7.1: miRNA Identification

Two approaches were undertaken to identify potential regulatory roles for sRNAs in the development and maintenance of the C₄ cycle. First, a sRNA library was compiled from total RNA extracts prepared from mature *C. gynandra* leaf tissue. This data was then explored using target sequences of known photosynthesis genes to identify potential candidate targets. This was combined with a study of *C. gynandra* transgenics expressing the p19 viral inhibitor of miRNA synthesis in order to identify effects of miRNA inhibition upon the C₄ cycle. It was considered that the effects of such a disruption of miRNA activity could be examined at multiple levels. Firstly, if a gene was being actively excluded from a given cell type due to suppression by a miRNA, an inhibition of the miRNA may lead to overaccumulation of the gene at the transcript or protein level. Secondly, it was considered that p19 activity may destabilise the C₄ cycle to the extent that net photosynthesis would be affected and that examination of the physiological effects of p19 expression would expand the scope of this

study beyond those components of the C₄ cycle with a known genetic origin. Finally, expression of p19 during leaf development would enable the roles that miRNAs play during leaf development in *C. gynandra* to be explored, specifically with regards to the formation of Kranz anatomy

1.7.2: Hybridisation Studies

As discussed above, the generation of hybrids between C₃, C₄ and C₃/C₄ species has been utilised to explore the effects of a mixed genetic background upon the performance of the C₄ cycle and the formation of Kranz anatomy. If fertile hybrid lines can be generated hitherto-undescribed genes required for the C₄ cycle may be identified through segregation studies. Successful hybridisations with *Cleome* were reported by Rajndrudu & Rama'Das (1982), and so attempts were made to hybridise *C. gynandra* with the C₃ *C. hassleriana*.

1.7.3: The Effects of Light during the Development of *C. gynandra* Cotyledons

The onset of the C₄ system in developing leaves may respond to a number of environmental or developmental triggers (as discussed above), and it was considered that an analysis of the effects of light exposure in *C. gynandra* may yield insights into possible environmentally-linked controls of the C₄ cycle during early leaf development. Therefore, a study was undertaken to quantify changes in gene expression after light exposure of etiolated cotyledons.

2. Materials and Methods

2.1: General Plant Cultivation

Individual lines of *Cleome gynandra*, *C. hassleriana* and *Arabidopsis thaliana* were obtained from laboratory stocks. Cultivation was carried out on Levington M3 potting compost (Scotts Miracle-Grow, Godalming, UK) supplemented with medium-coarse vermiculite (William Sinclair Horticulture Ltd., Lincoln, UK) (3:1). All soil was treated before use with Intercept® (Scotts Miracle-Gro) at a concentration of 200 mg L⁻¹ per 5 L of soil to prevent sciarid fly infestation. Young plants were kept under propagator lids (Stewart Ltd., Croydon, UK) until established and the first pair of true leaves had formed.

Arabidopsis thaliana: Seeds from the Columbia-0 ecotype were sown directly onto soil prior to stratification at 4 °C for 3 days in darkness before transfer to a growth chamber at 20 °C, a photon flux density of 200 µmol m⁻² s⁻¹ with either a short day (12 hours) or long day (16 hours) photoperiod. Plants grown for transformation by floral dipping were sown directly onto muslin in pots 9.5 x 8.5 cm and were thinned to c.25 plants per pot. Plants grown for vegetative analysis were grown in 24 well trays under a short day photoperiod.

Cleome gynandra: Seeds were sown onto moist filter paper discs (Whatman grade I, Whatman Ltd., Maidstone, UK) in dishes sealed with Parafilm® (Alpha Labs Ltd., Eastleigh, UK) were incubated at 30 °C for 24 hours in darkness. Germinated seedlings were transferred to soil in 9.5 x 8.5 cm pots and were cultivated at 22 °C, of 350 µmol m⁻² s⁻¹ with a 16 or 12 hour photoperiod. For light shift experiments, seeds were germinated in the normal way before transfer to Cg media (see below) for *in vitro* culture. The work was carried out under “green-safe” light filtered through a HT124 filter (Stage Electric Ltd., Bristol, UK), and the pots wrapped in aluminium foil before incubation at room temperature of 7 days.

C. hassleriana: Cultivation matched that of *C. gynandra*, except that germination was achieved by incubation for seven days at 16 hours light at 28 °C followed by 8 hours in darkness at 18 °C. Once fully established, the plants were transferred to 12 cm square pots to allow for maximal growth before flowering.

2.2: Molecular Techniques

2.2.1: DNA Amplification

Amplification of target DNA sequences was achieved through the use of the polymerase chain reaction (PCR, Kleppe *et al.*, 1971, Saiki *et al.*, 1985). A TC-312 thermocycler (Techne, Staffordshire, UK) was used to perform the reactions using either BioTAQ® DNA polymerase (Bioline) or Phusion High-fidelity DNA polymerase (Finnzymes, Espoo, Finland). Under general conditions, 0.2mM dNTPs (Bioline) and 2 ng μl^{-1} of primers (Invitrogen) were used against 1-100 ng of template DNA. When Phusion was employed, the reaction mix was heated to 98 °C for 30 s prior to the addition of 0.02 U μl^{-1} of the polymerase and the initiation of the reaction cycle. A typical reaction sequence is as follows: initial denaturisation at 94 °C for 3 minutes, the 25-30 cycles of 94 °C for 30 s, primer annealing at 55 °C for 30 s, extension at 72 °C for 1-2 minutes, then final extension for 7-10 minutes at 72 °C. Polymerase choice, PCR component concentration and cycling conditions were optimised in each case according to amplicon length, primer annealing temperature and the manufacturer's guidelines and are stated in the text accordingly.

Agarose Gel-phase Electrophoresis

DNA fragments and RNA extracts were visualised after size-separation on gels of 0.8–2% agarose (Melford Laboratories Ltd., Suffolk, UK) made with ½ strength tris-borate-EDTA buffer (TBE): 44.5 mM tris(hydroxymethyl)aminomethane (Tris, Melford), 44.5 mM boric acid (Fisher Scientific) and 1 mM diaminoethetetra-acetic acid disodium salt (EDTA, Fisher Scientific) at pH 8.0. After heating to dissolution, the agarose gel was cooled before pouring into casting moulds (Bio-Rad, Hercules, USA) followed by the addition of ethidium bromide (Sigma) to a concentration of 0.5 $\mu\text{g ml}^{-1}$ (Sambrook *et al.*, 1989). DNA samples were prepared for loading by the addition of DNA loading buffer (40% sucrose (Fisher Scientific), 0.4% bromophenol blue (Sigma), which was used at a 1:5 concentration. RNA samples were prepared with RNA loading buffer: 50% glycerol (Fisher Scientific), 0.4% bromophenol blue (Sigma), 1 mM EDTA (Fisher Scientific), 48% formamide (Sigma) and 0.05% TBE) used at a 1:5 concentration and the samples were heated to 65 °C for 5 minutes before loading. Hyperladder® II (Bioline) was used as a size marker, and the gels were run for c.40 minutes at 80 V in a ½x TBE running buffer in Wide Mini-Sub cell tanks (Bio-Rad). Gels were then visualised on an Alpha Imager UV transilluminator (Alpha Innotech, San Leandro, USA) before photographing with a MultiImage light cabinet and Alpha-Ease FC Imaging System software (Alpha Innotech).

Purification of DNA Bands

Gel extraction of DNA fragments separated by electrophoresis was performed using the QIAquick Gel Extraction Kit (Qiagen) following the manufacturer's guidelines. PCR products were run out on a 1% agarose gel as detailed above, and the required bands excised using a fresh razor blade. The resulting DNA extracts were eluted into 25µl of water before being quantified *via* spectrophotometry.

2.2.2: RNA Preparation and cDNA Synthesis

Young, fully developed leaf material was harvested at 10am and flash-frozen in liquid nitrogen before storage at -80 °C. Total RNA extraction was achieved through phenol/chloroform extraction (Chomczynski & Sacchi, 1987) using TriPure[®] Isolation Reagent (Roche Diagnostics Ltd., Burgess Hill). The RNA was precipitated from the aqueous phase after extraction with a 1:1 mix with 0.8 M sodium citrate, 1.2 M sodium chloride (all Fisher Scientific) and incubation at -20 °C for 16 hours. The RNA was pelleted by centrifugation at 16000g for 30 minutes at 4 °C before cleaning in 70% and 100% ethanol (Fisher Scientific) and resuspension in water. All water used in RNA-orientated reactions was treated with diethylpyrocarbonate in a 1 in 1000 dilution and autoclaved prior to use to inhibit RNase activity. After resuspension, the RNA was treated with RQ1 DNase (Promega, Madison, WI, USA) before column cleaning and purification (RNeasy[®] Kit, (Qiagen, Hilden, Germany). The RNA was the quantified directly using the Nanodrop[®] spectrophotometer (Thermo Scientific, Waltham, MA, USA). The quality of the RNA was confirmed either by microcapillary electrophoresis (2100 Bioanalyser, Agilent Technologies Ltd., Santa Clara, USA) or by electrophoresis on a 1% agarose gel. In the latter case, quality was assessed *via* the appearance of the rRNA bands, while in the former a RNA Integrity Number (RIN, Schroeder *et al.*, 2006) greater than 7 was considered good quality. The RNA was then stored at -80 °C prior to use. 1 µg of total RNA was used for cDNA synthesis using SuperScript[®] II reverse transcriptase (Invitrogen, Carlsbad, CA, USA) following the manufacture's guidelines using oligo (dT)₁₅ (Roche) to prime the reaction. The cDNA was diluted 1:5 before storage at -18 °C.

2.2.3: Quantitative RT-PCR

Relative transcript abundance of a given gene was assessed with quantitative real-time PCR (qRT-PCR, Bustin *et al.*, 2000). cDNA was obtained following the method given above, before qRT-PCR reactions were carried out using a Rotor-Gene Q centrifugal real-time thermocycler (Qiagen) and associated analytical software. cDNA synthesis was performed using 1µg of total RNA, the products of which were diluted 15-fold before use as a template in a 10µl reaction mix

based on SYBR Green Jump Ready Mix (Sigma). Initial denaturisation was carried out at 95°C for 5 minutes before 40 cycles of 95 °C for 20s, 58 °C for 30s, 72 °C for 30s and 75 °C for 5 s, at which point the sample fluorescence was recorded. After the completion of cycling, a melting curve was produced between 55-95 °C recording every 1°. Primers for qRT-PCR were designed to have a melting temperature of 60 °C ($\pm 1/2$ °C) and to produce an amplicon of 100-300bp. Actin was chosen as a basic reference gene due to consistent levels of expression in *C. gynandra* and *C. hassleriana* (Bräutigam *et al.*, 2010), so *ACTIN7* was used for *Cleome* qRT-PCR reactions, although *ACTIN8* was used in analysis of Arabidopsis transcripts. Primer pairs against *C4* genes in *Cleome* were taken from Bräutigam *et al.* (2010), except for those developed for this study which were designed using the IDT PrimerQuest software (<http://eu.idtdna.com/Scitools/Applications/Primerquest>) prior to synthesis by Invitrogen. All primer sequences are given Appendix 1. In each instance, C_t values were produced for three technical replicates of at least three biological replicates and were calculated using a threshold of 0.02 for all transcripts so that fluorescence was recorded in the exponential phase of amplification. Reference actin qRT-PCR reactions were run alongside each gene of interest, and the comparative $2^{-\Delta\Delta C_t}$ value was calculated to allow for quantification of transcript abundance (Livak & Schmittgen, 2001), and standard errors were calculated from each combination of biological replicates. If a given reaction produced C_t values smaller than 12, or with variation greater than 0.25 between technical replicates the reaction was repeated with a 1 in 10 dilution of the original template.

2.2.4: Small RNA Library Preparation

The sRNA population of *C. gynandra* was sequenced following the methods of Havecker (2011) using materials supplied with the Illumina® sRNA TruSeq™ library preparation kit (see Figure 2.1). RNA was extracted from mature leaf material following the methods described above until the stage of ethanol precipitation. In short, the 18-25nt fraction of the total leaf RNA was purified prior to ligation of 5' and 3' adaptors before reverse transcription and PCR amplification of the library.

The sRNA fraction was purified using a 15% TBU denaturing polyacrylamide gel comprised of 42% urea (w/v, Fisher Scientific), 1x TBE and 15% acrylamide (19:1 acrylamide:bisacrylamide, Severn Biotech Ltd., Worcestershire, UK) set with 0.05% ammonium peroxodisulphate (APS, w/v, BDH) and 0.05% N,N,N',N'tetramethylethylenediamine (TEMED, v/v, Severn Biotech Ltd.). The gel was prerun at 200 V in 1x TBE buffer and the lanes washed out prior to loading of 10 µg of total RNA that had been prepared for loading as described above. In addition to the

standard running ladder, a 20-100bp low ladder (Sigma) and Hyperladder II[®] were run alongside the sample. The gel was run in an AE-6450 Dual Mini Vertical PAGE system (Atto, Tokyo, Japan) at 150 V until the bromophenol blue front had reached the bottom of the gel.

The ladder portion of the gel was then placed in a 1xTBE solution containing 0.225 µg ml⁻¹ ethidium bromide for 5 minutes before being briefly rinsed in fresh TBE. The gel was visualised on a M26 UV transilluminator (Alpha Innotech) at 360nm and the RNA section of the gel corresponding to 15-30nt was excised with a fresh razor blade. The gel fragment was shredded by brief centrifugation through a microfuge tube that had been punctured with a 21-gauge needle before the addition of 500 µl 0.3 M NaCl. The gel was left at a slow rotation at 4 °C for 16 hours to elute the RNA. The gel/NaCl mix was then transferred to a Spin-X[®] cellulose/acetate filter (Sigma) and spun at 12000g for 2 minutes, followed by a second washing using 100µl of 0.3 M NaCl. The elutate was combined with 600 µl 100% isopropanol and 3 µl of a co-precipitant stain GlycoBlue[™] (Ambion, Austin, USA) before incubation at -80 °C for 1 hour. The RNA precipitate was then pelleted and washed as described above before resuspension in 5.7 µl of RNase-free water.

The 5.7 µl RNA eluate was heated to 90 °C for 30 s before snap cooling on ice prior to the ligation of the 5' adaptor following the manufacturer's guidelines. The ligation reaction consisted of the 5' adaptor at 1.3 µM, 10 units of T4 RNA ligase, 40 units of RNAaseOUT and 1x RNA ligation buffer. The reaction mix was incubated at 37 °C for one hour before termination of the reaction by the addition of 10 µl of RNA loading buffer. The reaction mix was then run on a 15% TBU gel at 200 V, before excision of a gel slice corresponding to the 40-60nt region. The gel slice was macerated, the RNA eluted in 0.3 M NaCl before precipitated as described above. The resultant RNA pellet was then resuspended into 6.4 µl of RNase-free water. The full RNA product was then used for the 3' adaptor ligation reaction, following the same procedure as given above, although the 3' adaptor concentration was at 0.5 µM. The product of the 3' ligation reaction was separated out using a 10% TBU gel, and the fraction corresponding to 60-80nt was excised and used for RNA elution into 4.5 µl of RNase free water, as outlined above.

The full 4.5 µl RNA elutate was used for the reverse transcription reaction. The reaction was carried out using SuperScript[™] II reverse transcriptase following the manufacturer's guidelines using a siRNA RT primer (Illumina) to prime the reaction. 4µl of the RT-PCR product was used in an 80 µl PCR reaction mix using Phusion[®] polymerase as described above, using Illumina[®]-supplied primers at a concentration of 0.625 µM. The reaction mix was subdivided into four separate reactions. Initial denaturisation at 98 °C for 30 s was followed by 15 cycles of

98 °C for 2 s, 58 °C for 30 s and 72 °C for 20 s before a final extension at 72 °C for 5 minutes. The separate reactions were then recombined prior to the addition of 8 µl 3 M sodium acetate, 200 µl ethanol and 3 µl GlycoBlue™ before incubation at -80 °C for one hour to precipitate the PCR products. After centrifugation at 18000g, the pellet was washed in 100% ethanol before air drying and resuspension in 20 µl of sterile water and 3µl of DNA loading buffer as described above prior to loading on a 6% TBE gel.

The gel was run at 100V until the xylene cyanol front reached the bottom of the gel before staining with ethidium bromide and excision of a gel slice corresponding to 92bp from the sample lane. The gel was then macerated, and the DNA extracted using the QIAquick gel extraction kit (Qiagen) following the manufacturer's guidelines. The concentration and quality of the amplified library was verified as described above before submission for Illumina® sequencing-by-synthesis method version 1.

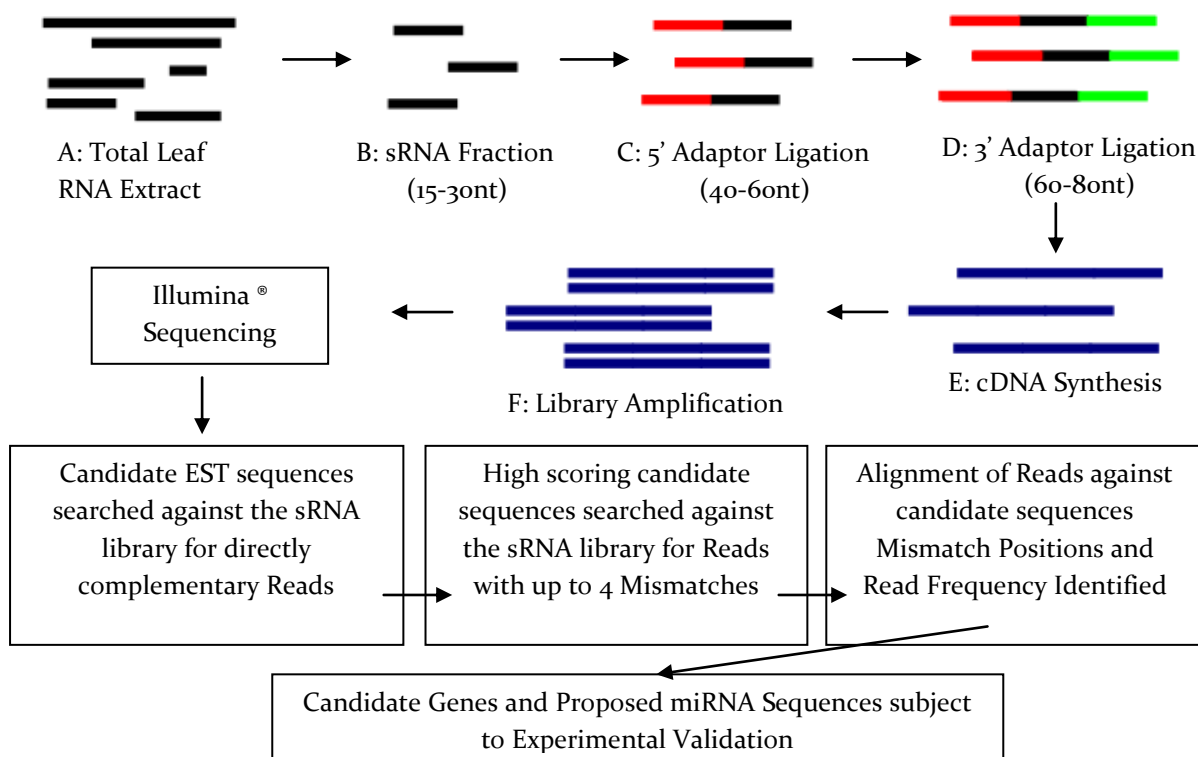


Figure 2.1: Sequencing and Processing of the sRNA Library

Total leaf RNA was extracted (A) before purification of the 15-30nt fraction using TBU-PAGE (B) was carried out. Separate reactions to ligate the 5' (C) and 3' (D) adaptor were then performed, each followed by purification of the 40-60nt and 60-80nt fraction respectively. The ligated RNA was then used for cDNA synthesis (E) to provide a ssDNA template for PCR amplification (F). The amplified library was subject to Illumina® sequencing v.1. After sequencing, the library was processed to remove noise reads (determined by length, composition and adaptor content) to provide a unique read library that was used as a basis for miRNA prediction based on direct and mismatched complementarity to candidate EST sequences. The reads were then subject to the given criteria for the *in silico* prediction of miRNA sequences as outlined.

2.2.5: Library Processing

On receipt of the library, the sequences were processed to produce a library of adaptor-free, non-redundant reads using the SIROCCO ADDAPTS processing pipeline of Nag *et al.* (In Submission). The sequences were first filtered for reads of lengths between 15-50nt, as the sequences obtained are comprised of the sRNA fused to the 3' adaptor. The starting 8nt of the 3' adaptor were then identified, and the sequences upstream from this site cleaved to leave the sRNA sequence. This was then subject to further filtering to produce a library of unique reads between 15-35nt in length. Due to the lack of a genome for *C. gynandra*, the library was initially examined using selected target EST sequences of the transcriptome data of Braütigam *et al.* (2011) as given in Appendix 2. Initial searches were made for direct complementarity using the algorithms of Moxon *et al.* (2008). Those sequences which showed an above average accumulation of hits against the library were then reanalysed using a modified form of the Bowtie alignment algorithm (Langmead *et al.*, 2009) to allow for alignment of sRNA sequences possessing up to 4 mismatches against an EST sequence of interest. Such sequences were then examined for high levels of abundance in the unfiltered library and for fulfilment of the miRNA targeting requirements as discussed above to identify any potential regulatory components (see Figure 2.1). Alignment visualisation was carried out using the Integrative Genomics Viewer of Robinson *et al.* (2011).

2.2.6: Cleavage Product Identification via 5' RACE

Validation of a predicted cleavage-directing miRNA was carried out using 5' Rapid Amplification of cDNA Ends (RACE, Frohman *et al.*, 1988) following methods of Llave *et al.* (2002b) and Kasschau *et al.* (2003) using the FirstChoice® RLM RACE kit (Ambion). Nested primer pairs were developed against the midsection of the target transcript (see Appendix 1), and were initially used following the full manufacturer's protocol to test for effectiveness of the primer pairs in amplifying the target transcript. The FirstChoice® kit includes treatment with Calf Intestinal Phosphatase to remove 5' terminal phosphates of non-degraded transcripts prior to treatment with Tobacco Acid Pyrophosphatase, 5' adaptor ligation and RT-PCR. 10 µg of total RNA taken from mature *C. gynandra* leaf material was used for each reaction. The product of the RT reaction was then used for two rounds of PCR using nested primers to obtain a high level of product specificity using hot start reactions mediated by the Phusion® high fidelity polymerase as described above.

The nested reverse primers were designed to match the forward primers supplied with the FirstChoice® kit, although melting temperature optimisation was carried out using

temperature-graded PCRs in a Techne TC-512 gradient thermocycler. The PCR products were run out on a 1% (w/v) agarose gel, and bands of the predicted size were excised from the gel prior to DNA extraction using the QIAquick gel extraction kit (Qiagen). The products were then cloned using the ZeroBlunt® TOPO PCR cloning kit (see below), and sequenced to obtain target verification. Once the products were fully identified, the process was repeated following the modified procedure of Llave *et al.* (2002b).

2.3: Quantification of Protein

2.3.1: Protein Extract Preparation

Material for protein extraction was flash frozen in liquid nitrogen before storage at -80°C. The material was then finely ground using a micropestle under liquid nitrogen before the addition of an extraction buffer comprised of 0.1 M sodium chloride, 1 mM magnesium chloride and 0.05 M tris at pH 7.8 to which had been added EDTA-free protease inhibitor cocktail (Roche). The material was vortexed briefly before pelleting at 4000g for 15 minutes at 4 °C before the removal of the supernatant. Total protein content was quantified *via* the methods of Bradford (1976) and Jones *et al.* (1989) using the Bio-Rad Protein Assay Reagent (Bio-Rad), following the manufacturers protocol. The supernatant was then mixed 5:1 with protein loading buffer comprised of 0.1 M dithiothreitol (DTT, Sigma), 0.3 M sodium dodecyl sulphate (SDS, Melford), 0.2 M tris, 1 M sucrose and 0.4% bromophenol blue before storage at -20 °C.

2.3.2: Separation of Proteins via Electrophoresis

Total leaf protein was separated *via* SDS/polyacrylamide gel electrophoresis after the methods of Maizel (1966) and Shapiro *et al.* (1966). A stacking gel of 5% acrylamide (37.5:1 acrylamide:bisacrylamide, (Severn Biotech Ltd.), 125 mM tris, 3.5 mM SDS, 0.05% ammonium peroxydisulphate and 0.05% TEMED at pH 6.8 was poured over a set resolving gel of varying percentage. 14% gels were used for resolving c.20 kDa proteins, while a 10% gel was used for proteins in the range of 50-100 kDa. Besides acrylamide, the resolving gel was composed of 375 mM tris, 3.5 mM SDS, 0.06% APS and 0.1% TEMED at pH 8.8. Electrophoretic separation was carried out using an AE-6450 Dual Mini Vertical PAGE system (Atto, Tokyo, Japan) using a running buffer comprised of 25mM tris, 0.2M glycine (Fisher Scientific) and 1.75 mM SDS at pH 8.5. Twin gels were run in tandem at 50 mA until the bands reached the bottom of the stacking gel, after which the current was increased to 70 mA until the bands reached the bottom of the gel. One gel was stained with Coomassie stained using InstantBlue™ (Expedeon, Cambridge, UK) for one hour to allow for protein visualisation, after which the gel was dried between two layers of gel drying film (Promega) for long-term preservation. Before loading,

aliquots of protein samples were heated to 95 °C for 5 minutes to ensure sufficient denaturation.

2.3.3: Immunoblot Analysis

The second gel produced by electrophoresis was used for immunoblotting following the methods of Towbin *et al.* (1979) and Renart *et al.* (1979). Transfer to a membrane was achieved through the use of a Mini Trans-Blot Cell (Bio-Rad) which was run using a running buffer of 50 mM tris, 40 mM glycine, 1.3 mM SDS and 20% methanol (Fisher Scientific) at 100 V for 1 hour, whilst cooling with an ice pack. The separated proteins were transferred onto Protran™ nitrocellulose transfer and immobilisation membrane (Perkin Elmer, Massachusetts, USA) with a pore size of 0.2 µm. The membrane was then incubated in blocking solution of 5% milk powder (Marvel™ dried skimmed milk powder, Premier International Foods Ltd., Lincolnshire, UK) in tween/tris-buffered saline (TTBS, 50 mM tris, 0.2 M sodium chloride with 0.1% Tween-20 at pH 7.5) for 1 hour at room temperature while shaking at 50 rpm. After rinsing briefly in TTBS, the primary antibody was applied at the appropriate dilution in TTBS and left to hybridise over night at 4°C while shaking at 50 rpm. The membrane was then washed in blocking solution five times (for five minutes each) before application of the secondary antibody, also in blocking solution, for 1 hour while shaking at room temperature. In all cases, the secondary antibody used was anti-Rabbit IgG biotinylated antibody raised in Donkey (GE Healthcare, Wisconsin, USA) which was used in a 1 in 1000 dilution. The membrane was then washed in blocking solution for a further five times before rinsing in TTBS before application of streptavidin-biotinylated horseradish peroxidase complex (GE Healthcare) in a 1 in 1000 dilution in TTBS for 30 minutes. The membrane was then rinsed three times in TTBS before two washes in sterile water, each for five minutes while shaking.

Enhanced chemiluminescent detection was carried out using the Western Lightning™ Plus-ECL substrate (Perkin Elmer), medical X-ray film (Konica Minolta, Tokyo, Japan) and a compact X4 X-ray film processor (Xograph Imaging Systems, Gloucestershire, UK) following the manufacturer's guidelines in each instance. Numerical data was derived from western blot images were calculated using the ImageJ (National Institutes of Health, USA) using the 'Rectangular Selections', 'Histogram Plot' and 'Measure' functions.

2.4: Plasmid Design and Construction

2.4.1: Design of Plasmids

The *35S::p19::nos* construct was obtained as a 13.5 kb binary vector (Voinnet *et al.*, 2003) while the *pOpON2.1* promoter (Moore *et al.*, 2006) was obtained as a 20.1 kb binary vector with an empty destination site for the Gateway™ cloning system (Invitrogen). The *p19* coding sequence was cloned from the *35S::p19::nos* construct and inserted into the Gateway™ destination site of the *pOp* promoter following the methods given below. The final plasmid blueprint is given in Figure 2.1, while full restriction site maps are given in Appendix 3.

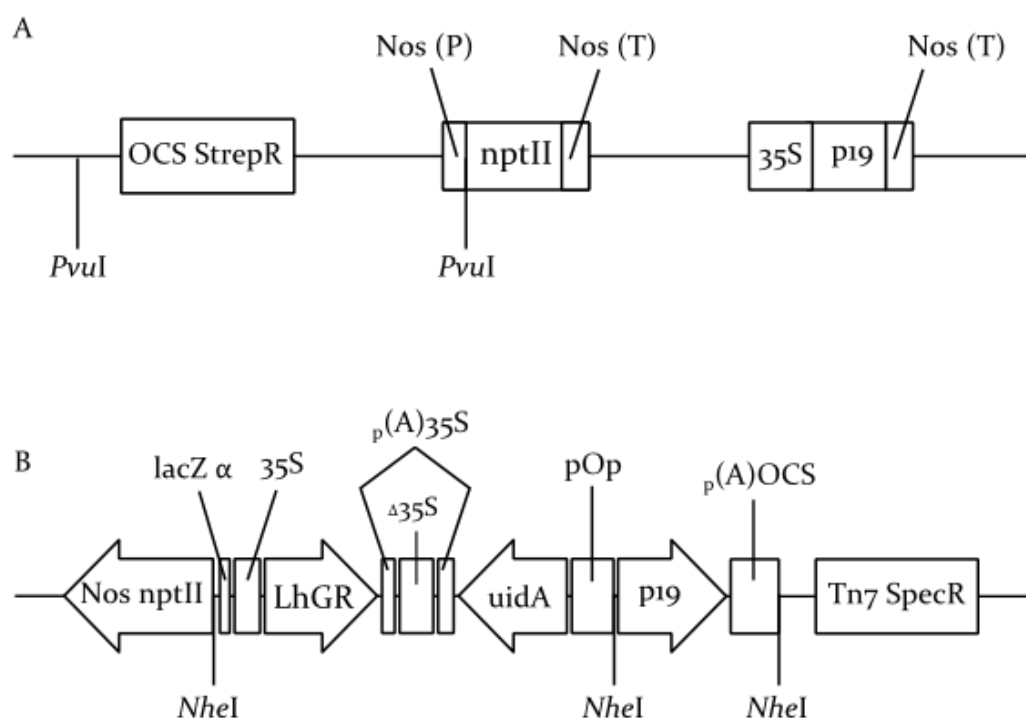


Figure 2.2: *p19* Expression Constructs

A: 35S::p19::nos: A 13.5kb binary vector carrying streptomycin resistance regulated by the octopine synthase (OCS) promoter, kanamycin resistance (neomycin transferase, *nptII*) regulated by the nopaline synthase (*nos*) promoter (P) and terminator (T) placed upstream of *p19* promoted by the CaMV 35S promoter and terminated by *nos* (T). *PvuI* restriction sites are marked, which yield fragments of 2781 and 10677bp upon digestion.

B: pOp::p19: A 19.3kb binary vector carrying the constitutively expressed spectinomycin (SpecR, regulated by T7), *nptII* (regulated by Nos (P) and (T)), and LhGR transcription factor, promoted by 35S. β -glucuronidase (*uidA*) and *p19* are promoted by the pOp promoter but are transcriptionally isolated by the presence of a 35S and OCR polyadenylation signal respectively. *NheI* restriction sites are marked, which yield fragments of 7006, 10931 and 1373 upon digestion.

2.4.2: Vector Production

The *pOpON2.1* binary vector was transformed into chemically competent *Escherichia coli* DH5 α cells (as described below) which were used to inoculate solid LB plates containing 100 $\mu\text{g ml}^{-1}$ spectinomycin (Melford) before incubation at 37 °C for 16 hours. A single colony was then used to inoculate 5ml LB liquid cultures with the same selective antibiotic which was incubated at 37 °C for 16 hours while shaking before being used to prepare the raw *pOpON2.1* plasmid *via* alkaline lysis and elution into TE buffer (10 mM Tris, 1 mM EDTA, pH 7.5). The plasmid was then verified by restriction enzyme digestion and sequence analysis as described below and above respectively. The plasmid was then stored at -20 °C until use.

The *p19* coding sequence was amplified as a blunt-ended PCR product using Phusion[®] high-fidelity polymerase as described above. Primers were designed to amplify the entirety of the *p19* coding sequence from the *35S::p19::nos* construct with the addition of a CACC sequence to the 5' terminus after the ATG site (see Appendix 1). After verification by sequencing, the *p19* amplicon was inserted into the pENTR/D-TOPO[®] vector using the Zero Blunt[®] TOPO[®] PCR cloning kit (Invitrogen) following the manufacturers guidelines to produce the pENT/*p19* entry vector. The product of the cloning reaction was transformed into chemically competent *E. coli* DH5 α cells which were cultured on solid LB media containing kanamycin (Melford) at 50 $\mu\text{g ml}^{-1}$ as a selective antibiotic. Single colonies were then used to inoculate 5ml LB liquid cultures with the same selective antibiotic which we incubated at 37 °C for 16 hours before being used to prepare the raw *pENTR/p19* plasmid *via* alkaline lysis and elution into TE buffer. The prepared plasmid was then verified by restriction enzyme digestion and sequencing before storage at -20 °C until use.

2.4.3: Gateway[™] Recombination of Vectors

Recombination between the *pOpON2.1* destination vector and *pENTR/p19* entry vector was achieved through the use of Gateway[™] LR clonase II Enzyme Mix (Invitrogen), following the manufacturers guidelines. The LR clonase mediates recombination between a region boarded by *att* sites in the entry and destination vectors. The insertion of the CACC sequence before the *p19* ATG site ensures this occurs in a directional manner so that the *p19* insert would be placed downstream of the *pOp* promoter in a 5' \rightarrow 3' orientation. Upon completion of the LR reaction, a lethality gene is removed from the destination vector and is replaced with the required insert so that only complete recombination products will proliferate in subsequent cultures. The products of the LR reaction were transformed into *E. coli* DH5 α cells, before subculturing and plasmid preparation as described below. The resultant *pOp::p19* construct

was then verified by restriction digests and sequencing prior to transformation into corresponding *Agrobacterium* strains as described below.

2.4.4: Plasmid Isolation and Verification

Plasmids were obtained *via* alkaline lysis (Bimboim & Doly, 1979) from cultures of *Escherichia coli* DH5 α cells produced by the methods discussed below. 5 ml liquid cultures of LB broth containing the appropriate antibiotics were established from streak plates and incubated at 37 °C for 20 hours. 2ml aliquots of cultures were pelleted twice in a bench-top centrifuge (260D, Denville Scientific Inc., Metuchen, USA) before plasmid extraction using the QIAprep Spin Miniprep kit (Qiagen) following the manufacturer's protocol. Final elution of the plasmid yield was made in either water or TE buffer (10 mM Tris-Cl (Melford), 1mM EDTA (Fisher Scientific) at pH 7.5 with NaOH) depending on the eventual downstream application. The extraction yield was then spectrophotometrically determined ($50 \mu\text{g ml}^{-1}$ dsDNA $A_{260} = 1.0$).

Plasmids were verified through a process of restriction digestion (see below) to test for fragment size, followed by sequencing *via* the chain-termination method (Sanger & Coulson, 1975, Sanger *et al.*, 1977). This was carried out by the DNA Sequencing Facility (Department of Biochemistry, University of Cambridge) using a 3730xl DNA Analyser (Applied Biosystems, Foster City, USA) using $1\frac{1}{2} \mu\text{g}$ of raw plasmid and primers designed against the predicted sequence. Chromatogram and sequence analysis was carried out using BioEdit (Hall, 1999) and BLAST (<http://blast.ncbi.nlm.nih.gov/Blast.cgi>).

Purified plasmids were subject to restriction digestion to release DNA fragments of sizes based on the analysis of their predicted sequence. 10 μl reactions were carried out using enzyme preparations and corresponding buffer solutions (NEB, Massachusetts, USA) and 0.5 μg of DNA. The reaction was performed following the manufacturer's guidelines before inactivation by heating to 65 °C for 15 minutes prior to visualisation on an agarose gel of a corresponding strength. The enzymes used with each plasmid are discussed above.

2.5: Microbial Techniques

2.5.1: Production of Competent *Escherichia coli* DH5 α Cells

Competent DH5 α cells were prepared following a method derived from Hanahan (1983). Cells were plated out on Luria-Bertani (LB) medium comprised of 1% Bacto™ tryptone (BD, Franklin Lakes, USA), 1% (w/v) sodium chloride (Fisher Scientific), 0.5% (w/v) yeast extract (Oxoid, Cambridge, UK) solidified with 1.5% (w/v) agar (Melford), pH 7.5 with NaOH. After incubation at 37 °C for 20 hours a single colony was used to inoculate 5ml of Ψ broth comprised of 2% Bacto™ tryptone (w/v), 0.5% yeast extract (w/v), 0.4% magnesium sulphate (w/v, Sigma), 10mM potassium chloride (w/v, Sigma) at pH 7.6 via NaOH. After incubation at 37 °C for 16 hours at a rotation of 200 rpm, 1ml of the culture was used to inoculate a further 100ml of Ψ broth which was then cultured until such time that the growth rate had entered the mid-log phase.

The culture was cooled on ice for 15 minutes before centrifugation at 1000g at 4 °C and resuspension in chilled TFBI (100mM rubidium chloride, 50mM magnesium chloride, 30mM potassium acetate, 10mM calcium chloride, 15% glycerol (v/v) taken to pH 5.8 with 0.2 M acetic acid (all Sigma)). After 15 minutes incubation on ice, the suspensions were centrifuged again before resuspension in 8ml of TBII (10 mM MOPS, 10 mM rubidium chloride, 75 mM calcium chloride, 15% glycerol (v/v) at pH 7.0 with NaOH (all Sigma)). 200 μ l aliquots of the resuspended cells were flash-frozen on dry ice before storage at -80 °C. The efficacy of the preparation was tested by a trial transformation with selective antibiotic genes.

2.5.2: Transformation of Competent *Escherichia coli* DH5 α Cells

Vectors were inserted into DH5 α cells using heat shock transformation (Hanahan, 1983). 5 μ l of chemically competent DH5 α cells were incubated with 2 μ l of the product of a cloning reaction on ice for 20 minutes before heating to 42 °C for 1 minute and then rapid cooling on ice for 3 minutes. 500 μ l of SOC medium was added (Super Optimal broth with Catabolite repression, 2% Bacto™ tryptone (w/v), 0.5% yeast extract (w/v), 0.05% sodium chloride (w/v), 25mM potassium chloride (w/v), 0.01M magnesium chloride (w/v) (all Sigma) with 20mM glucose (Fisher Scientific) at pH 7.0 with NaOH) before incubation at 37 °C for 1 hour while shaking at 200 rpm. 200 and 300 μ l of the resultant culture was spread on LB plates containing either 50 μ g ml⁻¹ kanamycin sulphate, 100 μ g ml⁻¹ streptomycin sulphate or 50 μ g ml⁻¹ spectinomycin dihydrochloride (All Duchefa Biochemie, The Netherlands). Colonies were screened for successful transgenic colonies after 20 hours incubation at 37 °C.

Confirmation of plasmid transfer was initially carried out *via* PCR screen before subsequent verification through sequencing of the purified plasmid (see 2.2.4). Primers complementary to the insert were used in an amplification reaction using 0.5 units BioTaq® DNA polymerase (Bioline) in a 10µl reaction mix containing 1 mM magnesium chloride (Bioline), 0.25 mM dNTPs (Bioline) with a primer concentration of 2 ng µl⁻¹ (Invitrogen). Colonies were selected using a sterile pipette tip were added to the reaction mix after streaking on a fresh LB plates containing the appropriate antibiotics. The thermocycler conditions were as follows: initial denaturation at 94 °C, then 27 cycles of 94 °C for 30s, 55 °C for 30s, 72 °C for 1 minute followed by a final extension period of 7 minutes at 72 °C. Streaks were identified as positive by visualisation of an amplification product on a 1% agarose gel as described previously. To establish bacterial stocks, positive streak colonies were used to inoculate 5ml LB liquid cultures containing the corresponding antibiotic and incubated at 37 °C for 20 hours while shaking. A 500µl aliquot of culture was combined with an equal volume of sterile 80% glycerol (v/v, Sigma) before storage at -80 °C.

2.5.3: Production of Electrocompetent *Agrobacterium tumefaciens* Cells

The production of electrocompetent *A. tumefaciens* cells was achieved *via* a protocol derived from Fisher & Guiltinan (1995) for both the LBA4404 and GV3101 strains. Cells taken from a central stock of each strain were streaked onto solid LB media before incubation at 30 °C for 24 hours. A single colony was then used to incubate a 5ml culture of LB medium containing either 25 µg ml⁻¹ rifampicin (GV3101, Melford) or 100 µg ml⁻¹ streptomycin sulphate (LBA4404) which was incubated at 30°C for 20 hours while shaking at 200rpm. 1ml of the resultant culture was then used to inoculate a 100ml liquid LB culture with selective antibiotics which was incubated for a further 3 hours until the bacteria reached the mid-log phase of growth with an OD₅₆₀ of 0.45-0.6. The culture was then pelleted by centrifugation at 4000g for 15 minutes at 4°C before resuspension in 100ml chilled 10% glycerol. This process was repeated with 50 ml, 20 ml and 4 ml of 10% glycerol. The cells were then separated into 45 µl aliquots before flash freezing on dry ice and storage at -80 °C.

2.5.4: Plasmid Entry into *Agrobacterium tumefaciens* Cells

Plasmids were inserted into either strain of *A. tumefaciens* by electroporation (Schen & Forde, 1989). 250 ng of purified plasmid DNA was added to a thawing 45 µl aliquot of cells and transferred to an electroporation cuvette (Bio-Rad) after 5 minutes incubation on ice. The cells were then subject to an electroporation pulse using a Bio-Rad Gene Pulser set to 400 Ω, 2.5 mV with a capacitance of 25 mF. Directly after electroporation 1ml of SOC media was applied

and the cells incubated at 30 °C while shaking at 180rpm for three hours. At this point, the cells were spread over solidified LB media containing the corresponding selective antibiotics (streptomycin for LBA4404, rifampicin for GV3101, kanamycin for *35S::p19::Nos*, spectinomycin for *pOp::p19*) and incubated at 30 °C for 36–48 hours to produce colonies. These were then subject to assessment by PCR screen to identify the positive colonies before the establishment of glycerol stocks as described for *E. coli* above.

2.6: Transformation of *Cleome gynandra*

The transformation of *C. gynandra* was performed *in vitro* from cotyledon and hypocotyl explant material following the method derived by Newell *et al.* (2010). All reagents were supplied by Duchefa Biochemie, unless otherwise stated. *Agrobacterium tumefaciens* strain LBA4404 was used for *C. gynandra* transformations.

2.6.1: Provision of Plant Material and Bacterial Stocks

Fresh seeds taken from unopened pods were sown directly onto moist sterile filter paper in sealed plates and incubated in darkness at 30 °C for 30 hours. Germinating seeds with a hypocotyl greater than 7mm were transferred to 9cm-diameter sterile pots containing MS medium (Murashige & Skoog, 1962) supplemented with the vitamins of B5 medium (Gamborg *et al.*, 1968) and 1% sucrose (Fisher Scientific) at pH 6.0 and set with 0.8% agar (Melford) at a density of 30 seeds per pot. The pots were then incubated at 24 °C at a light intensity of 50 $\mu\text{mol m}^{-2} \text{s}^{-1}$ with a 16 hour photoperiod for a period of 7 days.

200 μl of stock cultures were used to inoculate 50ml of YEP medium (An *et al.*, 1988), comprising of 1% Bacto™ Peptone (BD), 1% yeast extract (Oxoid) and 0.5% sodium chloride (Fisher Scientific) at pH 7.0 in a sterile 250ml conical flask. In all instances kanamycin sulphate (50 $\mu\text{g ml}^{-1}$) was used as a selective antibiotic, with the addition of streptomycin sulphate (100 $\mu\text{g ml}^{-1}$) for the *35S::p19::nos* construct and spectinomycin dihydrochloride (50 $\mu\text{g ml}^{-1}$) for the *pOp::p19* construct. The culture was incubated at 30 °C for 24 hours while shaking at 200rpm. The culture was cooled on ice for 15 minutes before centrifugation at 1000g at 4°C and resuspension in chilled SIM (Simplified Induction Medium, Alt-Mörbe *et al.*, 1989) comprised of 2% sucrose (Fisher Scientific), 0.59% trisodium citrate and 0.2mM acetosyringone (Acros Organics) at pH 5.5.

2.6.2: Transformation and Regeneration

Transformation of *C. gynandra* was achieved following the methods of Newell *et al.*, (2010). Explant material was prepared by excising each cotyledon at the base, followed by a second incision at the cotyledon apex to provide a second wound site. The root tip and apical bud was removed from the hypocotyl. Both hypocotyl and cotyledon (abaxial surface downwards) material were placed into the *Agrobacterium* inoculum at a density of 25 seedlings per 10ml of inoculum and left for 30 minutes with gentle shaking. The explant material was then transferred to co-culture plates comprised of 1/10 MS medium supplemented with 3% sucrose, 1mg l^{-1} benzylaminopurine (BAP), 0.1mg l^{-1} naphthalene acetic acid (NAA) at pH 5.5, set with 0.8% agar. The solidified medium was covered with a disc of sterile filter paper moistened with 1ml of liquid MSO (MS medium with 3% sucrose at pH 5.5) on top of which the explant material was placed, with the cotyledons placed abaxial surface placed downwards. Co-culture plates were incubated for 2 days under the conditions given above before the explant material was transferred to regenerative media comprised of MS medium supplemented with the vitamin cocktail of Nitsch & Nitsch (1969), 0.5 g l^{-1} 2-[N-morpholino]ethanesulfonic acid (MES, Sigma), 0.5 g l^{-1} poly(vinyl-pyrrolidone) (PVP, Sigma), 40 mg l^{-1} adenine hemisulphate, 10 mg l^{-1} silver nitrate (added after autoclaving), 0.1 mg l^{-1} NAA, 1 mg l^{-1} BAP, 2% sucrose at pH 5.7 and solidified with 0.8% agar. Kanamycin sulphate (60 mg l^{-1}) was added to the cooled media as a selective antibiotic in addition to carbenicillin (500 mg l^{-1}) to prevent *Agrobacterium* overgrowth.

The cultures were grown under the conditions given above for three weeks, at which point they were subcultured onto fresh selective medium. After 5 weeks, explant material showing regenerative callus was transferred to selective A6 medium (De Block *et al.*, 1989). After a further three weeks callus balls showing significant leaf formation were transferred to A7 medium (De Block *et al.*, 1989) to promote shoot formation, and were maintained on this media indefinitely with subculturing occurring every three weeks.

2.6.3: Recovery of Seed

Shoots greater than 1.5 cm in height and showing little to no hyperhydricity were selected for grafting attempts. Wild-type *C. gynandra* plants were grown at $24\text{ }^{\circ}\text{C}$ with a light intensity of $350\text{ }\mu\text{mol m}^{-2}\text{ s}^{-1}$ with a photoperiod of 12 hours for 6–8 weeks until a stem greater than 7.5cm was produced while still showing vegetative growth. The stem apex was removed after the third node, and the remaining leaves and auxiliary buds removed. Two diagonal slits were made in the exposed rootstock stem creating a narrow channel into which the transgenic

scion could be inserted. A plastic collar was wrapped around the join to strengthen the graft, and was secured with dental thread. A clear plastic bag was then placed entirely around the plant to maintain a humid atmosphere, which was in turn covered with a non-woven agricultural textile to prevent excessive light damage affecting the scion. Once the scion established and demonstrated positive growth, the bag and covering were incrementally removed to allow progressive acclimatisation to the ambient growth chamber conditions. The scion was then allowed to mature naturally before being both self-fertilised and providing pollen to artificially adjacent WT individuals.

2.7: Transformation of *Arabidopsis thaliana*

The production of transgenic *Arabidopsis* lines was achieved through the use of the floral dip method (Clough & Bent, 1998). Col-O *A. thaliana* seeds were cultivated as described above, and were used for transformation shortly after bolting, which typically occurred after 4 weeks of cultivation. Glycerol stocks were used to establish 500 ml liquid LB cultures in 2 L conical flasks containing the corresponding antibiotics, which were inoculated with 200µl of glycerol-stored cultures before incubation at 30 °C for 24 hours while shaking at 200 rpm. The cultures were then pelleted by centrifugation at 3000g at 4 °C for 15 minutes before resuspension in 250ml of a 5% sucrose solution containing 0.05% Silwett L-77 (GE Silicones, West Virginia, USA). The plants were immersed inflorescence-side down in the bacterial suspension for 30s while gently shaking. After inoculation, the plants were wrapped in cling film before replacement in the growth room out of direct light for 24 hours, after which the plants were returned to normal growth conditions (see 2.1) until seed pod formation was advanced and the plants were allowed to dry out prior to harvesting.

Seed recovered from dipped plants was cleaned by filtration before being subject to antibiotic selection following the methods of Harrison *et al.* (2006). Surface sterilisation was achieved by washing the seeds in 70% ethanol (Fisher Scientific) for three minutes followed by 15% sodium hypochlorite (Fisher Scientific) with 0.1% Tween®-20 (Sigma) for 20 minutes, after which the seeds were washed three times in sterile water. The seeds were then mixed in a 0.5% agarose gel (Melford) and poured over a 25 cm plate of MS medium supplemented with 1% sucrose and kanamycin sulphate at 60mg l⁻¹. The plates were sealed with parafilm and stratified at 4°C in darkness for three days before light pulsing for 4 hours at 200 µmol m⁻² s⁻¹. After four days of culturing at 24°C in darkness, the plates were transferred back into light with a 16 day photoperiod for a further week. Healthy, developing plants were then potted up and cultivated in the fashion discussed previously (2.1).

2.8: Analysis of Transgenics

2.8.1: Verification of Transgenic Recovery

Individuals from recovered seed and *in vitro* transgenics were tested for the presence of the target transgene through PCR screening using primer pairs complementary to the transgene. Total genomic DNA was tested through the use of the Extract-N-Amp™ Plant PCR Kit (Sigma) following the manufacturer's guidelines.

2.8.2: Dexamethasone Induction

Induction of transgenic lines containing the *pOpON2.1* promoter was achieved using the methods of Samalova *et al.* (2005). 20 mM ethanolic dexamethasone (dex, Sigma) stocks were kept at -20 °C until dilution to a working concentration of 100mM with sterile water. Transient induction was achieved by inserting cut leaf petioles into the induction solution. For *in vitro* induction, dex was added directly to the cooled media before pouring. Soil-grown plants were either induced by misting of the leaf surfaces with a dex solution containing 0.1% Tween-20 or by application to the soil surface every three days to the point soil saturation. Successful induction was validated by GUS screening.

2.8.3: β -glucuronidase (GUS) Assay

Stable lines of both *Arabidopsis* and *C. gynandra* containing the *pOpON* promoter system were assessed for GUS expression after induction. The *uidA* gene, expressed concurrently with the gene of interest after induction of the *pOpON* promoter, encodes for β -glucuronidase which cleaves the cyclohexylammonium salt of 5-bromo-4-chloro-3-indolyl- β -D-glucuronic acid (X-Gluc) to produce glucuronic acid and chloro-bromoindigo, the precipitate of which is coloured deep blue and is preserved through leaf clearing processes in ethanol and sodium hydroxide (Jefferson *et al.*, 1987). The GUS stain was comprised of 100mM disodium hydrogen orthophosphate (Fisher Scientific), 0.5mM potassium ferricyanide (Fisher Scientific), 0.5 mM potassium ferrocyanide (Sigma), 10mM EDTA, 0.06% Triton X-100 (Sigma) and 2 mM X-GlucA (Sigma) (Jefferson, 1987). Penetration of the GUS stain into foliar tissues was achieved by three rounds of vacuum infiltration, each of one minute long. The plant material was then left to incubate at 37 °C for 16 hours before fixing and clearing.

2.9: Anatomical Analysis

2.9.1: Clearing of Leaf Tissue

Leaf tissue, either freshly harvested or treated with GUS stain, was cleared for light microscopy with ethanol treatment. The material was first submerged in ethanol/acetic acid (3:1, both Fisher Scientific) for one hour before replacement with fresh 96% ethanol for 24 hours, both at 37°C. The material was then transferred to fresh 70% ethanol before storage at 4°C until required. Prior to examination the tissue was rehydrated by submersion in 50% ethanol followed by distilled water, each for 10 minutes.

2.9.2: Preparation of Material for Histology

Material was fixed and embedded for histological examination using a method adapted from Jackson (1992) and Langdale (1993). Leaf tissue was harvested directly from the plant and cut into sections 2x10mm before fixing in 4% paraformaldehyde with 0.1% Tween[®]20 and 0.1% Triton X-100 (all Sigma) before three rounds of 1 minute long vacuum infiltration on ice. The paraformaldehyde was replaced after infiltration and the material incubated for 24 hours at 4°C. The samples were then taken up an ethanol dehydration series of 30%, 40%, 50%, 60%, 70%, 85% ethanol on ice for 1 hour at each step before overnight incubation in 95% ethanol with 0.1% eosin (Sigma) to stain the tissue deep red. The material was then washed twice in 100% ethanol at 4°C for 30 minutes before transfer to a Leica TP1020 automated embedding machine (Leica Microsystems, Wetzlar, Germany). An overnight run was performed which consisted of three 1 hour washes in 100% ethanol, 1 hour wash in 50% ethanol/50% histoclear (National Diagnostics, Georgia, USA), three 1 hour washes in 100% histoclear and two 1½ hour treatments in molten Paraplast[®] embedding media (Sigma). The ethanol and histoclear washes were carried out at room temperature under a vacuum, while the paraplast treatment was carried out at 60°C, also under a vacuum. The samples were then aligned in the correct orientation in molten paraplast and set by rapid cooling in Peel-A-Way[®] embedding moulds (Polysciences, Inc., Pennsylvania, USA).

The resultant wax blocks were then cut down for sectioning before mounting on plastic cassettes (Histosette[®], Quebec, Canada) prior to sectioning on a Leica RM2135 rotary microtome. Sections cut to a thickness of 7µm using a fresh razorblade cleaned with 100% ethanol were floated on a layer of water on top of Polysine+[™] adhesive slides (VWR International, Pennsylvania, USA) and left to dry overnight at 42°C. Dry sections were then stripped of wax by the following process: two washes of 100% histoclear, 80% histoclear (made with 20% ethanol), then 50% histoclear, 30% histoclear, two washes of 100% ethanol followed

by 95%, 80%, 50%, 30% ethanol before a final water wash. Each treatment was for 2 minutes, and the process was performed at room temperature. The tissue was then placed in filtered 0.1% toluidine blue (Sigma) for 3-4 minutes before rinsing twice in water and examination using an Olympus BX41 microscope (Olympus, Tokyo, Japan) and were photographed using a MicroPublisher 3.3RTV camera (Q Imaging, Surrey, Canada).

2.10: Photosynthetic Analysis

2.10.1: Photosynthetic Pigment Quantification

The abundance of protochlorophyll (the precursor of chlorophyll *a*, Virgin, 1955) and chlorophyll *a/b* in *C. gynandra* cotyledons were determined by spectrophotometry following the extinction coefficients of Moran & Porath (1980). Three pairs of light-grown or ten pairs of etiolated cotyledons were incubated in 1.5 ml *N,N*-dimethylformamide (DMF, Sigma) for 24 hours in darkness at 4 °C before quantification in a Helios Gamma spectrophotometer (Unicam Ltd.). Readings were taken at 603, 625, 647 and 664 nm to enable accurate determination of the photosynthetic components utilising the following equations of Moran (1982). Absorption at 664 nm was kept below 0.8 by diluting extracts accordingly.

$$\begin{aligned}\text{Chlorophyll } a &= 12.81 A_{664} - 2.16 A_{647} + 1.44 A_{625} - 4.91 A_{603} \\ \text{Chlorophyll } b &= -4.93 A_{664} + 26.01 A_{647} + 3.74 A_{625} - 15.55 A_{603} \\ \text{Protochlorophyll} &= -2.52 A_{664} - 0.79 A_{647} + 36.55 A_{625} - 27.08 A_{603}\end{aligned}$$

2.10.2: Photosynthetic Capacity Analysis

Transgenic lines were cultivated in soil under the conditions given above (2.1) for a period of 4 weeks before induction with dexamethasone application for 1 week prior to photosynthetic quantification. Photosynthetic capacity was assessed using a 6400-40 leaf chamber fluorometer attached to a LI6400-XT portable open gas exchange system under illumination from a variable 6400-02B LED light source (all Li-COR Biosciences, Nebraska, USA). Measurements were taken from the central leaflet of the 3rd youngest leaf, which was allowed to acclimatise to a saturating light level of 1500 $\mu\text{mol quanta m}^{-2} \text{ s}^{-1}$ at an external CO₂ concentration of 400 $\mu\text{mol mol}^{-1}$. The chamber area was 2cm², and was maintained at a leaf temperature of 22 °C while the vapour pressure deficit was kept below 1.3kPa. A steady state was determined when the conductance remained in a constant for 5 minutes, after which the response to changing A_{Ci} and PAR levels were recorded. The photosynthetic rate was recorded relative to internal [CO₂] produced from external concentrations of 400, 400, 300, 200, 100, 50, 400, 400, 400, 500, 600, 800, 1000, 1200, 1500, 1800 and 400 $\mu\text{mol mol}^{-1}$. Light

responses were measured at levels of 3000, 2500, 2000, 1800, 1600, 1400, 1200, 100, 800, 600, 400, 200, 100, 50, 25 and 2000 $\mu\text{mol quanta m}^{-2} \text{s}^{-1}$.

2.11: Hybridisations of *C. hassleriana* and *C. gynandra*

2.11.1: Generation of Crosses

Cross pollination of *C. gynandra* and *C. hassleriana* plants was carried out following methods adapted from Rajendrudu & Rama'Das (1982). The reproductive biology of both taxa were examined as a preliminary study prior to establishing crosses. Given the high levels of self-fertility that have been reported in *Cleome* (Cane, 2008) it was necessary to emasculate the flowers on the day before anthesis, a point which was determined by the extension of the petals to the point that the anther filaments were visible at the base of the petal in *C. hassleriana*, and the anther filaments were drawn out of the flower bud, and the anthers removed before dehiscence. Anthesis of *C. gynandra* was determined by a loss of green pigmentation from the flower. The emasculated flowers were covered with thin paper bags ("Glassine" bags, Eastern Polyteine & Paper Ltd., St. Ives, UK), and all intact flowers surrounding the emasculated buds were removed. 20 plants of each species, each with 3-6 mature flowers were used for crossing. The following morning, the stigmatic surfaces of the emasculated flowers were pollinated with pollen grains taken from a freshly dehisced anther of the opposite species before rebagging and subsequent cultivation until maturity. The receptivity of the stigmatic surface was assessed by submersion of the stigma into 6% (v/v) hydrogen peroxide (Fischer), and evidence of oxygen evolution on the stigmatic surface was taken as an indicator of receptivity (Dafni & Maués, 1998).

Pollen germination and tube growth was examined through the use of fluorescent visualisation following the method of Martin (1959). The gynoecium was removed from sample flowers and fixed in 3:1 ethanol:acetic acid for 16 hours before clearing in 4 M sodium hydroxide for one hour. The gynoecia were then washed three times in a 50 mM potassium phosphate solution buffered to pH 8 with potassium hydroxide, before submersion in a 0.1% (w/v) aniline blue stain for two hours at 60 °C. The stain was prepared by dissolution of aniline blue diammonium salt (Sigma) in 50 mM potassium phosphate buffer (pH 8) before being left to decolourise in darkness at 4 °C for one week. After rinsing in fresh phosphate buffer the gynoecia were placed into 10% glycerol (v/v) before visualisation under UV light ($\lambda = c.350\text{nm}$) using a Leica M165FC dissecting microscope and photographing using the accompanying camera and software. Under such conditions, the callose-rich pollen grain and tube fluoresce while the surrounding styler tissue acquires a dark blue hue.

2.11.2: In vitro Ovule Culture

In order to attempt *in vitro* culture of developing hybrid ovules, a method was adapted from Quazi (1988) and Zhang *et al.* (2003). 7–10 days after pollination (see Chapter 5), the gynoecia were removed and were sterilised by washing in 70% ethanol for 5 minutes before soaking in 12.5% bleach for 20 minutes before washing three times in sterile water. The ovaries were then dissected along the replum, and the developing embryos excised under sterile conditions and were transferred to Embryo Rescue (ER) media. At this stage the undeveloped embryos could easily be identified and only maturing embryos were extracted. The ER medium was comprised of MS salts with Gamborg B5 vitamins (Murashige & Skoog, 1962; Gamborg *et al.*, 1968) supplemented with 3% sucrose (w/v), 1 g l⁻¹ casein hydrolysate (Sigma), 0.5 g l⁻¹ MES, 0.5 g l⁻¹ PVP, 40 mg l⁻¹ adenine hemisulphate at pH 5.7. The medium was either solidified with agar at 0.75% (w/v), or used in a liquid state. In the latter case, the liquid medium was placed in the bottom of a sterile 30 ml tube, into which was inserted a filter paper bridge (Whatman) onto which was placed the recovered embryos. In addition, cultures were established in slowly rotating liquid medium, which was cultured while shaking at 30rpm. The medium was supplemented with 0, 0.25 or 0.5 mg l⁻¹ NAA and 0, 0.5, 1.0, 1.5, 2.0 and 3.0 mg l⁻¹ BAP. The cultures were then incubated at the conditions given above (2.1) with subculturing occurring every three weeks. After 12 weeks, the weight of each callus ball was measured using an AB104/S balance (Mettler-Toledo, Inc., Columbus, USA).

3. Do miRNAs regulate the C₄ Cycle? Analysis of sRNAs and their Inhibition

3.1: Introduction

The primary goal of this study was to test the hypothesis that miRNAs regulate the development or maintenance of the C₄ pathway. If a miRNA targeting the C₄ pathway was identified, its function in a C₃ system could be tested in order to understand how the miRNA was recruited into regulating the C₄ pathway. This hypothesis is based on the report that a disproportionate accumulation of sRNA sequences align against certain components of the C₄ system in maize (Tolley *et al.*, unpublished), and so attempts to identify any regulatory miRNAs that target components of the C₄ cycle in *C. gynandra* were undertaken.

3.1.1: miRNA Identification

A novel miRNA can be defined under the basis of a number of criteria (Ambros *et al.*, 2003; Bonnet *et al.*, 2004). Firstly, most plant miRNAs show between 1–4 mismatches with their target transcript, although these mismatches must not occur within the proposed cleavage site. Secondly, the miRNA sequence must match precisely with a locus on the genome of the target organism which is capable of generating the mature miRNA: the flanking regions of the miRNA coding sequence must be capable of generating a minimal free-energy folding hairpin structure capable of generating a pre-miRNA duplex.

miRNA sequences can be identified by computational analysis of the target genome by identification of regions coding for pre-miRNA hairpins (e.g. Wang *et al.*, 2005) or by cloning and sequencing of the small RNA (sRNA) fraction of the transcriptome between 15–35nt. In both instances, the targets of the miRNAs must be identified computationally by exploring the genome for target transcripts. Combined computational/cloning based strategies have been utilised to identify miRNA sequences during mechanical stress-responsive miRNAs in *Populus* (Lu *et al.*, 2005), oxidative stress in rice (Li *et al.*, 2011) and varied stresses in *Arabidopsis* (Sunkar & Zhu, 2004). While the direct computational analysis of genomic sequences for miRNA precursors can yield predictions, the latter authors report the detection of miRNAs by cloning methods that would not have been predicted *in silico*. However, as the genome of *C. gynandra* has not been sequenced, global prediction of functional sRNA using these methods is not possible. Therefore, the construction of a library of sRNA sequences present in mature *C. gynandra* was undertaken as an initial step in the identification of miRNA sequences which may interact with components of the C₄ cycle.

Construction of sRNA libraries from total leaf RNA is well-established (Havecker, 2011). The production of libraries from M or BS cells would enable sRNAs with differential abundance in these cell types to be identified. Methods exist for cell-type specific RNA extraction in maize (Kanai & Edwards, 1973), but when this method was attempted in *C. gynandra* a high level of contamination from the opposing cell type was observed (Gage, unpublished). The use of Laser Capture Microdissection (Emmert-Buck *et al.*, 1996) has been applied to *C. gynandra* (Aubury *et al.*, in prep.), but the low yields of RNA from this method would make this approach unsuitable for isolation of sRNA. As a result, the construction of a library of sRNA reads from total mature leaf RNA extracts of *C. gynandra* was undertaken.

Previous studies have predicted miRNA sequences utilising Expressed Sequence Tag (EST) data (Prabu & Mandal, 2010; Wu *et al.*, 2010). An EST library is available for *C. gynandra* (Bräutigam *et al.*, 2011), and so ESTs for candidate genes were used as targets for the computation prediction of miRNA sequences present in the sRNA population of *C. gynandra*. Hits against target sequences were examined for abundance and targeting criteria that have been described for plant miRNAs (Rhoades *et al.*, 2002; Bonnet *et al.*, 2004), and were compared against previously described miRNA sequences to identify any conserved sequences from Arabidopsis.

Predicted miRNAs can experimentally validated by the detection of cleavage products of their predicted target transcripts that would indicate miRNA activity. Those transcripts which show a high level of sRNA accumulation to specific loci can be screened for such cleavage products using 5' Rapid Amplification of cDNA Ends (RACE, Frohman *et al.*, 1988). The cleavage reaction will produce a transcript missing the 5' cap so that additional treatment with Tobacco Acid Pyrophosphatase (TAP) prior to adaptor ligation is not required (unlike full length transcripts). The point of cleavage can then be determined by subsequent sequencing.

Using this approach, it should be possible to detect sRNA sequences which directly target the components of the C₄ cycle. In addition to this approach, the effects of expressing an inhibitor of miRNA activity in *C. gynandra* were examined in order to test whether miRNAs may play a role in regulating aspects of the C₄ cycle for which a genetic origin has yet to be described, such as the formation of Kranz anatomy.

3.1.2: Viral Inhibition of miRNA Activity

As discussed previously (Section 1.4.2), a number of plant viruses have evolved mechanisms to suppress siRNA. Due to the similarity between the biosynthesis pathways of siRNAs and

miRNAs, expression of such viral inhibitors can interfere with the function of endogenous miRNAs (Chapman *et al.*, 2004), promoting a phenotype that matches that of *dcl-1* mutants in Arabidopsis (Kasschau *et al.*, 2003; Dunoyer *et al.*, 2004). Variation is seen in the activity between different viral inhibitor proteins, and the p19 protein of the *TOMBUS* viral family is one of the most potent inhibitors (Lakatos *et al.*, 2006; Dunoyer *et al.*, 2004). Cytosolic p19 selectively binds to 21nt dsRNA (Vargason *et al.*, 2003) prior to RISC formation, but has no effect on existing functional RISC complexes (Lakatos *et al.*, 2006). In addition, Uhrig *et al.* (2004) reported a relocalisation effect of p19 upon nuclear ALY proteins, although the effects of this interaction are unclear.

As p19 has been shown to inhibit sRNA biosynthetic pathways it was chosen as an inhibitory protein for introduction into *C. gynandra*. The benefits of establishing a stable transgenic line would be three-fold. Firstly, leaf development could be examined to identify any effects of miRNA inhibition on the formation of Kranz anatomy. Secondly, analysis of photosynthetic performance may highlight any effects of disruption of miRNA activity. Finally, components of the C₄ cycle can be quantified at the transcript and protein level to screen for any p19-induced changes in abundance that could be associated with a relief from miRNA inhibition. This would test the hypothesis that if a component of the C₄ cycle was subject to miRNA-mediated repression, then an over-accumulation of the component could be identifiable when the miRNA activity is suppressed by the presence of p19.

3.1.3: Temporal Control of p19 Expression

Due to the effects of p19 expression on leaf development it was considered likely that high levels of constitutive p19 expression may limit the recovery of a viable transgenic line. Inducible promoters have been used previously to allow temporal control of genes (e.g. *CLAVATA1/2*, Schoof *et al.*, 2000) and so the placement of p19 under control of a chemically inducible promoter was investigated. The dexamethasone-inducible *pOpON* inducible promotion system has been shown to generate specific induction of transgenes in tobacco (Samalova *et al.*, 2005) and Arabidopsis (Craft *et al.*, 2005) and so this system was selected for temporal control of *p19*. The utilisation of such a promoter would ensure that transgenic lines could develop normally prior to the induction of p19 activity.

The *pOpON* system is comprised of two components (Figure 3.1). Firstly, the transgene (in this case *p19*) is placed downstream of the chimeric *pOp* promoter comprised of *lac* operators upstream of a 35S promoter with the addition of the *Tobacco Mosaic Virus* Ω translational enhancer in the 5' UTR region. This construct is inserted into the target organism along with

the constitutively expressed *LhGR* synthetic promoter which is comprised of a *lac* DNA-binding domain placed between a *GAL4* transcription activation domain taken from *Saccharomyces cerevisiae* and GR, the glucocorticoid binding domain taken from rat. The presence of the GR domain ensures that LhGR is bound to the heat-shock protein HSP90 until ligation of dexamethasone to the GR domain allows release of LhGR and subsequent activation of the pOp promoter (Moore *et al.*, 2006).

Due to the absence of dexamethasone from a standard cultivation system, transgene expression is effectively silent in the absence of induction. In contrast, high levels of transgene expression can be seen within 4 hours of dexamethasone application, either locally or systemically (Samalova *et al.*, 2005). Other glucocorticoid-inducible promoter systems have been reported to cause developmental defects unrelated to transgene expression (Kang *et al.*, 1999), Samalova *et al.* (2005), although this is not the case in the pOp/LhGR system. Therefore, this system should allow silencing of miRNAs *via* p19 induction in mature leaves to investigate the importance of the sRNA pathway in maintaining C₄ photosynthesis. Furthermore, long term exposure to dexamethasone during early plant development should enable the effect of removing small RNA activity on C₄ leaf anatomy to be examined.

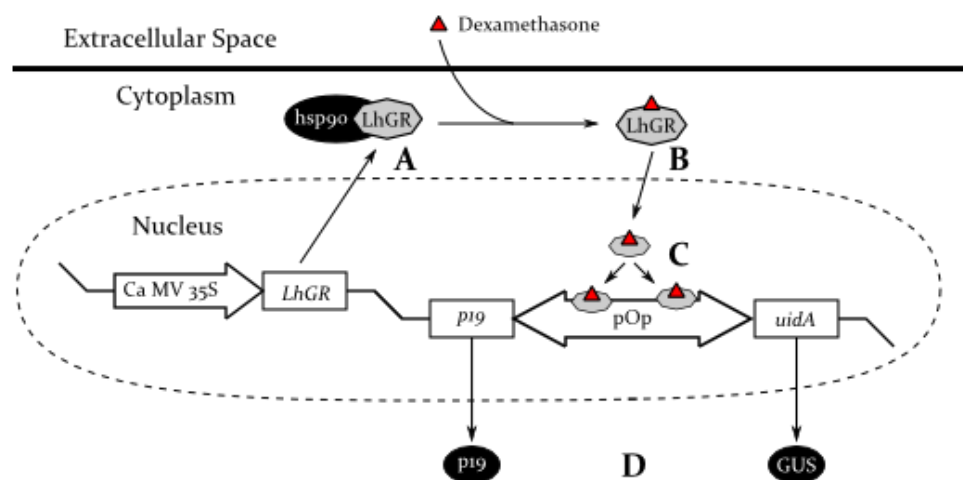


Figure 3.1: Function of the pOp promoter. The LhGR transcription factor is constitutively expressed, but when present in the cytosol it is bound to the heat-shock protein hsp90 (A). For induction, externally applied dexamethasone ligates to the GR domain of LhGR, releasing it from hsp90 and allowing it to pass into the nucleus (B) where it binds to the *lac* regions of the pOp promoter (C). The promoter drives transcription in both directions, leading to the expression of p19 and GUS in tandem (D).

3.1.4: Experimental Design

The sRNA population of mature leaf tissue of *C. gynandra* was sequenced in order to generate a library of reads as described previously. The EST sequences of candidate components of the C₄ cycle were then used as targets for exploring the library in order to identify miRNAs which

may target components of the C₄ cycle on the basis of sequence complementarity. Potential miRNA sequences were then verified by testing for the products of cleavage of their target transcript.

This work was underpinned by exploring the effects of inhibition of miRNA biosynthesis upon the C₄ cycle. The *35S::p19::nos* construct of Voinnet *et al.* (2003) was transformed into *C. gynandra in vitro* using the methods of Newell *et al.* (2010) in order to assess the effects of constitutive expression of p19. In addition, the same construct was transformed into *Arabidopsis* via the floral dip method (Clough & Bent, 1998) in order to validate the effects of p19 expression upon leaf development described from previous studies. *Agrobacterium*-mediated transgene insertion occurs at random sites (Townsend *et al.*, 1994), and as such generates variation in the extent of transgene expression due to positional effects of neighbouring loci (van Leeuwen *et al.*, 2001). In both *C. gynandra* and *Arabidopsis* the T₀ generation were assessed in order to examine dose-dependent effects of p19 expression by exploiting this variation.

In parallel to this, *p19* was cloned into the *pOpON2.1* promoter system (Moore *et al.*, 2006). This construct was then transformed into *C. gynandra in vitro*. Transgenic seed was obtained by grafting T₀ transgenic shoots (shoots recovered directly from *in vitro* culture) onto established WT rootstocks, and this T₁ generation was assessed for any impacts of p19 activity upon the C₄ cycle, either through changes in anatomy, photosynthetic capacity or transcript/protein abundance. The *pOp::p19* construct was also transformed into *Arabidopsis* in order to examine the effects of inducible p19 expression on the C₃ leaf.

The benefit of the *pOpON* system is that the effects of p19 expression can be examined at a number of levels. The effects of p19 expression on plant development at the cotyledon stage and beyond will be possible with the lines containing p19 under the control of the CaMV 35S promoter, but induction of mature plants will enable assessment of the effects of p19 expression on a developed, functioning C₄ leaf. Initially, induced plants were subject to gas exchange analysis in order to determine the effect of p19 expression on net photosynthesis by evaluating changes in CO₂ uptake under varying light and CO₂ regimes (Farquhar *et al.*, 1980; Caemmerer & Farquhar, 1981). Plants operating the C₄ cycle show reduced carbon compensation points and increased carboxylation efficiencies (as discussed previously). Therefore, if p19 activity impacted on the C₄ cycle, net photosynthesis should become more C₃-like. If a miRNA is directly regulating the accumulation of a component of the C₄ cycle, its method of acting is most likely to be *via* the negative regulation of the target gene in the

opposing cell type. In order to assess this, induced plants were examined for changes in transcript abundance using quantitative real-time PCR (qRT-PCR, Bustin *et al.*, 2000) and in protein abundance using the western blot method of Maizel (1966) and Shapiro *et al.* (1966). Given the wide number of roles that miRNAs have been linked with, it is likely that the expression of p19 is going to have a range of effects on multiple levels. By working with developed leaves it is hoped that developmental effects are going to be limited. However, it will be impossible to separate out any additional metabolic effects on a biochemical level. By working at the level of gas exchange analysis, and at transcript/protein abundance it is hoped that as greater focus on photosynthetic effects as possible will be achieved.

It was hoped that through the combination of sRNA cloning, computational prediction of targets and examination of p19 transgenic lines, any miRNAs which are targeting the C₄ cycle in *C. gynandra* could be identified. The use of the p19 inhibition is beneficial on two levels. Firstly, it may provide support for computationally-predicted miRNA sequences. Secondly, it will enable a broader examination of miRNA-mediated regulation of the C₄ cycle in that it will be possible to evaluate any effects of p19 expression upon traits for which no genetic basis has been determined, such as the formation of Kranz anatomy.

3.2: Results

3.2.1: sRNA Library Compilation and Analysis

A library of small RNA sequences present in mature *C. gynandra* leaf tissue was cloned and sequenced, yielding 2.4 million reads of which 660 thousand were unique (Table 3.1). Sizes ranged between 15-25nt in length and these demonstrated a distribution typical of the sRNA fraction, with the greatest abundance of reads being 24nt in length (Figure 3.2).

	Number of Reads	Total Number of Nucleotides	GC Content (%)	Percentage (%)
Raw Reads	2,437,396	87,746,256	46.43	100.00
Reads rejected due to Length	1,394,192	50,190,912	45.17	57.20
Reads rejected due to Noise	17,914	644,904	46.77	0.73
Reads rejected during Trimming	8,588	81,250	44.94	0.35
Duplicate Reads	354,548	7,981,925	44.95	14.53
Unique Reads	662,548	15,135,415	44.23	27.18

Table 3.1: Statistics relating to the sRNA library compiled for *C. gynandra*. 27.18% of the total reads were non-redundant and within the 15-25nt size threshold defined during the filtration process.

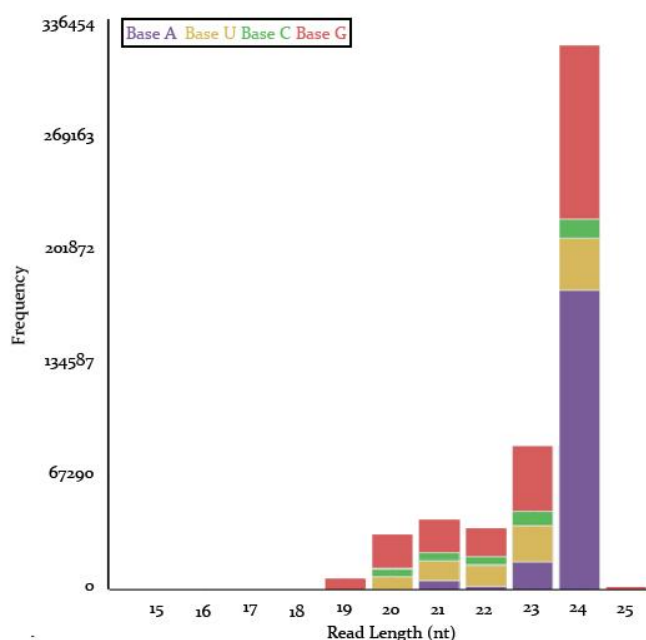


Figure 3.2: Size distribution of reads in the *C. gynandra* sRNA library. Read length was between 20-24nt, with a strong bias towards 24nt after adaptor removal. The sRNA library demonstrates a distribution and composition typical of this sequencing method. These data were obtained in collaboration with P. Shivaprasad.

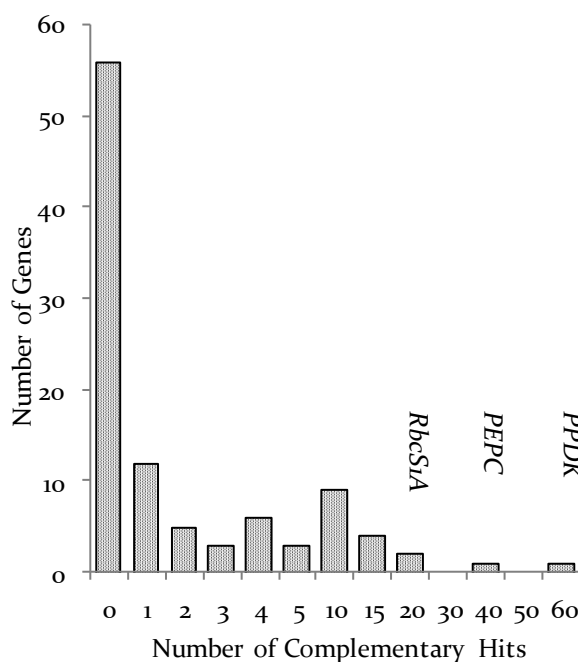


Figure 3.3: Reads from the *C. gynandra* sRNA library aligning against target EST sequences. The majority of EST sequences had no sRNA hits, with less than 15% of the targets obtaining more than 10 hits from the sRNA library. The decline in sequence number within each size threshold drops off rapidly.

Analysis of the library was preceded with a series of processing steps to produce a library of reads. The sequences were first filtered for reads of lengths between 15-50nt, as the sequences obtained are comprised of the sRNA fused to the 3' adaptor. The starting 8nt of the 3' adaptor were then identified, and the sequences upstream from this site cleaved to leave the sRNA sequence. This was then subject to further filtering to produce a library of unique reads between 15-35nt in length. These steps were achieved using the SIROCCO ADDAPTS processing pipeline of Nag *et al.* (in submission). The quality of the library was verified by the size distribution of its content (Figure 3.2) and by the identification of two known miRNA sequences. miR398 and miR165/166 which regulate copper superoxide dismutase (Jagadeeswaran *et al.*, 2009) and *PHABULOSA* (Mallory *et al.*, 2004) respectively. Sequences corresponding to these miRNAs were present in the sRNA library, which was taken as confirming its quality.

As a result of the lack of an annotated genomic sequence for *C. gynandra*, the library was initially explored using EST sequences of the transcriptome data of Braütigam *et al.* (2011). Initially, candidate target sequences were searched against the library for directly complementary reads using the algorithms of Moxon *et al.* (2008) (Figure 3.3, Table 3.2)

The candidate EST sequences (given in Appendix 2) were then used as targets in a search for direct complementarity to sequences in the non-redundant read library, the results of which are summarised in Figure 3.3. Only 15% of the ESTs had more than 10 hits, with the top scorers being represented by transcripts of *PPDK* (60), an isoform of *PEPC* (40) and *RbcS1A* (18). Given the rapid decline in hit rate seen within these data, these sequences were analysed with an additional set of the genes important for the C₄ pathway components for mismatches within sRNA/target pairings (see Appendix 2). Sequencing of the sRNAs present in *C. gynandra* leaf material indicated that a disproportionate accumulation of sRNA that map to some components of the C₄ cycle.

Functional plant miRNAs tend to show a measure of imperfection in pairing with their targets, as discussed previously. Therefore, a smaller subset of candidate genes were searched with relaxed targeting criteria to allow mismatched pairings. While increased numbers of reads aligning against the target sequences were seen, this increase was not equally distributed between genes (Table 3.3). While an average of 39 unique reads aligned against each EST, *ALAAT1*, *ASP1*, *CA4*, *DIT2.1*, *MDH*, *PEPC*, *PPCK* and *PyT1* sequences showed below average

sRNA alignment while *RbcS1A*, *RCA* and both isoforms of *PPDK* and *NAD-ME* had considerably above average alignment scores.

Table 3.3: sRNA reads aligning against photosynthesis genes in *C. gynandra*. The number of unique reads aligning against each target is unevenly distributed, with *PPDK*, *NAD-ME2*, *CA4*, *RbcS1A* and *RCA* showing alignment to an above average number of sRNA reads. *ALAAT1*: Alanine aminotransferase 1, *ASP1*: Aspartate aminotransferase 1, *DiT2.1*: Dicarboxylate Transporter 1, *MDH*: Malate Dehydrogenase, *NAD-ME*: NAD-malic enzyme, *PEPC2*: PEP carboxylase, *PPCK1*: PEP carboxylase kinase 1, *PPDK*: pyruvate, orthophosphate dikinase (including chloroplastic isoform and genomic DNA), *PyT1*: pyruvate transporter, *RbcS1A*: SSU of RuBisCO, *RCA*: RuBisCO Activase.

	Total Reads	Unique Reads
<i>ALAAT1</i>	25	25
<i>ASP1</i>	19	17
<i>CA4</i>	29	29
<i>DiT2.1</i>	12	12
<i>MDH</i>	30	11
<i>NAD-ME1</i>	39	38
<i>NAD-ME2</i>	64	60
<i>PEPC2</i>	6	6
<i>PPCK</i>	27	27
<i>PPDK</i>	47	41
<i>PPDK (Chp)</i>	33	29
<i>PPDK (gDNA)</i>	323	224
<i>PyT1</i>	24	24
<i>RbcS1A</i>	31	31
<i>RCA</i>	51	39

When the sRNA reads were aligned against the target sequences, a number of patterns were evident (Figure 3.4 and Table 3.4). sRNA reads mapped against some target sequences in a very diffuse pattern (e.g. *NADME2*, *ALAAT1*), while others showed a highly focused aggregation of sRNA reads to a narrow range of sites (e.g. *CA4*, *MDH*, *RCA*).

The direction, nature and mismatch content of sRNA alignments were grouped into a number of predominant classes (Table 3.4). The diffusive pattern of some alignments contained a number of loci at which multiple sRNA reads aligned although this was most pronounced in *NADME1&2* and *RCA*. Frequently, antisense alignment clusters contained both perfect and mismatched alignment loci and several sRNA reads aligned against a series of concurrent loci so that a contiguous sequence greater than 30nt was achieved, frequently with greater than 4 mismatches (e.g. alignment J in Figure 3.4). Due to the nature of the sequencing method involved, the reads are unidirectional and so primary analysis was concerned with antisense reads, as discussed previously. However, alignment parameters allowed sense alignments to be recorded in order to detect any aberrant accumulation patterns. In addition, the genomic sequence of a gene was also searched where available, and sense alignments in these conditions were considered. In several targets, perfect alignment (or alignments in which mismatches were not supported by all aligned reads) against a number of loci were recovered, and this was most pronounced in *ASP1*, *PyT1* and *RCA*. Perfectly aligned reads containing

mismatches and no mismatches are given in Table 3.4, although contiguous sequences are also stated.

Significant regions of antisense alignment (Figure 3.4) were found in *MDH* (**I**: 20nt, 22 reads), *CA₄* (**J**: 35nt, 17 reads), *NAD-ME₁* (**A**: 35nt, 11 reads), *RCA* (**G**: 15nt, 7 reads). A region of 26nt covered by 9 reads was seen in *NAD-ME₂* (**B**), although this was part of a greater sequence aggregation. Two significant sense alignments were also detected: 11 reads aligned to a 20nt region in *RCA* (**H**), and 11 reads aligned against a 42nt region of the chloroplastic isoform of *PPDK* (**C**). Interestingly, alignments against the genomic sequence of *PPDK* were found which were not detected in the chloroplastic isoform: 20 antisense reads aligned against a 50nt region (**D**), and 125 sense reads aligned against a region 29nt long (**E**), both of which rest in intronic regions. A perfect sense alignment was also recovered (**F**).

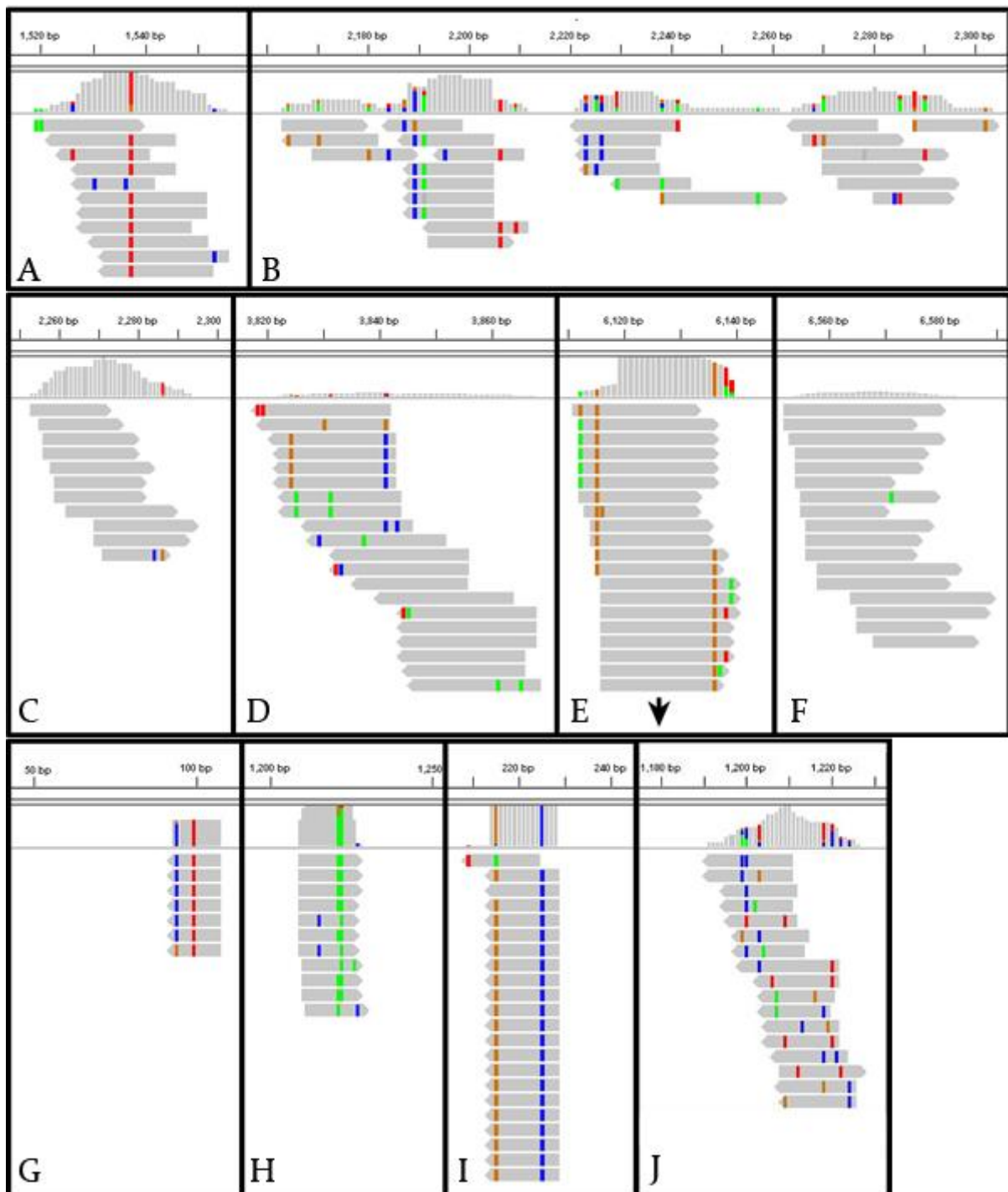


Figure 3.4: Alignments of sRNA reads against target sequences in *C. gynandra*. **A:** *NAD-ME1*, **B:** *NAD-ME2*, **C:** *PPDK* (chloroplasmic isoform), **D, E & F:** *PPDK* (genomic DNA), **G&H:** *RCA*, **I:** *MDH*, **J:** *CA4*. The scale bar at the top of each plot refers to the alignment position from the transcription start site. Right handed arrows are in the sense direction to the target, with left-handed arrows representing antisense. Grey alignments indicate perfect pairing, while a coloured band highlights single-base substitutions. The arrow in E represents the additional 105 reads which align at this position.

Target	Antisense						Sense					
	Perfect		Mismatch		>30 nt		Perfect		Mismatch		>30 nt	
	Nº	L	Nº	L	Nº	L	Nº	L	Nº	L	Nº	L
<i>ALT1</i>			1	24	4	44	3	20				
			4	29								
<i>ASP1</i>	7	25	1	18								
			1	18								
			2	22								
			3	18								
<i>DIT2.1</i>			2	26	8	32						
<i>PyT1</i>			1	19			2	44	6	27		
							5	37				
<i>NAD-ME1</i>			1	18	11	37	1	24				
			1	24			2	31				
			1	28			2	25				
			2	29			6	28				
			3	20								
<i>NAD-ME2</i>			1	20	4	37	2	18				
			2	25	11	48	2	24				
			5	23			2	26				
							3	27				
							3	34				
							7	40				
<i>PEPC2</i>												
<i>PPCK1</i>					5	47	3	39				
					5	34	3	13				
							4	28				
							5	19				

Table 3.4: sRNA read alignments against target sequences in *C. gynandra*. The number of reads aligning at a single site is given (Nº) with the total length of the alignment (L). Matches are separated on the basis of sense or antisense complementarity, and on the basis of perfect or mismatched alignment. The sequences which aligned to form a contiguous sequence greater than 30nt in length are also denoted. Those alignment clusters discussed in the text are given in bold. (Continued Overleaf)

Target	Antisense						Sense					
	Perfect		Mismatch		>30 nt		Perfect		Mismatch		>30 nt	
	Nº	L	Nº	L	Nº	L	Nº	L	Nº	L	Nº	L
<i>CA₄</i>			1	19	17	36						
			1	18								
			2	18								
<i>PPDK</i>			2	17			2	25	2	24	2	32
							4	17	2	26	3	40
											14	33
											17	33
<i>PPDK</i> (Chp)			1	18			4	28	1	21	11	41
									1	22		
									1	26		
									2	28		
									2	28		
<i>PPDK</i> (gDNA)	1	18	2	21	3	34	1	20	2	21	17	37
	1	19	4	26	4	32	1	24	2	21	4	33
	1	20	5	26	7	36	125	29	3	24		
	1	21	7	23	20	50						
			10	28								
<i>MDH</i>			2	22								
			2	20								
<i>Rbcs1A</i>									3	28	6	43
<i>RCA</i>			1	18	6	42	1	10			3	37
			3	18							10	51
			7	15							2	33

Table 3.4 (Continued): sRNA read alignments against target sequences. The number of reads aligning at a single site is given (Nº) with the total length of the alignment (L). Matches are separated on the basis of sense or antisense complementarity, and on the basis of perfect or mismatched alignment. The sequences which aligned to form a contiguous sequence greater than 30nt in length are also denoted. Those alignment clusters discussed in the text are given in bold.

Mismatches were highly conserved within a given alignment, and it was only within extended regions of alignment coverage that multiple mismatches were recorded (e.g. 3.4-J). Sequences that were abundant were searched against a database of mature miRNAs (miRBase, Kozomara & Griffiths-Jones, 2011). Five sequences were identified which showed similarity to the alignments recovered in this analysis (Table 3.5).

Target	Position	Sequence	Reference miRNA	Reference Origin
<i>PPDK Chp</i>	2263 +	GACGAAUAUGAACGAAGAAGA	miR5293	<i>Medicago truncatula</i>
<i>Rbcs1A</i>	419 +	UGUUAGCGGAGCUUGAAGAGG	miR4398	<i>Glycine max</i>
<i>NAD-ME2</i>	1014 +	CAAAGGAGAUGGGCU	miR399k	<i>Populus trichocarpa</i>
		CAAAGGAGAUGGGCU	miR399d	<i>Vitis vinifera</i>
		CAAAGGAGAUGGGCU	miR399f	<i>Ricinus communis</i>
	1303 +	ACUGAUCAGAAAGCAGAGGAC	miR2111	<i>Vitis vinifera</i>
<i>ALT1</i>	124 -	CUUCUUCAUUUGUUUCUACUU	miR5655	<i>Arabidopsis thaliana</i>

Table 3.5: Known miRNAs which show similarity to reads aligning to potential C₄ photosynthesis target genes in *C. gynandra*. The first site of alignment against the target sequence and orientation is given under **Position**, with the read itself quoted under **Sequence**. Bases given in red show a mismatch against the established miRNA sequence. The reference and species of origin according to miRBASE (see text) are also given.

While single sequences have been published for miR5293, miR4398 and miR5655, sequences for miR399 and miR2111 (both of which potentially target *NAD-ME2*) have been described in a sufficient number of species to produce alignments (Figure 3.5). A high level of sequence conservation is seen in miR2111 between lineages, and the only region present in the proposed *C. gynandra* *NAD-ME* sequence is a GAGG motif in the 5' region. A broader spectrum of variation is seen in miR399, both between and within lineages. Greater similarity was seen between the *C. gynandra* sRNA read aligning to position 1014 in *NAD-ME2* and miR399, with the first 10bp matching the conserved sequence, and the structure present in the 5' region bearing some resemblance to the miR399 sequence. However, the reduced length of the sRNA read does not allow for a full comparison to be made. The sequence of the proposed target site in *NAD-ME2* does not match miR399 at either the 5' or 3' end, so even if the sRNA read was part of a full length sequence it would not be possible to align against *NAD-ME2* and show a conserved sequence with miR399.

Given the abundance of sRNA sequences aligning against *PPDK*, it was chosen as a candidate to identify potential cleavage products via 5' RACE. Initially, attempts were made to produce

sequences for the first 250nt of the chloroplastic isoform of *PPDK*. These were successful, yielding a PCR product of the predicted length (Figure 3.6) which corresponded to the *C. gynandra* *PPDK* sequence of Bräutigam *et al.* (2011). However, subsequent attempts to increase the sequence obtainable via the 5'RACE protocol failed to produce amplicons that were distinguishable from non-specific products despite reaction optimisation.

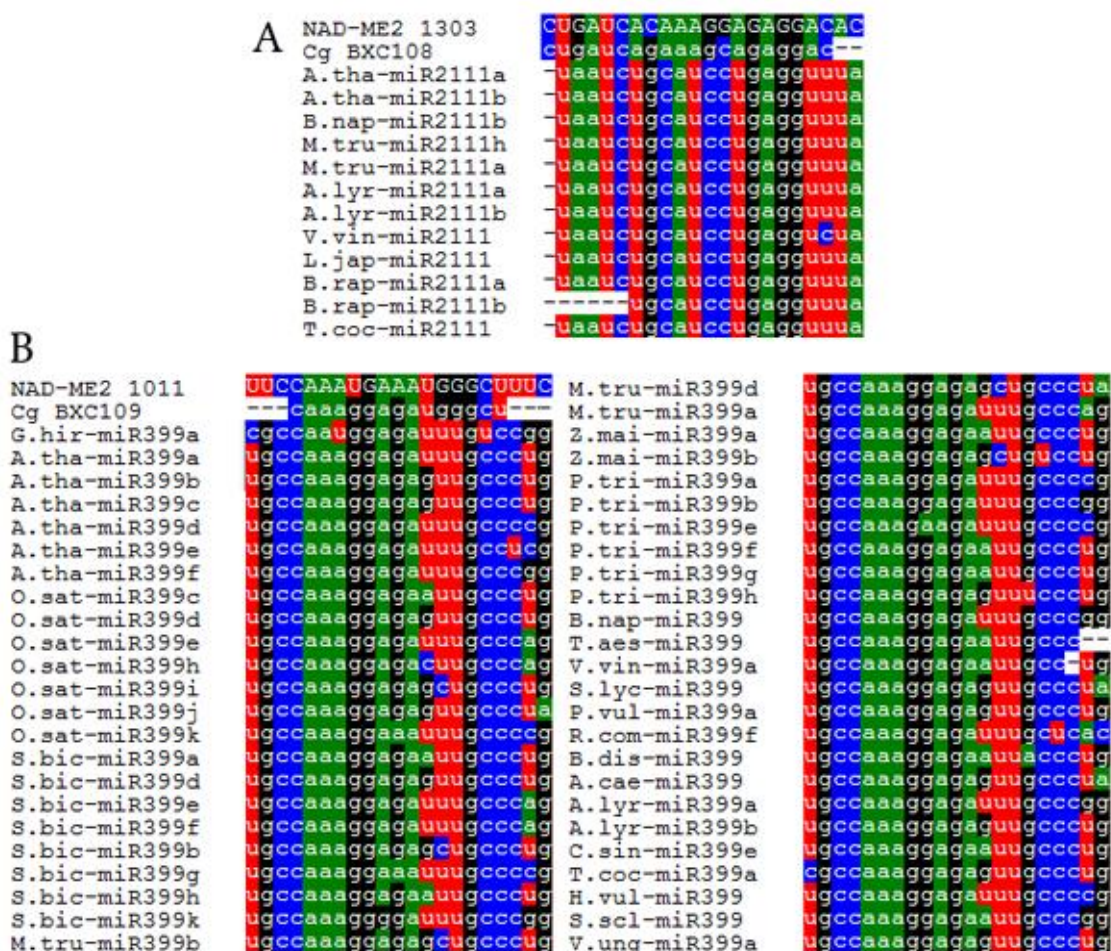


Figure 3.5: Alignments of potential miRNA sequences against *Cg* *NAD-ME2* show varying levels of similarity with described miR399 sequences. The proposed miRNA sequence (**Cg BXC10X**) underneath the target site (*NAD-ME2*, top), followed by published sequences for miR2111 (**A**) and miR399 (**B**). Sequence notation corresponds to the miRNA reference number on miRBase (see text). Neither sequence shows sufficient similarity to the conserved structure of the published miRNA, nor is a corresponding sequence between either miR399/miR2111 present in *NAD-ME2* transcripts.



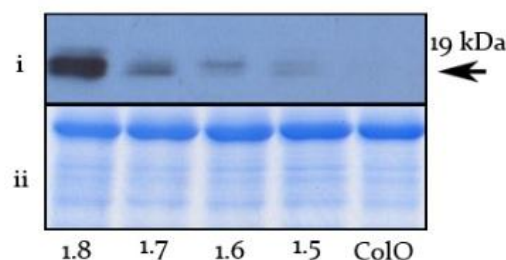
Figure 3.6: Amplification products of a 5'RACE reaction using nested primers against *PPDK* run out on a 1% agarose gel. The bands indicated correspond to the region of cytosolic isoform and chloroplastic isoform of *PPDK* after the addition of the zont RACE adaptor. The smearing on the gel is due to non-specific primer binding.

3.2.2: The Effects of p19 Expression

3.2.2.1: Constitutively Expressed p19 in Arabidopsis

The 35S::p19 construct (Voinnet *et al.*, 2001) was transformed into Arabidopsis in order to quantify the effects of constitutive expression of p19 upon leaf morphology. T₀ individuals were recovered at a rate of 1.8% although a loss of between 10-20% of individuals was seen within two weeks of transfer to soil. p19 protein was detectable by immunoblotting (Figure 3.7) and a strong phenotype was recordable in the T₀ generation (Figure 3.8). Individuals showed reduced vigour to the point of dwarfism (3.8-A) and leaves showed increased lobe formation and serration of the leaf margin. In the most severe lines shortened leaves with very limited blade expansion were seen (3.8-B). Internal leaf anatomy of these lines was disorganised so that the standard arrangement of palisade and spongy mesophyll was not identifiable, although the formation of the bundle sheath was still evident (3.8-C). While premature flowering was recorded in weakly expressing individuals, a number of variations in inflorescence anatomy were seen (Figure 3.9). The strongest leaf phenotype corresponded with delayed or inhibited flowering, in which extension of the raceme halted prematurely or failed completely. Increased cauline leaf formation was seen, although these showed similar developmental modifications to the rosette leaves (3.9-B). The primary raceme was subject to premature termination (3.9-C,D), although this did not always prevent development of the axillary racemes. The flowers produced on the ascendant racemes formed reduced sepals and petals, which were narrowed and curled (3.9-E,F). The stamens showed reduced anther and filament development, and pollen dehiscence was not detected (3.9-G). The presence of p19 at both the transcript and protein level was detectable, and a correlation was found between the extent of p19 accumulation and the severity of the recorded phenotype within the T₀ individuals (Figure 3.10). As a result of the altered floral anatomy caused by p19 expression, fertility was significantly impacted so that no T₁ seed was recovered.

Figure 3.7: p19 accumulation in stable lines of transgenic Arabidopsis. 20µg of total soluble leaf protein was loaded onto a 14% denaturing acrylamide gel. A signal is detectable at the 19 kDa point in lines 1.8-1.5 after conjugation with antibodies raised against p19 which is absent from the WT ColO control (i). Equal protein loading is shown by Coomassie staining (ii).



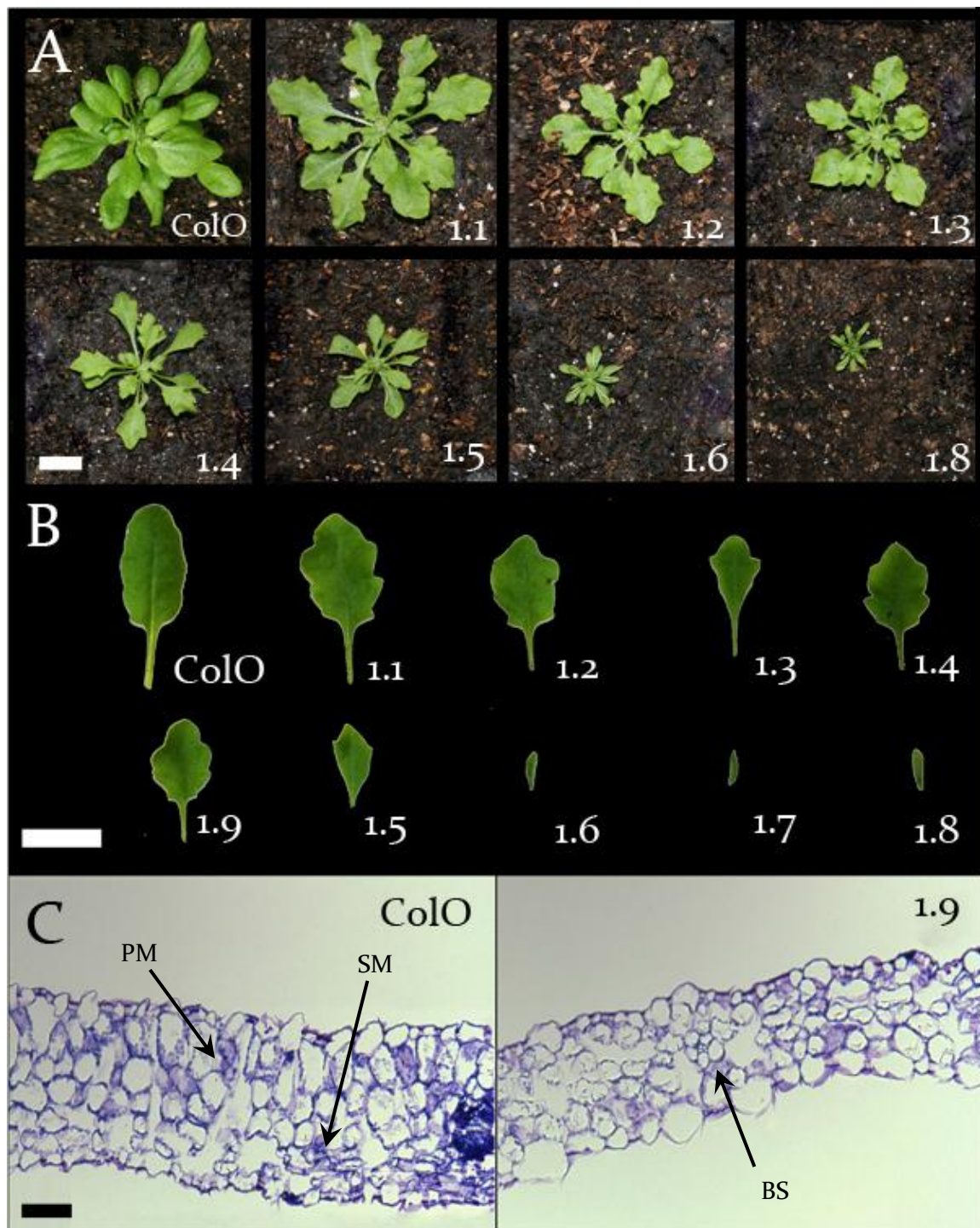


Figure 3.8: p19 expression alters leaf morphology in Arabidopsis. Varied expression is seen in T₀ lines (A), with extreme instances of the phenotype showing reduced vigour and stunting (lines 1.6 - 1.8). In addition to reduced leaf growth, increased serration of the leaf margin is seen in the more developed individuals (B, lines 1.1 - 1.4, 1.9) relative to the ColO WT leaf. While the palisade (PM) and spongy (SM) mesophyll is identifiable in sections of ColO leaf tissue (C), an increased level of disorganisation in p19-expressing lines (C - 1.9) renders these tissues indistinguishable, although the bundle sheath (BS) is still evident. Scale = 1cm (A,B), 100μm (C).

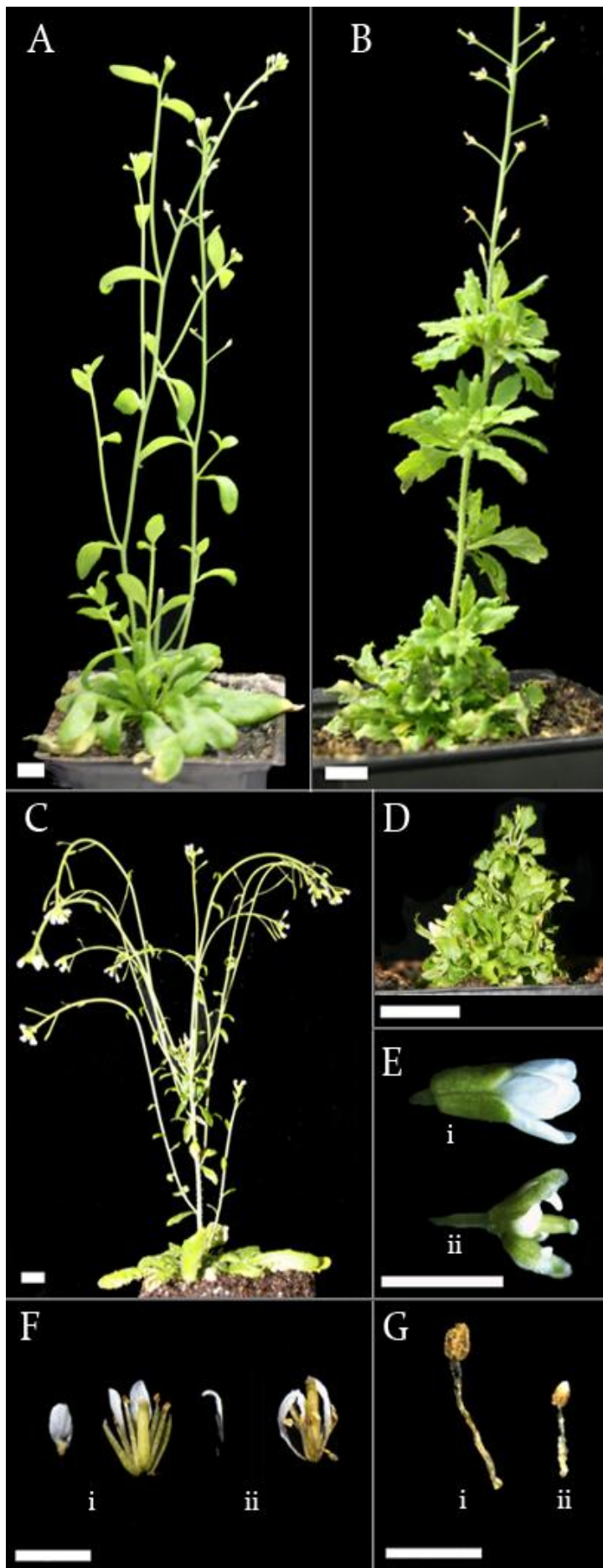


Figure 3.9: p19 expression effects reproductive anatomy in *Arabidopsis*. Increased formation of cauline leaves was observed, with the leaves showing the same increase in serration shown in the rosette leaves (**B**) relative to that of the WT Col-O (**A**) individuals. Premature termination of the primary raceme was seen although this did not always prevent the formation of axillary racemes (**C,D**). The flowers of p19-expressing individuals (**E,F-ii**) showed reduced, misformed petals and sepals when compared with ColO individuals (**E,F-i**). The anthers of p19-expressing lines (**G-ii**) failed to mature and pollen dehiscence was not observed by the stage that dehiscence was evident in ColO individuals (**G-i**). Scale = 1cm (**A-D**), 2mm (**E,F,G**).

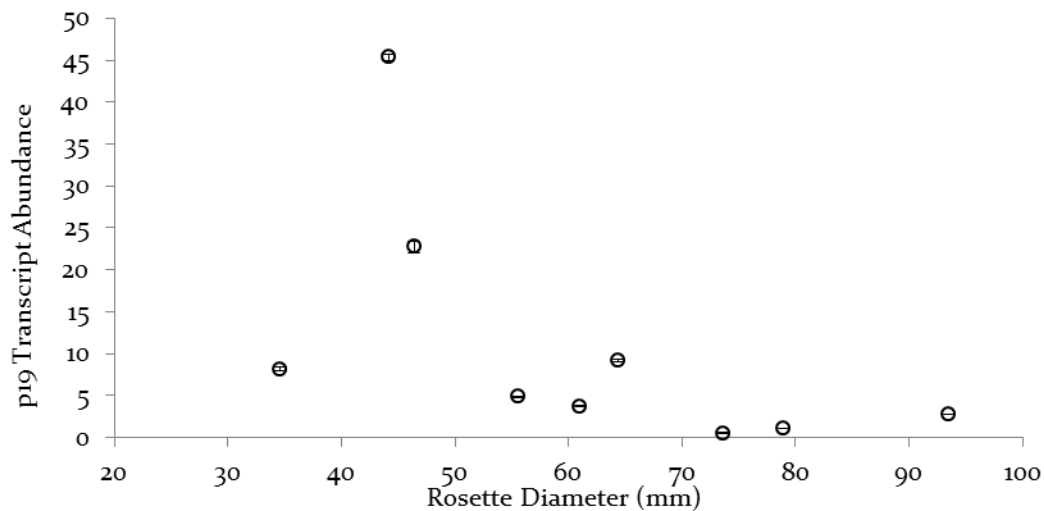


Figure 3.10: Arabidopsis rosette growth shows a negative correlation with *p19* transcript abundance. Increased abundance of *p19* leads to an increased severity of the dwarfing phenotype.

3.2.2.2: Constitutive Expression of *p19* in *C. gynandra*

Transformation of the *35S::p19* construct into *C. gynandra* was successful. Regenerative callus was produced from cotyledon and hypocotyl explant material within three weeks of culture, and early leaf formation was detectable within six weeks. While c.75% of explants produced 1–3 callus masses, leaf regeneration was only seen in 30–50% of the callus produced. Significant variation was seen between subsequent transformation attempts and explant age was found to be most significant with an optimum age of 6 days from initial sowing. Transgenic lines were identified on the basis of *p19* presence at the genomic and transcript level (Figure 3.11). The antisera raised against *p19* showed cross-reactivity to a c.20kDa residue in WT *C. gynandra* material, so it was not possible to test for the presence of *p19* protein.

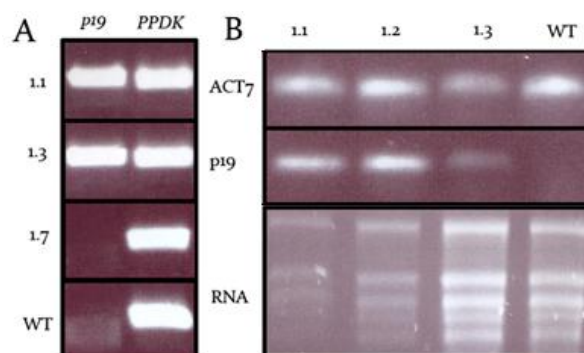


Figure 3.11: *p19* in transgenic *C. gynandra* lines. PCR screens of genomic DNA (A) showed the presence of *p19* in lines expressing the radialised phenotype (1.1, 1.3) which were absent in regenerative lines resembling WT (1.7) and in WT material. *PPDK* was used as a positive control. The presence of *p19* at the transcript level was detected through the use of RT-PCR (B). Total leaf RNA was used for cDNA synthesis to provide a template for PCR reactions to screen for the presence of *p19* transcripts. These were detectable in those lines expressing the radialised phenotype (1.1–1.3), but were absent from the WT. Primers for *ACT7* were used as a positive control for effective cDNA synthesis.

The *in vitro* regeneration of leaf material from non-transgenic control lines showed the formation of small but intact leaves of (Figure 3.12–WT). However, p19-expressing lines showed the formation of long, thin, radialised leaves which showed little to no mesophyll development (3.12–1.1, 1.3). These showed indeterminate growth, with a tortuous habit which showed little to no polarity. No shoots were recovered from these lines. The internal anatomy of p19-expressing lines showed a significant reduction in the extent of vein formation (Figure 3.13). While normal Kranz anatomy was seen in the leaves regenerated by non-transgenic material, the extent of primary and secondary vein formation was greatly reduced in p19 expressing lines. The reduction in mesophyll development was also notable.

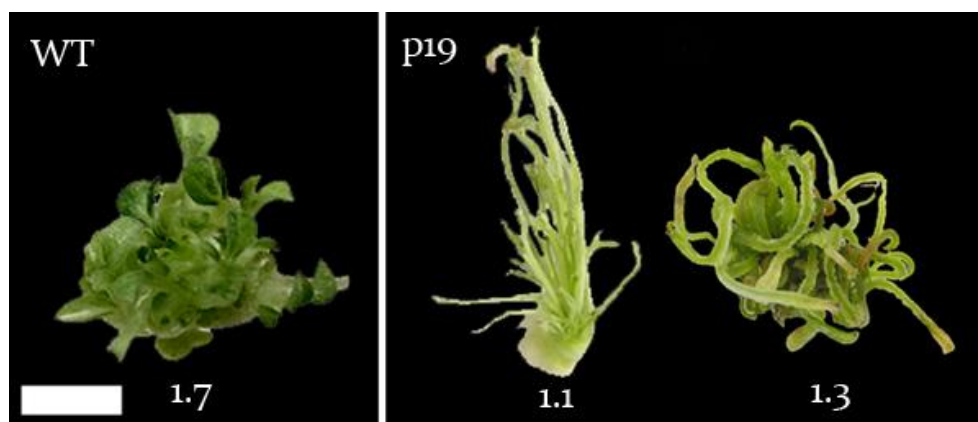


Figure 3.12: p19 expression in *C. gynandra* causes significant changes to leaf anatomy. The regeneration of WT *C. gynandra* material *in vitro* shows the formation of small leaves and shoots from callus (1.7). Transgenic lines 1.1 and 1.3 showed the production of thin, radialised leaves with little to no mesophyll development, and the formation and shoots was not seen. Scale = 1cm.



Figure 3.13: p19 expression causes a reduction in leaf venation and leaf expansion in *C. gynandra*. The radialised leaves of p19-expressing lines are narrow and thinned and demonstrate little mesophyll formation, while normal leaf development is seen in WT material. The extent of primary and secondary branching of the vasculature is decreased, and as a result the mesophyll area between such venation is equally decreased. Scale = 1mm.

3.2.3.3: Creation of the *pOp::p19* System

As a result of the significant morphological changes caused by constitutive expression of *p19* in *C. gynandra*, *p19* was placed under the control of the *pOpON2.1* dexamethasone inducible promoter. The stages involved in the production of this construct are shown in Figure 3.14. The coding sequence of *p19* was amplified from the original *35S::p19::nos* construct (3.14-A) using primers which would extend the 5' end of the coding region to include a CACC sequence to ensure that insertion of the amplified fragment could occur in the correct orientation when placed into the entry vector (3.14-B). Plasmid composition was verified through restriction enzyme digestion. A region of 1.2kb sits between the recombination sites of the *pOpON* destination vector, and this is replaced with the 0.5kb *p19* coding sequence. As a result, a 2.2kb fragment of the *pOpON* destination vector released by digestion with *NheI* was reduced to 1.5kb after recombination between the entry and destination vectors. Integration of the *p19* fragment into *pOp::p19* was confirmed by restriction digestion (3.14-D), followed by sequencing.

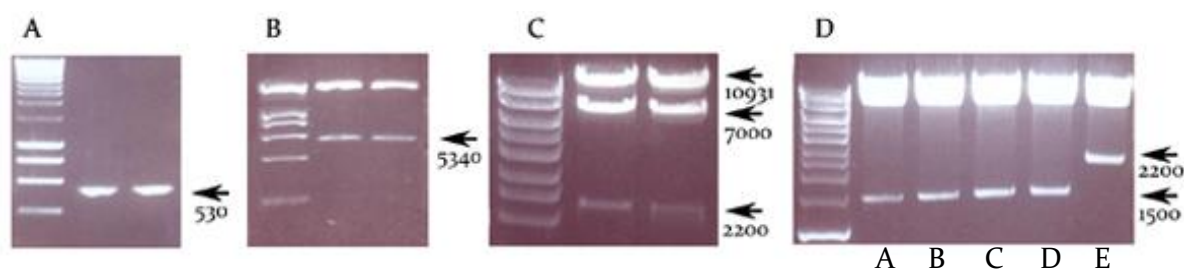


Figure 3.14: Creation of the *pOp::p19* Construct

Initially, the coding sequences of *p19* was amplified from the *35S::p19* construct. A 5' CACC sequence was added to allow for directional cloning, giving a total fragment size of 530bp, as visualised on a 1% agarose gel (A). This was inserted into a TOPO® entry vector, which was propagated in *E. coli* before extraction and digestion with *NheI*. A fragment of 5340bp containing the *p19* insert can be detected as a product of digestion, shown here on a 0.9% agarose gel (B). The *pOpON* destination vector produces fragments of 2208, 7006 and 10931bp after digestion with *AscI* and *NotI*, shown here on a 0.9% agarose gel (C). The *p19* entry and *pOpON* destination vectors were subject to recombination, producing the *pOpON::p19* construct. Upon digestion with *NheI*, the previous 2.2kp fragment of the *pOpON* destination vector is reduced to 1.5kb due to the recombination reaction inserting the shortened *p19* sequence, as visualised here on a 0.9% agarose gel (D). Lanes A to D show the 1.5kb fragment containing *p19*, while lane E contains the larger 2.2kb fragment produced by digestion of the empty *pOpON* destination vector shown in C.

3.2.3.4: *pOp::p19* in Arabidopsis

The *pOp::p19* construct was transformed into Arabidopsis using the floral dip method, and a transgenic recovery rate of around 0.25% was seen. T₀ individuals were grown on soil in the absence of dexamethasone for four weeks before induction was attempted. Initially, a single leaf was excised and placed in a 50 μ M aqueous dexamethasone solution for four hours before GUS staining. The dual-orientation promoter system of *pOpON* would ensure that both *uidA* and *p19* are expressed together, so the accumulation of GUS was taken as indicative of *p19* accumulation. GUS expression and accumulation was detectable within the four hour induction period, as indicated by the accumulation of GUS in the excised leaf tissue, and subsequent RNA extraction followed by qRT-PCR showed the accumulation of *p19* transcripts, although *p19* was not detectable in the absence of dexamethasone (Figure 3.15). T₀ individuals that had been cultivated on soil for four weeks were then subjected to a week-long period of induction through soil irrigation with 30 μ M dexamethasone on alternate days. After seven days, the youngest fully developed leaf was removed and used for RNA and protein extraction prior to profiling for *p19* transcript and protein accumulation. Transcripts and protein of *p19* were detectable only after induction with dex (Figure 3.15, 3.16).

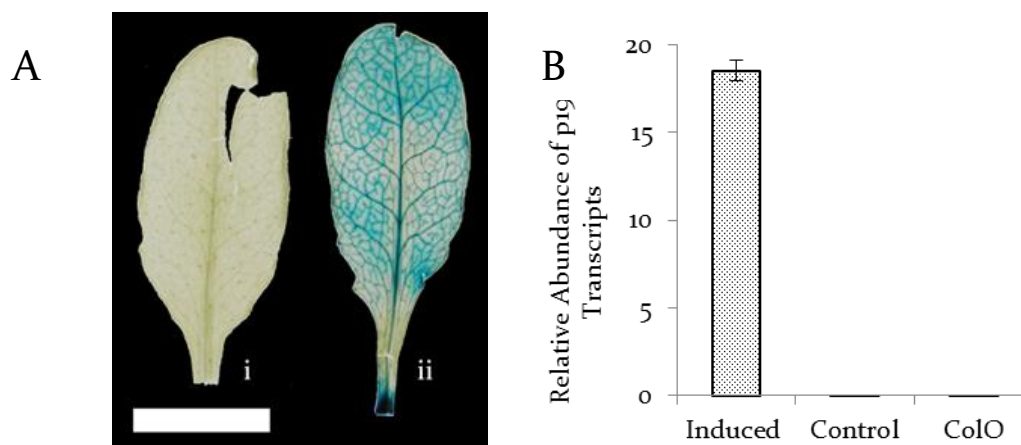


Figure 3.15: GUS expression is inducible by exposure to dexamethasone in transgenic Arabidopsis lines containing the *pOp::p19* construct. Scale = 1cm.

A: A pair of leaves that have been removed from the same T₀ individual and have been incubated in either a water control (**i**) or 50 μ M dexamethasone solution (**ii**) for four hours before GUS staining. GUS accumulation is specific to the induced leaf, indicating that GUS is not expressed in the absence of dexamethasone, but is capable of obtaining high levels of accumulation within 4 hours of dexamethasone exposure. **B:** The accumulation of *p19* transcripts follows a similar pattern. Leaves taken from a single T₀ individual show induction of *p19* after exposure to dexamethasone, generating a level of transcript accumulation not seen in the water-treated control or in a WT ColO individual.

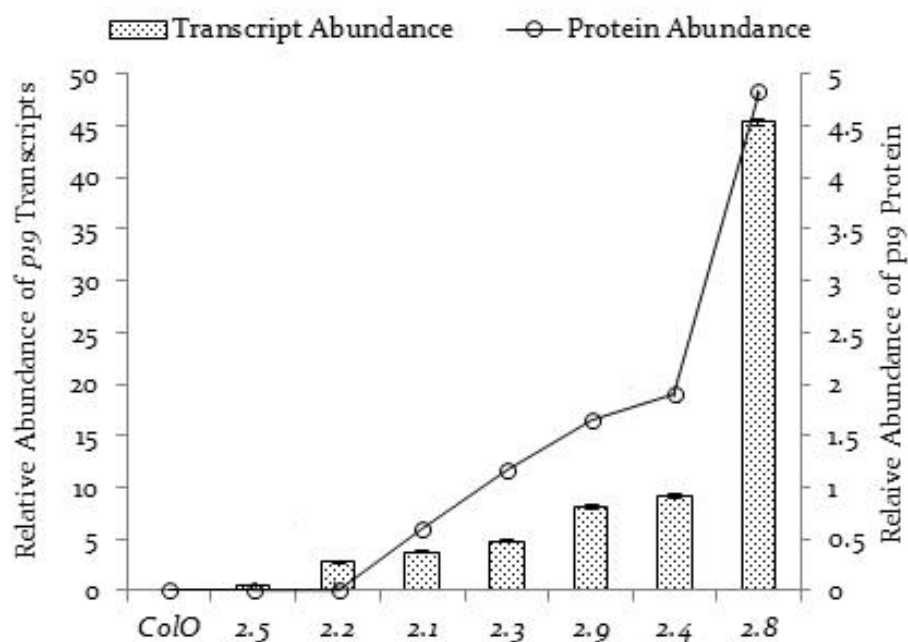
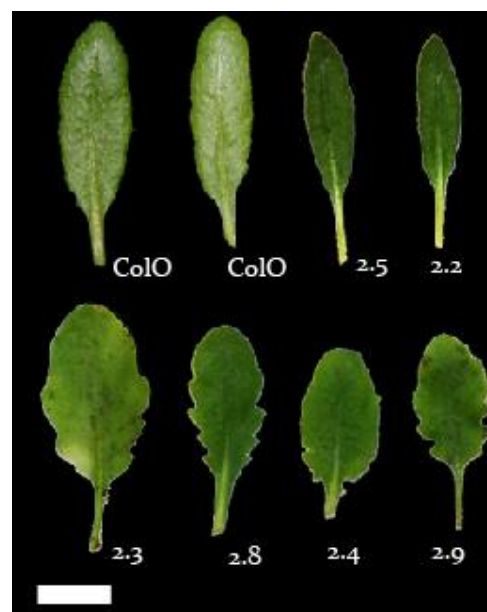


Figure 3.16: Induction of p19 and GUS in Arabidopsis lines containing *pOp::p19*. Multiple T₀ lines were irrigated with 30 μ M dexamethasone solution for a week prior to sampling. The abundance of *p19* transcripts relative to that of *ACT7* is given (dotted column) alongside the amount of protein given relative to the chemiluminescence of a ColO control sample as determined by immunoblotting (hollow circles).

Prolonged cultivation in the presence of dexamethasone led to serration of the leaf margin and the leaves showed reduced elongation (Figure 3.17). The severity of this effect correlated with the extent of p19 protein accumulation (Figure 3.16) and matched that seen in the lines containing p19 under the control of the 35S promoter described above. Induced plants reverted to a phenotype resembling that of ColO after the removal of dexamethasone, although a time lag of 1–2 weeks was seen before a return to normal leaf morphology, and in some instances altered floral morphology was seen a month after irrigation with dexamethasone was halted.

Figure 3.17: Chemically-induced expression of p19 effects leaf architecture in Arabidopsis. Transgenic lines grown on soil irrigated with dexamethasone for six weeks showed the formation of leaves with increased abundance of lobes and serration of the leaf margin. Control lines had a normal leaf phenotype, and the serrated leaf margin was only seen after dexamethasone application. The line number given correlates that that stated in Figure 3.16. Scale = 1cm.



3.2.3.5: *pOp::p19* in *C. gynandra*

The *pOp::p19* construct was transformed into *C. gynandra* via *Agrobacterium*-mediated *in vitro* transformation (Newell *et al.*, 2010). Between one and three regenerative callus balls were recovered from each explant within 4 weeks of culture, although organogenesis was seen within six weeks in about 60% of those recovered. The regeneration of shoots was seen within 12 weeks of culture at an average rate of two to five shoots per 20 callus balls. The induction of root formation was routinely unsuccessful, and only one intact plant was recovered. This was derived from callus tissue rather than a shoot/hypocotyl structure, and so was unsuitable for prolonged culture. Due to the lack of root induction, it was necessary to establish grafts between transgenic shoot scions and wild type root stocks that had already been established in soil.

The establishment of such grafts faced a number of significant technical challenges. The *in vitro* grown material tended to be somewhat hyperhydratic as a result of prolonged culture, which compounded the difficulties of establishing vascularisation between root stock and scion, leading to increased risk of desiccation. Secondly, while the sucrose supplementation of the culture media was reduced in the later stages of culture to promote self-sufficiency of the scions, the ambient light levels were constantly low-level which led to a risk of photodamage when exposed to the elevated light levels under which *C. gynandra* is grown in soil. Finally, *C. gynandra* plants only form substantial stems when approaching flowering. The axillary buds showed rapid induction after removal of the apical bud, often reaching functional maturity before the establishment of vasculature between root stock and scion was fully developed. To avoid problems relating to the maturity of the root stock, all lower leaves and axillary bud material was removed both at the point of grafting and at regular intervals until the graft had established.

The plants were transferred to low light, high humidity environments to prevent desiccation and photodamage. After establishment, it was found that a carefully graduated process of hardening off was necessary before exposure of the graft to normal cultivation conditions. Such a transfer, however, was necessary as it was found the prolonged growth under low light/high humidity promoted the formation of small, short lived leaves and inhibited flowering, as illustrated in Figure 3.18. This was necessary during establishment of the graft, but transfer to normal growing conditions led to normal leaf development and flowering. The production of vegetative stem tissue was promoted by growth under short day conditions, and

chemical fertilisation. Increased stem formation is seen in *C. hassleriana*, but attempts to establish interspecific grafts between *C. gynandra* and *C. hassleriana* were unsuccessful.

Figure 3.18: An established graft between a transgenic *C. gynandra* scion (**S**) and a WT root stock (**R**). The site the graft is indicated with an arrow. A vertical slit was made in the root stock, into which a notch was cut. The base of the scion was cut into a wedge, inserted into the notch and the graft secured with a plastic collar. All axillary buds of the rootstock were removed at the point of grafting, and the plant was left in a high humidity, low light environment to protect the scion from desiccative or photooxidative damage. This environment caused the leaves of the established graft to be small, curled and short lived (illustrated here) but a return to normal leaf morphology was seen upon return to standard cultivation conditions. Scale = 1cm.



Despite these modifications to the grafting procedure, only one transgenic *pOp::p19* line was recovered. This was back crossed with both itself and WT *C. gynandra* individuals in order to provide T₁ seed. As an initial test of the presence of the *pOp::p19* construct, a subset of leaves on the T₀ individual were painted with a 30 μM dexamethasone solution before GUS staining after 24 hours. Those leaves which had been treated with dexamethasone showed GUS activity in a pattern similar to that seen in the *Arabidopsis* transgenics, while the leaves which had not been induced did not show GUS activity (Figure 3.19-A). Once the efficiency of transient surface-applied dexamethasone induction was demonstrated, the effects of induction through soil irrigation were explored. Dexamethasone requires ethanol as a solvent, but the extent of dilution resulted in concentrations of 0.01% in the induction solution. The application of blank ethanol-containing mock induction (MI) solutions to the leaf surface was found to promote a measure of pitting and necrosis which may have been attributable to the effect of ethanol or optical effects of water droplets on the leaf surface promoting photodamage. Secondly, the induction of p19 expression in leaf primordia was desirable in order to assess the effects of p19 expression on the development of Kranz anatomy, but the nature of the apical meristem prevented direct surface application of dexamethasone. To avoid these effects, induction through the transpiration stream was investigated by irrigating the roots with a dexamethasone solution. This promoted systemic expression of GUS in both the cauline leaves and within developing leaf primordia (Figure 3.19-B,C).

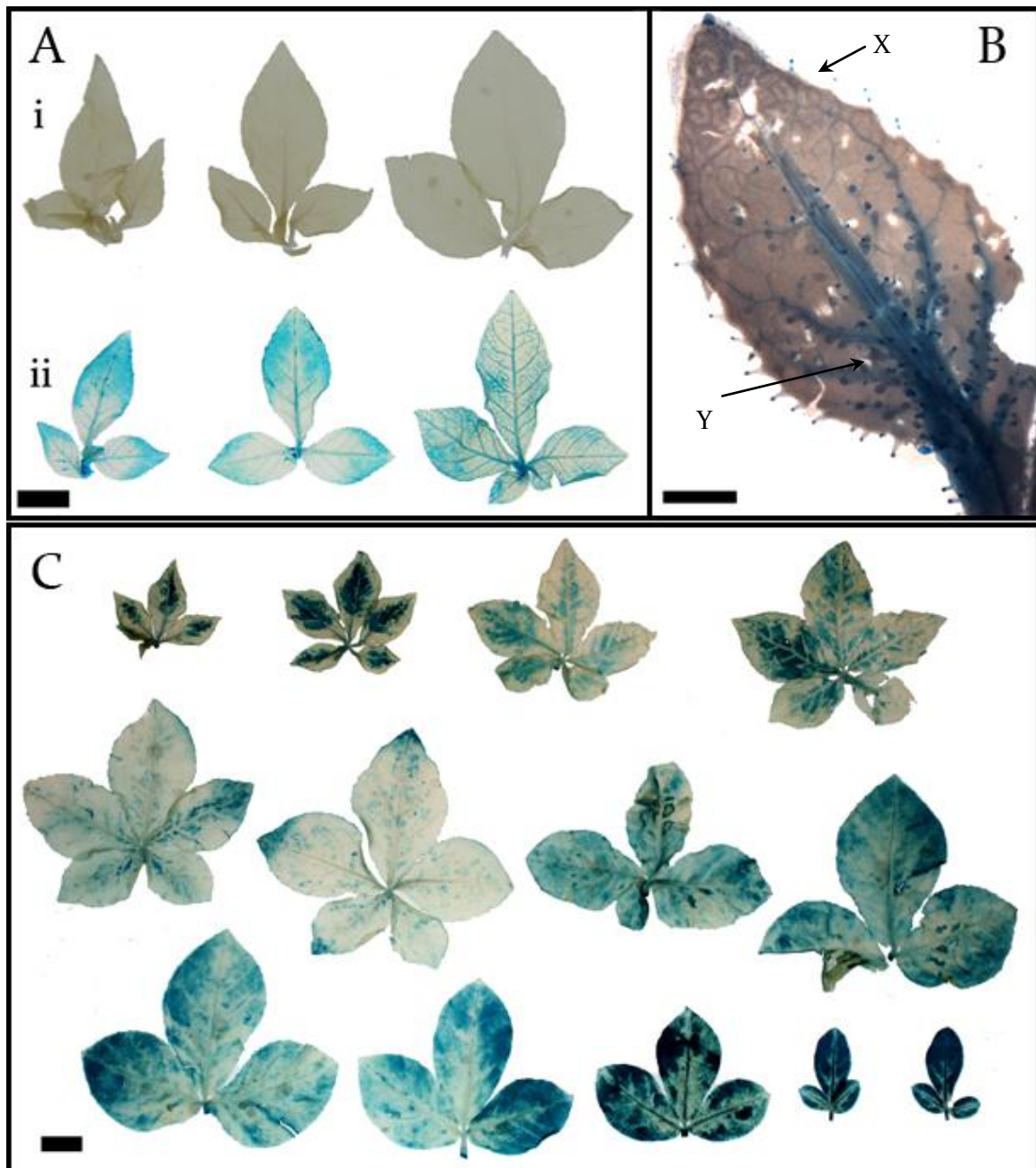
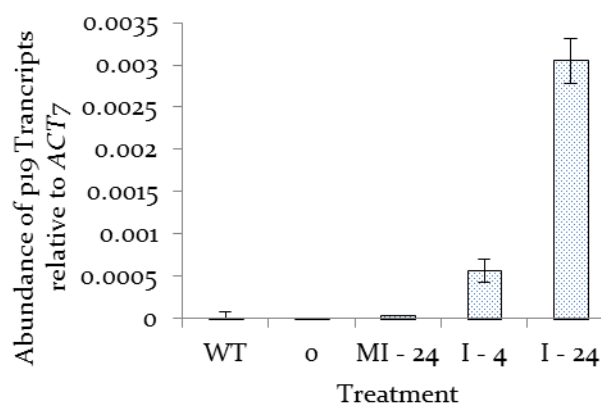


Figure 3.19: GUS expression is inducible in transgenic *C. gynandra* plants. Localised expression within an individual is possible by direct application to the leaf surface (A) as shown by induced (A-ii) and mock induced (A-i) leaves taken from the same individual. Systemic induction is possible through soil irrigation with dexamethasone, leading to GUS expression in all leaves (C, shown in age order). Induction through the transpiration stream is sufficient to generate GUS expression in developing leaf primordia, shown here accumulating in the veins prior to full vascular development (B). The developmental gradient of Kranz anatomy can be seen from the tip (X) to the leaf base (Y). Scale = 1cm (A,C), 1mm (B).

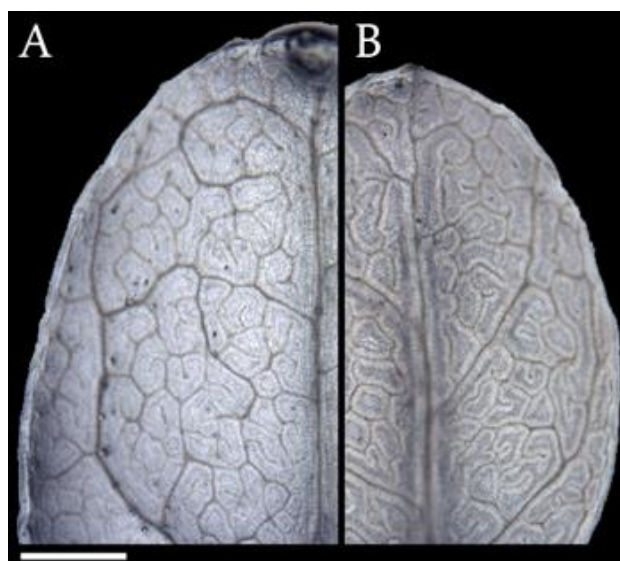
Once GUS induction was confirmed, attempts were made to assess the extent of *p19* accumulation after induction. Individuals from the T₁ generation were induced and sampled for the presence of *p19* transcripts after four and 24 hours, and a high level of *p19* expression was seen in induced (I) individuals between four and 24 hours which was absent in the mock induced (MI) individuals (Figure 3.20).

Figure 3.20: *p19* expression is inducible in transgenic *C. gynandra* individuals when irrigated with dexamethasone solution. No expression was seen at time point 0, and expression remained negligible in the mock induced individuals after 24 hours (MI - 24). Induced individuals (I) showed a marked increase in *p19* accumulation between 4 and 24 hours.



Given the correlation between GUS expression and *p19* accumulation, and that GUS expression was detectable in the developing primordia of induced *C. gynandra* plants, it was considered likely that *p19* could be induced before leaf development. The development of Kranz anatomy occurs in a basipetal direction when the leaf is 4-7mm in length, a period of development which can be seen occurring in Figure 3.19-B. Transgenic lines were cultivated in the presence of dexamethasone for a month before the developing leaves were examined. Samples were taken beyond the stage at which Kranz anatomy should have developed, and Kranz anatomy was evident in both the induced and MI lines (Figure 3.21). In addition, the developed leaves appeared normal, and no significant morphological phenotype was recovered.

Figure 3.21: *p19* expression does not alter the development of Kranz anatomy in *C. gynandra*. The leaves of plants cultivated on dexamethasone-containing soil showed fully developed Kranz anatomy in both mock-induced (A) and induced (B) plants. In addition, general leaf development appeared unaffected. Scale = 1mm.



Once successful systemic induction of *p19* expression was established through soil-based application of dexamethasone, a course of week-long induction of *p19* was carried out before photosynthesis was assessed. Successful induction was confirmed *via* GUS staining. *p19* expression had considerable impact on photosynthesis in *C. gynandra* (Figure 3.22, Table 3.6). While quantum efficiency was constant between induced and mock-induced (MI) individuals, the level of dark respiration was increased from -1.2 to -2.0 $\mu\text{mol CO}_2 \text{ m}^{-2} \text{ s}^{-1}$ in *p19*-expressing individuals ($p = 0.01$). The increased dark respiration combined with the constant quantum efficiency increased the light compensation point in *p19* expressing individuals by 17 $\mu\text{mol m}^{-2} \text{ s}^{-1}$ ($p = 0.03$). Analysis of the response of photosynthesis to internal concentrations of CO₂ allowed both carboxylation efficiency and the CO₂ compensation point to be derived. Induction of *p19* reduced carboxylation efficiency (an increase of 0.05 $\mu\text{mol mol}^{-1}$ from the MI individuals, $p = 0.08$) and increased the CO₂ compensation point (an increase of 13 $\mu\text{mol Q m}^{-2} \text{ s}^{-1}$ from the MI individuals, $p = 0.03$). Finally, the P_{Max} of induced individuals was reduced by 3.0 $\mu\text{mol CO}_2 \text{ m}^{-2} \text{ s}^{-1}$, but this was not statistically significant.

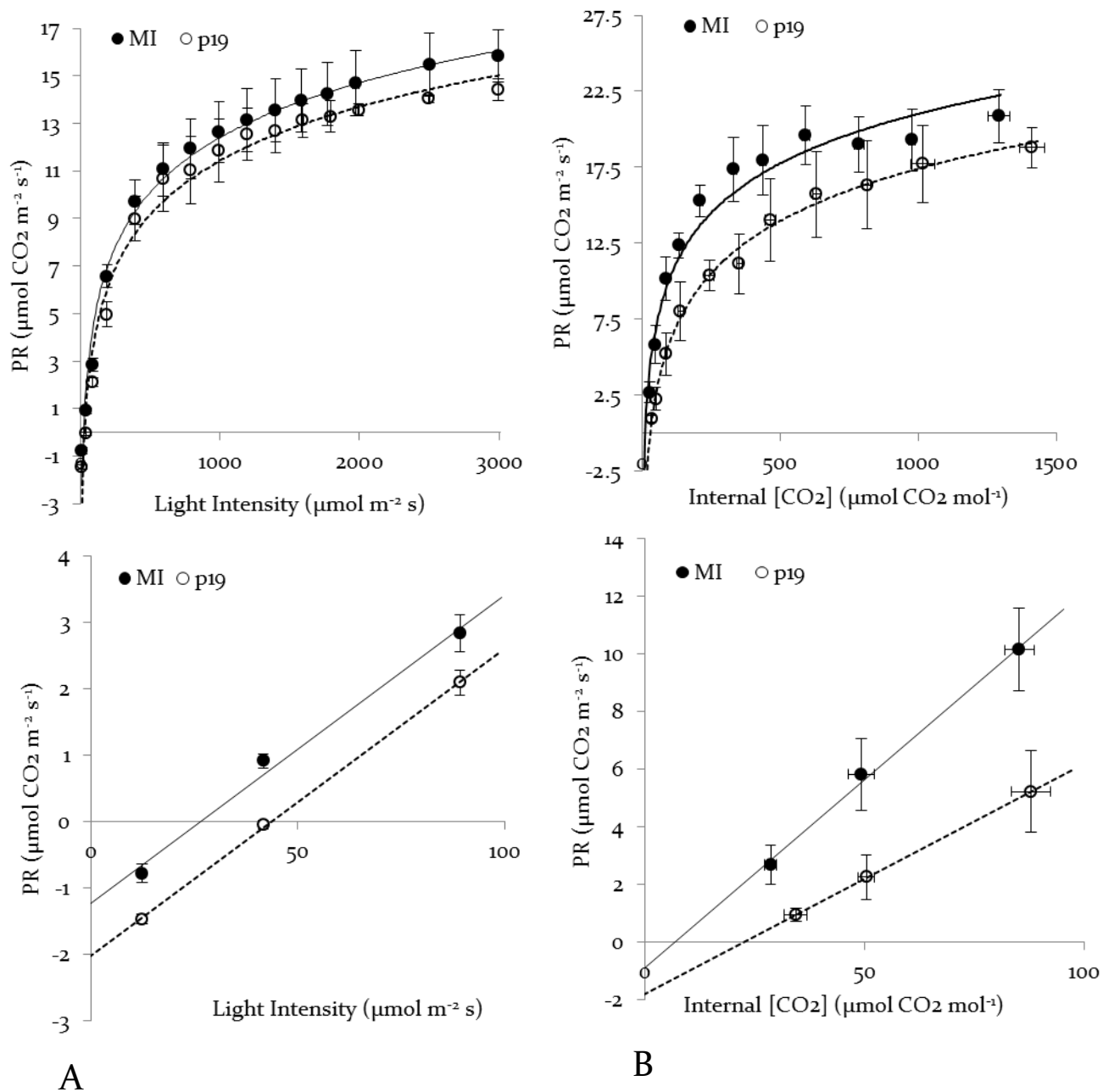


Figure 3.22: p19 expression effects photosynthesis in *C. gynandra*. Under changing light intensity (**A**) quantum efficiency is not altered, but an increase in dark respiration is evident. Under changing CO₂ concentrations (**B**) the carbon compensation point is increased, while carboxylation efficiency is depressed.

	Quantum Efficiency	Carboxylation Efficiency	Dark Respiration	Light Compensation Point	Γ	P_{Max}
MI	0.05 ± 0.003	0.13 ± 0.018	-1.22 ± 0.22	26.40 ± 4.61	8.97 ± 0.75	20.85 ± 1.77
p19	0.05 ± 0.002	0.08* ± 0.011	-2.01* ± 0.08	43.57* ± 2.10	21.98* ± 2.56	18.80 ± 1.32

Table 3.5: p19 expression effects photosynthesis in *C. gynandra*. While the quantum efficiency ($\mu\text{mol CO}_2 \mu\text{mol m}^{-2} \text{s}^{-1}$) remains constant between p19-expressing and mock induced (MI) individuals, an increase in dark respiration ($\mu\text{mol CO}_2 \text{m}^{-2} \text{s}^{-1}$) is seen which leads to a corresponding increase in the light compensation point ($\mu\text{mol Q m}^{-2} \text{s}^{-1}$) at 400 $\mu\text{mol mol}^{-1} \text{CO}_2$. A significant difference is not seen in the maximum rate of photosynthesis (P_{Max} , $\mu\text{mol CO}_2 \mu\text{mol Q m}^{-2} \text{s}^{-1}$). The carboxylation efficiency (Γ , $\mu\text{mol mol}^{-1}$) is increased with p19 expression, while the carboxylation efficiency ($\text{mol CO}_2 \text{m}^{-2} \text{s}^{-1}$) is decreased. Those values that showed a p value below 0.05 between MI and p19 values are marked (*).

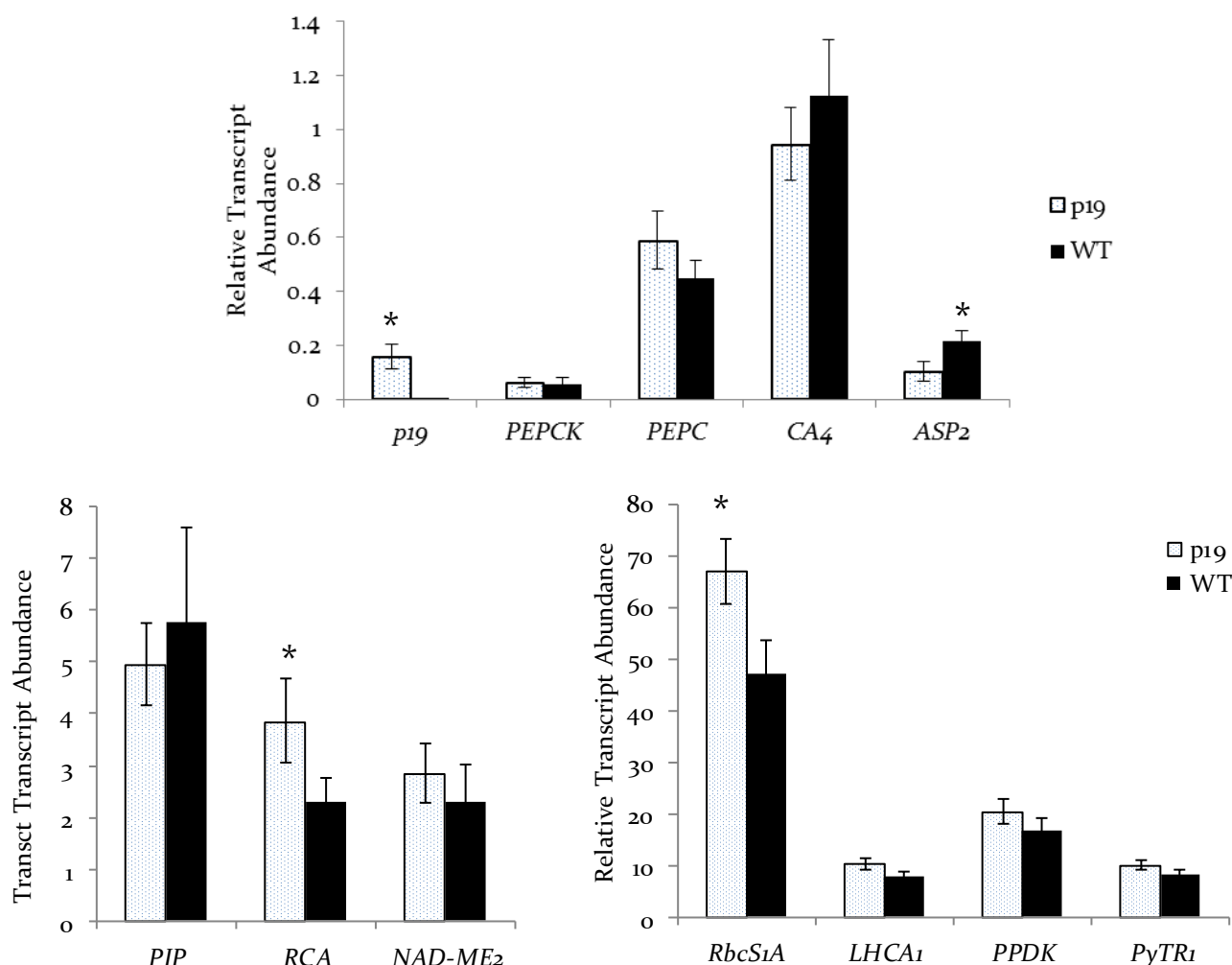


Figure 3.23: Changes in transcript abundance in *C. gynandra* are detectable that may be attributable to p19 expression. Some genes do not show significant changes in abundance between p19-expressing and mock-induced individuals (e.g. *PYR*, *CA4*, *PSBQ2*), while *PEPC*, *RbcS1A*, *RCA* and *ASP2* show levels of abundance which are significantly elevated relative to the MI individuals. Those transcripts which showed a difference with a p value less than 0.1 are marked with an asterisk (*). Transcript abundance is relative to *ACT7*.

Concurrent with the photosynthetic analysis, RNA and protein samples were prepared for quantification. Analysis of relative transcript abundance (Figure 3.23) showed that most components of the C₄ cycle maintained comparable levels of expression between p19-expressing and MI individuals. Although some average expression values differed, these were not statistically significant (e.g. *RbcS1A*, *PEPC*). However, two genes showed statistically significantly elevated levels of expression when p19 was expressed compared with the MI individuals: *RCA* (+ 53%) and *RbcS* (+ 23%). While such differences were detectable at the transcript level, no significant variation was seen in the abundance of protein (Figure 3.24). While antisera against all components of the pathway were not available, no changes were detected in the rate of accumulation of either subunit of RuBisCO. No antisera were available for *RCA* or *ASP2*, so the differences in transcript abundance that had been detected for these two genes could not be assessed.

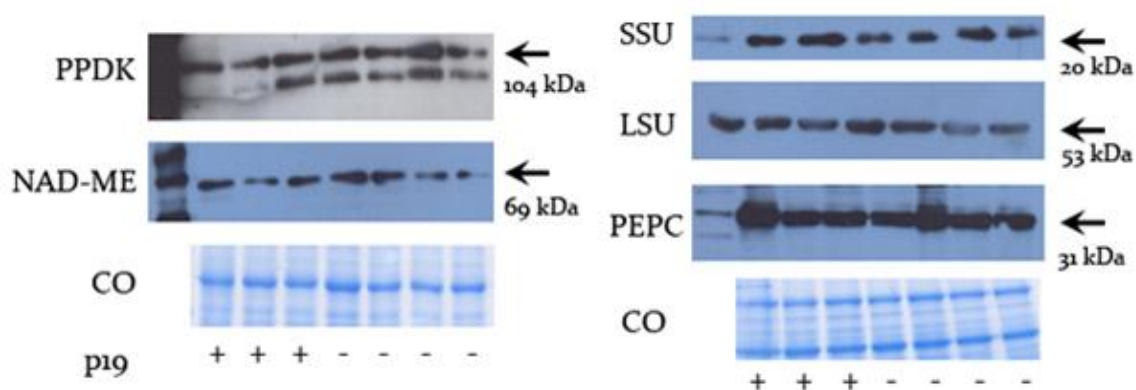


Figure 3.24: p19 expression does not affect protein accumulation in *C. gynandra*. Protein abundance for PPDK, NAD-ME, PEPC and the SSU/LSU of RuBisCO are constant between individuals expressing p19 (+) and the MI controls (-). 10µg of total protein extracts prepared from mature leaf tissue were run out on 10% denaturing polyacrylamide gels prior to treatment with an appropriate antisera. The molecular weight of the expected band is given next to each blot, and a Coomassie-stained parallel gel to demonstrate equal protein loading rates.

3.3: Discussion

3.3.1: miRNA Prediction

A library of sRNA sequences in *C. gynandra* was compiled with good coverage between 18-25nts. The presence of previously described miRNA sequences within the library showed not only that sRNAs in *C. gynandra* are conserved when compared with other species, but also that the method used to compile the library was sufficient to obtain reads for functional miRNAs. An initial search indicated that hits against potential target genes were over-represented in some C₄ genes (*RbcS*, *RCA*, both isoforms of *PPDK* and of *NAD-ME*) which corresponded with the over-representation of sRNA hits against C₄ genes in maize (Tolley *et al.*, unpublished). These reads may represent mRNA decay products or endogenous sRNAs (Kim & Nam, 2006). The absence of genomic DNA sequence for *C. gynandra* meant that it was not possible to identify miRNA sequences on the basis of a separately encoded hairpin precursor. The presence of such a precursor can be identified by RNA blots (Berezikov *et al.*, 2005), but this approach would be challenging due to the large number of candidates. Therefore, it was necessary to examine the alignment patterns of mismatch reads against ESTs.

3.3.2: Over-Representation of Hits against Certain C₄ Genes

A number of distribution patterns along target transcripts were evident. Some sequences (e.g. *PEPC2*) showed a diffuse pattern of reads with little overlap which was taken to indicate that the presence of an underlying miRNA sequence was unlikely. In some cases, an aggregation of reads aligned against a single site created a concatenated sequence greater than 24nt (e.g. *NAD-ME2*), and these may contain an underlying miRNA sequence. However, numerous alignments in the uni- or bidirectional orientation were recovered and in some instances these contained sequences in both orientations. The nature of the sequencing method used should ensure that read orientation is retained, and so reads in the sense direction were classified as probable decay products. While sense alignments may indicate DNA-based activity such as methylation (Chellappan *et al.*, 2010, Bao *et al.*, 2004), a broad screen of methylation sites would be challenging. In addition, methylation of base DNA would need to occur during the acquisition of C₄ competency, and so these miRNAs could not be regulated to maintain process in a mature C₄ leaf.

The genomic sequence of *PPDK* showed high read alignment in both sense (17 & 125 reads) and antisense (20 reads) directions. These sites were within introns and so are unlikely to represent a regulatory miRNA targeting the transcript. Interestingly, this pattern of over-

accumulation is present in the *C. gynandra* sRNA library compiled by Aubury (unpublished) but is absent from comparable data in Arabidopsis. These data may indicate a potential role for methylation, or transcript decay products. While attempts were made to screen for cleavage products of *PPDK*, the apparent inability to recover products greater than 500bp for a 5'RACE reaction limits the extent to which this method can be utilised to screen for cleavage products. The major sRNA alignment clusters against *PPDK* occurred far into the 3' region of the transcript (Figure 3.4: C-F), and it is likely that considerable optimisation of the RACE procedure would be required before a satisfactory level of amplification could be achieved to test for cleavage products at these sites.

22 antisense reads aligned to a single site in the transcripts of *MDH*, giving a sequence of 20nt with a pair of highly supported mismatches and so represent a good candidate miRNA sequence. A large amount of sequence aggregation exceeding the 24nt threshold was seen in other targets, such as the 36nt region covered by 17 reads in *CA₄*. Similar aggregations were seen against *RbcS*, *NAD-ME* and *ALT1*. The sequences covering these loci were examined for conserved sequences present in previously described miRNAs, as the high level of conservation within miRNA families has facilitated miRNA prediction previously (Zhang *et al.*, 2005).

Those sequences targeting *NAD-ME₂* bear the closest resemblance to miR399 and miR2111 which have been described as playing roles in regulating phosphatase transporters (Jones-Rhoades & Bartel, 2004) and phosphate metabolism (Hsieh *et al.*, 2009) respectively. miR5293 showed close relatedness to a sRNA read aligning against *PPDK*, although the activity of miR5293 has been related to the formation of mycorrhizal relationships in *Medicago* (Devers *et al.*, 2011). sRNA reads aligning against *RbcS* and *ALAAT1* showed similarity to miR4398 and miR5655 respectively, although the function of the targeted sequences for these miRNAs have yet to be established. While variation is seen in miR2111 and miR399 between divergent lineages, the extent of this variation is not sufficient to indicate that the proposed miRNA sequences are members of either family. Equally, the proposed target sites do not show complementarity to either miRNA family, making it unlikely that *NAD-ME* is targeted by members of the miR2111 or miR399 families.

While sequence conservation can be effective in identifying miRNAs (e.g. Zeng *et al.*, 2010) this approach is limited. For example, Lu *et al.* (2005; 2008) described over 50 miRNA sequences from *Populus trichocarpa* via sRNA cloning that were not found in Arabidopsis. Therefore, it is conceivable that novel miRNAs are active in *C. gynandra* which target

components of the C₄ cycle, but show no similarity to reads present in Arabidopsis. However, given the close phylogenetic proximity of *Cleome* to Arabidopsis (unlike *Populus*) some measure of sequence conservation is to be expected. Regulatory miRNAs could be recruited by two routes into the C₄ cycle: mutation of the miRNA to target a C₄ gene or by modification of the C₄ gene to possess a miRNA targeting site. In either scenario, some measure of ancestral conservation would be expected.

3.3.3: The Identification of Potential Regulatory miRNA Sequences in *C. gynandra*

While the approach outlined above did not specifically identify miRNA sequences that regulate the C₄ cycle, an uneven distribution of sRNA reads aligning against the components of the C₄ cycle was found, and this was similar to that reported in maize (Tolley *et al.*, unpublished). This pattern of sRNA alignments may indicate underlying miRNA activity in a number of instances.

While it is possible that novel miRNA sequences are active in *C. gynandra*, the lack of a sequenced genome means that miRNAs can only be compared to EST sequences. A key area of C₄ regulation which is poorly understood is the nature of *trans*-acting factors which may bring about the cell-type specific patterning associated with the C₄ cycle. Given that the vast proportion of miRNAs target transcription factor families (Carrington & Ambros, 2003), if miRNAs are involved with regulating the C₄ cycle then they are most likely to target the *trans* acting factors rather than the specific components. Therefore, a lack of understanding of the transcription factors involved with the C₄ cycle means that it is not possible to explore the most likely area of miRNA activity using bioinformatics with data taken from a sRNA library.

3.3.4: Establishing Transgenic Lines

In vitro transformation of the 35S::p19 construct into *C. gynandra* was successful, but the severity of the phenotype prevented establishment of transgenic lines. The successful utilisation of the inducible pOp::p19 construct in Arabidopsis therefore provided a method of by-passing this. Recovery of *C. gynandra* transgenics containing the pOp::p19 construct was limited to a single line. Two transgenic calli generated roots *in vitro* (this represents a recovery rate of less than 0.1%) and time restrictions meant that obtaining more rooted plantlets was not possible. While root formation can be impacted by a wide range of factors including osmotic conditions, nutrient composition, growth regulator choice and explant material (Marks & Simpson, 2000; Conner & Falloon, 1993; Parra & Amo-Marco, 1996), the formation of roots seen in this study indicates that the current system is capable of root induction. It is likely that root formation is triggered either by variation in media composition (e.g. localised

depletion of components, or accumulation of breakdown products) or callus stress, although further exploration of these aspects would be worthwhile if this study were to be extended.

As an alternative, transgenic scions were grafted onto wild type root stocks. While optimisation of the process was undertaken, it was still difficult to promote graft establishment, meaning that only one transgenic line was recovered. Therefore, the conclusions drawn from this study should be considered in this light. While the transformation of the *pOp::p19* into Arabidopsis was primarily carried out to test its functionality, it remains an effective system to explore the effects of the inhibition of miRNA activity in a spatial and temporal fashion.

3.3.5: Constitutive expression of p19 alters leaf and flower anatomy in Arabidopsis

Expression of p19 led to the formation of individuals with heavily lobed, serrated leaves which showed stunting, premature flowering and the formation of flowers with malformed sepals, petals and anthers which were effectively sterile. The depressed rate of transgenic recovery at the T₀ stage could be attributable to the effect of strongly expressing p19 lines in that highly expressing individuals were incapable of surviving after transfer to soil. *In vitro* cultivation of transgenics was attempted to bypass this, but this was prevented by the secondary phenotypic effects caused by prolonged *in vitro* culture of Arabidopsis.

Numerous pathways in leaf regulation are subject to miRNA regulation. For example, transgenic lines overexpressing the *TCP3* transcription factor show the formation of serrated leaf margins, matching that shown in the p19-expressing lines generated by this study (Koyama *et al.*, 2007). The *TCP* family is negatively regulated by miR164, the precursor to which is encoded by the *JAW* locus, and loss-of-function *jaw* mutants produce serrated leaf margins and altered leaf morphology (Palatnik *et al.*, 2003). Therefore, the effects of p19 expression can be attributed to its effects on miRNA activity rather than a direct effect on the p19 protein itself.

The effects of p19 expression on internal leaf anatomy have not been described previously, and this study indicates that p19 expression has a significant effect on internal leaf anatomy (Figure 3.8-C). While WT Col-O leaf material shows the standard arrangement of palisade and spongy mesophyll, this arrangement was greatly disrupted in p19-expressing individuals. In addition, p19 expressing lines demonstrated irregular and enlarged epidermal cells. Again, the loss of miRNA-mediated regulation of *PHAVOLUTA* promotes disorganised adaxial mesophyll and palisade development in *Nicotiana* (McHale & Koning, 2004), and over-expression of

TCP3 causes undifferentiated, rounded epidermal cells (Koyama *et al.*, 2007). Therefore, the effects of p19 expression on internal leaf anatomy are considered to be *via* interference with the miRNA regulatory pathway.

The expression of p19 causes a phenotype similar that which has been reported for miRNA inhibition by previous authors (e.g. Dunoyer *et al.*, 2004). The latter authors note, however, that the p19 phenotype remained constant despite variation in expression levels (unlike that of P1-HCPro which showed a dose-dependent response). This contrasts with the results of this study which illustrate a correlation between the phenotype severity and the extent of p19 accumulation. Due to the activity of p19 as a competitive inhibitor (Vargason *et al.*, 2003; Lakatos *et al.*, 2004), it is conceivable that elevated p19 accumulation will increase its effectiveness as a competitor for dsRNA, hence increasing of the resultant phenotype.

Flowering was seen only in weakly expressing Arabidopsis lines, and altered floral morphology was evident in these instances. p19-expressing lines showed a reduction in stem formation with maximum cauline leaf development, leading to a dense, conical growth habit (Figure 3.9-C,D) which eventually produced a prematurely terminated raceme, and pollen dehiscence was not recorded. Similar phenotypes have been reported in other instances of p19 and P1-HCPro expression (Dunoyer *et al.*, 2004; Lakatos *et al.*, 2006), further supporting the hypothesis that the p19-induced phenotype is attributable to its effects on miRNA activity.

3.3.6: p19 Expression can alter Leaf Anatomy of *C. gynandra*

C. gynandra containing *35S::p19* showed a strong phenotype with stick-like, radialised leaves and little to no mesophyll development. The lack of expansion of the leaf blade in p19-expressing transgenics is considered to be attributable to the lack of vein development. Mesophyll development does occur, but the reduction in venation has prevented the expansion of the leaf blade away from leaf midrib. This phenotype correlated with the accumulation of p19 at the transcript level, and so was presumably related to the activity of p19 at the protein level. The radialisation of leaf tissue correlates with loss-of-function mutants of *PHABULOSA* and *PHAVOLUTA* (Mallory *et al.*, 2004) which are subject to miRNA regulation, and to mutants deficient in *AGO1* (Kidner & Martienssen, 2004). The severity of the phenotype recovered in transgenic individuals exceeds that seen in the Arabidopsis *35S::p19* expressing lines. While it is difficult to draw comparisons between soil- and *in vitro*-grown material, it is conceivable that carbohydrate supplementation of the culture media used in *C. gynandra* cultures was sufficient to promote growth of organs that would be unsustainable in a soil-grown individual due to the lack of photosynthetic tissue production. The initial *in vitro*

cultures demonstrated that p₁₉ was effective in *C. gynandra*, but the severity of the phenotype meant that it was not possible to recover stable expressing lines from the established cultures. While RNA and protein quantification would have been possible, any changes may have been caused by the *in vitro* cultivation process rather than the effect of p₁₉ on the C₄ cycle.

3.3.7: p₁₉ Expression can be induced in *C. gynandra* and Arabidopsis

Placing p₁₉ under the control of the inducible *pOpON* promoter (Samalova *et al.*, 2005) facilitated transient expression of p₁₉ in both Arabidopsis and *C. gynandra*. Testing the system with Arabidopsis showed that GUS accumulation was detectable within 4 hours of the application of 20–50µM dexamethasone solution to the leaf surfaces, and p₁₉ was detectable at the transcript and protein level only after induction. Prolonged induction led to a phenotype matching that seen in plants containing p₁₉ under the control of the *CaMV 35S* promoter.

Surface application of dexamethasone led to the development of necrotic patches and curvature of the leaf in *C. gynandra*, but these effects were seen in mock-induced individuals and so the effects were attributed to the ethanol used as a solvent rather than dexamethasone itself, supporting the findings of Samalova *et al.* (2005). As root irrigation was used for induction throughout the study, these problems were bypassed. It was not possible to assess the impact of a functional *pOp* promoter in the absence of p₁₉ expression. Craft *et al.*, (2005) and Sheldon *et al.* (2008) reported no detrimental effects of *pOp* expression in control lines, but testing of an empty *pOpON* vector would be advisable if this study were extended.

In *C. gynandra*, systemic expression of GUS was detectable within 24 hours of soil irrigation with dexamethasone, to the extent that it could be detected in the apical bud and developing leaf primordia (Figure 3.9-B). The distribution of GUS was unequal, however, with highest levels of expression seen in the oldest and youngest leaves (Figure 3.9-C). Samalova *et al.* (2005) reported an unequal distribution of GUS expression, although the greatest GUS expression was seen in mid-aged leaves, with reduced expression in the youngest and eldest leaves. It is conceivable that differences in transpiration rates between leaves may be responsible for this variation. While the origin of the unequal GUS expression remains obscure, the leaf tissue sampled for this experiment was taken from the youngest mature leaf, a site which should have shown maximal p₁₉ expression.

3.3.8: Induced expression of p₁₉ does not affect the development of Kranz Anatomy

The accumulation of GUS in primordia of plants irrigated with dexamethasone was detectable at a stage before full development of Kranz anatomy had occurred (3.19-B). Prolonged

induction, however, did not yield any modification in leaf anatomy either in terms of gross leaf structure or formation of Kranz anatomy. Due to the low RNA yields from primordial tissue it was not possible to validate *p19* expression in the developing leaves, but given the correlation between the accumulation of GUS and *p19* seen in other tissues, it is likely that *p19* was being expressed in the developing leaves. As *p19* is capable of producing a vegetative phenotype in *C. gynandra* when controlled by the *35S* promoter, but follows a dose-dependent response in *Arabidopsis*, it is conceivable that the lack of a vegetative phenotype in the *pOp* promoter line is due to relatively low levels of *p19* expression.

3.3.9: *p19* expression negatively impacts photosynthesis in *C. gynandra*

Analysis of photosynthetic gas exchange of the *p19*-expressing and mock induced (MI) *C. gynandra* individuals demonstrated a number of significant differences. The MI individuals had a carbon compensation point (Γ) of 8.9 $\mu\text{mol m}^{-2} \text{s}^{-1}$, which is comparable to values published by Voznesenskaya *et al.* (2007) and Marshall *et al.* (2007). The average Γ values reported for other C₃ members of *Cleome* given by these authors is between 40–65 $\mu\text{mol m}^{-2} \text{s}^{-1}$. However, in *p19*-expressing individuals, Γ is increased to an average of 22.0 $\mu\text{mol m}^{-2} \text{s}^{-1}$, and while this does not approach the Γ of C₃ taxa (Marshall *et al.*, 2007), this is significantly higher than in functional C₄ leaves. The cause of this increase appears to be two-fold: firstly, the level of dark respiration in C₄ *p19*-expressing individuals is increased by 0.8 $\mu\text{mol CO}_2 \text{ m}^{-2} \text{ s}^{-1}$, and the carboxylation efficiency (CE) is decreased by 0.05 $\text{mol m}^{-2} \text{ s}^{-1}$. The quantum efficiency was not significantly different between MI and *p19*-expressing individuals, so initial photochemistry is not being disrupted.

While the effects of *p19* expression on photosynthesis have been quantified, the cause of these effects is yet to be identified, and a number of components may be responsible for the changes in Γ and CE. For example, Γ may increase due to changes in light-dependent non-photorespiratory CO₂ production (e.g. nitrate metabolism, Guo *et al.*, 2005), or to changes in photorespiration. Furthermore, dark respiration values are relatively equal between C₃ and C₄ species (Byrd *et al.*, 1992), so while a return to C₃-like values is seen in the CE, the increase in dark respiration may represent an effect independent of C₃ and C₄ photosynthesis. Therefore, it would be advisable to quantify the extent of photorespiration (Brooks & Farquhar, 1985) in order to separate these effects.

The observed changes in CE may be due to changes in the activity of RuBisCO or other components of the C₄ cycle. Changes in RuBisCO activity can lead to a depression in CE (Jacob & Lawlor, 1992), while CE and dark respiration can be altered by metabolic instability.

For example, exposure to ozone or heavy metal toxins can depress CE due to direct effects on photosynthetic pathways, while dark respiration increased in line with elevated protein turnover rates (McLaughlin *et al.*, 1991; Reich, 1983; Parys *et al.*, 1998). Therefore, the photosynthetic effects observed in this study may be due to single or multiple causes, which may or may not be directly attributable to photosynthesis.

If p19 is affecting photosynthesis directly, it may destabilise the patterns of gene expression associated with the C₄ cycle. For example, a collapse of cell-type specific expression caused by negative regulation *via* a miRNA may be detectable at the transcript or protein level. The establishment of strict C₄ patterning is considered integral to the optimisation of the C₄ pathway (Hibberd & Covshoff, 2010), so it is conceivable that a partial reversal of this may lead to increased inefficiency manifesting as the changes in Γ and CE recorded here.

3.3.10: p19 Expression alters Transcript, but not Protein Accumulation

If the changes in Γ and CE are attributable to reduced negative regulation of a component of the C₄ cycle, then the altered patterns of accumulation may be detectable at the transcript or protein level. At the transcript level, multiple genes show equal expression between the induced and MI individuals, indicating that p19 expression does not universally effect endogenous gene expression. While a number of genes showed a slight increase in relative abundance after p19 expression, transcripts of *RCA*, *RbcS* and *ASP2* show a statistically significant difference between p19 expressing a MI lines, with *RCA* and *RbcS* showing an increase in response to p19 expression. Both transcripts showed an abnormally high level of read accumulation during the analysis of the sRNA library. While no definitive miRNA sequences were identified from these alignments, they still represent potential sites of underlying miRNA activity, and the increase in transcript abundance seen with p19 expression may signify a reduction in negative repression.

Interestingly, the upregulation of RuBisCO and/or *RCA* may explain the observed changes in gas exchange properties seen after p19 induction. The effects of overexpressing a single component of the C₄ cycle has not been fully explored to date, and so it is not possible to state that the changes in photosynthesis observed in this study are derived from changes in overexpression of a C₄ component as a result of a removal of negative regulation by a miRNA. Sage (2004) notes that as part of optimisation of the pathway during its early evolution, significant changes in expression of both existing and newly recruited genes in order to maximise the efficiency of the cycle. Therefore, any disruption of the cycle caused by an over accumulation of a single component which upsets the core metabolite flow could lower net

photosynthetic efficiency. Quantification of enzyme activity was not included in this study, but screening the core components of the C₄ cycle for changes in activity after p19 expression may enable the identification of any induced changes, attributable to the specific enzyme or its regulators that may occur in a background of p19 expression.

While correlations may be seen between changes in transcript abundance and the small RNAs identified from sequencing, these effects are not seen at the protein level. Of the proteins assessed by this study, relatively equal levels of accumulation were seen between induced and MI plants, although abundance of RCA was not examined. Some discrepancy is seen between accumulation of transcripts and protein level, which may be indicative of two potential scenarios. Firstly, these genes may be subject to multiple levels of control: a failure of regulation at the transcript level is superseded by a second, redundant, regulatory pathway at the protein level, a system which has been described in *Amaranthus* (McCormac *et al.*, 1997). Alternatively, the changes in photosynthetic response may be due to changes in abundance or activity of a variety of other genes which have not been explored in this study.

A key extension for this work, in addition to profiling enzyme activities, would be the utilisation of *in situ* immunolocalisation or RNA hybridisation to identify any changes in the cell specificity of the components of the C₄ cycle. This would not only bypass the problems associated with whole-tissue qRT-PCR analysis, but would provide definitive evidence of any loss of expression patterning as a result of p19. In addition, utilisation of a single transgenic line in this study means that it has not been possible to explore any dose-dependent response of photosynthesis. Therefore, it would be advisable to expand this study to include additional lines.

Additional lines of exploration would be possible if two key areas were addressed. Firstly, the provision of an annotated genome for *C. gynandra* would allow for the identification of both target and miRNA-precursor site identification (Wang *et al.*, 2005; Lu *et al.*, 2005). The ability to screen for both sequences would not only enable more effective prediction of miRNAs, but also of their targets. Secondly, an improved transformation protocol for *C. gynandra* would enable a number of transgenic routes to be explored. For example, fusion of proposed target sites to *uidA* sequences could be a rapid way of testing for M/BS specificity of proposed miRNAs (e.g. Millar & Gubler, 2005). Mutants deficient in miRNA silencing pathways have been used to identify regulatory miRNAs previously (e.g. Vaucheret *et al.*, 2004), although these examinations have mostly focused on developmental pathways. Generation of such mutants in *C. gynandra* may be prohibitively complex, and it was hoped that similar effects

could be achieved through the use of the p19 protein in this study. Finally Srivastava *et al.* (2012) identified stress-induced miRNAs in *Brassica juncea* through microarray analysis using probes against known miRNA sequences, and it is possible that this method could be applied to *C. gynandra* upon further exploration of the sRNA library. These mechanisms could be adapted to *C. gynandra*, and may prove effective in obtaining more finite miRNA predictions.

3.3.11: Concluding Remarks

Overall, these data may provide support for the hypothesis that miRNA-mediated regulation may play a role in regulating C₄ photosynthesis. This has been demonstrated in a transgenic *C. gynandra* line that has shown a reduction in carboxylation efficiency and an increase in the carbon compensation point in response to inhibition of miRNA biosynthesis by the p19 protein. Two genes (*RbcS* and *RCA*) show high levels of sRNA alignment and statistically significant increases in relative transcript abundance after p19 expression, although this does not appear to persist to the protein level, indicating that these changes may not be the origin of the observed changes in photosynthetic capacity.

Through the utilisation of sRNA profiling, it has been demonstrated that a disproportionate accumulation is seen in sRNA reads aligning against certain genes of the C₄ cycle in *C. gynandra*. While it has not been possible to specifically identify a conserved miRNA sequence targeting known components of the C₄ cycle, a number of focused accumulations of sRNA reads are sufficiently disproportionate to warrant further examination to test whether an underlying miRNA sequence may be present.

While a specific regulatory miRNA has been identified by this study, there are indications that miRNAs may have a role to play in establishing or maintaining the C₄ photosynthetic cycle. Several areas of this study could be extended to further in order to evaluate the areas highlighted by the data here reported.

4. Changes in Gene Regulation during Cotyledon Development

4.1: Introduction

4.1.1: Both Environmental and Developmental Factors may Influence the C₄ Cycle

One approach to examine gene regulation associated with the C₄ cycle is to investigate changes which occur during development. The onset of C₄ photosynthesis may occur at a predetermined developmental stage (Wang *et al.*, 1993b) or in response to environmental stimulation (e.g. Langdale *et al.*, 1988). While variation may be seen within and between lineages, the changes in gene expression that occur during maturation of a C₄ leaf or cotyledon may yield insights into methods of regulation of the C₄ cycle.

Illumination can trigger significant changes in gene expression, and is both sensed and transduced in a variety of ways (Desprez *et al.*, 1998, Ma *et al.*, 2001). For example, specific wavelengths can be detected *via* photosensitive pigments such as phytochrome and cryptochrome (e.g. Neff *et al.*, 1994; Lin, 1998). Alternatively, light responses may be mediated by electrochemical gradients across the thylakoid membrane such as in the translational repression of *psaA&B* (Klein & Mullet, 1987; Kim & Mullet, 2003). Light has been shown to have a significant regulatory effect on the C₄ cycle in various species. In maize, neither PEPC nor PPDK accumulate to detectable levels in darkness and light is necessary for cell-type specific upregulation of both enzymes (Langdale *et al.*, 1984, Matsuoka *et al.*, 1993). RuBisCO accumulates at the same developmental stage in light- and dark-grown leaves of maize, albeit at lower levels in darkness (Nelson *et al.*, 1984), with proteins of both subunits accumulating in both the mesophyll and bundle sheath until exposure to light triggers cell specificity (Langdale *et al.*, 1988). Similarly, light is required for the correct cell-type patterning of PPDK, PEPC and the small subunit of RuBisCO in *Flaveria*, indicating that light-mediated responses are required for the acquisition of full C₄ competency (Shu *et al.*, 1999). Finally, dark-grown cotyledons of *Amaranthus* fail to show NAD-ME accumulation, and high levels of transcript accumulation are seen only after illumination (Long & Berry, 1996).

Several instances have been described where promoter regions give both a light-mediated response and cell specificity, for example the *PPDK* and *PEPC₁* promoters of maize (Matsuoka *et al.*, 2003; Kausch *et al.*, 2001). However, enhanced expression and cell type-specific repression may be attributable to separate components. Shu *et al.* (1999) note that a lack of coordinated light-induced expression between PPDK and RuBisCO suggests that light-mediated effects on the C₄ cycle are likely to be effected *via* indirect light-induced developmental signals rather than a direct effect of light upon the C₄ cycle itself. This

correlates with the observation that red light itself is insufficient to exclude *RbcS* transcripts from mesophyll cells in maize (Bilang & Bogorad, 1996) and the finding that RuBisCO specificity occurs as a response to metabolic changes associated with illumination rather than in response to light itself (Langdale & Kidner, 1994).

In contrast to *Flaveria* and maize, PPDK and PEPC show mesophyll-specific expression in *Amaranthus* in darkness (Wang *et al.*, 1993a), indicating that light is not required for the correct cell-type expression patterning in these species. In light-grown leaves, the restriction of both RuBisCO transcripts and protein to the bundle sheath of *Amaranthus* occurs concurrently with the sink-to-source transition (Wang *et al.*, 1993b). However, the development of C₄-like expression patterns of both subunits occurs in etiolated cotyledons indicating that light is not required for this transition (Wang *et al.*, 1993a). Light does influence the accumulation of RuBisCO, however, as transcripts of both subunits are subject to translational repression in darkness *via* modified ribosome interaction (Berry *et al.*, 1986; 1990). While similar processes are present in C₃ plants (Kim & Mullet, 2003), the use of multiple levels of regulation is likely a common theme in the regulation of the C₄ cycle (Hibberd & Covshoff, 2010). A lack of congruence between transcript and protein abundance is also seen in *Amaranth* meristems and developing leaf primordial (Ramsperger *et al.*, 1996). For example, NAD-ME transcripts in *Amaranthus* only develop cell specificity once immature leaves have expanded beyond a given threshold, although the NAD-ME α subunit polypeptide shows specificity throughout this period (Long & Berry, 1996). It therefore appears that a common theme in these processes is the development of the C₄ expression pattern over an existing C₃-like pattern. In conditions where a transcript is undetectable in darkness it is not possible to state whether its upregulation in light automatically generates cell specificity, or whether additional regulatory processes are in operation to provide high levels of cell-type specific expression.

4.1.2: The Development of the C₄ Cycle in *C. gynandra*

Given that previous studies of the effects of de-etiolation upon gene expression have enabled the identification of the mechanisms of regulation associated with the C₄ cycle (e.g. Wang *et al.*, 1993a), a similar study was undertaken in *C. gynandra* to provide an additional C₄ dicot species in which the extent of light-induction of gene regulation is described. Photosynthetic tissue grown in darkness will lack the necessary stimuli to trigger gene responses which are mediated either by direct light exposure or the metabolic changes associated with the acquisition of photosynthetic ability. After exposure to light, any changes in gene expression

in response to illumination can then be detected. In maize, the production of leaf tissue is seen in darkness (Langdale *et al.*, 1988), but etiolation tends to limit cotyledon development and prevents the formation of leaf tissue in some dicots. Attempts to produce etiolated leaf material in *C. gynandra* were unsuccessful, which indicates that leaf formation is inhibited in dark-grown *C. gynandra* plants, a similar situation to that described in *Amaranthus* (Wang, *et al.*, 1993a). However, functional Kranz anatomy is present in the cotyledons of *Amaranthus* and *Flaveria*, and this has been utilised in previous studies of the effects of etiolation on the C₄ cycle (e.g. Shu *et al.*, 1999; Wang *et al.*, 1993a). Kranz anatomy is present in the cotyledons of the C₄ members of *Cleome* (Koteyeva *et al.*, 2011), and so cotyledon material of *C. gynandra* was used in this study in the absence of etiolated true leaf material.

4.1.3: Experimental Design

In order to examine the effects of illumination on cotyledon development in *C. gynandra*, concurrent experiments were established. Seedlings germinated in darkness were transferred to MS medium supplemented with 1% sucrose and set with 0.8% agar (Brown *et al.*, 2011; Kajala *et al.*, 2011). Seeds kept in darkness were manipulated under a green safe lamp, and while previous reports have suggested such wavelengths are sufficient to produce a light-inductive response (Baskin & Baskin, 1979), the limited wavelengths and exposure was deemed sufficient to prevent undue influence. Seedlings were then placed in light, or in darkness prior to exposure to light after seven days, with sampling of tissue occurring during the first six hours after light exposure. This period was deemed sufficient to identify changes in gene expression linked directly to illumination. Beyond this point, developmental and metabolite flux changes are likely to be considerable and so it will no longer be possible to separate any causative mechanisms in observed changes in gene expression based on the data obtainable. Light grown seedlings were harvested concurrently so that any influence of circadian rhythms or developmentally-linked changes could be taken into account. Changes in gene expression were then assessed through the use of qRT-PCR and immunoblotting to quantify abundance of transcripts and proteins respectively. In addition, the abundance of chlorophyll was examined as an indicator of the extent of cotyledon development. Finally, the anatomy of cotyledons grown in light and in darkness were examined to verify the presence of Kranz anatomy in both treatments. This experiment was performed three times, with three replicates in both light treatments in each instance.

4.2: Results

4.3.1: Effects of Etiolation on Cotyledons

Cultivation in darkness triggered the formation of stereotypical etiolated cotyledons: hypocotyl growth was advanced while the cotyledons failed to expand and retained yellow pigmentation. The seed coat did drop from the cotyledons, however, and etiolated cotyledons demonstrated full Kranz anatomy comparable with that of light-grown seedlings (Figure 4.1; 4.2). The intervein distance was reduced in etiolated cotyledons, and cell density appeared to be increased. Therefore, the development of Kranz anatomy occurs early in cotyledon formation independent of illumination, and cotyledon expansion is achieved through expansion of existing mesophyll cells, increasing the intervein distance as the cotyledons develop. The presence of stomata on both the adaxial and abaxial epidermis was also notable. The presence of the cotyledons after seven days means that the assessment of light exposure at this point is justified.

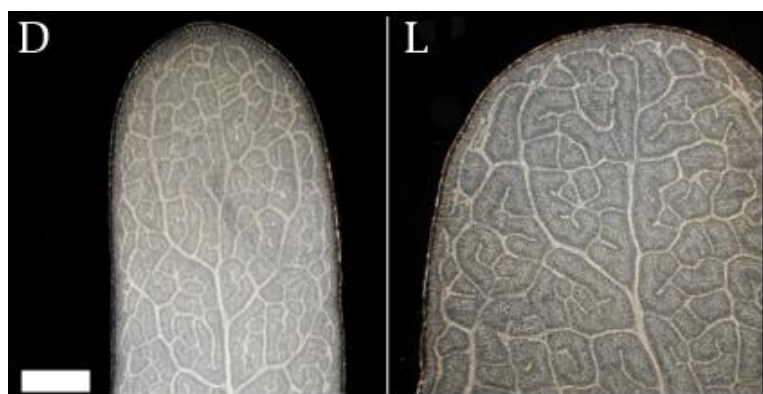


Figure 4.1 Etiolated cotyledons possess Kranz anatomy. Cotyledons grown in darkness (**D**) form Kranz anatomy, which is characterised by high levels of venation. This is comparable with light-grown cotyledons (**L**) showing normal development of Kranz anatomy. Scale = 25µm.

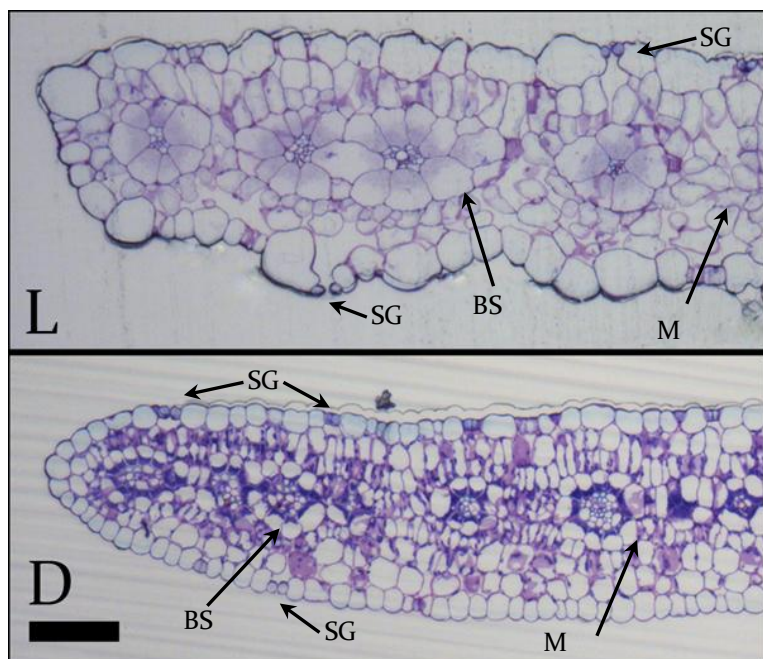


Figure 4.2: Internal anatomy of light-grown and etiolated (dark-grown) cotyledons of *C. gynandra*. The development of enlarged bundle sheath (BS) cells distinct from the mesophyll (M) is evident in both cotyledons, indicative that the cotyledons develop a functional Kranz anatomy. Scale = 100µm. Images produced in collaboration with B. Kumpers.

Total chlorophyll concentrations showed an increase within six hours of light exposure in etiolated cotyledons (Figure 4.3). While concentrations of chlorophyll remained relatively constant in light grown cotyledons at around 1.53 μg per mg of fresh tissue, chlorophyll was undetectable in etiolated cotyledons until two hours after exposure to light. The increase in total chlorophyll appeared linear at a rate of 0.06 $\mu\text{g mg}^{-1} \text{hr}^{-1}$. Mature leaf tissue of *C. gynandra* showed an average chlorophyll content of 2.25 (± 0.31) μg per mg of fresh tissue.

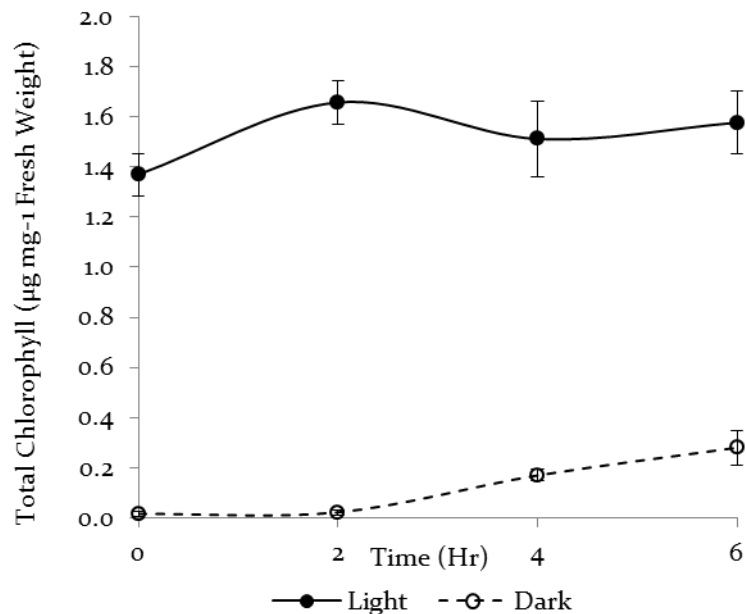


Figure 4.3: An increase in total chlorophyll concentration can be seen in etiolated cotyledons within six hours of illumination. Chlorophyll abundance remains relatively constant in light-grown seedlings, while it was not detectable in etiolated cotyledons at the point of transfer into illumination ($t=0$).

6.3.2: Transcriptional Effects

Exposure to light had a significant effect on transcript accumulation in etiolated *C. gynandra* cotyledons (Figure 4.4 & 4.5). Only *LHCA1* showed a complete absence in etiolated tissue, but it was detectable after 2 hours of light exposure. *PPDK*, *CA4*, *NAD-ME* and the transporters *DiT2* and *Bass2* were present in etiolated tissue, but showed a significant upregulation after light exposure. In the case of *PPDK*, *CA4* and *Bass2* this upregulation leads to levels which exceeded that seen in light-grown seedlings. *PEPC* and *RCA* accumulation fluctuated in etiolated tissue, although *PEPC* showed a level of accumulation greater than that seen in the light-grown tissue at $t=6$. Variation in transcript abundance was also seen in light-grown cotyledons, although this was most pronounced in *DiT2* and *Bass2*. Overlaid on this was a general decline in transcript abundance seen throughout the course of the study. In light-grown material, the abundance at $t=6$ was around half that seen at $t=0$ in *LHCA1*, *NAD-ME*, *RCA* and *CA4*. The increase in expression seen in the etiolated material appears transient in *NAD-ME* and *CA4*, and levels began to decline within a period of time after the initial peak in expression. The extent of this decline, however, was within the boundaries set by variation seen within the result and was not considered to be significant. The only gene which showed increased levels of accumulation in etiolated seedlings was *RbcS1A*, which showed a level of accumulation some 1.5x that seen in light-grown cotyledons. Within the first 2 hours of light exposure this value had decreased to below that of the light-grown seedlings, although a gradual increase in expression was seen between $t=2$ and $t=6$, by which point levels of accumulation approximated that seen in the light grown tissue.

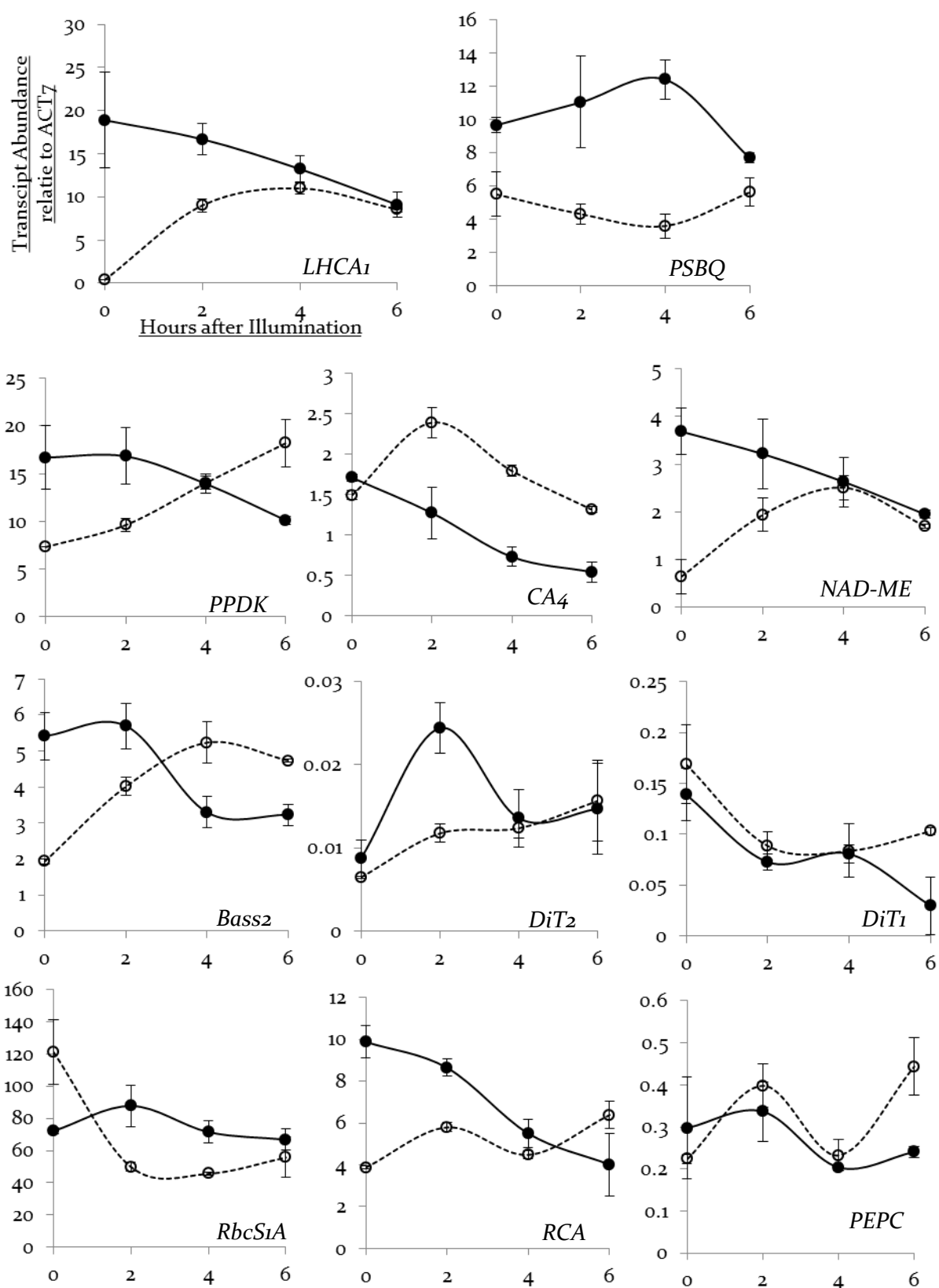


Figure 4.4: Light induction causes changes in transcript accumulation. Of the genes profiled, only *LHCA* is not present in etiolated cotyledons. Upregulation of gene expression in response to illumination is seen, but the extent and point of onset of this increase varies between gene. Only *RbcS* shows an initial decline in accumulation levels after light exposure. Etiolated cotyledons are shown with a broken line, while light-grown seedlings are given a solid line.

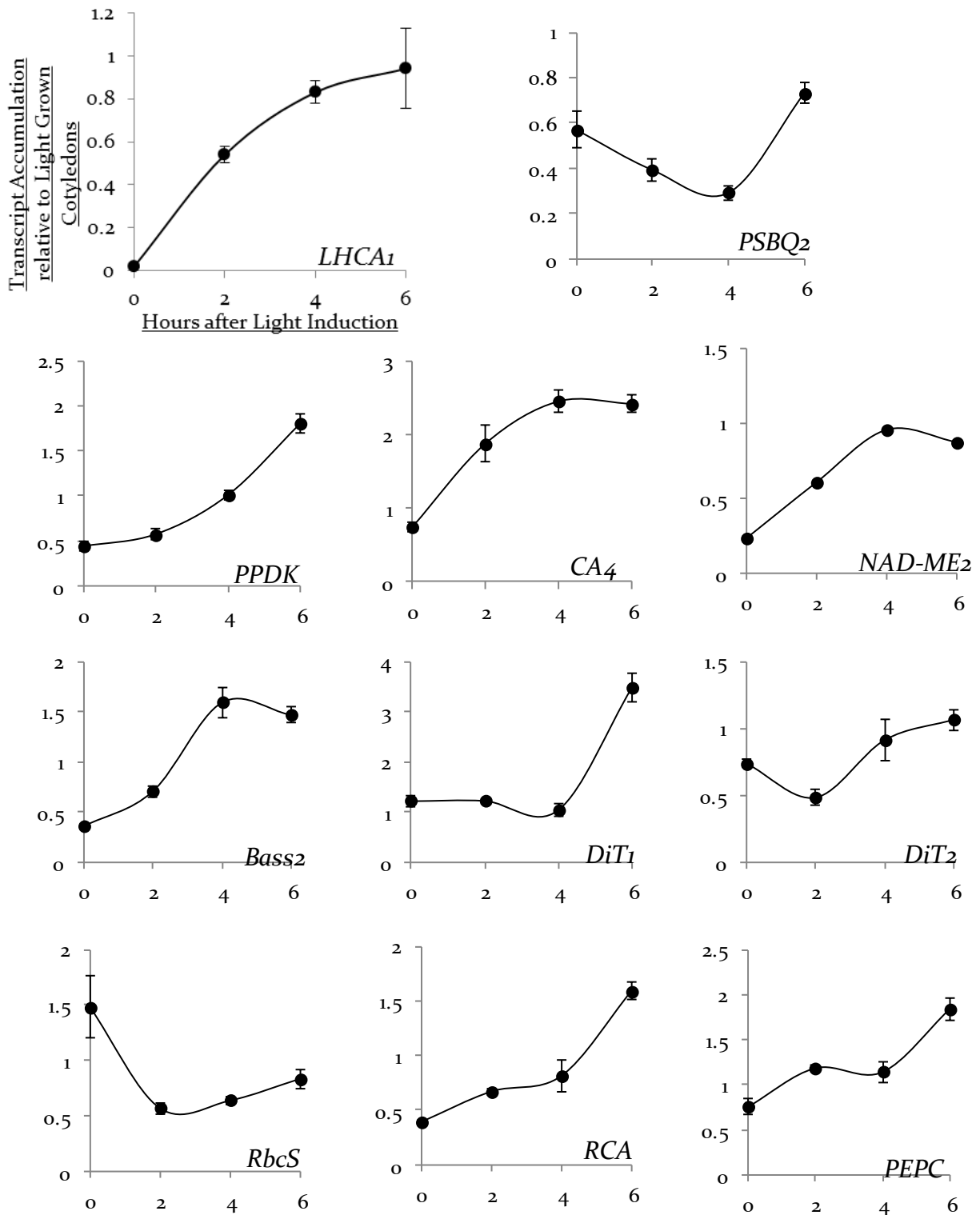
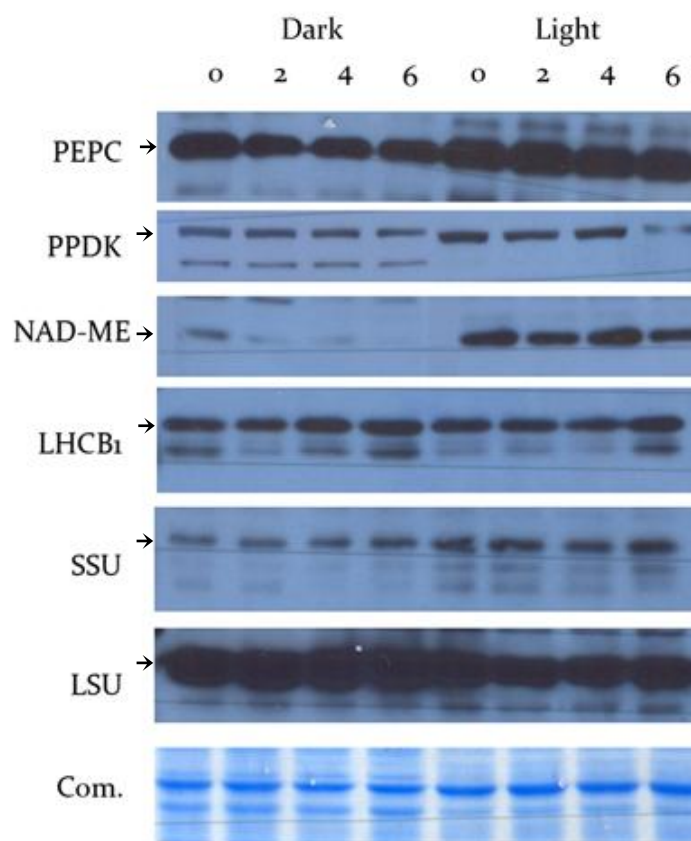


Figure 4.5: Light induction causes changes in transcript accumulation. Transcript abundance (relative to *ACT7*, and between light and dark grown plants) are given. A general increase is seen in transcript abundance after illumination (*PEPC*, *PPDK*, *NAD-ME2*) and while these increases may be transient (e.g. *PEPC*) some transcripts remain elevated (e.g. *CA4*). *RbcS* shows an initial decline in accumulation after illumination.

4.3.3: Changes in Protein Accumulation

The increase in transcript accumulation associated with illumination corresponds to the abundance of protein (Figure 4.6), although the levels of protein accumulation appear more constant throughout the course of sampling. PEPC and PPDK were detectable in dark-grown cotyledons, although at lower levels, indicating that light exposure was required for increased levels of accumulation. This is seen to a greater extent in NAD-ME, which was largely undetectable in etiolated material. Both subunits of RuBisCO were present in etiolated material, although the SSU appeared to be at a lower level of abundance compared with light-grown material indicating that increased expression is seen in light-grown cotyledons. The LSU appears more constant, although the abundance of this protein made it difficult to fully quantify.

Figure 4.6: Changes in protein accumulation occur after illumination. PEPC, PPDK and NAD-ME are detectable in etiolated cotyledons, but at lower levels than light grown individuals. NAD-ME shows significant depression in dark grown cotyledons, but is still detectable. Similarly, an increase in the abundance of the SSU of RuBisCO is seen between are relatively constant between dark and light grown samples. Equal loading of total protein is shown by in the Coomassie-stained gel (Com.).



4.3: Discussion

4.3.1: Post-germination Cotyledon Development in *C. gynandra*

While some C₄ species produce cotyledons that are C₃ (e.g. *Salsola gemmascens*, Pyankov *et al.*, 2000), others produce cotyledons with a functional C₄ cycle (e.g. *Flaveria* (Shu *et al.*, 1999), *S. laricina* (Pyankov *et al.*, 2000). These data demonstrate that *C. gynandra* is in the latter group, forming developed Kranz anatomy in its cotyledons, an observation that matches the observations of Koteyeva *et al.* (2011). While the contrasting origins and functions of cotyledons when compared with mature leaf material may result in differing photosynthetic types, a limited number of mutations may yield leaf-like development of cotyledons (Meinke *et al.*, 1992) which would suggest that genetic control is malleable. In addition, if the C₄ cycle can be considered an ecological adaptation (Sage, 2004), then it is to be expected that cotyledons would possess the same photosynthetic type as that present in mature plants to enable maximal exploitation of a given ecological niche. However, from this data it is not possible to define whether Kranz formation occurs during cotyledon formation or maturation after germination. The latter instance has been demonstrated in *S. richeteri* (Voznesenskaya *et al.*, 2003), and it may be worth extending the time course over which samples are prepared in order to properly quantify this.

While Kranz anatomy is considered likely to be present in cotyledons prior to germination, the reduced development of the mesophyll in etiolated cotyledons suggests that maturation of the cotyledon is achieved predominately by the expansion of these cells. The vein density of the light-grown cotyledons is similar to that of mature *C. gynandra* leaves but this is lower than that of etiolated cotyledons (Figure 4.1, 4.2). Again, this matches expected developmental pathways: if Kranz anatomy is present prior to maturation then it would be necessary to expand existing tissues rather than forming *de novo* structures. Such a process has been observed in *Arabidopsis*, whereby cell numbers within the cotyledon remain relatively constant during development, while expansion is achieved through increases in cell volume with a corresponding reduction in cell density (Mansfield & Briarty, 1996). A reduction in the ratio of mesophyll to bundle sheath cells is seen during the expansion of *Amaranthus tricolor* leaves (Wang & Nii, 2001) so similar developmental processes have been recorded in other C₄ dicots.

The response of *C. gynandra* cotyledons to darkness is typical of dicotyledons: the elongation of the hypocotyl is considerable, while the cotyledons do not expand and do not accumulate chlorophyll. The accumulation of chlorophyll in response to illumination is recordable within

six hours of illumination (Figure 4.3). Little to no change is evident in the abundance of chlorophyll of light-grown seedlings over the duration of this experiment, which would infer that a steady state of chlorophyll abundance may have been reached at around $1.53 \mu\text{g mg}^{-1}$ of fresh weight. This is lower than that seen in mature leaf material, which showed total chlorophyll content of $2.25 \mu\text{g mg}^{-1}$ of fresh weight, although this value is comparable to that reported for *C. gynandra* previously (Kulya *et al.*, 2011). A diverse range of species reach maxima of chlorophyll production around the 7–8 day point of cotyledon development (Moore *et al.*, 1972) so this situation in *C. gynandra* is not without precedent, although the reduced abundance of chlorophyll may depress the photosynthetic capacity of the cotyledons relative to the mature plant.

4.3.2: Light regulates Components of the C₄ cycle in *C. gynandra*

The exposure of etiolated cotyledons of *C. gynandra* to light triggers significant changes in gene expression. *CA₄*, *NAD-ME₂*, *LHCA₁* show a rapid increase in transcript abundance within 2 hours of illumination, reaching or exceeding the level of accumulation seen in light-grown cotyledons (Figure 4.4). *LHCA₁* shows a more significant increase than the other genes examined in this study, but given its relative absence in etiolated cotyledons this may be a proportionate response. The absence of *LHCA₁* from etiolated cotyledons corresponds with the absence of chlorophyll from these tissues, and so it is likely that the upregulation the light-harvesting complexes (LHC) is concurrent with the increased abundance of chlorophyll although the changes in LHC abundance may be triggered by changes in redox potential rather than light sensitivity *per se* (Maxwell *et al.*, 1995). An up-regulation of *LHCA₁* occurs within the first two hours after light exposure, while an increase in chlorophyll abundance was not detectable until four hours after exposure. This would suggest that the regulation of *LHCA₁* is not linked to changes in redox potential due to the lack of functioning chlorophyll during the initial period of its upregulation. A general increase in transcript accumulation is seen, although the majority of transcripts profiled in this study appear to have reached a plateau of expression within 6 hours of light exposure. However, only *RbcS*, *LHCA₁* and *PSBQ₂* are at levels equal to or lower than the light-grown samples which may indicate that the elevated level of expression is transient, and will be subject to a decline once the cotyledons become photosynthetically active.

All the genes examined by this study show a measure of accumulation at the transcript level before illumination, with the exception of *LHCA₁*. A general increase in abundance is seen after illumination, which indicates that light is required to induce expression to levels seen in

photosynthetically active tissue. The exception to this is *PSBQ* which appears to be relatively constant, albeit it at a lower level than light grown material. In addition, *RbcS* shows a sharp decrease in abundance within the first 2 hours of illumination, which may suggest that light has a suppressive effect on the accumulation of its transcripts, potentially similar to that which has been described in maize (Langdale *et al.*, 1988)

4.3.3: Circadian Regulation may be active in *C. gynandra*

Interestingly, a general decline was seen in the levels of gene expression seen in light-grown cotyledons over the course the experiment (Figure 4.4). As $t=0$ occurred between 9 and 10am in the morning, this may correspond to a decline in expression linked to a pre-dawn or dawn-promoted upregulation of expression. Circadian regulation has been shown to have a significant impact on the expression of genes associated with photosynthesis such as the production of chlorophyll and LHC-binding proteins (Gehring *et al.*, 1977; Paulsen & Bogorad, 1988). The decline in transcription levels observed here may be linked to circadian rhythms promoting peak expression at dawn with a subsequent decline over time. While light-grown seedlings were subject to a long-day photoperiod, etiolated seedlings were kept in constant temperature and darkness from the point of germination so that a circadian rhythm may not have been entrained, although circadian rhythms have been described in *Arabidopsis* seedlings deprived of both light and temperature stimuli (Salomé *et al.*, 2008). A significant proportion of genes may be placed under circadian control (Michael & McClung, 2003), and a number of key C_4 genes in maize follow a circadian rhythm which peaks around dawn (Khan *et al.*, 2010). Therefore, it is conceivable that the general decline in transcription seen in this experiment may be linked to intrinsic rhythms. It would be interesting to address whether such non-photosynthesis genes are under circadian control in a C_3 environment prior to their recruitment into the C_4 cycle as this could represent an additional evolutionary requirement.

It is beyond the scope of this study to explore the effects of circadian rhythms upon the C_4 cycle. However, should this study be extended, it would be beneficial to examine gene expression levels over a longer time period to properly quantify this decline, and to assess what, if any, impact circadian regulation has upon these genes.. In the context of this exploration, however, the scale of differences in expression between the etiolated and light-grown cotyledons is likely to have exceeded any changes in expression linked to the circadian clock. It would be beneficial to adjust the culturing process so that light grown seedlings were grown under continuous illumination to remove the impact of any periodicity upon expression patterns should this study be extended.

Of those genes that show a reduction in accumulation, either initially (e.g. *RbcS*) or after an initial increase after illumination (e.g. *DiT2*), a feature which may alter the interpretation of this data is that of RNA stability. Not only do these reductions indicate that transcription has been depressed, but that the stability of these transcripts show half-life values within 2-4 hours based on the reduction in relative abundance implied by these data. The control of mRNA stability has been implicated as a key feature of gene regulation, and it is likely that significant variation will occur between transcripts (Abler & Green, 1996). Transcript stability in *C. gynandra* has yet to be fully explored, and significant variation exists in published values for *Arabidopsis* (Gutiérrez *et al.*, 2002; Narsai *et al.*, 2007) so it is not possible to explore this area. Should such data become available, however, it may be possible to test whether the changes in accumulation seen in this study are attributable to alteration in transcript stability either between genes or in response to illumination.

4.3.4: Metabolic Flux may also direct Development in *C. gynandra*.

Of the transporters examined in this study, *DiT1/2* and *Bass2* show similar up-regulation after illumination. The onset of this increase occurs between 2-4 hours after illumination, representing a delay from that seen in the majority of genes profiled by this study. The data indicates that the regulation of these genes is not linked directly to light exposure (given that their non-C₄ roles are unlikely to be associated with photosynthetic activities), and so it is conceivable that their regulation is targeted more towards the concentrations of metabolites with which they interact (Bräutigam *et al.*, 2008). A role for metabolite-led development has been described in *Amaranthus* as the C₃ to C₄ switch corresponds with a gain of net productivity (Wang *et al.*, 1993b). Therefore, these may indicate that metabolite flux may have an impact on regulation of the onset of the C₄ cycle in *C. gynandra*, but testing this is far beyond the scope of this study.

4.3.5: Protein Accumulation in Etiolated Cotyledons

While this study has highlighted that an upregulation of many of the components of the C₄ cycle at the transcript level occurs in response to light, the actual cause of this response remains to be examined. Those genes such as *LHCA1* which show the most rapid response to illumination may be attributable to the direct effect of illumination, but those that show a more delayed response (e.g. *DiT2*, *PPDK*) may be subject to additional regulation based on metabolic flux, or the activity of intermediate regulators.

At the protein level, expression patterns largely mirror those seen at the transcript level. *PPDK*, *PEPC* and *NAD-ME* are detectable in etiolated cotyledons, but at levels significantly

depressed from that of light-grown seedlings. The difference in abundance of PEPC between the treatments is less than that seen in NAD-ME and PPDK, which reflects the lower levels of transcript accumulation seen at $t=0$ in the latter two instances. The presence of NAD-ME, PPDK and PEPC in etiolated cotyledons would suggest that light is not required for their expression, but that light is required to achieve high levels of accumulation. This mirrors the situation in *Amaranthus*, where both PPDK and PEPC show localisation to the mesophyll in etiolated cotyledons (Wang *et al.*, 1993a).

However, a lack of correlation between transcript and protein abundance appears to be present in the expression of *RbcS*, which is also the only gene examined here which shows a reduction within the first two hours of light exposure. Levels drop from about 1.5x that of light-grown cotyledons to around 0.5x, before returning to c.1x after six hours. This may indicate that the steady-state level of *RbcS* expression is elevated in darkness, and a light-mediated mechanism reduces expression of *RbcS* upon illumination. At the protein level, however, the SSU appears to increase in abundance after illumination, which would indicate an incongruity between transcript and protein accumulation in darkness. This would mean that if increased levels of *RbcS* transcripts are present during etiolation, then a secondary level of regulation exists which prevents increased abundance at the protein level. In *Amaranthus*, both subunits show the correct patterning in darkness (albeit at greatly reduced levels), although multiple levels of regulation *via* transcription and translation have been reported (Wang *et al.*, 1993a; McCormac *et al.*, 2000). For the data presented here it is not possible to define whether the changes in abundance of either protein or RNA are concurrent with a change in cell-specificity, but this would be worthwhile exploring further.

A key extension of this study would be to develop *in situ* localisation of RNA and protein accumulation. Primarily, this would provide better quantification of any changes in gene expression patterns. The data utilised to date has been derived from whole-cotyledon extracts so that it has not been possible to explore changes in the BS or M cells in isolation. *In situ* localisations would enable visualisation of any changes that occur in either protein or transcript abundance in a cell type-specific fashion, improving the clarity of the examination. Additionally, it would enable assessment to be carried out on a cotyledon-specific basis. While lower levels of *PPDK* and *PEPC* were recorded in etiolated plants, the up-regulation of both genes may be independent of the acquisition of cell specificity. In *Amaranthus*, both show the correct cell patterning from the onset of cotyledon development in both light and dark (Wang *et al.*, 1993a). It could be argued that as both genes have been recruited from non-

photosynthetic roles, the acquisition of direct light-mediated regulation would require an additional step in the recruitment process. However, *PPDK* expression is induced by light in maize, an effect attributable to *cis*-acting elements in its promoter (Matsuoka *et al.*, 1993). In addition, both enzymes are subject to light-mediated post-translation regulation (Vidal & Chollet, 1997; Astley *et al.*, 2011), so it is likely that additional transcriptional or post-transcriptional controls are in place which are directly regulated by illumination. Finally, the development of *C. gynandra* lines expressing an inhibitor of sRNA synthesis may provide an opportunity for the study of the effects of sRNA/miRNA activity during the de-etiolation process. miRNAs have been implicated in light sensitivity in roots (Sorin *et al.*, 2005), but whether this extends to light-mediated physiological changes in foliar tissue remains to be explored. Replicating this experiment using cotyledons expressing the p19 inhibitor that was transformed into *C. gynandra* as part of this would enable testing of a potential miRNA-mediated role in the decline in transcript accumulation that has been demonstrated in this study.

4.3.6: Concluding Remarks

This study has confirmed the presence of Kranz anatomy in the cotyledons of *C. gynandra*, and that light is not required for its development. Genes associated with light harvesting, and the formation of chlorophyll, are only demonstrated after illumination of etiolated cotyledons. The other components of the C₄ cycle are present at the transcript level prior to illumination, although a measure of upregulation occurs after light exposure indicating that environmental stimuli are required if accumulation at the transcript level is to reach levels comparable with that seen in light grown cotyledons. Accumulation of PEPC, PPDK, NAD-ME polypeptides match the increase in accumulation after illumination seen at the transcript level. A decrease in the accumulation of *RbcS* transcripts is seen within the first two hours of light exposure, however, although levels of the SSU remain lower than that seen in light-grown cotyledons. This may indicate that a secondary level of regulation is in effect which uncouples the levels of transcript and peptide accumulation of SSU which is relieved upon illumination. While the data presented here are insufficient to fully test the effects of illumination upon cell-specificity, a number of areas have been highlighted that may benefit from further exploration.

5. The Generation of Hybrids within *Cleome*

5.1: Introduction

5.1.1: The Assessment of Hybrids between Photosynthetic Types

The occurrence of C₃, C₄ and C_{3/4} intermediates within close phylogenetic groups offers an opportunity to examine the C₄ cycle through hybridisation studies. The generation of hybrids could allow the assessment of C₄ traits in a C₃ environment and *vice versa* in order to be able to identify the regulatory processes that have been modified during the evolution of a given trait into the C₄ cycle. While this experimental approach has been used on a gene-specific basis (e.g. Brown *et al.*, 2011) this can be a slow and laborious process, and is not applicable to traits for which no genetic basis has been identified. The generation of an artificial C₃ x C₄ hybrid lineage would enable the identification of loci associated with the C₄ cycle *via* mapping of an introgression line, a method which has been previously used to identify features of complex polygenic traits (e.g. Eshed & Zamir, 1995). Analysis of hybrids would also enable the identification of linked traits within the C₄ cycle which may indicate a shared regulatory or evolutionary process, as well as assessing whether components of the C₄ cycle would be dominant or recessive in a C₃ leaf.

The hybridisation studies published to date tend to show hybrids with reduced vigour and levels of photosynthesis which are depressed towards if not below that of the C₃ parent (e.g. Byrd *et al.*, 1992; Pearcy & Björkman, 1970), although C₄-like dominance is seen in some single-gene instances (e.g. NADP-malate dehydrogenase, Holaday *et al.*, 1988). The dominance of the C₃ cycle may be attributable to C₃ representing the “default” state over which the C₄ cycle is placed (which would correlate with the delayed onset of C₄ photosynthesis during leaf development discussed in Section 1.1.6). The dominance of C₃ or C₄ traits in the opposing environment may test this, in addition to enabling the identification of *trans*-acting factors, and so it is considered important to explore this aspect in a wider context. In addition, the presence of heterologous SSU/LSU combinations may enable screening for altered RuBisCO kinetics. C₃ and C₄ species show a measure of altered catalytic efficiency (Sage, 2001), and so the production of hybrid holoenzymes may enable this aspect to be explored further. It will be necessary to carry out reciprocal crosses to screen for differences in parental dominance. Brown *et al.* (1992) reported paternal dominance patterns of $\delta^{13}\text{C}$ values in reciprocal crosses between *Flaveria brownii* and *F. linearis*, so production of bidirectional crosses would be required to fully test any hypothesis of dominance.

A number of successful hybridisation attempts have been made between members of *Panicum* ($C_3 \times C_3/C_4$, Brown *et al.*, 1985; Sternberg *et al.*, 1986), *Flaveria* ($C_3 \times C_3/C_4$, $C_3 \times C_4$, Brown *et al.*, 1986, Holaday *et al.*, 1988; Bryd *et al.*, 1992) and *Atriplex* (Björkman *et al.*, 1970), although these studies were generally restricted to analysis of gas exchange parameters, enzyme activity and anatomical structures with no global assessment of changes in transcript or protein abundance of components of the C_4 cycle. To test whether interspecific crosses between C_3 and C_4 members of *Cleome* could be generated to address these questions, hybridisations between *C. gynandra* and *C. hassleriana* were undertaken. Rajndrudu & Rama'Das (1982) reported successful hybridisation between *C. gynandra* and *C. viscosa* L. (C_3) using conventional breeding techniques, and while their study was limited to seed coat morphology it does indicate the potential for interspecific crosses within *Cleome*. *C. hassleriana* was chosen as the C_3 parent in this instance due to the availability of molecular resources for this species (Bräutigam *et al.*, 2011).

5.1.2: Production of Hybrid Lines

A number of barriers may be present to prevent the production of hybrids at both the pre- and postzygotic level. At the prezygotic level, heterospecific pollen grains may fail to germinate or may show abnormal growth through the stylar tissue (Chen & Gibson, 1972), preventing fertilisation. After fertilisation the hybrid embryos may abort before full development can be achieved, most likely as the result of a halting of development of the endosperm leading to a cessation of the supply of resources to the developing seed (Briggs *et al.*, 1987; Abbo & Ladizinsky, 1991). Once hybrids are obtained, they may demonstrate sterility or unviability, potentially through an uncoupling of coadapted subspecific gene complexes or negative interactions between divergent loci (Wu & Palopoli, 1994; Li *et al.*, 1997). In addition, successful hybridisation events may be asymmetrical, so that the cross is unidirectional in that viable plants are obtained with a specific maternal/paternal mix (Smith, 1970). This is especially relevant in this situation due to the benefit of carrying out reciprocal crosses. Rajndrudu & Rama'Das (1982) were unsuccessful in obtaining viable seed when *C. gynandra* was the maternal partner when crossed with *C. viscosa*, although only a 5.5% success rate was reported in the reciprocal cross.

5.1.3: Experimental Approach

In order to minimise the impact of fertility barriers upon the generation of hybrids within *Cleome*, it was decided to supplement traditional crossing methods with a regime of *in vitro* cultivation of excised hybrid embryos in order to minimise any negative effects of continued

development *in planta*. Such methods have improved the recovery of interspecific hybrids in *Brassica* (Bajaj *et al.*, 1986; Quazi, 1988), and given that *C. gynandra* (Newell *et al.*, 2010) and *C. spinosa* (Albarello *et al.*, 2006) have been successfully cultured *in vitro* it was hoped that such techniques could be adapted to interspecific hybrids within *Cleome*. In addition to *in planta* development of embryos, a three tailed approach was undertaken to attempt *in vitro* culturing of hybrid embryos. Liquid suspension cultures of Quazi (1988), rotating liquid cultures of Harberd (1969) and gel-phase cultures of Zhang *et al.* (2003) were adapted, with the primary focus of ensuring adequate contact between the medium and embryo. Additionally, a hormone regime matrix was established to identify optimum concentrations to ensure either continued embryo development or the formation of regenerative callus.

The crossing methods employed by Rajndrudu & Rama'Das (1982) first involved the emasculation and isolation of flowers prior to anthesis, an approach which is considered valid given the reported occurrence of self-compatibility within *Cleome* (Cane, 2008). It was also necessary to identify the reproductive morphology of both species as hermaphroditic, andromonoecious (flowers lacking gynoecia) and staminate flowers (flowers which originate as hermaphroditic, but show halted pistal growth) have been reported within *Cleome* (Cane, 2008; Machado *et al.*, 2006). Successful ovule penetration by the pollen tube was assessed using the methods of Martin (1959) to enable visualisation of tube growth, although this will be used as a tentative indicator of successful fertilization as pollen-tube penetration may not directly correspond to fertilisation success rates (Rieseberg *et al.*, 1995).

Reciprocal heterospecific crosses between *C. gynandra* and *C. hassleriana* were therefore attempted. In addition to maturation *in planta*, attempts to recover mature embryos *via in vitro* embryo cultured were undertaken. The unknown hormonal requirements of *C. hassleriana* and of the potential hybrids required a hormone matrix to be established to highlight optimum concentrations for embryo maturation. In addition, the potentially conflicting requirements of nutrient and gas exchange requirements were screened through the use of three alternative culture systems. Solid-state cultures were achieved by solidifying the media with 0.9% agar, while liquid-phase culturing was achieved through the direct placement of the excised embryos into agitated liquid medium. Finally, liquid-suspension cultures were achieved through the placement of the excised embryos onto filter paper bridges placed over a vessel of liquid medium, which could then be drawn up to the suspended embryo. The latter two methods were considered to represent the two extremes of nutrient/gas supply, although these were chosen in an attempt to overcome any problems

associated with the unequal distribution of nutrients or by-products within the solid-state medium.

5.2: Results

5.2.1: Reproductive Biology

C. gynandra and *C. hassleriana* both demonstrated the formation of heteromorphic flower types (Figure 5.1). The development of hermaphrodite flowers interspaced with staminate flowers which show aborted gynoecium development at c.3mm of growth was seen in layers progressing up a simple raceme. In both instances the dehiscence of the anthers occurred 2-4 days after anthesis. The petals of *C. gynandra* were greatly reduced and shortened, although the gynoecium and anthers were borne on an extend androgynophore. Such extension was absent from *C. hassleriana*, but the extension of both petals, anther filaments and style ensure that the projection of the reproductive organs away from the petals was roughly equal between the two species (5.1-A,B). The anthers and stigma of *C. hassleriana* remain enclosed within the flower bud until anthesis, although the anther filaments and style curved outwards forming a hook shape prior to anthesis (5.1-B). In *C. gynandra*, the stigma and anther tips are visible above the edge of the developing petal whorl, resulting in the exposure of the stigma considerably prior to anthesis (5.1-C). When treated with hydrogen peroxide, the stigmatic tissue of *C. hassleriana* demonstrated receptivity before emergence from the flower bud, and *C. gynandra* showed receptivity before the extension of the androgynophore away from the petals (Figure 5.2).

5.2.2: Pollen Grain Germination and Seed Set

Pollen tube tissue was readily discernible from that of the style under UV light after aniline staining (Figure 5.3). The gynoecia of isolated plants of both species that had received a heterospecific pollen load showed high levels of pollen grain germination. Tube growth showed no abnormal growth through the style, and growth was sufficient to reach the ovules. A subset of plants that had been cross pollinated were left to set seed naturally. While no seed production was seen in maternal *C. gynandra* plants, maternal *C. hassleriana* pods developed at a rate comparable with plants which had received a homospecific pollen load, although the number of seeds set was depressed to less than 25% of that seen in WT crosses. When the seeds were harvested, they showed no difference in size from WT seeds to *C. hassleriana*, although the surface was discoloured, the seed coat was thinned and brittle, and the seeds were incompletely filled. No successful germination occurred from seeds obtained from heterospecific crosses.



Figure 5.1: Sexually dimorphic flowers are present in *Cleome*. Staminate (i) and hermaphrodite (ii) flowers are produced by both *C. gynandra* (A) and *C. hassleriana* (B). The gynoecium of each type is marked with an arrow. The gynoecium of the staminate flowers shows halted development resulting in a reduced ovary and stigma at the base of the anther filaments in both species. The vestigial ovary is identifiable by its retention of green pigmentation while the other floral organs acquire pink/purple pigmentation during maturation. The *C. hassleriana* flowers are shown prior to anthesis, with the hook of the elongating style evident in the hermaphrodite flower. In the developing flowers of *C. gynandra* (C), the anthers (Y) and stigma (X) project above the petal whorl prior to anthesis. Scale: 1cm (A,B), 1mm (C).

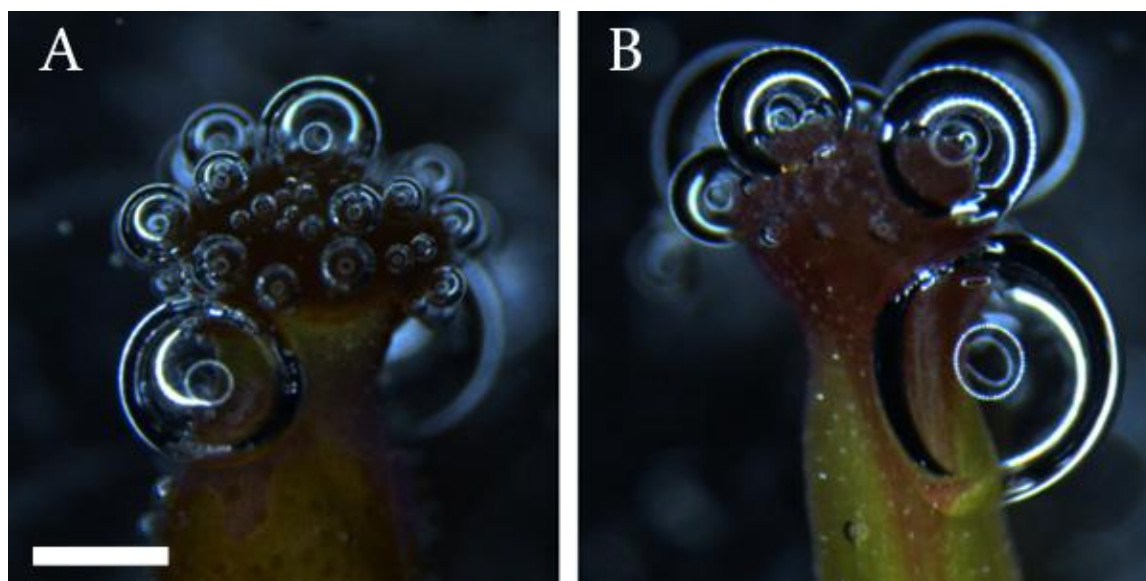


Figure 5.2: Oxygen evolution at the stigmatic surface of *C. gynandra* (A) and *C. hassleriana* (B). Both stigmas were removed shortly before anthesis and submerged in 6% hydrogen peroxide solution. The production of oxygen bubbles was taken as an indicator of stigma receptivity. Scale = 250µm.

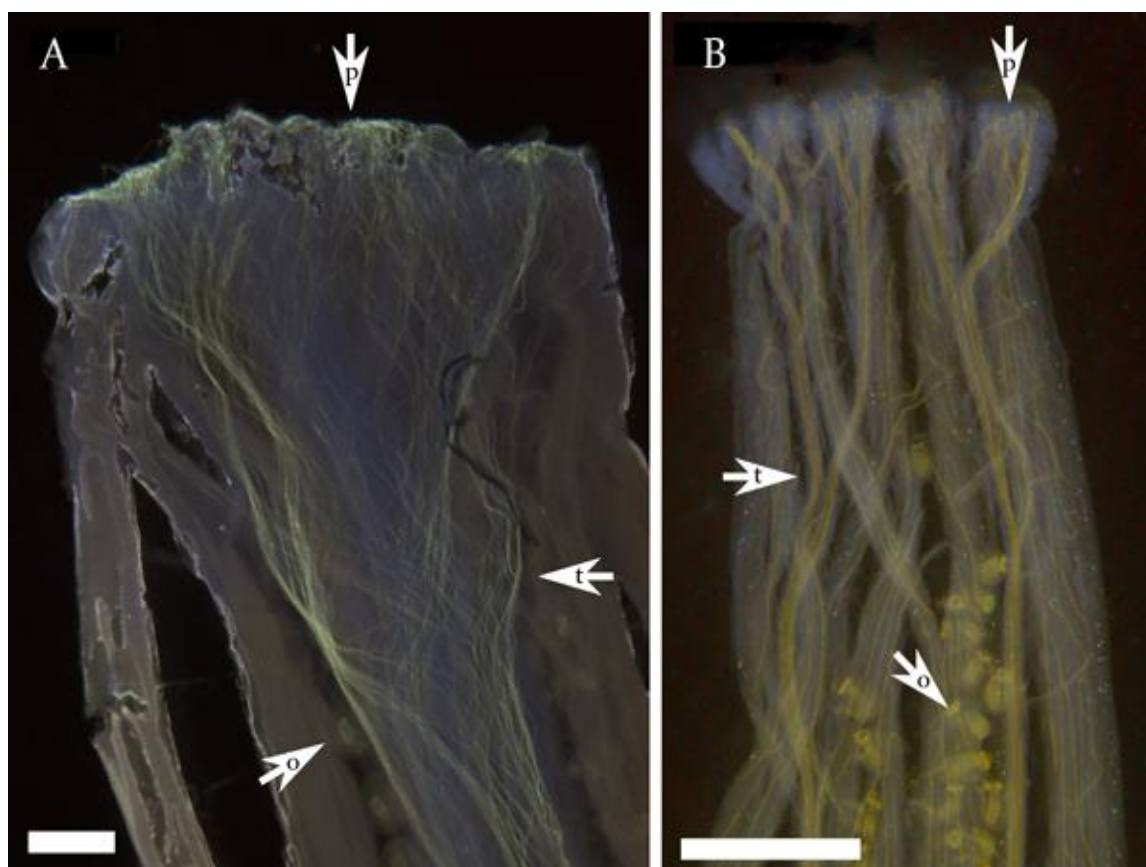


Figure 5.3: Heterospecific pollen tube growth in *C. gynandra* (A) and *C. hassleriana* (B). The growth of the pollen tube (t) from the germinating grains on the stigmatic surface (p) down the style into the ovary (o) is distinguishable from the stylar tissue by staining with aniline blue. No pollen tubes were evident in unfertilised flowers. The gynoecia were flattened between glass slides before examination. Scale: 500µm.

5.2.3: Embryo Extraction and Culture

The method of embryo extraction discussed above was sufficient for the establishment of aseptic cultures. Maternal *C. gynandra* crosses did not produce any viable embryos, although between 5 and 10 embryos per ovary were recoverable from maternal *C. hassleriana* crosses. The 7-day window after fertilisation was sufficient to produce enlarged embryos that were approaching the globular/heart boundary and were discernible from the unfertilized ovules (Figure 5.4).



Figure 5.4: Embryo growth in *C. hassleriana*. The ovary was cut down the replum, revealing the extent of ovule growth 7 days after fertilisation. A pair of unfertilised ovules (i) can be identified relative to the developing fertilised embryo (ii). The stigmatic tissue and remaining embryos/ovules were removed prior to photography. Scale = 1mm.

The induction of callus was successful in the solid-phase culture, although considerable variation was seen in the extent of callus formation (Figure 5.5). The extent of callus formation at levels of 0.5 mg l⁻¹ NAA was considerably higher over 0 and 0.25 mg l⁻¹ NAA, although a slight increase in callus weight was seen at 0.25 mg l⁻¹ NAA when placed in tandem with increased concentrations of BAP. Increases of callus weight correlated well with BAP concentration, which showed a peak at 1 mg l⁻¹, with NAA concentrations of 0.5 mg l⁻¹ NAA. For the duration of this experiment, no organogenesis was demonstrated, and senescence of the callus occurred sporadically after 16 weeks. Callus formation was only recordable in the solid-state cultures as no growth was recorded and senescence occurred within two weeks of the establishment of the liquid-suspension and liquid phase cultures.

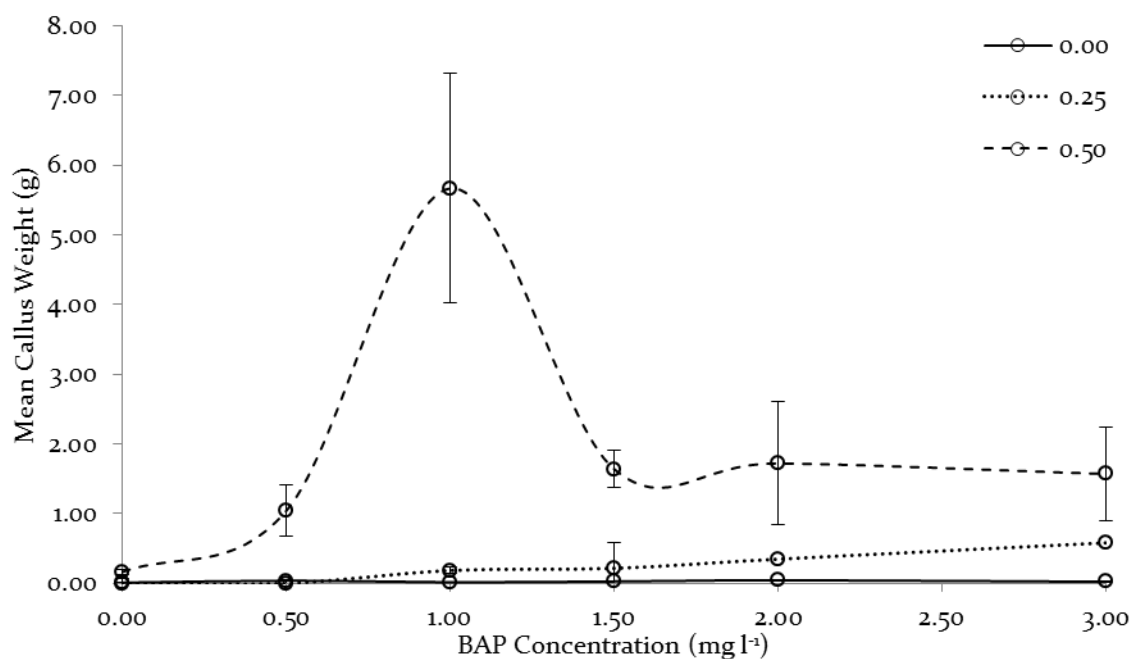


Figure 5.5: Response of embryos cultured *in vitro* to varying BAP concentrations in tandem with 0, 0.25 and 0.5 mg l⁻¹ of NAA. Limited growth was seen in cultures with 0 and 0.25 mg l⁻¹ NAA at all concentrations of BAP. Maximal callus regeneration was seen at concentrations of 1.0 mg l⁻¹ BAP/ 0.5 mg l⁻¹ NAA.

5.3: Discussion

5.3.1: Reproductive Biology of *C. gynandra* and *C. hassleriana*

The production of heteromorphic flower types by *C. gynandra* and *C. hassleriana* match similar reports of other members of the genus (Stout, 1923; Cane, 2008) although the male flowers were found to be staminate (flowers in which the gynoecium halted development) rather than andromonoecious (the gynoecium is absent entirely) which agrees with the observation of Cane (2008). Cane also notes the receptivity of the stigma from the point of anthesis as was found in both *C. gynandra* and *C. spinosa*, with the delayed dehiscence of the anthers potentially acting as a method of limiting the extent of selfing. While the stigma of *C. hassleriana* was receptive prior to anthesis, its encapsulation in the developing bud means that its isolation and cross pollination can be performed with minimal risk of contamination with homospecific pollen.

The lack of seed recovered from crosses in which *C. gynandra* was the maternal partner matches the report of Rajendrudu & Rama'Das (1982) that *C. gynandra* was incapable of acting as a maternal parent in such crosses. The data presented here suggests that this is not due to a failure of pollen tube penetration. This would infer that additional post-zygotic barriers are in place which halts the development of the embryo after fertilisation, as discussed above. The

failure of *C. hassleriana* to produce viable seed through normal crossing methods also indicates that post-zygotic barriers are active within *Cleome*. The embryos produced in the maternal *C. hassleriana* crosses show viability at the 7 day harvesting threshold, while no such development is present in crosses in which *C. gynandra* is the maternal partner. This would indicate that abortion of the hybrid embryos occurs early in development before the globule stage has been passed, as has been reported in other interspecific crosses (e.g. Barone *et al.*, 1992).

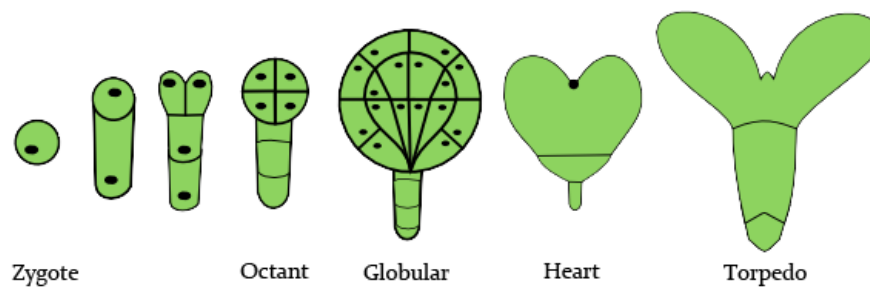


Figure 5.6: Developmental patterning of the fertilised zygote. Once the octant stage has passed into the global stage, enlargement of the cotyledon precursor cells shows passage into the heart stage, before further development leads to torpedo formation. (After Steeves & Sussex, 1989)

5.3.2: Receptivity of Hybrid Material to *In Vitro* Culture

The rapid senescence of excised embryos placed in either form of liquid culture limited the extent to which this experimental system could be evaluated. The success of the solid-state culture medium in obtaining callus may indicate the negative effects of liquid culture are due to physical parameters rather than biochemical ones. Due to the nature of liquid culture, it was not possible to ensure the embryos remained on the surface of the liquid medium, and such submersion is likely to have significant impact on the gas exchange properties of the embryos. The relative quantity of atmosphere within the culture vessel, and especially oxygen abundance, has been shown to be significant in promoting embryo growth in other systems (Dunwell, 1979) and so it is feasible that a lack of aeration prevented development *in vitro*. If gas exchange limits were a feature in the failure of the liquid-based cultures, then the opposing situation may be seen in the liquid-suspension cultures. The lack of growth in the liquid-suspension cultures is considered most likely to be attributable to a lack of nutrients resulting from poor contact with the culture media. Cultivation in the solid-state media enabled the embryos to be partially imbedded in the media, which may have allowed for sufficient exposure to the culture vessel atmosphere while ensuring good contact with the nutrient source.

An aspect that was difficult to examine using embryo material as explant matter was the effect of the osmotic potential of the media. Variation in the osmotic potential of the media due to changes in the nature or abundance of the carbohydrate source (Biahoua & Bonneau, 1998) or alternative osmoticum (e.g. sorbitol, Finkelstein & Crouch, 1986) may help to promote embryo development in both the liquid and solid-phase culture. Finally, the choice of synthetic hormone analogue may have an impact on the extent of callus development due to a variety of interactions between the carbohydrate source, hormone analogue and sterilisation method which can occur (Mendoza & Kaeppeler, 2002). As such, a considerable number of aspects may have an impact on the level of embryo development *in vitro*. The diversity of these factors, and the large number of possible interactions between them limited the extent to which they could be examined in this experiment. While it would be advisable to explore these aspects further should this study be extended, it may be advisable to optimise the culture process using fertilised embryos obtained from homospecific crosses in order to ensure that the failure of the culturing system is not due to base genetic incompatibility present in the hybrid material.

The key variable that has been assessed by this experiment is the effect of varying hormone regimes upon the recovery of viable material. Optimal callus recovery was seen at 0.25 mg l⁻¹ NAA and 1.5 mg l⁻¹ of BAP. This range is significantly higher than the concentrations required for the propagation of *C. gynandra* described by Newell *et al.* (2010), and concentrations that have shown to be effective in *Brassica* embryo culture. The ranges used within this experiment are comparable to those used by Bajaj *et al.* (1986) and the range found optimum by Zhang *et al.* (2003) reported peak rates of callus production 0.3 mg l⁻¹ NAA and 2 mg l⁻¹ of BAP. This concentration of BAP exceeds that which was found to be optimum in this experiment for callus growth in *Cleome* hybrids, although the NAA concentration is comparable. Quazi (1988) reported successful maturation and germination of hybrid *Brassica* embryos *in vitro* on a relatively simple media lacking hormone supplements, although the embryos were harvested 22 days after pollination. The results of this experiment indicate that embryo development does not continue in the absence of supplemental hormones.

It may be the case that the embryos were harvested at a stage where there is still some dependence on maternally-derived signals such as auxin (Weijers & Jürgens, 2004) although it would be hoped that any such signal could be replaced by supplemental hormone addition to the culture media. Liu *et al.* (1993) reported successful culture of proembryos that were extracted at the 8–36 cell stage and *in vitro* fertilisation of excised ovules has been effective in

a number of taxa, including *Brassica* (Zenkteler, 1990). Stewart & Hsu (1978) report increased cotton embryo recovery after 22 days onto media supplemented with auxin, although it is noted the external application of hormones may predispose the embryos to form callus rather than develop normally. If this were to be the case in *Cleome* hybrids then the level of hormonal supplementation required to promote embryo development would coincide with that required for callus induction, so the organogenesis step may be inevitable. The production of potentially hybrid callus as demonstrated by this experiment may still prove informative if organogenesis can be induced, despite the complications of achieving whole plant regeneration from *in vitro* cultures of *C. gynandra* (see section 3.3.3.5). If this work is continued further, the hormone regime should be more closely explored to identify optimal concentrations to promote embryo development, callus production and promote organogenesis to increase the probability of hybrid recovery.

5.3.3: Genetic Incompatibility within *Cleome*

Difficulties in obtaining viable hybrids from *C. gynandra* x *C. hasseleriana* crosses may be due to genetic incompatibility rather than experimental methods. Rajndrudu & Rama'Das (1982) reported successful hybridisation between *C. gynandra* and *C. viscosa* although the genetic distance between these two taxa is relatively limited according to the phylogeny of Inda *et al.* (2008). In contrast, *C. hasseleriana* is placed at considerable genetic distance from both *C. gynandra* and *C. viscosa*. The increased divergence between *C. gynandra* and *C. hasseleriana* relative to *C. viscosa* may have facilitated a higher level of evolution of heterologous loci which negatively interact in the hybrid environment leading to detrimental heterosis effects (Orr & Turelli, 2001). The application of such theory (as described by the Dobzhansky-Muller model) has been described in other plant systems (e.g. Tomato, Moyle & Nakazato, 2010) so it is conceivable that such barriers may exist within *Cleome*. In addition to genetic incompatibility, effects may also be seen due to differences in karyology. *C. gynandra* shows a base chromosome number ($x = 16$ or 17) that differs from both *C. viscosa* ($x = 10$) and *C. hasseleriana* ($x = 10$), although the latter taxon is tetraploid (Ruiz-Zapata *et al.*, 1996). It is possible that chromosomal variation prevents hybridisation, as diploid x tetraploid crosses have been reported to show lower than expected progeny yields in other plant systems (Griffiths *et al.*, 1971).

A possible method of overcoming both genetic incompatibility and problems associated with the *in vitro* culture of excised embryos may be the generation of somatic hybrids. The production of somatic hybrids *via* the fusion of isolated protoplasts has been demonstrated

between members of *Brassicaceae* (e.g. Forsberg *et al.*, 1994; Terada *et al.*, 1987). The utilisation of this method would have the additional benefit of producing “cybrids” containing a mixed parental inheritance of organelles that would not have been possible in sexual crosses. Utilisation of such methods would require an effective protocol for the isolation and regeneration of protoplasts from *Cleome*, and this has not been explored experimentally to date. Additionally, the inability to recover root tissue would place a bottleneck on the recovery of hybrid material as discussed previously. Therefore, this method would require considerable experimental exploration before it could be practically utilised.

This experiment has illustrated that it is possible to obtain potentially hybrid callus material from crosses between *C. gynandra* and *C. hassleriana* in which the latter taxon is used at the maternal parent. The inability to obtain viable embryos from the reciprocal cross matches that which has been reported previously (e.g. Smith, 1970) and may represent asymmetrical hybridisation potential between these two taxa. Genetic and chromosomal aspects of the cross may act as incompatibility barriers between the cross, although such barriers may be overcome through *in vitro* culture. While normal embryonic development *in vitro* has been not been achieved, the production of callus has been demonstrated with a potential for the recovery of hybrid individuals should organogenesis be realised through further exploration of the effects of supplementary hormone control.

6. Final Discussion

6.1: The potential for miRNAs to regulate the C₄ Cycle

This study has explored the roles that sRNA may play in regulating photosynthesis in *C. gynandra*. Since their original description as a mechanism of viral defence (Hamilton & Baulcombe, 1999), miRNAs have been implicated in an ever-increasing number of regulatory roles including leaf development (e.g. Kidner & Martienssen, 2004; Chuck *et al.*, 2007), phase change (e.g. Aukerman & Sakai 2003) and responses to plant growth regulators (e.g. Reyes & Chua 2007). Besides developmental roles, miRNAs have been described in regulating aspects of plant metabolism, notably in response to abiotic stress (e.g. Lu *et al.*, 2005; Ding *et al.*, 2009) and nutrient availability (Beauclair *et al.*, 2010). A role for miRNA activity in the C₄ cycle was initially indicated by the disproportionate alignment of sRNA sequences to components of the C₄ cycle in maize (Tolley *et al.*, unpublished). While no previous role for sRNA activity in the regulation of photosynthesis has been published, computational prediction of miRNAs in *Glycine max* has identified miRNAs which may target proteins associated with photosynthesis (Katara *et al.*, 2010) and a broader role for miRNA activity in plants has been suggested given the extent to which such regulatory processes are active in animals (Rhoades *et al.*, 2002).

miRNAs are attractive as potential regulatory elements of the C₄ cycle for a number of reasons. Firstly, miRNAs have been shown to function in a cell-specific fashion (Parizotto *et al.*, 2004) so that BS/M differentiation could enable a unique miRNA population to be present in each cell type, allowing for selective inhibition of a target gene in a cell-specific fashion. Secondly, as *trans*-acting factors a variety of separate evolutionary pathways would enable cell-type specific gene expression to be achieved without direct modification of the transcriptional regulation of the target gene itself. Finally, miRNAs appear to be subject to rapid rates of evolutionary turnover, and their limited size may mean that significant changes in their target range can be caused by a limited number of base substitutions (Fahlgren *et al.*, 2007). Given these considerations, an exploration of the roles that sRNAs play in regulation in *C. gynandra* was considered justified, and the results of this study support the hypothesis that sRNAs may regulate the C₄ cycle in *C. gynandra*.

6.2: miRNAs actively regulate Development in *C. gynandra*

The expression of the viral p19 inhibitor of miRNA biosynthesis in transgenic Arabidopsis and *C. gynandra* lines has highlighted the extent to which miRNAs are involved in regulating leaf development in both species. In Arabidopsis, expression of p19 lead to reduced vigour, the formation of leaves with increased serration of the leaf margin and modified inflorescence

structure (Figure 3.8 & 3.9), the extent of which correlated with the abundance of p19 protein which varied between lines (Figure 3.10). The severity of this phenotype is considered to be the maximum obtainable in unsupported plants grown on soil. In contrast, *C. gynandra* transgenic lines demonstrating a more advanced foliar phenotype were obtained by growth *in vitro* when supported by exogenous supplies of nutrients and growth regulators. These cultures demonstrated the formation of radialised leaves with little to no mesophyll development (Figure 3.12). These effects are consistent with previously reported phenotypes where miRNA activity has been disrupted either by the presence of viral inhibitors (Dunoyer *et al.*, 2004; Chapman *et al.*, 2004) or a loss-of-function mutation of miRNA-encoding genes (Palatnik *et al.*, 2003). The same phenotype was found in *Arabidopsis* when *p19* was placed under inducible control, although a phenotype was not recovered in the *C. gynandra* transgenic line. The accumulation of *p19* transcripts in these plants was considerably less than the relative abundance of *p19* in the *Arabidopsis* lines and so the extent of *p19* expression may have been insufficient to trigger the foliar phenotype even though *p19* expression in the developing primordia was inferred from GUS accumulation patterns (Figure 3.19).

From these data it can be inferred that miRNA-led regulatory pathways are active in *C. gynandra* that are comparable to those present in *Arabidopsis*, and the utilisation of the *p19* protein as a method of studying miRNA-mediated effects is effective.

6.3: sRNAs may act as Regulators of the C₄ Cycle in *C. gynandra*

6.3.1: Computational Prediction of miRNAs in *C. gynandra*

A key stage in the assessment of potential sRNA regulators of the C₄ cycle was the development of a library of sRNA sequences present in mature photosynthetic tissue, and the compilation of a sequence library has enabled the core components of the C₄ cycle to be subject to miRNA prediction. While the vast proportion of candidate sequences showed little to no alignment to sRNA reads, a limited subset of candidates showed above-average alignment counts (*NAD-ME1&2*, *PPDK*, *RCA*, *MDH* and *CA₄*). When the alignment of mismatched sequences against these transcripts was explored, it was found that the distribution of hits along each sequence was not equal, and that sRNA reads aligned against a limited number of loci. These positions tended to exceed the 21-24nt size window for miRNA functionality, and the presence of a conserved sequence from previously described miRNAs was not identified. Therefore, while a specific miRNA sequence has not been predicted, the unequal distribution of sRNA reads aligning against C₄ genes reported in maize (Tolley *et al.*, unpublished) has also been demonstrated in *C. gynandra*.

The full utilisation of this resource is not yet possible, however, and this limits the scope of this study. Traditional miRNA prediction methods are dependent upon an annotated target genome (Rhoades *et al.*, 2002) or candidate EST sequence lists (Prabu *et al.*, 2010), the former of which is unavailable for *C. gynandra*. Therefore, direct prediction of targets or precursor miRNA coding sequences is not possible, and the incomplete genetic blueprint for the C₄ system means that a full exploration of potential candidates is not possible with extant resources. The analysis that is possible, however, supports the suggestion that sRNAs exert a regulatory influence on the C₄ cycle. A primary extension would be to obtain similar sequence data for the C₃ *C. hassleriana*. The availability of an annotated EST database for this species (Bräutigam *et al.*, 2011) would enable a replication of the analysis performed on the *C. gynandra* sRNA library as well as direct comparison of sRNA sequences. Not only would this enable identification of sRNA sequences which are over-represented in *C. gynandra*, but this may facilitate the detection of novel miRNA sequences which do not any show conserved sequence identity with *Arabidopsis*.

Secondly, a more comparative approach may enable the identification of miRNA targets which play a role in the C₄ cycle but which have hitherto unidentified roles. The foliar tissue used to construct the library was taken from fully expanded and photosynthetically active leaves (net CO₂ fixation was demonstrable) so any regulatory miRNAs targeting components of the C₄ cycle could be expected to be present in the subsequent RNA extracts. An additional hypothesis that was to be tested by this experiment was that miRNAs play a role in regulating the development of Kranz anatomy early in leaf development. This, however, cannot be tested using the library compiled for this experiment as the genes underlying Kranz anatomy have not been identified in *C. gynandra*. In addition to anatomical development, *C. gynandra* shows some measure of age-related variation in the extent and nature of C₄ cycle, especially with regards to the decarboxylation steps (Sommer *et al.*, 2012). Therefore, a key extension would be a compilation of similar sRNA libraries along a developmental gradient from prior to the onset of Kranz formation to the point of leaf maturity. This would enable the identification of sRNA sequences which showed a high level of abundance before or during the development of Kranz anatomy that may serve as potential regulators of the maturation process. Target prediction using such libraries would be limited by the lack of known target sequences, and so a second extension would be necessary to include data from a C₃ relative of *C. gynandra*, most likely *C. hassleriana*. The availability of data relating to sRNA reads present in both a C₃ and a C₄ species along a developmental gradient would enable the identification of sequences which

show altered abundance during the development of Kranz anatomy relative to the maturation of a C₃ leaf.

6.3.2: The Efficacy of p19 as a System to test miRNA Activity

Besides direct target prediction, this study has validated the feasibility of utilising the viral p19 inhibitor of miRNA biosynthesis to examine the roles of miRNA action in *C. gynandra*. Constitutive expression of p19 *in situ* lead to significant morphological changes, reducing the leaves to a radialised structure with little to no mesophyll development, a finding which is concurrent with previously reported effects of miRNA-related disruption during leaf formation (Palatnik *et al.*, 2003). This confirms that the developmental control of leaf formation in *C. gynandra* follows parallel routes to that seen in Arabidopsis. The utilisation of the *pOp* promoter enabled p19 expression to be examined in developed tissue, and while p19 expression was implied in developing leaf primordia (as inferred by GUS activity) no change in leaf development was observed. This may suggest that inhibition of sRNA activity does not impact the formation of Kranz anatomy. However, a dose-dependent response was evident in the effects of p19 expression in Arabidopsis, and the relative levels of p19 accumulation in the *C. gynandra* transgenics are below the threshold where developmental effects were seen in transgenic Arabidopsis lines developed for this study. This issue should be addressed by the establishment of additional transgenic lines of *C. gynandra* containing the *pOp::p19* construct which would show elevated levels of p19 expression to better quantify the effects of p19 expression upon leaf development. Interestingly, the dose-dependent response of transgenic Arabidopsis lines to p19 expression demonstrated by this study contrasts with that reported by previous studies, which reported a consistent phenotype despite varied p19 expression (Dunoyer *et al.*, 2004).

6.3.3: The Effects of p19 Expression in *C. gynandra*

The key physiological effect of p19 expression demonstrated by this experiment was the depression in carboxylation efficiency (CE) and increase in the level of dark respiration in p19-expressing individuals relative to WT plants. The exact cause of the decrease in CE and increase of Γ is unclear from the data presented here. If the changes in these parameters are attributable to a relaxation of negative regulation, then the effects could be attributable to the increased activity of a component of the pathway: such an increase may indicate a loss of cell-type specificity leading to an overall reduction in efficiency. The effects of overexpression of components of the C₄ system have yet to be fully explored, although hybrid systems have been useful in exploring the effects of destabilised C₄-expression profiles.

Hybrids that were generated between various species of *Flaveria* showed an increase in the Γ values, and while this did not fully return to that of the C₃ parent, it represented a substantial increase from that of the C₄ or C₄-like parent (Byrd *et al.*, 1992; Holaday *et al.*, 1988). A similar increase in Γ , and a marked decrease in CE was seen in C₃×C₄ hybrids within *Atriplex*, to the extent that some hybrid lines showed photosynthetic characteristics which were reduced below that seen in either parent (Björkman *et al.*, 1970; Pearcy *et al.*, 1970). While the latter authors were unable to attribute the depressed CE to the activity of a single component of the C₄ cycle, it was felt the mixed genetic environment of the C₃×C₄ hybrid may lead to a combination of gene expression profiles that have a negative net effect on photosynthesis. Given the frequency of such incidences among C₃×C₄ hybrids (see Chapter 5), and the high level of orchestration that is believed to be required for efficient operation of the C₄ cycle (Sage, 2004) this is considered to be the most likely hypothesis. Given these effects, it is unfortunate that the complete regeneration of hybrids from the *C. gynandra* × *C. hasseleriana* crosses was not achieved by this study, although the validity of this approach has been confirmed and it would be advisable to optimise this process should the study be continued.

No changes in gene accumulation capable of causing the changes in Γ or CE have been recovered by this study, however. An increase in the relative abundance of *RbcS* and *RCA* transcripts was recordable, although levels of SSU polypeptides appeared to remain constant. Therefore, it is considered that the changes in photosynthesis are either attributable to changes in the activity of the components of the pathway (as manifested by changes in abundance of a *trans*-regulatory factor not profiled in this study) or to changes in the abundance of a component of the pathway hitherto unquantified. Therefore, an essential extension of this study would be to identify the reason for the increase in dark respiration in order to address the origin of these changes as discussed previously. If the effects of non-photorespiratory CO₂ production can be discounted, then the direct effects of photosynthesis can be explored. Given that no change in protein abundance sufficient to cause these effects is present in the data presented here, it is considered that the changes in photosynthetic capacity are due to either changes in a component not profiled by this study, or to changes in the activity of the existing components of the cycle. Numerous components of the C₄ cycle have been described as being subject to significant post-translational modification as a regulatory method (e.g. *PPDK*, Astley *et al.*, 2011). While the known regulatory proteins were included in this analysis, it is possible that additional mechanisms of transient regulation of enzyme activity have been affected by *p19* expression. Hypothetically, a relaxation of miRNA-mediated negative regulation of a secondary regulatory protein may lead to increased activity

of its target which in turn may lead to the changes in photosynthesis reported in this study. This would require significant experimentation to validate this hypothesis, however, and this study has highlighted the areas which would most benefit for further exploration in order to fully explore this possibility.

6.4: Light Influences Development in *C. gynandra*

Besides the effects of p19 expression, an increased accumulation of *RbcS* transcripts was also demonstrated in etiolated cotyledons of *C. gynandra* (Figure 4.5). In *Amaranthus*, *RbcS* transcripts do not associate ribosomes in darkness, and light-mediated increases in the SSU is attributable to a relaxation of translational inhibition rather than an increase in transcription rates (Berry *et al.*, 1986; 1990), a light exerts a suppressive effect on RuBisCO expression in maize (Langdale *et al.*, 1988). Therefore, the reduced abundance of the SSU in etiolated cotyledons of *C. gynandra* relative to transcript abundance correlates with this observation, although the light-mediated nature of this response means that is unlikely to be the cause of the discrepancy between transcript and peptide accumulation in the p19-expressing individuals. Secondly, it does not sufficiently explain the decline in *RbcS* transcripts that occurred within the first two hours of illumination. It is possible that the decline in transcript abundance indicates an acquisition of cell-specificity of *RbcS* (due to the exclusion of *RbcS* transcripts from the mesophyll). However, the developmentally-linked control of *RbcS* accumulation seen in *Amaranthus* (Wang *et al.*, 1992; 1993a) suggests that such regulation is most probable in *C. gynandra*, and that cell-specificity is likely to have already been in place prior to illumination. Additionally, a collapse of cell-specificity of *RbcS* transcripts does not lead to a corresponding collapse of BS-specific SSU accumulation in *A. tricolor* (McCormac *et al.*, 1997) so it is likely that *RbcS* is subject to multiple levels of regulation. The elevated levels of *RbcS* accumulation in p19-expressing plants appears to be similar to the increased abundance of *RbcS* in etiolated cotyledons, although again this does not appear to persist to the protein level.

The rate of decline seen in *RbcS* transcripts after illumination would infer a transcript half-life for *RbcS* that would be in the order of two hours. While transcript stability data is not available for *C. gynandra*, this would be considerably faster than values reported for other transcripts in *Arabidopsis* (Gutiérrez *et al.*, 2002; Narsai *et al.*, 2007), inferring that negative regulation of transcript abundance would be required if this decline were attributable to illumination alone. It would be attractive to speculate that such negative regulation could take the form of miRNA-mediated decay, but the data presented here is not sufficient to address

this hypothesis. While a number of sRNA reads aligned against *RbcS*, no underlying miRNA sequence was identifiable on the basis of conserved sequence or adherence to accepted targeting rules, and the frequency of aligned reads was considerably below that seen in other candidate genes profiled. However, this hypothesis might be supported by the increased abundance of *RbcS* transcripts after induction of p19 which may indicate a relaxation of active negative suppression beyond the transcriptional level. If these two conditions are linked, then it could be hypothesised that a light-induced miRNA may exert some regulatory effect upon *RbcS*. While a direct miRNA response to light has not been fully established, UV-B radiation has shown to modulate miRNA expression (Zhou *et al.*, 2007), and a role of miRNA activity in regulating adventitious rooting *via* influence on light-dependant auxin homeostasis (Sorin *et al.*, 2005). This is largely speculation, however, and it would be necessary to undergo significant experimentation to justify this. As noted previously, an ability to perform *in situ* RNA hybridisations and immunolocalisations would enable a specific gain or collapse of cell-specificity in response to illumination or expression of p19 to be identified. In addition, the repetition of the light-induction experiments with cotyledons of transgenic lines expressing p19 would enable a further examination of the decline in *RbcS* accumulation after illumination.

6.5: Final Conclusions

Overall, this study has demonstrated the depth of possible regulatory mechanisms that may be active in *C. gynandra*. The disproportionate alignment of sRNA sequences against C₄ genes in maize has also been identified in *C. gynandra*. Not only were high numbers of sRNA reads aligning against a limited subset of candidate genes but the distribution of these reads was not equal. No specific miRNA sequence was isolated, but alignments produced by this study may contain underlying miRNA sequences which could be identified with further study. A role of miRNA activity in leaf formation of *C. gynandra* is also supported by the significant phenotype caused by the expression of the p19 miRNA biosynthesis inhibitor. The severity of this phenotype required the use of a transient expression system so that the effects of p19 on a pre-existing functional C₄ system could be examined. The effectiveness of chemically inducing p19 expression was demonstrated, although the low levels of p19 expression seen under these conditions prevented a full exploration of any potential effects of an inhibition of miRNA activity on the formation of Kranz anatomy.

When p19 is transiently expressed in *C. gynandra*, carboxylation efficiency was reduced while the extent dark respiration increased which would indicate the photosynthesis in *C. gynandra*

is comprised when miRNA inactivity is reduced. While some changes were detected in transcript abundance these did not persist to the protein level, indicating that the effects of p19 upon photosynthesis are due either to a secondary cause not profiled in this study, or due to altered activity of the existing components of the C₄ system. *RbcS* appears to be negatively regulated at a number of levels due to a discrepancy between transcript and protein accumulation seen in both the p19-expressing systems and in etiolated cotyledons, although it is not possible to identify the nature of this regulation based upon the data obtained in this study.

7. References

- Abbo, S., Ladizinsky, G. (1991) Anatomical aspects of hybrid embryo abortion in the genus *Lens* L. *Botanical Gazette* **152**(3): 316–320.
- Abler, M.L., Green, P.J. (1996) Control of mRNA stability in higher plants. *Plant Molecular Biology* **32**(1–2): 63–78.
- Akyildiz, M., Gowik, U., Engelmann, S., Koczor, M., Streubel, M., Westhoff, P. (2007) Evolution and function of a cis-regulatory module for mesophyll-specific gene expression in the C₄ dicot *Flaveria trinervia*. *The Plant Cell* **19**(11): 3391–402.
- Albarello, N., Simões, C., Rosas, P.F.G., Castro, T.C., Gianfaldoni, M.G., Callado, C.H., Mansur, E. (2006) *In vitro* propagation of *Cleome spinosa* (Capparaceae) using explants from nursery-grown seedlings and axenic plants. *In Vitro Cellular & Developmental Biology - Plant* **42**(6): 601–606.
- Alt-Mörbe, J., Kühlmann H., Schröder, J. (1989) Differences in induction of Ti plasmid virulence genes *virG* and *virD*, and continued control of *virD* expression by four external factors. *Molecular Plant-Microbe Interactions* **2**(6):301–308.
- Ambros, V. (2004) The functions of animal microRNAs. *Nature* **431**: 350–355.
- An, G., Ebert, P.R., Mitra, A., Ha, S.B. (1988) Binary vectors. In: S.B. Gelvin and R.A. Schilperoort (Eds.), *Plant Molecular Biology Manual*, Kluwer Academic Publishers, Dordrecht, Netherlands, pp. A3: 1–19.
- Andrews, T.J., Lorimer, G.H. (1987) RuBisCO: structure, mechanisms and prospects for improvement. *The Biochemistry of Plants* **10**: 131–218.
- Aoyagi, K., Bassham, J. A., Greene, F.C. (1984) Pyruvate orthophosphate dikinase gene expression in developing wheat seeds. *Plant Physiology* **75**(2): 393–6.
- Astley, H.M., Parley, K., Aubry, S., Chastain, C.J., Burnell, J.N., Webb, M.E., Hibberd, J.M. (2011) The pyruvate, orthophosphate dikinase regulatory proteins of *Arabidopsis* are both bifunctional and interact with the catalytic and nucleotide-binding domains of pyruvate, orthophosphate dikinase. *The Plant Journal* **68**(6): 1070–1080.
- Aukerman, M.J, Sakai, H. (2003) Regulation of flowering time and floral organ identity by a MicroRNA and its APETALA2-like target genes. *The Plant cell* **15**(11): 2730–41.
- Bajaj, Y.P.S., Mahajan, S.K., Labana, K.S. (1986) Interspecific hybridization of *Brassica napus* and *B. juncea* through ovary, ovule and embryo culture. *Euphytica* **35**(1): 103–109.
- Bao, N., Lye, K., Barton, M.K. (2004) MicroRNA binding sites in *Arabidopsis* class III HD-ZIP mRNAs are required for methylation of the template chromosome. *Developmental Cell* **7**(5): 653–662.
- Barone, A., Giudice, A., Ng, N.Q. (1992) Barriers to interspecific hybridization between *Vigna unguiculata* and *Vigna vexillata*. *Sexual Plant Reproduction* **5**(3): 195–200.
- Bartel, D.P., Lee, R., Feinbaum, R. (2004) MicroRNAs: Genomics, Biogenesis, Mechanism, and Function Genomics. *Genes* **116**: 281–297.
- Baskin, J.M., Baskin, C.C. (1979) Promotion of germination of *Stellaria media* seeds by light from a greensafe lamp. *New Phytologist* **82**(2): 381–383.

- Beauclair, L., Yu, A., Bouché, N. (2010) microRNA-directed cleavage and translational repression of the copper chaperone for superoxide dismutase mRNA in Arabidopsis. *The Plant Journal* **62**(3): 454–62.
- Berezikov, E., Gurye, V., van de Belt, J., Wienholds, E., Plasterk, R.H.A. (2005) Phylogenetic shadowing and computational identification of human microRNA genes. *Cell* **120**(1): 21–24.
- Berry, J.O., Breiding, D.E., Klessig, D.F. (1990) Light-mediated control of translational initiation of ribulose-1, 5-bisphosphate carboxylase in amaranth cotyledons. *The Plant Cell* **2**(8): 795–803.
- Berry, J.O., Nikolau, B.J., Carr, J.P., Klessig, D.F. (1986) Translational regulation of light-induced ribulose 1,5-bisphosphate carboxylase gene expression in amaranth. *Molecular Cellular Biology* **6**(7): 2347–2353.
- Biahoua, A., Bonneau, L. (1999) Control of *in vitro* somatic embryogenesis of the spindle tree (*Euonymus europaeus* L.) by the sugar type and the osmotic potential of the culture medium. *Plant Cell Reports* **19**(2): 185–190.
- Bilang, R., Bogorad, L. (1996) Light-dependent developmental control of *RbcS* gene expression in epidermal cells of maize leaves. *Plant Molecular Biology* **31**(4): 831–841.
- Bimboim, H.C., Doly, J. (1979) A rapid alkaline extraction procedure for screening recombinant plasmid DNA. *Nucleic Acids Research* **7**(6): 1513–1523.
- Björkman, O., Gauhl, E., Nobs, M.A. (1969) Comparative studies of *Atriplex* species with and without B-carboxylation photosynthesis and their first-generation hybrid. *Carnegie Institute of Washington Yearbook* **68**: 620–633.
- Björkman, O., Nobs, M. A., Berry, J.A. (1971) Further studies on hybrids between C₃ and C₄ species of *Atriplex*. *Carnegie Institute of Washington Yearbook* **70**: 507–511.
- Björkman, O., Percy, R W., Nobs, M.A. (1970) Hybrids between *Atriplex* species with and without β-carboxylation photosynthesis. Photosynthetic characteristics. *Carnegie Institute of Washington Yearbook* **69**:640–48
- Boinski, J.J., Wang, J.L., Xu, P., Hotchkiss, T., Berry, J. O. (1993) Post-transcriptional control of cell type-specific gene expression in bundle sheath and mesophyll chloroplasts of *Amaranthus hypochondriacus*. *Plant Molecular Biology* **22**(3): 397–410.
- Bollman, K.M. (2003) HASTY, the Arabidopsis ortholog of exportin 5/MSN5, regulates phase change and morphogenesis. *Development* **130**(8): 1493–1504.
- Bonnet, E., Wuyts, J., Rouzé, P. Van de Peer, Y. (2004) Detection of 91 potential conserved plant microRNAs in *Arabidopsis thaliana* and *Oryza sativa* identifies important target genes. *Proceedings of the National Academy of Sciences of the United States of America* **101**(31): 11511–11516.
- Bouton, J.H., Brown, R.H., Evans, P.T., Jernstedt, J.A. (1986) Photosynthesis, leaf anatomy, and morphology of progeny from hybrids between C₃ and C₃/C₄ *Panicum* species. *Plant Physiology* **80**(2): 487–492.
- Bradford, M. (1976) A rapid and sensitive method for the quantitation of microgram quantities of protein utilizing the principle of protein-dye binding. *Analytical Biochemistry* **72**: 248–254.
- Bräutigam, A., Hoffmann-Benning, S. (2008) Comparative proteomics of chloroplast envelopes from C₃ and C₄ plants reveals specific adaptations of the plastid envelope to C₄ photosynthesis and candidate proteins required for maintaining C₄ metabolite fluxes. *Plant Physiology* **148**(1): 568–579.

- Bräutigam, A., Kajala, K., Wullenweber, J., Sommer, M., Gagneul, D., Weber, K.L., Carr, K.M. (2011) An mRNA blueprint for C₄ photosynthesis derived from comparative transcriptomics of closely related C₃ and C₄ species. *Plant Physiology* **155**(1): 142–156.
- Briggs, C.L., Westoby, M., Selkirk, P.M., Oldfield, R.J. (1987) Embryology of early abortion due to limited maternal resources in *Pisum sativum* L. *Annals of Botany* **59**(6): 611–619.
- Brodersen, P., Sakvarelidze-Achard, L., Bruun-Rasmussen, M., Dunoyer, P., Yamamoto, Y. Y., Sieburth, L., Voinnet, O. (2008) Widespread translational inhibition by plant miRNAs and siRNAs. *Science* **320**: 1185–1190
- Brooks, A., Farquhar, G.D. (1985) Effect of temperature on the CO₂/O₂ specificity of ribulose-1,5-bisphosphate carboxylase/oxygenase and the rate of respiration in the light. *Planta* **165**(3): 397–406.
- Brown, N.J., Newell, C.A., Stanley, S., Chen, J.E., Perrin, A.J., Kajala, K., Hibberd, J.M. (2011) Independent and parallel recruitment of preexisting mechanisms underlying C₄ photosynthesis. *Science* **331**: 1436–9.
- Brown, R.H., Bassett, C.L., Cameron, R.G., Evans, P.T., Bouton, J.H., Black, C.C., Sternberg, L.O. (1986) Photosynthesis of F(1) hybrids between C₄ and C₃-C₄ species of *Flaveria*. *Plant Physiology* **82**(1): 211–217.
- Brown, R.H., Bouton, J.H. (1993) Physiology and genetics of interspecific hybrids between photosynthetic types. *Annual Review of Plant Physiology* **44**: 435–456.
- Brown, R.H., Bouton, J.H., Evans, P.T., Malter, H.E., Rigsby, L.L. (1985) Photosynthesis, morphology, leaf anatomy, and cytogenetics of hybrids between C₃ and C₃/C₄ *Panicum* species. *Plant Physiology* **77**(3): 653–658.
- Brown, R.H., Byrd, G.T., Black, C.C. (1992) Degree of C₄ Photosynthesis in C₄ and C₃-C₄ *Flaveria* species and their hybrids: II Inhibition of apparent photosynthesis by a phosphoenolpyruvate carboxylase inhibitor. *Plant Physiology* **100**(2): 947–950.
- Brutnell, T.P., Sawers, R.J., Mant, A., Langdale, J.A. (1999) BUNDLE SHEATH DEFECTIVE2, a novel protein required for post-translational regulation of the *rbcl* gene of maize. *The Plant Cell* **11**(5): 849–64.
- Burnell, J.N., Suzuki, I., Sugiyama, T. (1990) Light induction and the effect of nitrogen status upon the activity of carbonic anhydrase in maize leaves. *Plant Physiology* **94**(1): 384–387.
- Bustin, S. (2000) Absolute quantification of mRNA using real-time reverse transcription polymerase chain reaction assays. *Journal of Molecular Endocrinology* **25**(2): 169–193.
- Byrd, G.T., Brown, R.H., Bouton, J.H., Bassett, C.L., Black, C.C. (1992) Degree of C₄ photosynthesis in C₄ and C₃-C₄ *Flaveria* species and Their Hybrids: I. CO₂ Assimilation and metabolism and activities of phosphoenolpyruvate carboxylase and NADP-malic enzyme. *Plant Physiology* **100**(2): 939–46.
- Byrd, G.T., Sage, R.F., Brown, R.H. (1992) A comparison of dark respiration between C₃ and C₄ plants. *Plant Physiology* **100**(1): 191–198.
- Cabido, M., Pons, E., Cantero, J.J., Lewis, J.P., Anton, A. (2007) Photosynthetic pathway variation among C₄ grasses along a precipitation gradient in Argentina. *Journal of Biogeography* **35**(1): 131–140.
- Caemmerer, S., Farquhar, G.D. (1981) Some relationships between the biochemistry of photosynthesis and the gas exchange of leaves. *Planta* **153**(4): 376–387.

- Cane, J.H. (2008) Breeding biologies, seed production and species-rich bee guilds of *Cleome lutea* and *Cleome serrulata* (Cleomaceae). *Plant Species Biology* **23**(3): 152–158.
- Carrington, J.C., Ambros, V. (2003) Role of microRNAs in plant and animal development. *Science* **301**: 336–338.
- Chapman, E.J., Prokhnovsky, A.I., Gopinath, K., Dolja, V.V., Carrington, J.C. (2004) Viral RNA silencing suppressors inhibit the microRNA pathway at an intermediate step. *Genes & development* **18**(10): 1179–86.
- Chastain, C.J., Heck, J.W., Colquhoun, T.A., Voge, D.G., Gu, X.Y. (2006) Posttranslational regulation of pyruvate, orthophosphate dikinase in developing rice (*Oryza sativa*) seeds. *Planta* **224**(4): 924–34.
- Chastain, C.J., Xu, W., Parsley, K., Sarath, G., Hibberd, J.M., Chollet, R. (2008) The pyruvate, orthophosphate dikinase regulatory proteins of *Arabidopsis* possess a novel, unprecedented Ser/Thr protein kinase primary structure. *The Plant Journal* **53**(5): 854–863.
- Chellappan, P., Xia, J., Zhou, X., Gao, S., Zhang, X., Coutino, G., azquez, F., Zhang, W., Jin, H. (2010) siRNAs from miRNA sites mediate DNA methylation of target genes. *Nucleic Acids Research* **38**(20): 6883–6894.
- Chen, C.C., Gibson, P.B. (1972) Barriers to hybridization of *Trifolium repens* with related species. *Canadian Journal of Genetics and Cytology* **14**(2): 381–389.
- Chen, X. (2004) A microRNA as a translational repressor of APETALA2 in *Arabidopsis* flower development. *Science* **303**: 2022–2025.
- Cheng, S.H., Keefe, D., Mets, L., Ku, M.S.B. (1987) Photosynthetic characteristics of reciprocal backcrosses between F₁ hybrid (C₃-C₄ x C₄) and C₄ *Flaveria* species. *Plant Physiology* **83**:4.
- Chitwood, D.H., Timmermans, M.C.P. (2007) Target mimics modulate miRNAs. *Nature Genetics* **39**(8): 935–936.
- Chitwood, D.H., Nogueira, F.T., Howell, M.D. (2009) Pattern formation via small RNA mobility. *Genes and Development* **23**: 549–554.
- Chollet, R., Ogren, W.L. (1975) Regulation of photorespiration in C₃ and C₄ species. *The Botanical Review* **41**(2): 137–179.
- Chomczynski, P., Sacchi, N. (1987) Single-step method of RNA isolation by acid guanidinium thiocyanate-phenol-chloroform extraction. *Analytical Biochemistry* **162**: 156–159.
- Christin, P.A., Salamin, N., Muasya, A.M., Roalson, E.H., Russier, F., & Besnard, G. (2008) Evolutionary switch and genetic convergence on *rbcl* following the evolution of C₄ photosynthesis. *Molecular biology and Evolution* **25**(11): 2361–2368.
- Chuck, G., Cigan, M., Saetern, K., Hake, S. (2007) The heterochronic maize mutant Corngrass1 results from overexpression of a tandem microRNA. *Nature Genetics* **39**(4): 544–549.
- Clough, S.J., Bent, A.F. (1998) Floral dip: a simplified method for *Agrobacterium*-mediated transformation of *Arabidopsis thaliana*. *The Plant Journal* **16**(6): 735–743.
- Collins, R.P., Jones, M.B. (1986) The influence of climatic factors on the distribution of C₄ species in Europe. **64**: 121–129.

- Conner, A.J., Falloon, P.G. (1993) Osmotic versus nutritional effects when rooting in vitro asparagus minicrowns on high sucrose media. *Plant Science* **89**(1): 101–106.
- Craft, J., Samalova, M., Baroux, C., Townley, H., Martinez, A., Tsiantis, M., Moore, I. (2005) New pOp/LhG4 vectors for stringent glucocorticoid-dependent transgene expression in Arabidopsis. *The Plant Journal* **41**(6): 899–918.
- Dafni, A., Maués, M.M. (1998) A rapid and simple procedure to determine stigma receptivity. *Sexual Plant Reproduction* **11**(3), 177–180.
- De Block, M., De Brouwer, D., & Tenning, P. (1989) Transformation of *Brassica napus* and *Brassica oleracea* using *Agrobacterium tumefaciens* and the expression of the *bar* and *neo* genes in the transgenic plants. *Plant Physiology* **91**(2): 694–701.
- Dengler N.G., Dengler R.E., Donnelly P.M., Hattersley P.W. (1993) Quantitative leaf anatomy of C₃ and C₄ grasses (Poaceae): bundle sheath and mesophyll surface area relationships. *Annals of Botany* **73**: 241–255.
- Dengler N.G., Nelson T. (1999) Leaf structure and development in C₄ plants. In: Sage RF, Monson RK, eds. *C₄ Plant Biology*. San Diego, CA, USA: Academic Press, pp.133–172.
- Desprez, T., Amselem, J., Caboche, M., Hofte, H. (1998) Differential gene expression in Arabidopsis monitored using cDNA arrays. *The Plant Journal* **14**(5): 643–652.
- Devers, E.A., Branscheid, A., May, P., Krajinski, F. (2011) Stars and symbiosis: microRNA- and microRNA*-mediated transcript cleavage involved in arbuscular mycorrhizal symbiosis. *Plant physiology* **156**(4): 1990–2010.
- Ding, D., Zhang, L., Wang, H., Liu, Z., Zhang, Z., Zheng, Y. (2009) Differential expression of miRNAs in response to salt stress in maize roots. *Annals of Botany* **103**(1): 29–38.
- Dunoyer, P., Lecellier, C., Parizotto, E.A., Himber, C., Voinnet, O. (2004) Probing the microRNA and small interfering RNA pathways with virus-encoded suppressors of RNA silencing. *The Plant Cell* **16**(5): 1235–50.
- Dunwell, J.M. (1979) Anther culture in *Nicotiana tabacum*: The role of the culture vessel atmosphere in pollen embryo induction and growth. *Journal of Experimental Botany* **30**(3): 419–428.
- Edwards, G.E., Ku, M.S.B. (1987) Biochemistry of C₃-C₄ Intermediates. *The Biochemistry of Plants* **10**: 275–325.
- Edwards, G.E., Ku, M.S.B., Hatch, M.D. (1982) Photosynthesis in *Panicum milioides*, a species with reduced photorespiration. *Plant Cell Physiology* **23**(7): 1185–1195.
- Ehleringer, J., Björkman, O. (1977) Quantum yields for CO₂ uptake in C₃ and C₄ plants. *Plant Physiology* **59**(1): 86–90.
- Ehleringer, J.R., Sage, R.F., Flanagan, L.B., Pearcy, R.W. (1991) Climate change and the evolution of C₄ photosynthesis. *Trends in Ecology & Evolution* **6**(3): 95–99.
- Emmert-Buck, M.R., Bonner, R.F., Smith, P.D., Chaqui, R.F., Zhuang, Z., Goldstein, S.R., Weiss, R.A., Liotta, L.A. (1996) Laser Capture Microdissection. *Science* **274**: 998–1001.

- Eshed, Y., Zamir, D. (1995) An introgression line population of *Lycopersicon pennellii* in the cultivated tomato enables the identification and fine mapping of yield-associated QTL. *Genetics* **141**: 1147–1162.
- Evans, L.T., Fischer, R.A. (1999) Yield potential: its definition and significance. *Crop Science* **39**(6): 1544 – 1551.
- Evenson, R.E, Gollin, D. (2003) Assessing the impact of the Green Revolution, 1960 – 2000. *Science* **300**: 75 –762.
- Farquhar, G.D., Caemmerer, S., Berry, J.A. (1980) A biochemical model of photosynthetic CO₂ assimilation in leaves of C₃ species. *Planta* **149**(1): 78–90.
- Finkelstein, R.R., Crouch, M.L. (1986) Rapeseed embryo development in culture on high osmoticum is similar to that in seeds. *Plant Physiology* **81**(3): 907–912.
- Fisher, D.K., Gultinan, M.J. (1995) Rapid, efficient production of homozygous transgenic tobacco plants with *Agrobacterium tumefaciens*: A seed-to-seed protocol. *Plant Molecular Biology Reporter* **13**(3): 278–289.
- Fischer, G., Heilig G.K. (1997) Population momentum and the demand on land and water resources. *Philosophical Transactions of the Royal Society B* **352**(1356): 869–889.
- Forsberg, J., Landgren, M., Glimelius, K. (1994) Fertile somatic hybrids between *Brassica napus* and *Arabidopsis thaliana*. *Plant Science* **95**(2): 213–223.
- Frohman, M.A. (1988) Rapid production of full-length cDNAs from rare transcripts: Amplification using a single gene-specific oligonucleotide primer. *Proceedings of the National Academy of Sciences* **85**(23): 8998–9002.
- Fujii, H., Chiou, T.-J., Lin, S.-I., Aung, K., Zhu, J.-K. (2005) A miRNA involved in phosphate-starvation response in Arabidopsis. *Current Biology* **15**(22): 2038–2043.
- Furbank, R.T. (2011) Evolution of the C₄ photosynthetic mechanism: are there really three C₄ acid decarboxylation types? *Journal of Experimental Botany* **62**(9): 3103–3108.
- Furumoto, T., Yamaguchi, T., Ohshima-Ichie, Y., Nakamura, M., Tsuchida-Iwata, Y., Shimamura, M., Ohnishi, J. (2011) A plastidial sodium-dependent pyruvate transporter. *Nature* **476**: 472–475.
- Gallaher, R.N., Brown, R.H. (1977) Starch storage in C₄ vs. C₃ grass leaf cells as related to nitrogen deficiency. *Crop Science* **17**(1): 85.
- Gamborg, O.L., Miller, R.A., Ojima, K. (1968) Nutrient requirements of suspension cultures of soybean root cells. *Experimental Cell Research* **50**(1): 151–158.
- Gehring, H., Kasemir, H., Mohr, H. (1977) The capacity of chlorophyll-a biosynthesis in the mustard seedling cotyledons as modulated by phytochrome and circadian rhythmicity. *Planta* **133**(3): 295–302.
- Gowik, U., Burscheidt, J., Akyildiz, M., Schlue, U., Koczor, M., Streubel, M., Westhoff, P. (2004) cis-Regulatory elements for mesophyll-specific gene expression in the C₄ plant *Flaveria trinervia*, the promoter of the C₄ phosphoenolpyruvate carboxylase. *The Plant Cell* **16**: 1077–1090.
- Griffiths, D.J., Pegler, R.A.D., Tonguthaisri, T. (1971) Cross compatibility between diploid and tetraploid perennial ryegrass (*Lolium perenne* L.). *Euphytica* **20**(1): 102–112.

- Guo, S., Schinner, K., Sattelmacher, B., Hansen, U.P. (2005) Different apparent CO₂ compensation points in nitrate- and ammonium-grown *Phaseolus vulgaris* and the relationship to non-photorespiratory CO₂ evolution. *Physiologia Plantarum* **123**(3): 288–301.
- Gutierrez, R.A., Ewing, R.M., Cherry, J.M., Green, P.J. (2002) Identification of unstable transcripts in Arabidopsis by cDNA microarray analysis: rapid decay is associated with a group of touch- and specific clock-controlled genes. *Proceedings of the National Academy of Sciences of the United States of America* **99**(17): 11513–11518.
- Haberlandt, D.G. (1882) *Vergleichende anatomie des assimilatorischen gewebesystems der pflanzen*. Pringsheim Jahrbuch fur Wiss. Botanischer Boded 13.
- Hall, L.N., Rossini, L., Cribb, L., Langdale, J.A. (1998) GOLDEN 2: a novel transcriptional regulator of cellular differentiation in the maize leaf. *The Plant Cell*, **10**(6): 925–936.
- Hall, T.A. 1999. BioEdit: a user-friendly biological sequence alignment editor and analysis program for Windows 95/98/NT. *Nucleic Acids Symposium Series* **41**: 95–98.
- Hamilton, A.J., Baulcombe, D.C. (1999) A species of small antisense RNA in posttranscriptional gene silencing in plants. *Science* **286**: 950–952.
- Hanahan, D. (1983) Studies on transformation of *Escherichia coli* with plasmids. *Journal of Molecular Biology* **166**(4): 557–580.
- Harberd, D.J. (1969) A simple effective embryo culture technique for *Brassica*. *Euphytica* **18**(3): 425–429.
- Harrison, S.J., Mott, E.K., Parsley, K., Aspinall, S., Gray, J.C., Cottage, A. (2006) A rapid and robust method of identifying transformed *Arabidopsis thaliana* seedlings following floral dip transformation. *Plant Methods* **2**(1): 19.
- Hartwell, J., Gill, A., Nimmo, G.A., Wilkins, M.B., Jenkins, G.I., Nimmo, H.G. (1999) Phosphoenolpyruvate carboxylase kinase is a novel protein kinase regulated at the level of expression. *The Plant Journal*, **20**(3): 333–342.
- Hatch, M.D. (1971) The C₄ pathway of photosynthesis. Evidence for an intermediate pool of carbon dioxide and the identity of the donor C₄ -dicarboxylic acid. *The Biochemical journal*, **125**(2): 425–32.
- Hatch, M.D., Slack, C.R. (1966) Photosynthesis by sugar-cane leaves. A new carboxylation reaction and the pathway of sugar formation. *The Biochemical Journal*, **101**(1), 103–11.
- Havecker, E. (2011) Detection of small RNAs and microRNAs using deep sequencing technology. *Methods in Molecular Biology* **732**: 55–68.
- Hibberd, J.M., Sheehy, J.E., Langdale, J.A. (2008) Using C₄ photosynthesis to increase the yield of rice—rationale and feasibility. *Current Opinion in Plant Biology*, **11**(2): 228–31.
- Holaday, A.S., Brown, R.H., Bartlett, J.M., Sandlin, E.A., Jackson, R.C. (1988) Enzymic and photosynthetic characteristics of reciprocal F₁ hybrids of *Flaveria pringlei* C₃ and *Flaveria brownii* (C₄-Like Species). *Plant Physiology* **87**(2): 484–490.
- Hsieh, L.C., Lin, S.I., Shih, A.C.C., Chen, J.W., Lin, W.Y., Tseng, C.Y., Li, W.H., Chiou, T.J. (2009) Uncovering small RNA-mediated responses to phosphate deficiency in Arabidopsis by deep sequencing. *Plant Physiology* **151**(4): 2120–2132.

- Hudson, G., Dengler, R., Hattersley, P., Dengler, G. (1992) Cell-specific expression of Rubisco small subunit and Rubisco activase genes in C₃ and C₄ species of *Atriplex*. *Australian Journal of Plant Physiology*: **19**(1): 89.
- Hunt, S., Smith, A.M., Woolhouse, H.W. (1987) Evidence for a light-dependent system for reassimilation of photorespiratory CO₂, which does not include a C₄ cycle, in the C₃/C₄ intermediate species *Moricandia arvensis*. *Planta* **171**(2): 227–234.
- Inda, L.A., Torrecilla, P., Catalán, P., Ruiz-Zapata, T. (2008) Phylogeny of *Cleome* L. and its close relatives *Podandroyne* Ducke and *Polanisia* Raf. (Cleomoideae, Cleomaceae) based on analysis of nuclear ITS sequences and morphology. *Plant Systematics and Evolution* **274**(1-2): 111–126.
- Jackson, D.P. (1992) In situ hybridization in plants. In *Molecular Plant Pathology: A Practical Approach* (D.J. Bowles, S.J. Gurr and M. McPherson, Eds) Oxford University Press, Oxford, pp. 163–174.
- Jacob, J., Lawlor, D.W. (1992) Dependence of photosynthesis of sunflower and maize leaves on phosphate supply, ribulose-1,5-bisphosphate carboxylase/oxygenase activity, and ribulose-1,5-bisphosphate pool size. *Plant Physiology* **98**(3): 801–807.
- Jefferson, R.A. (1987) Assaying chimeric genes in plants: The GUS gene fusion system. *Plant Molecular Biology Reporter* **5**(4): 387–405.
- Jefferson, R.A., Kavanagh, T.A., Bevan, M.W. (1987) GUS fusions: beta-glucuronidase as a sensitive and versatile gene fusion marker in higher plants. *The EMBO journal* **6**(13): 3901–3907.
- Jiao, J., Chollet, R. (1988) Light/dark regulation of maize leaf phosphoenolpyruvate carboxylase by in vivo phosphorylation. *Archives of Biochemistry and Biophysics* **261**(2): 409–417.
- Jones, C.G., Daniel Hare, J., Compton, S.J. (1989) Measuring plant protein with the Bradford assay. *Journal of Chemical Ecology* **15**(3): 979–992.
- Jones-Rhoades, M.W., Bartel, D.B. (2004) Computational identification of plant microRNAs and their targets, including a stress-induced miRNA. *Molecular Cell* **14**(6): 787–799.
- Kajala, K., Brown, N.J., Williams, B.P., Borrill, P., Taylor, L.E., & Hibberd, J.M. (2011) Multiple Arabidopsis genes primed for recruitment into C₄ photosynthesis. *The Plant Journal* **69**(1): 47–56.
- Kalamajka, R., Hahnen, S., Cavalari, M., Töpsch, S., Weier, D., Peterhänsel C. (2003) Restriction accessibility in isolated nuclei reveals light-induced chromatin reorganization at the PEPC promoter in maize. *Plant Molecular Biology* **52**(3): 669–678.
- Kanai, R., Edwards, G.E. (1973) Separation of mesophyll protoplasts and bundle sheath cells from maize leaves for photosynthetic studies. *Plant Physiology* **51**(6): 1133–1137.
- Kanai, R., Edwards, G.E., (1999) Structure-Function of the C₄ Syndromes In: Sage RF, Monson RK, eds. *C₄ Plant Biology*. San Diego, CA, USA: Academic Press, pp.49–80.
- Kang, H.G., Fang, Y., Singh, K.B. (1999) A glucocorticoid-inducible transcription system causes severe growth defects in Arabidopsis and induces defense-related genes. *The Plant Journal* **20**(1): 127–133.
- Kasschau, K.D., Xie, Z., Allen, E., Llae, C., Chapman, E.J., Krizan, K.A., Carrington, J.C. (2003) P1/HC-Pro, a viral suppressor of RNA silencing, interferes with Arabidopsis development and miRNA function. *Developmental Cell* **4**(2): 205–217.

- Katara, P., Gautam, B., Kuntal, H., Sharma, V. (2010) Prediction of miRNA targets, affected proteins and their homologs in *Glycine max*. *Bioinformation* **5**(4): 162–5.
- Khush, G.S. (1999) Green revolution: preparing for the 21st century. *Genome* **42**(4): 646 – 655.
- Kausch, A.P., Page Owen, T., Zachwieja, S.J., Flynn, A.R., & Sheen, J. (2001) Mesophyll-specific, light and metabolic regulation of the C₄ PPCZm₁ promoter in transgenic maize. *Plant Molecular Biology* **45**(1): 1–15.
- Kellogg, E.A. (1999) Phylogenetic aspects of the evolution of C₄ photosynthesis In: Sage RF, Monson RK, eds. *C₄ Plant Biology*. San Diego, CA, USA: Academic Press, pp.411–439.
- Khan, S., Rowe, S.C, Harmon, F.G. (2010) Coordination of the maize transcriptome by a conserved circadian clock. *BMC Plant Biology* **10**(1):126.
- Kiniry, J.R., Jones, C.A., O'Toole, J.C., Blanchet, R., Cabelguenne, M., Spanel, D.A. (1989) Radiation-use efficiency in biomass accumulation prior to grain filling for five grain-crop species. *Field Crops Research* **20**(1): 51–64.
- Kidner, C.A., Martienssen, R.A. (2004) Spatially restricted microRNA directs leaf polarity through ARGONAUTE1. *Nature* **428**: 81–84.
- Kim, J. (2003) A Mechanism for Light-Induced Translation of the *rbcL* mRNA Encoding the Large Subunit of Ribulose-1,5-bisphosphate Carboxylase in Barley Chloroplasts. *Plant and Cell Physiology* **44**(5): 491–499.
- Kim, V.N., Nam, J.W. (2006) Genomics of microRNA. *Trends in Genetics* **22**(3): 165–73.
- Kiniry, J.R., Jones, C.A., O'Toole, J.C., Blanchet, R., Cabelguenne, M., Spanel, D.A. (1989) Radiation-use efficiency in biomass accumulation prior to grain-filling for five grain-crop species. *Field Crops Research* **20**(1), 51–64.
- Klein, R.R., Mullet, J.E. (1987) Control of gene expression during higher plant chloroplast biogenesis. Protein synthesis and transcript levels of *psbA*, *psaA-psaB*, and *rbcL* in dark-grown and illuminated barley seedlings. *Journal of Biological Chemistry* **262**(9): 4341–4348.
- Kleppe, K., Ohtsuka, E., Kleppe, R., Molineux, I., Khorana, H.G. (1971) Studies on polynucleotides. *Journal of Molecular Biology* **56**(2): 341–361.
- Knapp, A.K., Cocke, M., Hamerlynch, E.P., Owensby, C.E. (1994) Effect of elevated CO₂ on stomatal density and distribution in a C₄ grass and a C₃ forb under field conditions. *Annals of Botany* **74**(6): 595–599.
- Koteyeva, N.K., Voznesenskaya, E.V., Roalson, E.H., & Edwards, G.E. (2011) Diversity in forms of C₄ in the genus *Cleome* (Cleomaceae). *Annals of Botany* **107**(2): 269–283.
- Koyama, T., Furutani, M., Tasaka, M., Ohme-Takagi, M. (2007) TCP transcription factors control the morphology of shoot lateral organs via negative regulation of the expression of boundary-specific genes in *Arabidopsis*. *The Plant Cell* **19**(2): 473–484.
- Kubicki, A., Steinmaller, K., Westhoff, P., Disseldorf, H. (1994) Differential transcription of the plastome-encoded genes in the mesophyll and bundle-sheath chloroplasts of the monocotyledonous NADP-malic enzyme-type C₄ plants maize and Sorghum. *Plant Molecular Biology* **25**(4): 669–679.

- Kulya, J., Lontom, W., Bunnag, S., Theerakulpisut, P. (2011) *Cleome gynandra* L. (a C₄ plant) shows higher tolerance of salt stress than its C₃ close relative, *C. viscosa* L. *Advances in Agriculture & Botany* **3**(1): 59–66.
- Kurihara, Y., Watanabe, Y. (2004) Arabidopsis micro-RNA biogenesis through Dicer-like 1 protein functions. *Proceedings of the National Academy of Sciences of the United States of America* **101**(34): 12753–12758.
- Lakatos, L., Csorba, T., Pantaleo, V., Chapman, E., Carrington, J.C., Liu, Y.P., Calino, L.F., Lopez-Moya, J., Burgyán, J. (2006) Small RNA binding is a common strategy to suppress RNA silencing by several viral suppressors. *The EMBO Journal* **25**(12): 2768–2780.
- Lakatos, L., Szittyá, G., Silhavy, D., Burgyán, J. (2004) Molecular mechanism of RNA silencing suppression mediated by p19 protein of tombusviruses. *The EMBO Journal* **23**(4): 876–884.
- Langdale, J.A. (1993) In situ hybridization. In: *The Maize Handbook*. (Eds: V. Walbot and M. Freeling) pp. 165–180.
- Langdale, J.A., Kidner, C.A. (1994) bundle sheath defective, a mutation that disrupts cellular differentiation in maize leaves. *Cell* **68**(1): 673–681.
- Langdale, J.A., Metzler, M.C., Nelson, T. (1987) The argentia mutation delays normal development of photosynthetic cell-types in *Zea mays*. *Developmental Biology* **122**(1): 243–255.
- Langdale, J.A., Nelson, T. (1991) Spatial regulation of photosynthetic development in C₄ plants. *Trends in Genetics* **7**(6): 191–196.
- Langdale, J.A., Taylor, W.C., Nelson, T. (1991) Cell-specific accumulation of maize phosphoenolpyruvate carboxylase is correlated with demethylation at a specific site greater than 3 kb upstream of the gene. *Molecular & General Genetics* **225**(1): 49–55.
- Langdale, J.A., Zelitch, I., Miller, E., Nelson, T. (1988) Cell position and light influence C₄ versus C₃ patterns of photosynthetic gene expression in maize. *The EMBO Journal* **7**(12): 3643–3651.
- Langmead, B., Trapnell, C., Pop, M., Salzberg, S.L. (2009) Ultrafast and memory-efficient alignment of short DNA sequences to the human genome. *Genome Biology* **10**:R25
- Li, T., Li, H., Zhang, Y.X., Liu, J.Y. (2011) Identification and analysis of seven H₂O₂-responsive miRNAs and 32 new miRNAs in the seedlings of rice (*Oryza sativa* L. ssp. *indica*). *Nucleic acids Research* **39**(7): 2821–2833.
- Li, Z., Pinson, S.R.M., Paterson, A.H., Park, W.D., Stansel, J.W. (1997) Genetics of hybrid sterility and hybrid breakdown in an intersubspecific rice (*Oryza sativa* L.) population. *Genetics* **145**: 1139–1148.
- Lin, C. (1998) Enhancement of blue-light sensitivity of Arabidopsis seedlings by a blue light receptor cryptochrome. *Proceedings of the National Academy of Sciences* **95**(5): 2686–2690.
- Liu, C.M., Xu, Z.H., Chua, N.H. (1993) Proembryo culture: in vitro development of early globular-stage zygotic embryos from *Brassica juncea*. *The Plant Journal* **3**(2): 291–300.
- Liu, J., Wu, Y.H., Yang, J.J., Liu, Y.D., & Shen, F.F. (2008) Protein degradation and nitrogen remobilization during leaf senescence. *Journal of Plant Biology* **51**(1): 11–19.

- Livak, K.J., Schmittgen, T.D. (2001) Analysis of relative gene expression data using real-time quantitative PCR and the $2^{-\Delta\Delta C(T)}$ Method. *Methods* **25**(4): 402–408.
- Llave, C., Kasschau, K. D., Rector, M. A., Carrington, J. C. (2002a) Endogenous and Silencing-Associated Small RNAs in Plants. *Society* **14**: 1605–1619.
- Llave, C., Xie, Z., Kasschau, K.D., Carrington, J.C. (2002) Cleavage of Scarecrow-like mRNA targets directed by a class of Arabidopsis miRNA. *Science* **297**: 2053–2056.
- Long, S.P., Ainsworth, E.A., Leakey, A.D.B, Nosberger, J., Ort, D.R. (2006) Food for thought: lower-than-expected crop yield simulation with rising CO₂ concentrations. *Science* **312**: 1918–1921.
- Lobell, D.B., Burke, M.B, Tebaldi, C., Mastrandrea, M.D., Falcon, W.P., Naylor, R.L. (2008) Prioritising climate change adaptation needs for food security in 2030. *Science* **319**: 607–610.
- Long, J.J., Berry, J.O. (1996) Tissue-specific and light-mediated expression of the C₄ photosynthetic NAD-dependent malic enzyme of Amaranth mitochondria. *Plant Physiology* **112**(2): 473–482.
- Love, A.C., Andrews, M.E., Raff, R.A. (2007) Gene expression patterns in a novel animal appendage: the sea urchin pluteus arm. *Evolution & Development* **9**(1): 51–68.
- Lu, S., Sun, Y.H., Chiang, V.L. (2008) Stress-responsive microRNAs in *Populus*. *The Plant Journal* **55**(1): 131–151.
- Lu, S., Sun, Y.H., Shi, R., Clark, C., Li, L., Chiang, V.L. (2005) Novel and mechanical stress-responsive MicroRNAs in *Populus trichocarpa* that are absent from Arabidopsis. *The Plant Cell* **17**(8): 2186–203.
- Ma, L., Li, J., Qu, L., Hager, J., Chen, Z., Zhao, H., Deng, X.W. (2001) Light control of Arabidopsis development entails coordinated regulation of genome expression and cellular pathways. *Plant Cell* **13**(12): 2589–2607.
- Machado, I.C., Lopes, A.V., Leite, A.V., de Brito Neves, C. (2006) *Cleome spinosa* (Capparaceae): polygamodioecy and pollination by bats in urban and Caatinga areas, northeastern Brazil. *Botanische Jahrbücher* **127**(1): 14.
- Maizel, J.V. (1966) Acrylamide-gel electrophorograms by mechanical fractionation: Radioactive adenovirus proteins. *Science* **151**: 988–990.
- Mallory, A.C., Reinhart, B.J., Jones-Rhoades, M.W., Tang, G., Zamore, P.D., Barton, M.K., Bartel, D.P. (2004) MicroRNA control of PHABULOSA in leaf development: importance of pairing to the microRNA 5' region. *The EMBO Journal* **23**(16): 3356–64.
- Mansfield, S.G., Briarty, I.G. (1996) The dynamics of seedling and cotyledon cell development in *Arabidopsis thaliana* during reserve mobilisation. *International Journal of Plant Science* **157**(3): 280–295.
- Marks, T., Simpson, S. (2000) Interaction of explant type and indole-3-butyric acid during rooting in vitro in a range of difficult and easy-to-root woody plants. *Plant Cell, Tissue and Organ Culture* **62**(1): 67–74.
- Marshall, D.M., Muhaidat, R., Brown, N.J., Liu, Z., Stanley, S., Griffiths, H., Sage, R.F. (2007) *Cleome*, a genus closely related to Arabidopsis, contains species spanning a developmental progression from C₃ to C₄ photosynthesis. *The Plant Journal* **51**(5): 886–896.

- Martin, F.W. (1959) Staining and observing pollen tubes in the style by means of fluorescence. *Biotechnic & Histochemistry* **34**(3): 125–128.
- Matsuoka, M. (1993) Tissue-specific light-regulated expression directed by the promoter of a C₄ gene, maize pyruvate, orthophosphate dikinase, in a C₃ Plant, Rice. *Proceedings of the National Academy of Sciences* **90**(20): 9586–9590.
- Malthus, T.R. (1798) *An essay on the principle of population* in *Oxford World's Classic Reprints*, Chapter 1, pp.13.
- Maxwell, D.P., Laudendach, D.E., Huner, N.P.A. (1995) Redox regulation of light-harvesting complex II and cab mRNA abundance in *Dunaliella salina*. *Plant Physiology* **109**(3): 787–795.
- McCalla, A.F. (1994) Agriculture and food needs to 2025: Why we should be concerned.
- McCormac, D., Boinski, J.J., Ramsperger, V.C., Berry, J.O. (1997) C₄ Gene expression in photosynthetic and nonphotosynthetic leaf regions of *Amaranthus tricolor*. *Plant Physiology* **114**(3): 801–815.
- McCormac, D.J., Litz, H., Wang, J., Gollnick, P.D., & Berry, J.O. (2001) Light-associated and processing-dependent protein binding to 5' regions of rbcL mRNA in the chloroplasts of a C₄ plant. *The Journal of Biological Chemistry* **276**(5): 3476–83.
- McHale, N.A., Koning, R.E. (2004) MicroRNA-directed cleavage of *Nicotiana sylvestris* PHAVOLUTA mRNA regulates the vascular cambium and structure of apical meristems. *The Plant Cell* **16**(7): 1730–1740.
- McLaughlin, S.B., Andersen, C.P., Hanson, P.J., Tjoelker, M.G., Roy, W.K. (1991) Increased dark respiration and calcium deficiency of red spruce in relation to acidic deposition at high-elevation southern Appalachian Mountain sites. *Canadian Journal of Forest Research* **21**(8): 1234–1244.
- Meierhoff, K., Westhoff, P. (1993) Differential biogenesis of photosystem II in mesophyll and bundle-sheath cells of monocotyledonous NADP-malic enzyme-type C₄ plants: the non-stoichiometric abundance of the subunits of photosystem II in the bundle-sheath chloroplasts and the translational. *Planta* **191**(1): 23–33.
- Meinke, D.W. (1992) A Homoeotic Mutant of *Arabidopsis thaliana* with Leafy Cotyledons. *Science* **258**: 1647–1650.
- Mendoza, M.G., Kaepler, H.F. (2002) Auxin and sugar effects on callus induction and plant regeneration frequencies from mature embryos of wheat (*Triticum aestivum* L.). *In Vitro Cellular & Developmental Biology - Plant* **38**(1): 39–45.
- Michael, T.P., McClung, C.R. (2003) Enhancer trapping reveals widespread circadian clock transcriptional control in *Arabidopsis*. *Plant Physiology* **132**(2): 629–639.
- Millar, A.A., Gubler, F. (2005) The *Arabidopsis* GAMYB-Like genes, MYB33 and MY65, are microRNA-regulated genes that redundantly facilitate anther development. *The Plant Cell* **17**(3): 705–721.
- Monson, R., Rawsthorne, S. (2004) CO₂ assimilation in C₃-C₄ intermediate plants. *Photosynthesis* **9**: 533–550.
- Monson, R.K., Moore, B.D. (1989) On the significance of C₃-C₄ intermediate photosynthesis to the evolution of C₄ photosynthesis. *Plant, Cell & Environment* **12**(7): 689–699.

- Moore, B.D., Ku, M.S.B., Edwards, G.E. (1989) Expression of C₄-like photosynthesis in several species of *Flaveria*. *Plant, Cell and Environment* **12**(5): 541–549.
- Moore, I., Samalova, M., Kurup, S. (2006) Transactivated and chemically inducible gene expression in plants. *The Plant Journal* **45**(4): 651–683.
- Moore, K.G., Bentley, K., Lovell, P.H. (1972) A comparative study of chlorophyll production in cotyledons. *Journal of Experimental Botany* **23**(2): 432–439.
- Moran, R., Porath, D. (1980) Chlorophyll determination in intact tissues using n,n-dimethylformamide. *Plant Physiology* **65**(3): 478–479.
- Moxon, S., Schwach, F., Dalmay, T., Maclean, D., Studholme, D.J., Moulton, V. (2008) A toolkit for analysing large-scale plant small RNA datasets. *Bioinformatics* **24**(19): 2252–2253.
- Moyle, L.C., Nakazato, T. (2010) Hybrid incompatibility snowballs between *Solanum* species. *Science* **329**: 1521–1523.
- Murashige, T., Skoog, F. (1962) A revised medium for rapid growth and bioassays with Tobacco tissue cultures. *Physiologia Plantarum* **15**(3): 473–497.
- Nambudiri, E.M.V., Tidwell, W.D., Smith, B.N., Hebbert, N.P. (1978) A C₄ plant from the Pliocene. *Nature* **276**: 816–817.
- Narsai, R., Howell, K.A., Millar, A.H., O’Toole, N., Smmall, I., Whelan, J. (2007) Genome-wide analysis of mRNA decay rates and their determinants in *Arabidopsis thaliana*. *The Plant cell* **19**(11): 3418–3436.
- Neff, M.M., Van Volkenburgh, E. (1994) Light-stimulated cotyledon expansion in *Arabidopsis* seedlings (the role of Phytochrome B). *Plant Physiology* **104**(3): 1027–1032.
- Nelson, T. (1984) Light-regulated gene expression during maize leaf development. *The Journal of Cell Biology* **98**(2):558–564.
- Newell, C.A., Brown, N.J., Liu, Z., Pflug, A., Gowik, U., Westhoff, P., & Hibberd, J.M. (2010) *Agrobacterium tumefaciens*-mediated transformation of *Cleome gynandra* L., a C₄ dicotyledon that is closely related to *Arabidopsis thaliana*. *Journal of experimental Botany* **61**(5): 1311–1319.
- Nitsch, J.P., Nitsch, C. (1969) Haploid plants from pollen grains. *Science* **163**: 85–87.
- Obernosterer, G., Leuschner, P.J.F., Alenius, M., Martinez, J. (2006) Post-transcriptional regulation of microRNA expression. *RNA* **12**(7): 1161–1167.
- Orr, H. A., & Turelli, M. (2001) The evolution of postzygotic isolation: Accumulating Dobzhansky-Muller incompatibilities. *Evolution* **55**(6): 1085–1094.
- Palatnik, J.F., Allen, E., Wu, X., Schommer, C., Schwab, R., Carrington, J.C.C, Weigel, D. (2003) Control of leaf morphogenesis by microRNAs. *Nature* **425**: 257–263.
- Parizotto, E.A., Dunoyer, P., Rahm, N., Humber, C., Voinnet, O. (2004) In vivo investigation of the transcription, processing, endonucleolytic activity, and functional relevance of the spatial distribution of a plant miRNA. *Genes & Development* **18**(18): 2237–2242.
- Parra, R., Amo-Marco, J.B. (1996) Effect of plant growth regulators and basal media on in vitro shoot proliferation and rooting of *Myrtus communis* L. *Biologia Plantarum* **38**(2): 161–168.

- Parry, M., Rosenzweig, C., Iglesias, A., Fischer, G., Livermore, M. (1999) Climate change and world food security: a new assessment. *Global Environmental Change* **9** (S1): 51–67.
- Parys, E., Jastrzebski, H. (2006) Light-enhanced dark respiration in leaves, isolated cells and protoplasts of various types of C₄ plants. *Journal of Plant Physiology* **163**(6): 638–647.
- Parys, E., Romanowska, E., Siedlecka, M., Poskuta, J.W. (1998) The effect of lead on photosynthesis and respiration in detached leaves and in mesophyll protoplasts of *Pisum sativum*. *Acta Physiologiae Plantarum* **20**(3): 313–322.
- Patel, M., Corey, A.C., Yin, L.P., Ali, S., Taylor, W.C., Berry, J.O. (2004) Untranslated regions from C₄ Amaranth AhRbcS₁ mRNAs confer translational enhancement and preferential bundle sheath cell expression in transgenic C₄ *Flaveria bidentis*. *Gene Expression* **136**: 3550–3561.
- Patel, M., Siegel, A.J., Berry, J.O. (2006) Untranslated regions of FbRbcS₁ mRNA mediate bundle sheath cell-specific gene expression in leaves of a C₄ plant. *The Journal of Biological Chemistry* **281**(35): 25485–25491.
- Paulsen, H., Bogorad, L. (1988) Diurnal and circadian rhythms in the accumulation and synthesis of mRNA for the light-harvesting chlorophyll a/b-Binding protein in Tobacco. *Plant Physiology* **88**(4): 1104–1109.
- Pearcy, R.W., Björkman, O. (1970) Hybrids between *Atriplex* species with and without β -carboxylation photosynthesis: Biochemical characteristics. *Carnegie Institute of Washington Yearbook* **69**: 632–640.
- Prabu, G.R., Mandal, A.K.A. (2010) Computational identification of miRNAs and their target genes from expressed sequence tags of tea (*Camellia sinensis*). *Genomics, Proteomics & Bioinformatics* **8**(2): 113–121.
- Pyankov, V.I., Voznesenskaya, E.V., Kuz'min, A.N., Ku, M.S.B, Ganko, E., Franceschi, V.R., Black, C.C. (2000) Occurrence of C₃ and C₄ photosynthesis in cotyledons and leaves of *Salsola* species (Chenopodiaceae). *Photosynthesis Research* **63**(1): 69–84.
- Quazi, M.H. (1988) Interspecific hybrids between *Brassica napus* L. and *B. oleracea* L. developed by embryo culture. *Theoretical and Applied Genetics* **75**(2): 309–318.
- Rajendrudu, G., Rama'Das, V.S. (1982) Seed surface study of possible hybrids between C₃ and C₄ species of *Cleome* (Capparidaceae) *Current Science* **51**(16): 795–797.
- Ramsperger, V.C., Summers, R.G., Berry, J.O. (1996) Photosynthetic gene expression in meristems and during initial leaf development in a C₄ dicotyledonous plant. *Plant Physiology* **111**(4): 999–1010.
- Reich, P.B. (1983) Effects of low concentrations of O₃ on net photosynthesis, dark respiration, and chlorophyll contents in aging hybrid poplar leaves. *Plant Physiology* **73**(2): 291–296.
- Renart, J. (1979) Transfer of proteins from dets to diazobenzylxymethyl-paper and detection with antisera: A method for studying antibody specificity and antigen structure. *Proceedings of the National Academy of Sciences* **76**(7): 3116–3120.
- Reyes, J.L., Chua, N.H. (2007) ABA induction of miR159 controls transcript levels of two MYB factors during Arabidopsis seed germination. *The Plant Journal* **49**(4): 592–606.
- Rhoades, M.W., Reinhart, B.J., Lim, L.P., Burge, C.B., Bartel, B., Bartel, D.P. (2002) Prediction of plant microRNA targets. *Cell* **110**(4), 513–520.

- Rieseberg, L.H., Desrochers, A.M., Youn, S.J. (1995) Interspecific pollen competition as a reproductive barrier between sympatric species of *Helianthus* (Asteraceae). *American Journal of Botany* **82**(4): 515–519.
- Robinson, J.T., Thorvaldsdóttir, H., Winckler, W., Guttman, M., Lander, E.S., Getz, G., Mesirov, J.P. (2011) Integrative genomics viewer. *Nature Biotechnology* **29**(1): 24–26.
- Ruiz-Zapata, T., Huérfano, A.A., Xena de Enrech, N. (1996) Contribución al estudio citotaxonómico del género *Cleome* L. (Capparidaceae). *Fyton* **59**: 85–94.
- Sage, R.F. (2004) The evolution of C₄ photosynthesis. *New Phytologist* **161**(2): 341–370.
- Sage, R.F., Christin, P.A., Edwards, E.J. (2011) The C₄ plant lineages of planet Earth. *Journal of Experimental Botany* **62**(9): 3155–3169.
- Sage, R.F., Monson, R.K. (1999) *C₄ Plant Biology*. San Diego, CA, USA: Academic Press.
- Saiki, R., Scharf, S., Faloona, F., Mullis, K., Horn, G., Erlich, H., & Arnheim, N. (1985) Enzymatic amplification of beta-globin genomic sequences and restriction site analysis for diagnosis of sickle cell anemia. *Science* **230**: 1350–1354.
- Salomé, P.A., Xie, Q., McClung, C.R. (2008) Circadian timekeeping during early Arabidopsis development. *Plant Physiology* **147**(3): 1110–1125.
- Samalova, M., Brzobohaty, B., Moore, I. (2005) pOp6/LhGR: a stringently regulated and highly responsive dexamethasone-inducible gene expression system for tobacco. *The Plant Journal* **41**(6): 919–935.
- Sambrook, J., Fritsch, E., Maniatis, T. (1989) Quantitation of DNA and RNA In: *Ford N, Nolan C, Ferguson M, eds. Molecular Cloning. A Laboratory Manual*. Cold Spring Harbor, NY: Cold Spring Harbor Laboratory Press, 1989:E.5 (Appendix)
- Sanger, F., Coulson, R.A. (1975) A rapid method for determining sequences in DNA by primed synthesis with DNA polymerase. *Journal of Molecular Biology* **94**(3): 441–448.
- Sanger, F., Nicklen, S., Coulson, A.R. (1977) DNA sequencing with chain-terminating inhibitors. *Proceedings of the National Academy of Sciences* **74**(12): 5463–5467.
- Schoof, H., Lenhard, M., Haecker, A., Mayer, K.F.X., Jurgens, G., Laux, T. (2000) The stem cell population of Arabidopsis shoot meristems is maintained by a regulatory loop between the CLAVATA and WUSCHEL Genes. *Cell* **100**(6): 635–644.
- Schroeder, A., Mueller, O., Stocker, S., Salowsky, R., Leiber, M., Gassmann, M., Lightfoot, S. (2006) The RIN: an RNA integrity number for assigning integrity values to RNA measurements. *BMC Molecular Biology* **7**(1): 3.
- Shapiro, A.L., Scharff, M.D., Maizel, J.V., Uhr, J.W. (1966) Polyribosomal synthesis and assembly of the H and L chains of gamma globulin. *Proceedings of the National Academy of Sciences of the United States of America* **56**(1): 216–21.
- Sheen, J. (1990) Metabolic repression of transcription in higher plants. *The Plant Cell* **2**(10): 1027–38.
- Shu, G. 1999. Light Induction of cell type differentiation and cell-type-specific gene expression in cotyledons of a C₄ Plant, *Flaveria trinervia*. *Plant Physiology* **121**(3): 731–741.

Smith, E.D. (1970) Pollen competition and relatedness in *Haplopappus* section *Isopappus* (Compositae) II. *American Journal of Botany* **57**(7): 874–880.

Sommer, M.A., Bräutigam, A., Weber, A.P.M. (2012) The dicotyledonous NAD malic enzyme C₄ plant *Cleome gynandra* displays age-dependent plasticity of C₄ decarboxylation biochemistry. *Plant Biology* Published Online (June 2012)

Sorin, C., Bussel, J.D., Camus, I., Ljung, K., Kowalczyk, M., Geiss, G., McKhann, H., Garcion, C., Vaucheret, H., Sandberg, G., Bellini, C. (2005) Auxin and light control of adventitious rooting in *Arabidopsis* require ARGONAUTE1. *The Plant Cell* **17**(5): 1343–59.

Srivastava, S., Srivastava, A.K., Suprasanna, P., D'Souza, S.F. (2012) Identification and profiling of arsenic stress-induced microRNAs in *Brassica juncea*. *Journal of Experimental Botany* **Advanced Online Publication**, 16th November 2012.

Steeves, T.A., Sussex, I.M. (1989) *Plant Developmental Patterning* pp 6–26. Cambridge University Press, UK.

Sternberg, L.S., Deniro, M.J., Sloan, M.E., Black, C.C. (1986) Compensation point and isotopic characteristics of C₃/C₄ intermediates and hybrids in *Panicum*. *Plant Physiology* **80**(1): 242–245.

Stewart, J.M., Hsu, C.L. (1978) Hybridization of diploid and tetraploid cottons through in-ovulo embryo culture. *Journal of Heredity* **69**(6): 404–408.

Stockhaus, J., Schlue, U., Koczor, M., Chitty, J.A., Taylor, W.C., Westhoff, P. (1997) The promoter of the gene encoding the C₄ Form of phosphoenolpyruvate carboxylase directs mesophyll-specific expression in transgenic C₄ *Flaveria* spp. *The Plant Cell* **9**(4): 479–489.

Stout, A.A. (1923) Alternation of sexes and intermittent production of fruit in the spider flower (*Cleome spinosa*). *American Journal of Botany* **10**(2): 57–66.

Sunkar, R., Zhu, J.K. (2004) Novel and stress-regulated microRNAs and other small RNAs from *Arabidopsis*. *The Plant Cell* **16**(8): 2001–2019.

Taylor, L., Nunes-Nesi, A., Parsley, K., Leiss, A., Leach, G., Coates, S., Wingler, A. (2010) Cytosolic pyruvate, orthophosphate dikinase functions in nitrogen remobilization during leaf senescence and limits individual seed growth and nitrogen content. *The Plant Journal* **62**(4): 641–652.

Terada, R., Yamashita, Y., Nishibayashi, S., Shimamoto, K. (1987) Somatic hybrids between *Brassica oleracea* and *B. campestris*: selection by the use of iodoacetamide inactivation and regeneration ability. *Theoretical and Applied Genetics* **73**(3): 379–384.

Tolley, B.J., Woodfield, H., Wanchana, S., Bruskiwich, R., & Hibberd, J.M. (2011) Light-regulated and cell-specific methylation of the maize PEPC promoter. *Journal of Experimental Botany* **63**(3): 1381–1390.

Towbin, H., Staehelin, T., Gordon J. (1979) Electrophoretic transfer of proteins from polyacrylamide gels to nitrocellulose sheets: procedure and some applications. *Proceedings of the National Academy of Science* **76**(9): 4350–4354.

Townsend, J.A., Thomas, L.A. (1994) Factors which influence the *Agrobacterium*-mediated transformation of soybean. Keystone Symposium on Molecular and Cellular Biology. *Journal of Cell Biochemistry Supplement* **18A**.

- Uhrig, J.F., Canto, T., Marshall, D., MacFarlane, S.A. (2004) Relocalization of nuclear ALY proteins to the cytoplasm by the tomato bushy stunt virus P19 pathogenicity protein. *Plant Physiology* **135**(4): 2411–2423.
- van Leeuwen, W. (2001) Characterization of position-induced spatial and temporal regulation of transgene promoter activity in plants. *Journal of Experimental Botany* **52**(358): 949–959.
- Vargason, J.M., Szittyá, G., Burgyán, J., Hall, T.M.T. (2003) Size selective recognition of siRNA by an RNA silencing suppressor. *Cell* **115**(7): 799–811.
- Vidal, J., Chollet, R. (1997) Regulatory phosphorylation of C₄ PEP carboxylase. *Trends in Plant Science* **2**(6): 230–237.
- Viret, J. (1994) Transcriptional photoregulation of cell-type-preferred expression of maize rbcS-m3: 3' and 5' Sequences are involved. *Proceedings of the National Academy of Sciences*, **91**(18): 8577–8581.
- Virgin, H.I. (1955) Protochlorophyll formation and greening in etiolated Barley leaves. *Physiologica Plantarum* **8**(3): 630 – 643.dx
- Viswanathan, S.R., Daley, G.Q., Gregory, R.I. (2008) Selective blockade of microRNA processing by Lin28. *Science* **320**: 97–100.
- Voinnet, O., Rivas, S., Mestre, P., Baulcombe, D. (2003) An enhanced transient expression system in plants based on suppression of gene silencing by the p19 protein of tomato bushy stunt virus. *The Plant Journal* **33**(5): 949–956.
- Voinnet, O. (2005) Non-cell autonomous RNA silencing. *FEBS Letters* **579**: 5858–5871.
- Voznesenskaya, E.V., Franceschi, R., Artyushea, E.G., Black, C.C., Pyankov, I., Edwards, G.E. (2003) Development of the C₄ photosynthetic apparatus in cotyledons and leaves of *Salsola richteri* (Chenopodiaceae). *International Journal of Plant Sciences* **164**(4):471–487.
- Voznesenskaya, E.V., Koteyeva, N.K., Chuong, S.D.X., Akhani, H., Edwards, G.E., Franceschi, V.R. (2005) Differentiation of cellular and biochemical features of the single-cell C₄ syndrome during leaf development in *Bienertia cycloptera* (Chenopodiaceae). *American journal of Botany* **92**(11): 1784–1795.
- Voznesenskaya, E.V., Koteyeva, N.K., Chuong, S.D.X., Ivanova, A N., Barroca, J., Craven, L.A., Edwards, G.E. (2007) Physiological, anatomical and biochemical characterisation of photosynthetic types in genus *Cleome* (Cleomaceae). *Functional Plant Biology* **34**(4): 247.
- Wallace, J.S. (2000) Increasing agricultural water use efficiency to meet future food production. *Agriculture, Ecosystems & Environment* **82**: 105–119
- Wang, J.L., Long, J.J., Hotchkiss, T., Berry, J.O. (1993a) C₄ photosynthetic gene expression in light- and dark-grown Amaranth cotyledons. *Plant Physiology* **102**(4), 1085–1093.
- Wang, J.L., Turgeon, R., Carr, J.P., Berry, J.O. (1993b) Carbon Sink-to-Source Transition Is Coordinated with Establishment of Cell-Specific Gene Expression in a C₄ Plant. *The Plant Cell* **5**(3): 289–296.
- Wang, J.L., Klessig, D.F., Berry J.O. (1992) Regulation of C₄ gene expression in developing Amaranth leaves. *The Plant Cell* **4**: 173–184.
- Wang, X., Zhang, J., Li, F., Gu, J., He, T., Zhang, X., Li, Y. (2005) MicroRNA identification based on sequence and structure alignment. *Bioinformatics* **21**(18): 3610–3614.

- Wang, Y., Nii, N. (2002) Anatomical development and biochemical alteration in ribulose biphosphate carboxylase-oxygenase accumulation during leaf enlargement in *Amaranthus tricolor*. *Journal of the Japanese Society for Horticultural Science* **70**(6): 675–681.
- Waters, M.T., Wang, P., Korkaric, M., Capper, R.G., Saunders, N.J., Langdale, J.A. (2009) GLK transcription factors coordinate expression of the photosynthetic apparatus in Arabidopsis. *The Plant Cell* **21**(4): 1109–1128.
- Weber, A.P.M., von Caemmerer, S. (2010) Plastid transport and metabolism of C₃ and C₄ plants-comparative analysis and possible biotechnological exploitation. *Current opinion in Plant Biology* **13**(3): 257–265.
- Weijers, D., Jürgens G. (2005) Auxin and embryo axis formation: the ends in sight? *Current Opinion in Plant Biology* **8**(1): 32–37.
- Wu, C., Palopoli, M.F. (1994) Genetics of postmating reproductive isolation in animals. *Annual Review of Genetics* **27**: 283–308.
- Wu, X.M., Liu, M.Y., Xu, Q., Guo, W.W. (2010) Identification and characterization of microRNAs from citrus expressed sequence tags. *Tree Genetics & Genomes* **7**(1): 117–133.
- Xie, Z., Kasschau, K.D., & Carrington, J.C. (2003) Negative feedback regulation of Dicer-Like₁ in Arabidopsis by microRNA-Guided mRNA degradation. *Current Biology* **13**(9): 784–789.
- Yanagisawa, S. (2000) Dof1 and Dof2 transcription factors are associated with expression of multiple genes involved in carbon metabolism in maize. *The Plant Journal* **21**(3): 281–288.
- Yang, Z., Ebright, Y.W., Yu, B., Chen, X. (2006) HEN1 recognizes 21-24 nt small RNA duplexes and deposits a methyl group onto the 2' OH of the 3' terminal nucleotide. *Nucleic acids research* **34**(2): 667–675.
- Zenkter, M. (1990) In vitro fertilization and wide hybridization in higher plants. *Critical Reviews in Plant Sciences* **9**(3): 267–279.
- Zhang, G.Q., Zhou, W.J., Gu, H.H., Song, W.J., Momoh, E.J.J. (2003) Plant regeneration from the hybridization of *Brassica juncea* and *B. napus* through Eembryo culture. *Journal of Agronomy and Crop Science* **189**(5): 347–350.
- Zhang, Y. (2005) miRU: an automated plant miRNA target prediction server. *Nucleic acids Research* **33**: W701–704.
- Zhou, X., Wang, G., Zhang, W. (2007) UV-B responsive microRNA genes in Arabidopsis thaliana. *Molecular Systems Biology* **3**: 103.

Appendix 1: Primer List

The sequences of primers used in this study are tabulated below, along with a brief explanation of their purpose. The origin of each primer is given, adhering to the following code: KK: Kaisa Kajala (of Bräutigam *et al.*, 2011), NB: Naomi Brown, HA: Holly Astley, EG: E. Gage, AM: Ambion, Inc., IN: Invitrogen, Inc.

Primer	Sequence	Purpose	Origin
<i>ACT7</i> F	TCCGACCCGATGTGATGTTATGGT	qRT-PCR of <i>ACTIN7</i>	KK
<i>ACT7</i> R	CAATCACTTTCCGGCTGCAACCAA	qRT-PCR of <i>ACTIN7</i>	KK
<i>CA4</i> F	AGACCACTCCTTCCGTTGCTTCT	qRT-PCR of <i>CA4</i>	KK
<i>CA4</i> R	CACGAACACATCTCTGTGGTGTAGGAC	qRT-PCR of <i>CA4</i>	KK
<i>LHCA1</i> F	GACATCATCATCCCTATTCCCTTTCTCCC	qRT-PCR of <i>LHCA1</i>	KK
<i>LHCA1</i> R	AGTGATCAAATTACAGAGAGAGAGGGCT	qRT-PCR of <i>LHCA1</i>	KK
<i>NADME2</i> F	AGGATCGTGAAGGATGTTGAGGCT	qRT-PCR of <i>NADME2</i>	KK
<i>NADME2</i> R	TTCCTGAATTCCGGTATGGCGTCT	qRT-PCR of <i>NADME2</i>	KK
<i>PEPC</i> F	TCGACATTGCCCTCATCGGATTCT	qRT-PCR of <i>PEPC</i>	KK
<i>PEPC</i> R	AATCCAAGAACCTTCTCCGGGTCA	qRT-PCR of <i>PEPC</i>	KK
<i>PPCK</i> F	CTTGTCAATGGTCTTGCAGGCGAA	qRT-PCR of <i>PPCK</i>	KK
<i>PPCK</i> R	CCCAAACACTTCACAACAGCAGCA	qRT-PCR of <i>PPCK</i>	KK
<i>PPDK</i> F	GCAGGACTTGATTATGTCTCTTGCTC	qRT-PCR of <i>PPDK</i>	KK
<i>PPDK</i> R	GGGACAGCCATCTAACATTCTTCC	qRT-PCR of <i>PPDK</i>	KK
<i>PYR</i> F	TGCGGCATTCCGGTATTGGCTATTG	qRT-PCR of <i>PyT1</i>	KK
<i>PYR</i> R	TAACGGCAGAAGGAACGGCTACAA	qRT-PCR of <i>PyT1</i>	KK
<i>RbcS1A</i> F	TGGATTTCGACAACTCCCGTCAAGT	qRT-PCR of <i>RbcS1A</i>	KK
<i>RbcS1A</i> R	TTACAGCCAGAAGGCCGTGTGATA	qRT-PCR of <i>RbcS1A</i>	KK
<i>RCA</i> F	AGAGAGTCCAACCTGGCCGATAAGT	qRT-PCR of <i>RCA</i>	KK
<i>RCA</i> R	AACTGGCAGATTCACTTGCTGTGC	qRT-PCR of <i>RCA</i>	KK
<i>35S</i> F	AAGCTTGCATGCCTGCAGGTCA	Sequencing of TOPO Insert	NB
<i>35S</i> R	TCCTCTCCAAATGAAATGAAC	Sequencing of TOPO Insert	NB
<i>5' RACE</i> Adapter	GCUGAUGAAUGAACACUGCGUUUGC UGGCUUUGAUGAAA	Adapter for <i>5' RACE</i>	AM
<i>5' RACE</i> Inner	CGCGGATCCGAACACTGCGTTTGCTG GCTTTGATG	Adapter primer for <i>5' RACE</i> Inner PCR	AM
<i>5' RACE</i> Outer	GCTGATGGCGATGAATGAACACTG	Adapter primer for <i>5' RACE</i> Outer PCR	AM

Appendix 1: Primer List

Primer	Sequence	Purpose	Origin
<i>ACT8</i> F	CAGATGTGGATCGCAAAGGCA	qRT-PCR of <i>ACTIN8</i> - At	HA
<i>ACT8</i> R	AAACCCGGCTTGAGAAATGGTC	qRT-PCR of <i>ACTIN8</i> - At	HA
<i>ASP2</i> F	TGTACAGCGATTGGACCATTGAGC	qRT-PCR of <i>ASP2</i>	EG
<i>ASP2</i> F	TCACCAGGTGTGCCTTTAGCT	qRT-PCR of <i>ASP3</i>	EG
<i>CA</i> F	GTCAGAGCCCAAAGTATCTGGTATTTGC	qRT-PCR of <i>CA</i>	KK
<i>CA</i> R	TCACAGCTTCCTTCTCACATTGGGTGC	qRT-PCR of <i>CA</i>	KK
<i>NADME</i> F	ATTGCAACAACATCGTCTCGACGGTG	qRT-PCR of <i>NAD-ME</i>	NB
<i>NADME</i> R	AATAGAAAACGCCTCTTGTGGAGTGC	qRT-PCR of <i>NAD-ME</i>	NB
<i>p19</i> F	AACAGTGAACGTTGGGATGGAGGA	qRT-PCR of <i>p19</i>	EG
<i>p19</i> R	ACATCCGATCTGGTTCGAAACCGAA	qRT-PCR of <i>p19</i>	EG
<i>p19W</i> F	CACCATGGAACGAGCTATAACAAGG	Cloning of <i>p19</i> Coding Sequence	EG
<i>p19W</i> R	TTACTCGCTTTCGAAGGTCT	Cloning of <i>p19</i> Coding Sequence	EG
<i>pOpp19</i> F	AGAATGAACCGAAACCGGCGGTA	Directional Sequencing of pOp:: <i>p19</i>	EG
<i>pOpp19</i> R	GGCAAGCTGTAGCAGTTCTTGCTTT	Directional Sequencing of pOp:: <i>p19</i>	EG
<i>PPCK</i> F	CTGGTCTCTTTCTGAGGCTCAAACG	qRT-PCR of <i>PPCK</i>	KK
<i>PPCK</i> R	CCATGGATGCCTTAGTGATTGCTCTGC	qRT-PCR of <i>PPCK</i>	KK
<i>PPDK</i> F ₂	CAAGCACGTGCGATTTTCCAAGCAGC	qRT-PCR of <i>PPDK</i>	KK
<i>PPDK</i> R	CACATATTCCAACCTTGAGGTTAGGTGC	qRT-PCR of <i>PPDK</i>	KK
<i>PPDK</i> InA R	CACCGAATTTTACCACTTACCA	Internal Primer for <i>PPDK</i> 5' RACE	EG
<i>PPDK</i> InB R	AAAGTGGTGAGGATGGGTTG	Internal Primer for <i>PPDK</i> 5' RACE	EG
<i>PPDK</i> InC R	TGTAAAGTGGGTAAAATTCCGGTG	Internal Primer for <i>PPDK</i> 5' RACE	EG
<i>PPDK</i> InD R	CCTTCCAAGCCTCTTCTCCT	Internal Primer for <i>PPDK</i> 5' RACE	EG
<i>PPDK</i> InE R	AAGCAAAACGTTCTCCACTTTT	Internal Primer for <i>PPDK</i> 5' RACE	EG
<i>PPDK</i> InF R	TCCTAGGTTAAGAACTGTATCCATC	Internal Primer for <i>PPDK</i> 5' RACE	EG
<i>PPDK</i> InG R	ATGCCGGGTATGATGGATACAGTTC	Internal Primer for <i>PPDK</i> 5' RACE	EG
<i>PPDK</i> InH R	GATATGTTCCGGCAATGTTGTGATGATGG	Internal Primer for <i>PPDK</i> 5' RACE	EG
<i>PPDK</i> InI R	GAAGTGTATCCATCATAACCCGGCAT	Internal Primer for <i>PPDK</i> 5' RACE	EG
<i>PPDK</i> InJ R	CCATCACAACATTGCCGAACATATC	Internal Primer for <i>PPDK</i> 5' RACE	EG
<i>PPDK</i> InK R	CACTGCTATCTTACCAGCACCTTT	Internal Primer for <i>PPDK</i> 5' RACE	EG
<i>PPDK</i> InL R	CTGCCTTGATCGCCAATTCCAA	Internal Primer for <i>PPDK</i> 5' RACE	EG

Appendix 1: Primer List

Primer	Sequence	Purpose	Origin
<i>PPDK IRnA F</i>	GAGATGGCCAGCATAGGTCT	Internal Primer for <i>PPDK</i> 5' RACE	EG
<i>PPDK IRnB F</i>	CAACCCATCCTCACCACCTTTTCTT	Internal Primer for <i>PPDK</i> 5' RACE	EG
<i>PYR F</i>	TCATGACAACATGTTCAACCATTGGAGC	qRT-PCR of <i>PyT1</i>	KK
<i>PYR R</i>	CCACCGAGCGCCATACAGACAACGC	qRT-PCR of <i>PyT1</i>	KK
<i>Spec F</i>	ATTCATTCAAGCCGACACCGCTTC	Spectinomycin resistance (sequencing)	EG
<i>Spec R</i>	CGTCGTGCACAACAATGGTGACTT	Spectinomycin resistance (sequencing)	EG
<i>T3</i>	ATTAACCCTCACTAAAGGGA	PCR screen of TOPO vectors	IN
<i>T7</i>	TAATACGACTCACTATAGGG	PCR screen of TOPO vectors	IN
<i>uidA</i>	TGATCGCGTCAGCGCCGTC	Verification of <i>uidA</i>	NB

Appendix 2: sRNA Target List

The data of sequences used in the initial search of the sRNA library are given below. “Contig” refers to the sequence reference number in the EST database of Bräutigam *et al.* (2011). The EST identification is given, along with the number of sRNA hits against each sequence.

Contig	Blast Results	Hits
5	RbcS1A	4
11	RbcS1A	13
15	RbcS3B	4
16	PPDK	60
30	PEPC2	40
32	CA1	2
33	NAD(P)H:Plastoquinone Dehydrogenase subunit O	7
55	NDH-M (subunit NDH-M OF NAD(P)H:Plastoquinone Dehydrogenase complex)	0
63	RbcS1A	7
90	RbcS1a	7
98	CA1	0
114	RbcS1A	12
115	RbcS1A	9
120	RbcS1A	10
144	RbcS3B	4
148	MDH	4
164	RbcS1A	18
166	CA	0
212	RCA	1
213	RCA	0
233	Starch Synthase	3
242	NADPH dehydrogenase/electron transporter,	3
528	PEPCK1	2
1078	NDH-N of NAD(P)H:plastoquinone dehydrogenase complex (Ndh complex)	0
1223	PEPCK1	3
1708	RCA	0
1963	NAD(P)H:Plastoquinone Dehydrogenase subunit O	6
2049	PDK (Pyruvate Dehydrogenase Kinase)	0
2052	MDH	1
2081	Bundle-sheath defective protein 2 family / bsd2 family	0
2085	Malate dehydrogenase (NAD), mitochondrial	0
2236	DIT1 (Dicarboxylate transporter; oxoglutarate:malate antiporter)	1
2459	(NADP-malic enzyme 2); malate dehydrogenase (oxaloacetate-decarboxylating)	0
2466	Pyruvate decarboxylase family protein	0
2488	RuBisCO Large subunit, putative	0

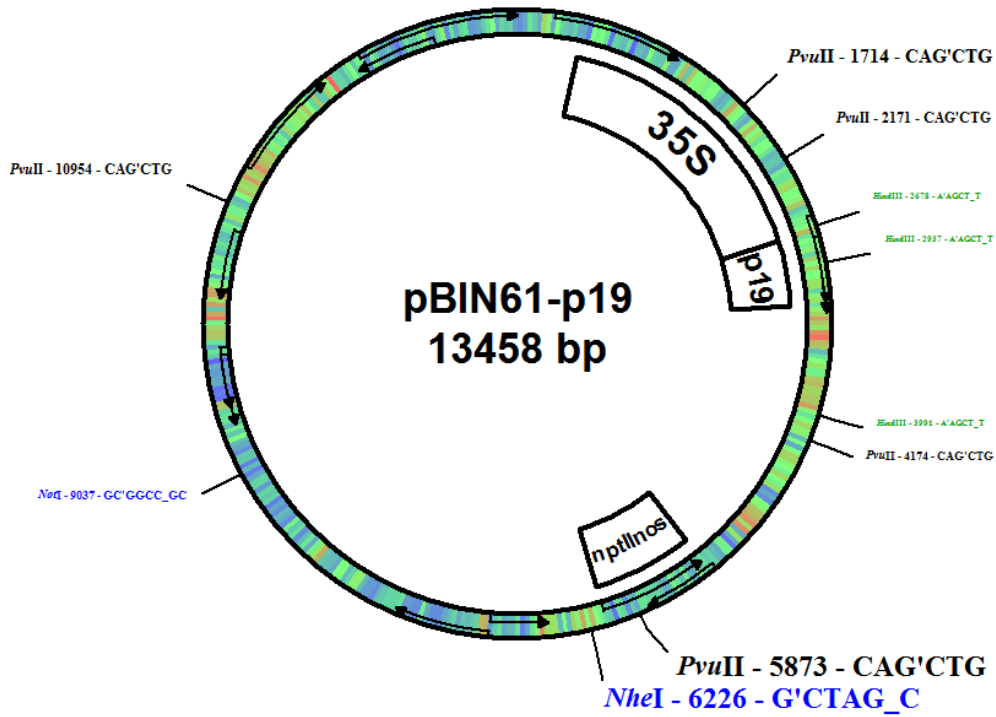
Appendix 2: sRNA Target List

Contig	Blast Results	Hits
2637	ASP ₃ (Asparatate aminotransferase 5)	1
2891	PPDK	2
2916	PEPC ₂	1
2924	Rbcs _{1A}	8
2955	Rbcs _{1A}	18
2957	PEPC ₁	6
2958	CA family protein	0
2964	Rbcs _{1A}	12
2984	PEPC ₂	1
3005	RbcS _{1A}	4
3058	PEPC ₁	6
3070	PPDK	5
3098	PEPC ₂	2
3099	PEPC ₂	2
3136	PEPC ₂	1
3138	Rbcs _{1A}	12
3167	CA family protein	0
3212	ASP ₃ (Asparatate aminotransferase 1)	0
3213	ASP ₁ (Asparatate aminotransferase 1)	5
3214	ASP ₁ (Asparatate aminotransferase 1)	5
3221	RCA	4
3486	PEPCK ₂	1
4520	MDH	0
5745	RuBisCO Large subunit, putative	0
5822	MDH	0
7150	Pyruvate dexcarboxylase family protein	0
7482	(NADP-malic enzyme 2); malate dehydrogenase (oxaloacetate-decarboxylating)	0
7993	MDH	0
8199	PEPC ₁	0
8389	DIT _{2.1} (Dicarboxylate transporter; oxoglutarate:malate antiporter)	0
8584	(NADP-malic enzyme 4); malate dehydrogenase (oxaloacetate-decarboxylating)	1
8736	pyruvate decarboxylase	0
9100	ASP ₃ (Asparatate aminotransferase 5)	0
9469	DIT _{2.1} (Dicarboxylate transporter; oxoglutarate:malate antiporter)	0
9719	RBCS _{1A} ; ribulose-bisphosphate carboxylase	0
10016	DIT _{2.1} (Dicarboxylate transporter; oxoglutarate:malate antiporter)	1
10211	PEPKR ₁ (PEPC-related kinase ₁)	0
10422	ALAAT ₂ (Alanine transferase 2)	0
10609	ALAAT ₂ (Alanine transferase 2)	0
11028	RbcS _{3B}	0
12043	MDH	0

Appendix 2: sRNA Target List

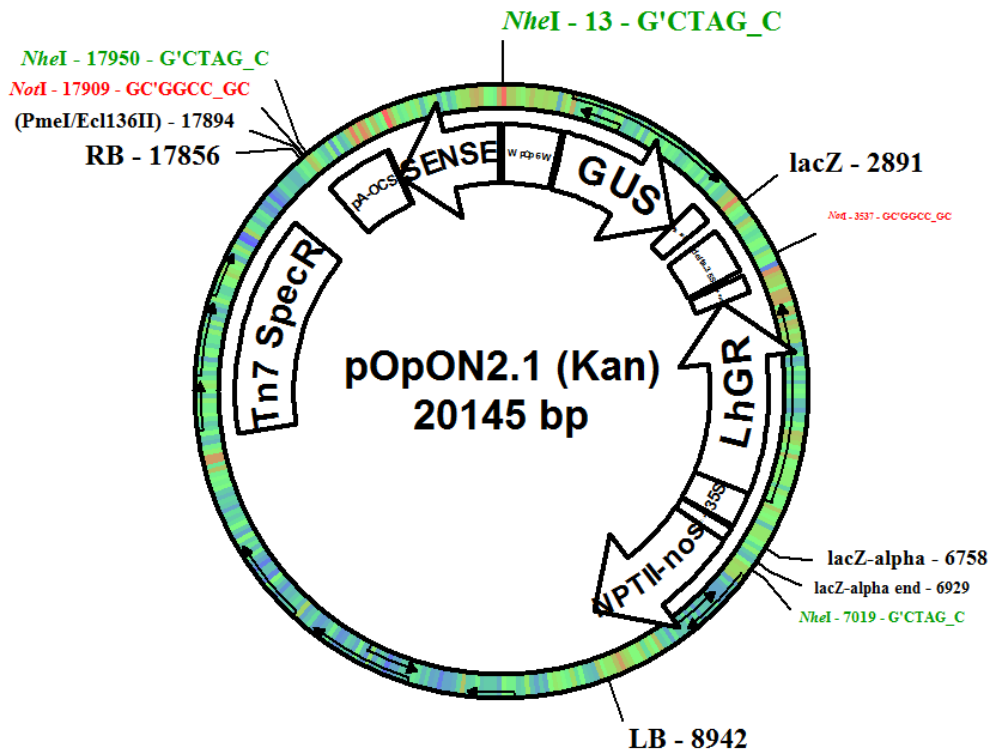
Contig	Blast Results	Hits
12274	MDH	0
13440	PEPCK ₁	0
13495	PEPC ₃	0
13682	ALAAT ₂ (Alanine aminotransferase 2)	0
13684	ALAAT ₂ (Alanine aminotransferase 2)	1
13685	ALAAT ₂ (Alanine aminotransferase 2)	0
13686	ALAAT ₁ (Alanine aminotransferase 1)	0
13689	ALAAT ₁ (Alanine aminotransferase 1)	0
13691	ALAAT ₂ (Alanine aminotransferase 2)	0
13692	ALAAT ₂ (Alanine aminotransferase 2)	0
13693	ALAAT ₂ (Alanine aminotransferase 2)	0
13812	Malate dehydrogenase, cytosolic, putative	0
14367	Pyruvate decarboxylase	0
14704	DIT _{2.1} (Dicarboxylate transporter; oxoglutarate:malate antiporter)	0
14714	PEPKR ₁ (PEPC-related kinase ₁)	0
14821	RCA	0
14941	Pyruvate decarboxylase family protein	0
14951	ASP ₃ (Asparatate aminotransferase 3)	0
15046	(NADP-malic enzyme 3); malate dehydrogenase (oxaloacetate-decarboxylating)	0
15107	ALAAT ₂ (Alanine aminotransferase 2)	0
15566	PEPC ₂	1
15934	RCA	0
16083	PEPC ₃	0
16651	PEPC ₂	0
16712	ASP ₃ (Asparatate aminotransferase 2)	0
17220	pyruvate decarboxylase family protein	0

Appendix 3: Plasmid Maps

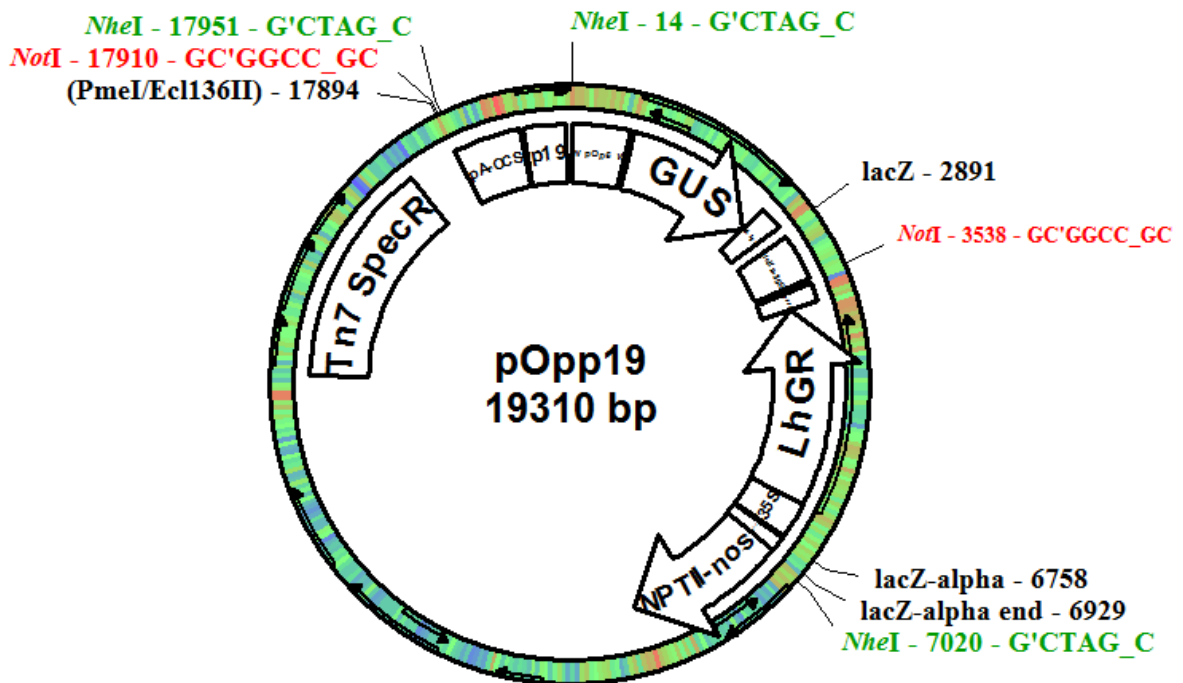


35S::p19::nos (Voinnet *et al.*, 2003)

Appendix 3: Plasmid Maps



Empty pOpON2.1 Vector (Moore et al., 2006)



pOp::p19 Expression Vector

